The role of nitric oxide as a hypoxic cell radiosensitizer

A thesis submitted for the degree of Doctor of Philosophy

University of Oxford

Lisa Folkes

CR-UK/MRC Gray Institute for Radiation Oncology and Biology

Linacre College, Oxford

Department of Oncology

Trinity Term 2013

Abstract

Many tumours contain regions of hypoxia which are difficult to treat by conventional radiotherapy. There is much interest in the ability of nitric oxide (•NO) to radiosensitize hypoxic mammalian cells as a possible adjunct to radiotherapy but mechanisms for its action are unclear. It has been proposed that •NO may radiosensitize cells by 'fixing' radiation-induced DNA free radicals, and elevated radiation response by •NO in cells has been partly attributed to increased formation of DNA double strand breaks.

In the work carried out for this thesis it is shown that reaction of •NO with radiation-induced nucleobase radicals produces some novel products. New pathways for the reactions of radiation-induced hydroxyl radicals with purine radicals are proposed. In addition, the effects of •NO on the yields of radiation-induced single strand breaks in anoxic plasmid DNA, and on anoxic mammalian cell radiosensitivity are investigated. Kinetics of formation and repair of radiation-induced double strand breaks indicate different effects of •NO on radiation-induced clustered and non-clustered DNA damage involving replication-induced DNA breaks.

As •NO is an inhibitor of ribonucleotide reductase, some of the radiosensitizing properties of •NO may be due to reduction in the availability of 2′-deoxyribonucleotides. Through studying reactions of •NO with tyrosine radicals, essential components of ribonucleotide reductase, this work has enhanced understanding into how •NO may inhibit the enzyme, which may offer new insights into the development of •NO-releasing anti-cancer agents.

The potential for delivery of •NO to hypoxic tissue for radiotherapy has also been investigated in this work, through the development of bioreductively-activated pro-drugs. These novel agents are stable until reduced by one-electron reductants, when a •NO-releasing pro-drug is rapidly evolved, only in those regions which are sufficiently hypoxic.

By increasing our understanding into the mechanisms involved in the ability of •NO to radiosensitize hypoxic cells, especially the reactivity of •NO with DNA radicals, knowledge has been gained into the identification, development and repair of radiation-induced DNA damage in cells, including clustered damage, in the presence of •NO. These studies contribute to further development of novel anti-cancer therapies based upon the release of •NO in hypoxic cells.

Acknowledgments

I would like to thank my supervisors; Professor Peter O'Neill for his valuable discussions and teaching me so much about radiation-induced DNA damage and repair; and Professor Borivoj Vojnovic for his varied technological support, advice and encouragement during my studies. The work would not have been possible without the valuable discussions with Dr. Peter Wardman, whose knowledge and ideas instigated this project and Dr. Mike Stratford who has always been there offering advice and help especially with HPLC analysis and whose patience is second to none. Thanks to Professor Rafael Radi for introducing me to the reactions of tyrosine. Thanks must also go to Mick Woodcock for his help and advice with flow cytometry and cell sorting and general assistance in times of need; Dr. Pamela Reynolds and Dr Jennifer Anderson for their immense patience with my discoveries into the world of immunofluorescence; Dr. James Thomson and John Prentice for their help in setting up the steady state radiolysis apparatus used in these studies way back at the beginning and to Dr. Iain Tullis who gave me the push to finally take the plunge and register for these studies after years of not having the courage to do so.

Of course none of this would have been possible without the support of The Gray Institute for Radiation Oncology and Biology and the Gray Trust who offered me a Gray Scholarship and gave me this fantastic opportunity. I cannot thank the department enough for believing in me when I did not believe in myself. I am still shocked that you said yes! Of course, thanks must also go to the funding bodies, Cancer Research UK and the Medical Research Council.

Finally I have to thank my family for their huge emotional support; my husband for coping with my worries and self-doubt, which must have been considerably hard, and his attempts at helping me with free-radical chemistry – I know two-electron reactions are much easier to understand; my children for losing their mother to science for so many hours, but always being there to welcome me home with a hug; my mum for checking up on me so often; and other colleagues, friends and family for their continued interest in my progress over the years.

Thanks to all who have helped to keep me plodding on through a sometimes difficult but very rewarding journey.

List of abbreviations

A	adenine
AP site	apurinic/apyrimidinic site
AscH	ascorbate
8AzaA	8-azaadenine
8AzadGMP	2′-deoxy-8-azaguanosine monophosphate
BER	base excision repair
$Br_2^{\bullet-}$	bromide radical
BSO	buthione sulfoxide
BSA	bovine serum albumin
C	cytosine
°C	degree Celsius
cm^3	cubic centimetre
$CO_3^{\bullet-}$	carbonate radical
DDR	DNA damage response
DEANO	diethylamine diazeniumdiolate
dI	2′-deoxyinosine
Dityr	3-3′-dityrosine
dG	2′-deoxyguanosine
dGMP	2′-deoxyguanosine monophosphate
dT	2′-deoxythymidine
dTMP	2′-deoxythymidine monophosphate
dCMP	2′-deoxycytidine monophosphate
dNTPs	2′-deoxyribonucleotide triphosphates
dXMP	2′-deoxyxanthosine monophosphate
DMEM	Dulbecco’s modified medium
DNA	deoxyribonucleic acid
DSB	double strand break(s)
Da	Daltons
EDTA	ethylenediamine tetraacetic acid
EMEM	Eagle’s modified medium
eNOS	endothelial nitric oxide synthase
ES	electrospray
ε	molar extinction coefficient
Fpg	formamidopyrimidine DNA glycosylase
FaPyA	4,6-diamino-5-formamidopyrimidine
FaPyG	2,6-diamino-4-hydroxy-5-methylformamidopyrimidine
G	guanine
g	gram(s)
Gy	gray(s)
GSH	glutathione
$GS^{\bullet}$	glutathionyl radical

HIF	hypoxia inducible factor
HF-19	human foetal lung fibroblast cells
HepG2	human Negroid hepatocyte carcinoma cells
HR	homologous recombination
HU	hydroxyurea
HPLC	high performance liquid chromatography
HRP	horseradish peroxidase
HCl	hydrochloric acid
$HClO_4$	perchloric acid
HOCl	hypochlorous acid
HX	hypoxanthine
h	hour(s)
HNO	nitroxyl
IR	ionizing radiation
iNOS	inducible nitric oxide synthase
LET	linear energy transfer
l	litre(s)
LCMS	HPLC with mass spectrometry detection
m/z	mass of the ion (in dalton) divided by its charge
min	minutes
ml	millilitre(s)
µl	microlitre(s)
mg	milligram(s)
µg	microgram(s)
M	molar
mM	millimolar
µM	micromolar
Mwt	molecular weight
MPA	metaphosphoric acid
$3NO_2$tyr	3-nitrotyrosine
3NOtyr	3-nitrosotyrosine
NHEJ	non-homologous end joining
NF	5-nitrofuran
NB	4-nitrobenzyl ether
NI	2-nitroimidazole
$^{\bullet}NO_2$	nitrogen dioxide radical
$N_3^{\bullet}$	azide radical
$^{\bullet}NO$	nitric oxide
NO^+	nitrosonium ion
NO_2^-	nitrite
3OHtyr	3-hydroxytyrosine (L-DOPA)
8oxoG	8-oxo-7,8-dihydroguanine
ONOOH	peroxynitrite
$^{\bullet}OH$	hydroxyl radical
PAA	4-hydroxyphenylacetic acid
PBS	phosphate buffered saline

PI	propidium iodide
PFA	paraformaldehyde
RT	room temperature
RR	ribonucleotide reductase
RNOS	reactive nitrogen species
s	second(s)
SER	survival enhancement ratio
SF	surviving fraction
SSB	single strand break(s)
T	thymine
Tyr	tyrosine
$Tyr^{\bullet}$	tyrosine phenoxyl radical
TBAOH	tetrabutyl ammonium hydroxide
U	units
UV	ultra-violet
V79-4	hamster fibroblast cells
w/v	weight/volume
X	xanthine

Table of Contents

2 Materials and Methods

List of Figures

List of Tables

List of Schemes

1 Introduction

1.1 Cancer

Although cancer is generally a disease of the elderly, it can affect all ages and long term survival is highly variable. Tumours arise from the uncontrolled growth of mutated cells which can overcome the normal function of tissue. Treatment of cancer is increasingly successful, but with average lifetime rising, about one in three of us is likely to suffer from the disease at some point. The location of a tumour within the body can be very varied which often determines the chosen treatment schedule. Although resection of a solid tumour is preferable, surgery is not possible for all tumours, especially if metastases are present. Radiotherapy can be an effective treatment, but deep tumours are difficult to treat and damage to overlying normal tissue can occur. Chemotherapy can also be limited by access of drugs to solid tumours, and in some cases only be successful for patients expressing certain genes. Combination therapy can be the most efficient treatment but clinical trials often focus on single-agent anti-cancer therapy in the first instance because of the danger of toxicity. Many tumour types can develop as secondary tumours throughout the body, for example in the liver, brain, lungs and bones. Metastasis is an enormous problem for therapy and reduces survival considerably and treatment can result in becoming only palliative. The choice of treatment is a difficult decision for oncologists and patients alike, and quality of life is an important factor to consider. We are constantly striving to improve therapy techniques and reduce unwanted side effects for those unfortunately struck with this horrific disease, in the hope that we will achieve a cure for all cancers.

1.2 Chemotherapy

Traditionally, chemotherapy drugs are cytotoxic agents used as a form of systemic treatment, showing some specificity to tumours generally through the higher metabolic rates of tumours compared to that of normal tissues. Toxic side effects can be an unpleasant consequence of the treatment, including severe nausea, vomiting and hair loss. With treatment schedules spanning many weeks, patients may have to stop treatment through ill health. In addition, tumours which initially respond extremely well to drugs can become resistant and unresponsive as treatment progresses.

There have been huge advances into chemotherapy in recent years, particularly in targeted therapies. For example, combretastatins target immature tubulin within tumours and induce vasoconstriction for up to 24 h, starving a tumour of nutrients and inducing cell death (Rustin *et al.* 2003; Patterson *et al.* 2012). It is becoming more apparent that cancer therapy can be most successful by screening for biomarkers and personalising treatment. Antibodies have been raised against tumour cells which express specific proteins or receptors and bind to and kill only those cells expressing the antigen (reviewed in (Weiner *et al.* 2009)). Rituximab, for example, is an antibody against CD20 antigens present on non-Hodgkins lymphoma cells and shows great promise against this disease (Maloney *et al.* 1997). Conjugation of a cytotoxic drug to an antibody is also a therapy used in current chemotherapy trials (reviewed in (Lambert 2012)). For example, Trastuzumab-DM1 (Herceptin-DM1) targets human epidermal growth factor receptor 2 (HER2) positive cells and shows promise for the treatment of pre-treated metastatic breast cancer (Burris III *et al.* 2011).

In all cases, diffusion of a drug into a solid tumour is essential for success, but this can be a difficult process to achieve (Jain 1994; Heldin *et al.* 2004), although different approaches are evolving to try and improve tumour uptake (Choi *et al.* 2013). Tumour uptake is a difficult process to study *in vitro* using cell cultures and spheroids, as the structure of a tumour and its network of blood vessels can not be represented. In addition, success in the laboratory is often

impossible to replicate in *in vivo* studies and even between different *in vivo* models and species. Development of new drugs for chemotherapy is therefore a slow and difficult process but one that is constantly evolving and becoming increasingly successful, particularly in the area of personalised medicine.

1.3 Radiotherapy

Radiotherapy can be a very effective treatment for some cancers and is used to treat ~50% of cases. The therapy includes external conventional beam radiotherapy and brachytherapy, where radioactive isotopes are inserted close to the tumour within the body. Side effects are generally less severe than with chemotherapy, but localised normal tissue damage around the region of the radiation beam can vary hugely, from mild discomfort and reddening of the skin to severe mucositis, for example in the treatment of head and neck cancers. Long term damage is also a risk, the side-effects including infertility and normal tissue damage, generally sited around the area of treatment, including permanent hair loss, oral dryness, heart disease and even further cancers. Enhanced targeting of the radiotherapy beam to the tumour with spatial collimation by for example intensity modulated radiotherapy (IMRT) or recently by the use of proton therapy or carbon ion therapy gives the potential for an increased dose to the tumour and with it a reduction in damage to surrounding normal tissues, thereby improving the quality of life of the patient (reviewed in (Bhide and Nutting 2010)).

In the United Kingdom conventional radiotherapy is generally delivered using a megavoltage linear accelerator to deliver high energy X-rays to the region of the body containing the tumour. Radiation dose is measured in grays (Gy) where 1 Gy = 1 J/kg. The dose necessary to kill a tumour is dependent upon the tumour type, stage and location, and ranges from a total dose of 20 – 80 Gy. For example leukaemias and lymphomas are generally very radiosensitive although difficult to treat because of the diffuse nature of the cancer

throughout the body; however, melanomas and renal cell carcinomas are very radioresistant. The total dose to a tissue must be closely regulated as too low a dose will not kill tumour cells and too high a dose, below that which would induce cytotoxicity, can induce further tumour growth within normal tissue through the induction of mutations. The dose delivery plan is always calculated on a case by case basis. Treatment can be carried out over many weeks using fractionated doses of ~2 Gy per day, five days a week, although hyperfractionation (Continuous Hyperfractionated Accelerated Radiotherapy, CHART) is also successful for lung cancer where three low doses are given a day (Saunders *et al.* 1999). Fractionation is important as it allows damaged normal cells to recover and dormant radioresistant tumour cells to become more radiosensitive as they start to replicate again or become re-oxygenated. The five R's of radiobiology (repair, reassortment, repopulation, reoxygenation and radiosensitivity) are mechanisms which are important in determining a response to fractionated radiotherapy (Steel *et al.* 1989). Radiotherapy can be extremely successful and constant advances in the treatment are being made, either in combination therapies (Begg *et al.* 2011), through changes in fractionation scheduling or in the types of radiation used (Bhide and Nutting 2010). However, successful radiotherapy may be limited by tumour oxygen tensions present in the tumour.

1.3.1 Tumour hypoxia

Success of radiotherapy is very dependent upon the concentration of oxygen in a tumour (Gray *et al.* 1953). These regions of a tumour are very problematic to effective therapy (Harrison and Blackwell 2004; Harrison *et al.* 2002); indeed patients displaying highly hypoxic tumours have a much lower life expectancy than those with well oxygenated tumours (Nordsmark *et al.* 2005).

It was shown over 60 years ago that tumours contain hypoxic regions (Thomlinson and Gray 1955) where chemo- and radiotherapy are much less effective. These regions still remain an important target for treatment. Solid tumours are very heterogeneous with

uncontrolled growth of blood vessels, many of which are blind-ended or have transiently restricted blood flow (Heldin *et al.* 2004). As distance is increased from these blood vessels (100 – 150 μm) O_2 concentration is decreased, leading to areas of mild (<1% v/v O_2) or severe (<0.01% O_2) hypoxia. These areas may be adjacent to necrotic tissue where cell death has occurred from O_2 and nutrient deprivation (Figure 1-1). Hypoxic regions of tumours contain dormant radioresistant cells which may be able to replicate and repopulate a tumour post-irradiation, if O_2 supply is returned following death of the adjoining well oxygenated radiosensitive cells (Kim and Tannock 2005).

Mechanistically, the radiosensitizing effect of O_2 can in part be explained through its extremely rapid reaction, within a few milliseconds, with radiation-induced DNA radicals (Eq. 1-1, § 1.4.4). These reactions are in competition, particularly in hypoxia, with repair of radiation-induced DNA radicals by cellular antioxidants like thiols (Eq. 1-2).

$$DNA^{\bullet} + O_2 \rightarrow DNA\text{-}OO^{\bullet} \rightarrow DNA\text{-}OOH + \text{strand breaks} \qquad (1\text{-}1)$$

$$DNA^{\bullet} + R\text{-}SH \rightarrow DNA + RS^{\bullet} \rightarrow \text{no strand breaks.} \qquad (1\text{-}2)$$

Apart from hypoxia affecting the chemistry of radiation-induced DNA damage, hypoxia can also affect the repair of radiation-induced DNA damage. For example levels of deoxyribonucleotides, the building blocks of DNA are depleted in hypoxia (Pires *et al.* 2010), (see §1.7.1). Expression or function of DNA repair proteins can alter, increasing the probability of radiation-induced DNA damage leading to genetic instabilities (Kumareswaran *et. al* 2012). In addition, tumour cells can have altered gene expression which confers resistance to radiotherapy (reviewed in Bristow *et. al* 2008). For example, hypoxia inducible factor (HIF-1) allows cells to adapt to changes in oxygen concentration through the expression of vascular endothelial growth factor (VEGF) and up-regulation of angiogenesis (see §1.6.3.2 for further discussion) which allows greater tumour growth. In addition, although hypoxia may induce wild type p53-dependent apoptosis, hypoxic tumours could

develop mutated p53 (Graeber *et. al* 1996), meaning that tumour cells could become radioresistant through inhibition of apoptosis.

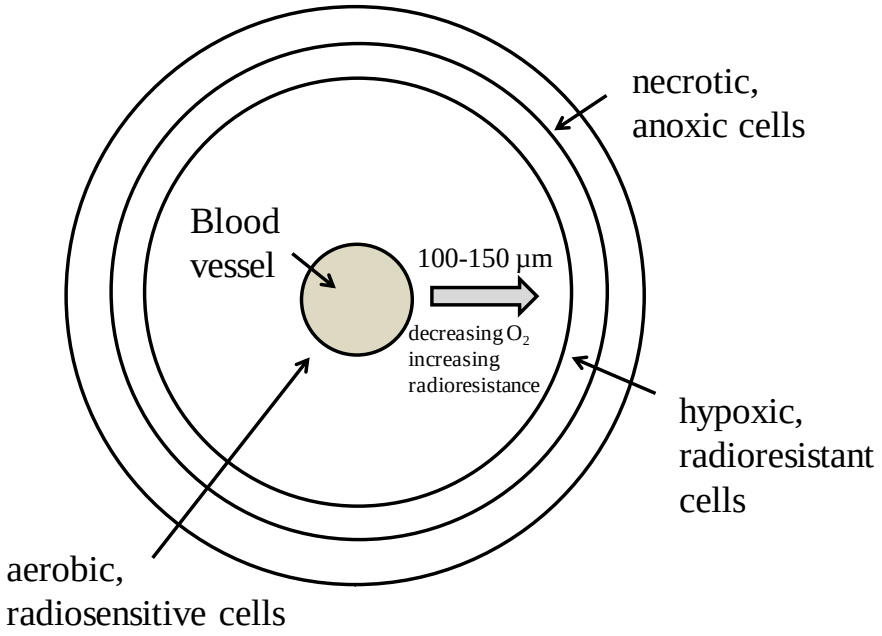

Figure 1-1 Diagrammatic representation of the formation of hypoxic cells distal from tumour blood vessels.

1.3.1.1 *Biomarkers of hypoxia*

Identification of biomarkers of hypoxia for radiotherapy would allow individualization of treatment protocols for patients. Such identification is necessary to further improve local cure and reduce treatment-based toxicity, which will vary between patients, dependent upon their tumour microenvironment and genetic make up (Yaromina *et al.* 2012). Hypoxia markers have been developed and have been used as predictive tests for radiotherapy response. For example, pimonidazole is a 2-nitroimidazole drug which is preferentially reduced in hypoxia and the resulting hydroxylamine (or the nitroso product) is able to react with protein thiols (Raleigh and Koch 1990) to form adducts which can be detected by immunohistochemistry, ELISA or flow cytometry. Pimonidazole is well tolerated in patients

and by using multiple punch biopsies, staining was observed in hypoxic tissue but not in necrotic tissue of primary cervical tumours 24 h after infusion (Varia *et al.* 1998). Further studies indicated its use as a hypoxia marker to select for patients specifically requiring hypoxia-modifying treatments (Kaanders *et al.* 2002). High osteopontin levels in plasma can also identify hypoxic tumours (Overgaard *et al.* 2005). Less invasive imaging methods for detecting hypoxic tumours include positron emission tomography (PET) imaging with ^{18}F-misonidazole as an example (Rischin *et al.* 2006). However, it has been reported recently that because the tumour microenvironment varies considerably following radiotherapy, that measurement of hypoxia biomarkers during the course of treatment may give better indications of radioresistant tumours compared to pre-treatment measurements (Yaromina *et al.* 2011; Yaromina *et al.* 2012).

1.3.2 Therapies against hypoxia including radiosensitizers

The difficulties of treating hypoxic tumours with radiotherapy can be partially overcome by the use of drugs. These can cause hypoxia-specific cell toxicity or can act through mimicking the oxygen effect or by increasing the oxygen concentration in a tumour for radiotherapy. Electron-affinic molecules are oxygen mimetics and react with free radicals generated during radiation and increase cytotoxicity under hypoxia. In particular nitro compounds were found to be very effective hypoxic cell radiosensitizers (Chapman *et al.* 1972). They work in part by reacting with free radicals generated at DNA bases following ionizing radiation (IR), inducing strand breaks in a similar manner to O_2 (Eq. 1-3) (Bamatraf *et al.* 1998; Wardman 2007).

$$DNA^{\bullet} + Ar\text{-}NO_2 \rightarrow DNA\text{-}ONO^{\bullet}\text{-}Ar \rightarrow DNA\text{-}ONOH\text{-}Ar + \text{strand breaks.} \qquad (1\text{-}3)$$

Electron affinity is directly correlated with rate of reduction and metabolism of a drug (Wardman and Clarke 1976; Olive 1979); however, early studies did not show that the most highly electron-affinic compounds were the best hypoxic radiosensitizers. Nitrofurans are

very electron affinic, but despite good results *in vitro* (Chapman *et al.* 1972), early studies with nitrofurans showed little success as radiosensitizers *in vivo* and they showed high toxicities (Durand and Olive 1981). 5-nitroimidazoles (e.g. metronidazole) also showed some early promise but 2-nitroimidazoles (e.g. misonidazole) were even better radiosensitizers (Brown 1981). However, success of misonidazole as a radiosensitizer was limited by its neurotoxicity. The 5-nitroimidazole nimorazole (Overgaard *et al.* 2005) and the 3-nitrotriazole, sanazole (Dobrowsky *et al.* 2007; Yamazaki *et al.* 2013) are now the main electron-affinic compounds being utilised clinically.

Radiosensitization can also occur through increasing tumour oxygenation. This can be achieved either through patients breathing hyperbaric oxygen (95%) or through the use of vasoactive compounds like nicotinamide. Pre-clinical studies into mice breathing hyperbaric oxygen containing 5% CO_2 (carbogen) during radiotherapy showed decreases in the tumour hypoxic fraction and radiosensitization, for example (Kjellen *et al.* 1991). The ARCON trial combined accelerated radiotherapy, carbogen breathing and nicotinamide, which together counteract tumour repopulation and hypoxia (Kaanders *et al.* 2002).

Drugs have also been developed which target and are cytotoxic to hypoxic cells compared to normoxic cells. For example, tirapazamine selectively kills hypoxic cells through mechanisms which include the induction of DNA strand breaks (Jones and Weinfeld 1996); however, no enhancement in cell toxicity was observed in combination with radiotherapy (Rischin *et al.* 2010).

1.3.3 Bioreductive drugs for cancer treatment

Nitro compounds can also show hypoxia-dependent cytotoxicity through enzymatic reduction of the drugs into toxic metabolites. This concept has been taken forward through the development of bioreductive pro-drugs (Denny *et al.* 1996; Rauth *et al.* 1998; Stratford and Workman 1998; Wilson and Hay 2011).

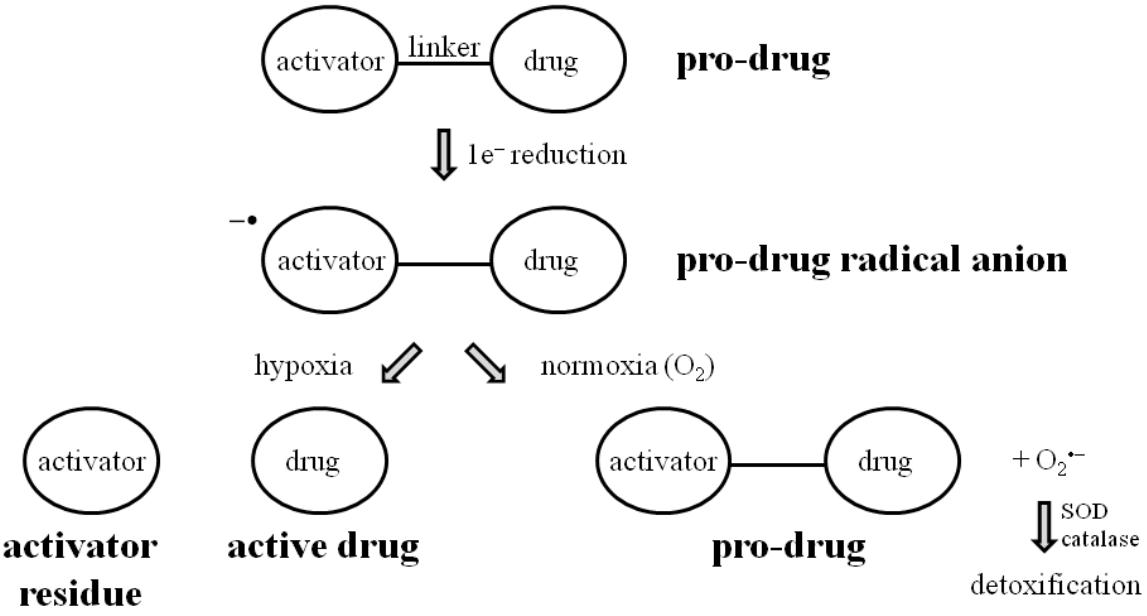

Figure 1-2 Schematic showing the concept for bioreductive release of an active drug from an inactive pro-drug in hypoxia (adapted from (Wardman 2007)).

Drugs containing different chemical groups including quinones, nitro groups, aromatic and aliphatic N-oxides and transition metals have been investigated for their ability to be reduced by intracellular enzymes. The subsequent release of the active drug from the one-electron reduced pro-drug depends upon sufficient activity of one-electron bioreductive enzymes within tumour tissue compared to normal tissue and also sufficiently low levels of oxygen (Figure 1-2) as well as the leaving group chemistry (Everett *et al.* 2002). Active drug levels are kept low in oxygenated and normal tissue through re-oxidation of the intermediate radical by O_2, producing $O_2^{\bullet-}$, a term known as futile redox cycling. This was first demonstrated using nitro compounds (Mason and Holtzman 1975) (Scheme 1-1). Superoxide production from the reaction will increase oxidative stress in oxygenated tissue. However, the tumour specificity of these drugs is potentially more important and cytotoxic, and the antioxidant enzymes superoxide dismutase and catalase are able to detoxify $O_2^{\bullet-}$.

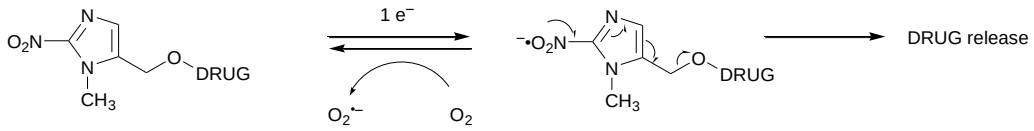

Scheme 1-1 Proposed mechanism for release of active drug from a reduced 2-nitroimidazole pro-drug with futile redox cycling.

Access of pro-drugs into hypoxic regions of tumours for bioreductive activation is potentially problematic, not only for pro-drug delivery, which is highly dependent upon blood vessels and diffusion, but also to achieve sufficient metabolism by cellular reductases like cytochrome P450s. Tumour regions containing oxygen at ~1-10 μM (~0.1 - 1%) are thought to be the most relevant for targeting and achieving cell death. Such regions are potentially able to re-oxygenate and re-populate a tumour after the more oxygenated cells are killed; this could lead to tumour re-growth. However, extreme hypoxia (O_2 <0.1 μM) can also be targeted, especially by 5-nitroquinoline compounds, where re-oxidation of the nitro radical is extremely O_2 sensitive (Siim *et al.* 1994). Release of an active drug in these severely hypoxic regions would then depend upon diffusion of the active drug to the adjoining less hypoxic but chemoresistant cells, to induce toxicity in all hypoxic tissue between 0.1 and 10 μM O_2.

These types of drugs could also be used as chemotherapeutic agents used in conjunction with radiotherapy, either activated by radiation to release a cytotoxin or reduced in hypoxia to release compounds which can radiosensitize during therapy.

1.4 Radiation-induced DNA damage

DNA damage, especially double strand breaks (DSB), is the most lethal of damage induced by radiation in cells and therefore it is a huge area of research, applied both to the study of the induction of damage and the subsequent repair or the resulting cell death which

follows. In contrast, if not repaired efficiently, DNA damage may lead to mutations in normal cells and be a forerunner to the onset of cancer.

1.4.1 DNA composition

DNA is comprised of 4 major bases; purines (adenine and guanine) and pyrimidines (cytosine and thymine) (Figure 1-3). Bases are linked to C-1′ of a deoxyribose sugar in DNA forming 2′-deoxynucleosides. Phosphate esters are formed with the C-5′ hydroxyl group of the sugar as shown in Figure 1-4, to form 2′-deoxynucleotides. These are the component blocks of DNA and are linked with neighbouring 2′-deoxynucleotides by the formation of further phosphate esters at the C-3′ hydroxyl groups.

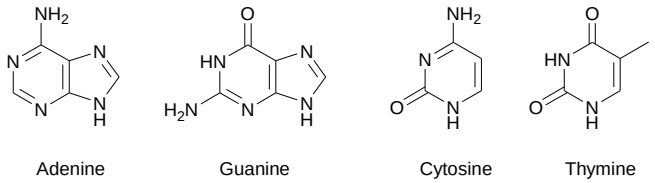

Figure 1-3 Structures of DNA bases.

Strands of 2′-deoxynucleotides are arranged in opposite directions with guanine pairing opposite cytosine and adenine pairing opposite thymine, all held together by hydrogen bonding. The strands are coiled into a double helix. Further secondary and tertiary structures involve compaction of DNA with the double helix coiling around histone proteins to form nucleosomes which are packaged into chromatin in the nucleus of a cell.

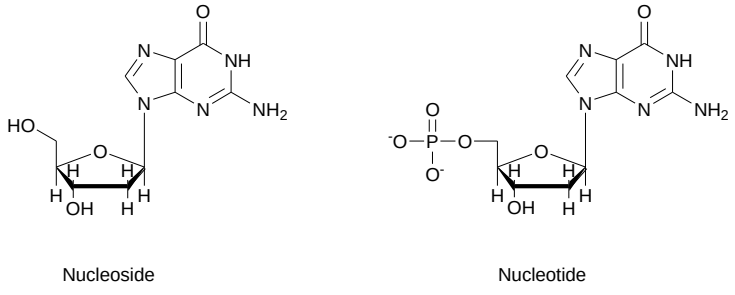

Figure 1-4 Structures of guanine nucleoside and nucleotide.

1.4.2 DNA damage from low LET ionizing radiation

Low linear energy transfer (LET) radiation like γ-rays and X-rays induce a variety of types of DNA damage including base damage, single strand breaks (SSB) and DSB (Figure 1-5) (von Sonntag 2006). In a mammalian cell it can be estimated that 1 Gy of low-LET γ-radiation induces ~100,000 ionizations in the nucleus with ~2000 occurring directly in the DNA. Approximately 1000 SSB and 40 DSB result, along with base modifications and DNA-protein cross-links. Of these ~0.2-0.8 are lethal effects and ~1 chromosome aberration can occur (Goodhead 1994; Ward 1994).

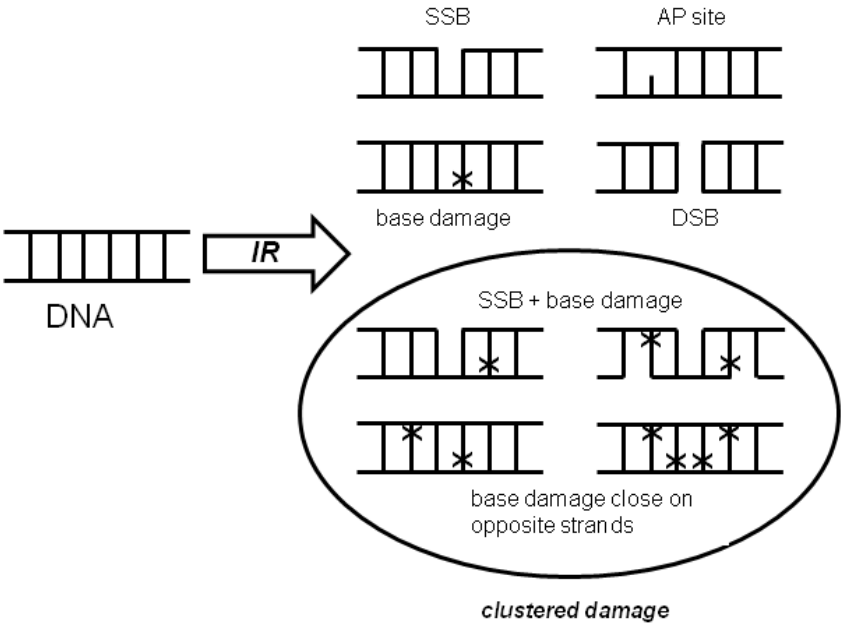

Figure 1-5 Some of the types of damage occurring to double-stranded DNA following ionizing radiation, including simple isolated lesions and simple and more complex clusters of lesions (adapted from (von Sonntag 2006; Eccles *et al.* 2011)).

Ionizing radiation (IR) produces tracks and spurs of high energy radicals which can react directly with the DNA. 1 Gy of low LET radiation may induce 1000 tracks in a cell nucleus and account for ~30-40% of damage by direct ionization of DNA (Goodhead 1994). Due to track structure, these nanometre regions may induce more than one DNA lesion within about 1 or 2 helical turns of the DNA in a single track and are termed clustered damage.

Clustered damage is more difficult to repair (Jenner *et al.* 1993; Eccles *et al.* 2011) and can lead to SSB, DSB, replication-induced DSB, mutations and cell death. These clusters are particularly prominent and complex with many more lesions in a cluster following high LET radiation (Goodhead 1994) (Figure 1-5).

DNA damage from IR can also occur as a result of DNA nucleotides reacting with hydroxyl radicals ($^{\bullet}OH$), hydrated electrons (e_{aq}^{-}) and hydrogen atoms ($H^{\bullet}$) produced from the ionization of water (Eq. 1-(4-7)), but only when they are generated within a few nanometres of the DNA, a distance short enough to avoid competitive reaction with other cellular biochemicals.

$$H_2O + IR \rightarrow H_2O^{\bullet+} + e^{-} \quad (1\text{-}4)$$

$$e^{-} + H_2O \rightarrow e_{aq}^{-} \quad (1\text{-}5)$$

$$H_2O^{\bullet+} + H_2O \rightarrow {}^{\bullet}OH + (H_3O^{+} = H^{+}) \quad (1\text{-}6)$$

$$H^{+} + e_{aq}^{-} \rightarrow H^{\bullet}. \quad (1\text{-}7)$$

This type of damage is termed an indirect effect and is more a feature of low LET radiation. $^{\bullet}OH$ is a strong oxidant and one of the most highly studied radicals which damage DNA. In cells (which are ~70% water) there are many other compounds in the cell which will also react with radiation-induced $^{\bullet}OH$ before they can diffuse to DNA. These reactions represent the so-called scavenger effect. Unless a $^{\bullet}OH$ is produced in close proximity to DNA it is unlikely to react with the DNA molecules as diffusion distances of $^{\bullet}OH$ are only ~4 nm, as verified in cells using radical scavengers (Roots and Okada 1975). When generated close enough, $^{\bullet}OH$ can form radical adducts with bases and abstract H-atoms from the deoxyribose backbone of DNA; these reactions can lead to base alterations, base release and strand breaks; mis-pairing of the bases and attenuation of DNA replication can also occur.

Therefore, the spatial distribution of DNA lesions resulting directly, or through indirect effects from IR, reflect the structure and energy of the radiation track. The types of damage range from simple isolated lesions to clusters of lesions, including complex DSB and

tandem lesions (Figure 1-5). The complexity of the damage reflects the cell's ability to repair the damage which will be discussed further in §1.5.

1.4.3 Hydroxyl radical-induced base modifications

Ionizing radiation induces DNA damage in particular by reaction of the bases with radiolytically formed •OH to form radical adducts. The reactions of •OH with nucleobases has been highly studied (see (Dizdaroglu and Jaruga 2012) for a recent review) and the major DNA modifications formed in oxygenated and non-oxygenated systems are well characterised. Variations are observed between naked DNA, chromatin and cellular DNA (Fuciarelli *et al.* 1990; Gajewski *et al.* 1990; Breen and Murphy 1995; Wiseman and Halliwell 1996; Pouget *et al.* 2002) (Table 1-1).

Nucleobases are oxidised by •OH more efficiently than the sugar residues in DNA. All of the bases react with •OH with similar efficiencies. Short-lived •OH-adducts are formed at a variety of positions within the molecules. Addition is favoured at C-4, C-8 and to a lesser extent at C-5 of the purines, and at C-5 and C-6 of the pyrimidines (von Sonntag 2006). These •OH adduct intermediates lead to stable structural changes, where products and yields vary depending upon the presence or absence of O_2 (Table 1, Figure 1-6), as discussed further in Chapter 3.

The chemistry associated with the pyrimidines is well documented and the majority of products arising from •OH reacting with free pyrimidines are dimers, glycols and hydrates. Thymine glycol is one of the most studied radiation-induced products in cellular DNA. The purine guanine is the most easily oxidized of the bases and 8-oxo-7,8-dihydroguanine (8oxoG) is the most studied product from guanine in oxygenated DNA. This product not only arises from reactions with •OH (§3.2) but could also form through electron transfer reactions from guanine to neighbouring pyrimidine peroxyl radicals or through the formation of tandem lesions with adjacent pyrimidine peroxyl radicals (Bergeron *et. al* 2010). Notably, the presence of 8oxoG (including the enol form, 8-hydroxyguanine) in plasma and urine is used

as a marker for oxidative stress and as a predictor of disease (Wu *et al.* 2004; Valavanidis *et al.* 2009).

	Naked DNA [a] nmol/J		**Chromatin** [b] nmol/J		**Cells** [c] lesions/ 10^9 bases/Gy
Base lesion	**N_2O**	**N_2O/O_2**	**N_2O**	**N_2O/O_2**	**Air**
thymine glycols	10.2	43.4	0.094	0.4	97
5-hydroxymethyluracil	n.d.	n.d.	0.064	0.052	29
cytosine glycols	10.7	25.6	0.95	2.3	n.d.
8oxoG	16.2	46.7	1.35	8.05	20
FaPyG	12.4	3.6	1.81	1.81	39
8oxoA	5.3	15.8	0.8	3.5	3
FaPyA	8.7	5.9	0.96	1.02	5

Table 1-1 γ-Radiation yields of some of the major base lesions isolated from DNA under anaerobic or aerobic conditions. data referenced from a- (Fuciarelli *et al.* 1990); b- (Gajewski *et al.* 1990); c- THP-1 malignant monocytic cells, data referenced from (Pouget *et al.* 2002). Structures of the base lesions are shown in Figure 1-6.

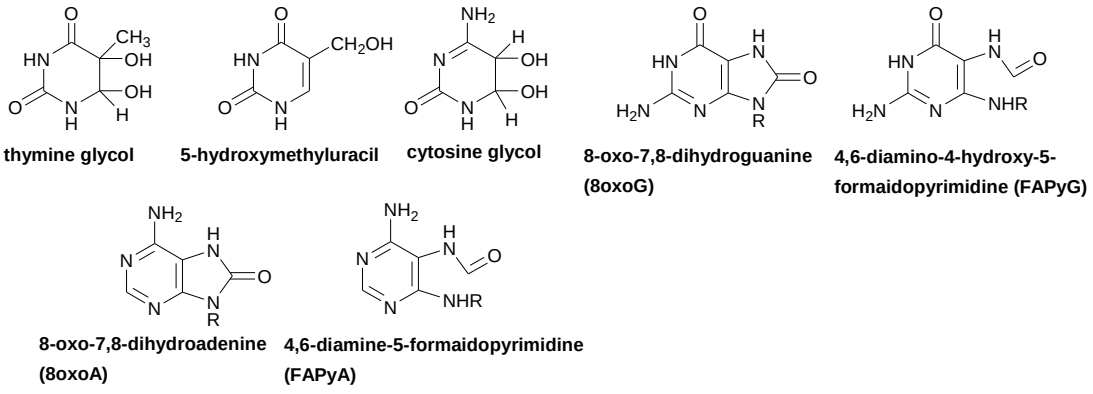

Figure 1-6 Structures of the most common base products observed following oxidation of DNA by •OH in aerated or non-aerated systems.

1.4.4 Induction of strand breaks from reactions of •OH with bases and sugars

Single strand breaks (SSB), which are usually non-lethal, can be formed by the direct reaction of •OH with the sugar moiety in DNA, a reaction which accounts for in the region of

>20% of ˙OH radicals, and may be even lower for pyrimidine nucleotides (von Sonntag 1987). However, not all direct reactions of ˙OH with sugars lead to strand breaks. ˙OH is thought to abstract H-atoms from the carbon atoms of the deoxyribose sugar dependent upon solvent accessibility, with 5′ H-atoms being easiest to abstract, followed by 4′ and then 3′, 2′ and 1′ being abstracted with similar lower efficiencies (Balasubramanian *et al.* 1998). It is thought that in DNA in the absence of O_2, SSB formation is mainly due to H-atom abstraction from C-4′ of the sugar, followed by in the majority, cleavage of the neighboring C-3′ phosphate group. Further hydration and oxidation reactions can then lead to base and nucleoside release by cleavage of the C-5′ and C-1′ bonds, leaving a modified sugar on the remaining DNA strand (Dizdaroglu and Sonntag 1975; Miaskiewicz and Osman 1994; Dizdaroglu and Jaruga 2012) (Scheme 1-2).

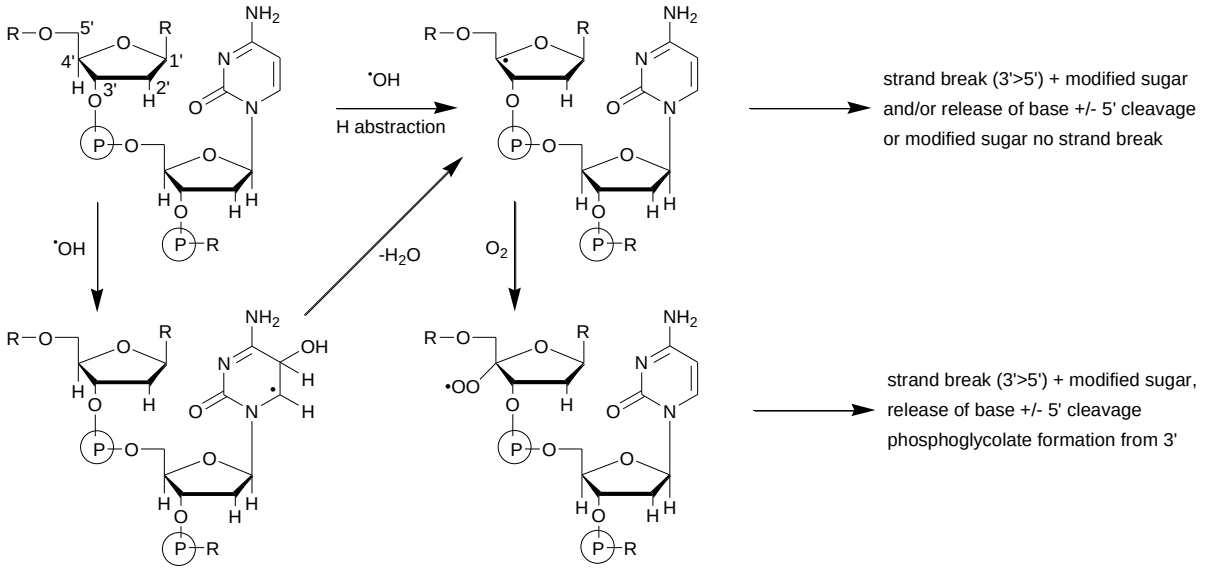

Scheme 1-2 Simplified mechanisms for the formation of SSB following ˙OH-induced H-atom abstraction, or base radical-induced H atom abstraction from C-4′

In oxygenated systems, O_2 can react with the C-4′ radical to form a long-lived peroxyl radical which can also induce a SSB with the formation of 3′-phosphoglycolate, and base release (Scheme 1-2) (von Sonntag 2006; Breen and Murphy 2012). Sugar radicals could also be

generated through the ability of •OH-induced base radicals to abstract a H-atom from the adjacent sugar (Jones and O'Neill 1991) which could then lead to a SSB as shown in Scheme 1-2.

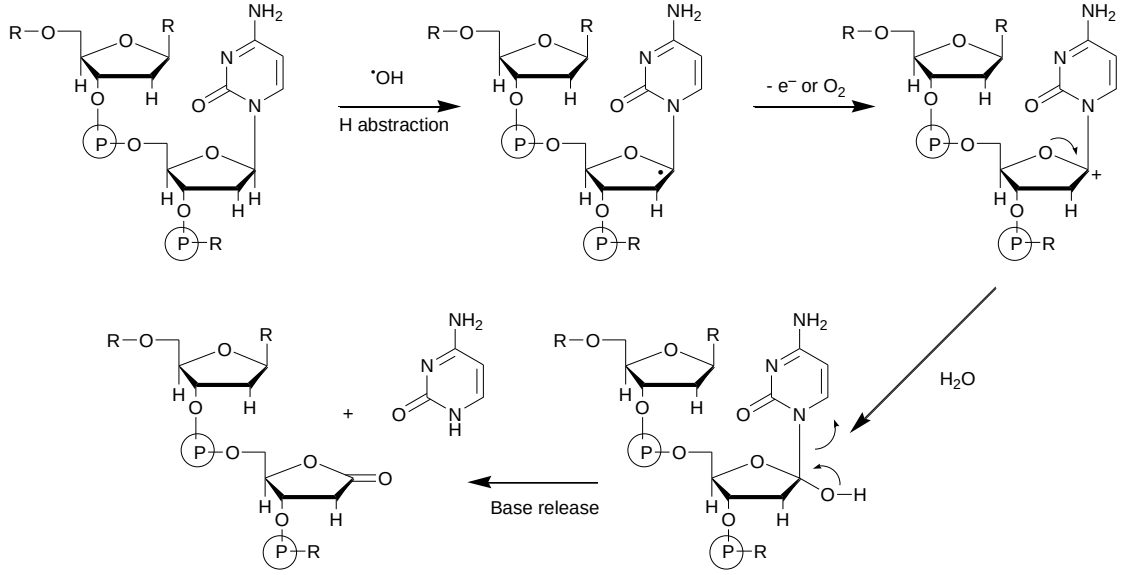

Scheme 1-3 Mechanism for the formation of a radiation-induced AP site.

Hydroxyl radical induced H-atom abstraction from C-1′ does not create SSB directly; however, oxidation of the deoxyribose radical can induce the release of an unaltered base, forming an apurinic/apyrimidic (AP) site e.g. 2-deoxyribonolactone (Scheme 1-3). Cleavage of the sugar-phosphate backbone does not occur except in mild alkaline conditions or through the actions of endonucleases to result in a SSB. Post-irradiation base release can also occur but the mechanisms involved are still largely unknown (von Sonntag 2006).

Radiation-induced •OH react mostly with the bases in DNA, but this does not in the main create strand breaks, except following repair processes. However, in the presence of O_2 SSB may occur through further radical reactions. Oxygen is a very efficient radiosensitizer through in part its rapid reaction with base-•OH adducts (~10^9 M^{-1} s^{-1} (Willson 1970)). Long-lived peroxyl radicals are formed which may interact with the adjoining sugar in the DNA strand, and abstract an H-atom forming a SSB and a modified base on the remaining nucleotide (Scheme 1-4). This mechanism for the formation of SSB is thought to be far less

important, if involved at all, for purine polyribose nucleotides compared to pyrimidine polyribose nucleotides (Jones and O'Neill 1990; Jones and O'Neill 1991), although this may not be the case in DNA. In similar mechanisms, nitroarenes can radiosensitize through interactions between the nitro group and the base radical forming a nitroxyl radical adduct which can abstract a proton from the adjoining sugar (Bamatraf *et al.* 1998; Wardman 2007).

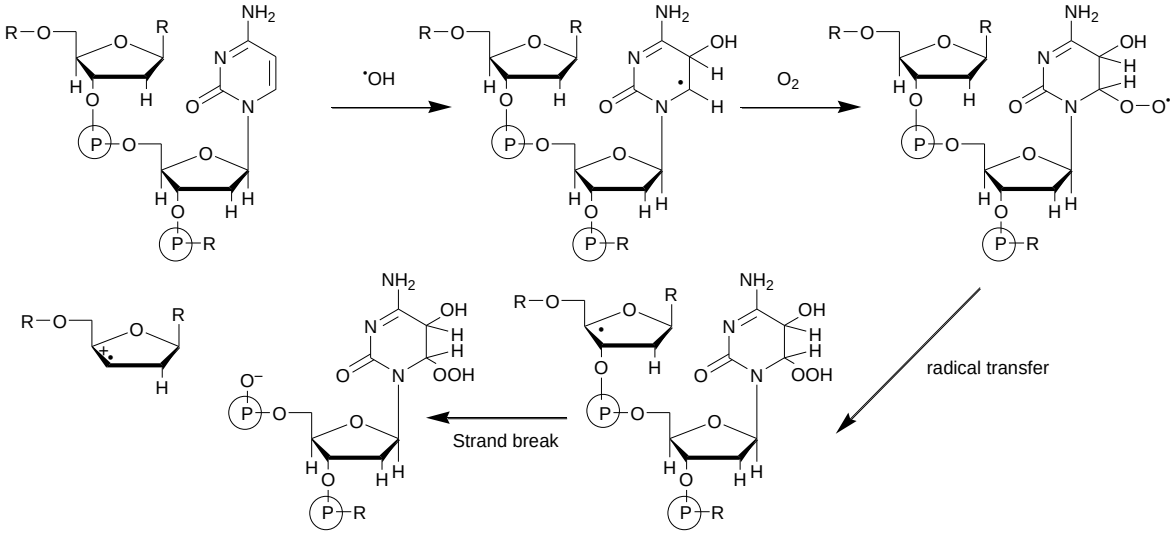

Scheme 1-4 Mechanism for the formation of •OH-induced DNA strand breaks in the presence of oxygen (adapted from (Wardman 2007)).

1.5 DNA repair

Radiation-induced DNA damage includes the formation of damaged bases, AP sites, SSB, DSB and combinations of all of them (Figure 1-5). Mechanisms occur which can repair the DNA with different fidelities. Inaccurate or incomplete repair can lead to mutations or cell death and cells which have defects in their ability to repair can be highly radiosensitive. Understanding the types of DNA damage including clustered damage sites and the DNA repair pathways involved to process these different damage sites is therefore paramount to developing new anti-cancer therapies (reviewed in (Aziz *et al.* 2011)), as many cancer cells have such defects. Increasing tumour cell radiosensitivity through enhancing the persistence of various types of DNA damage is an area of research under active investigation.

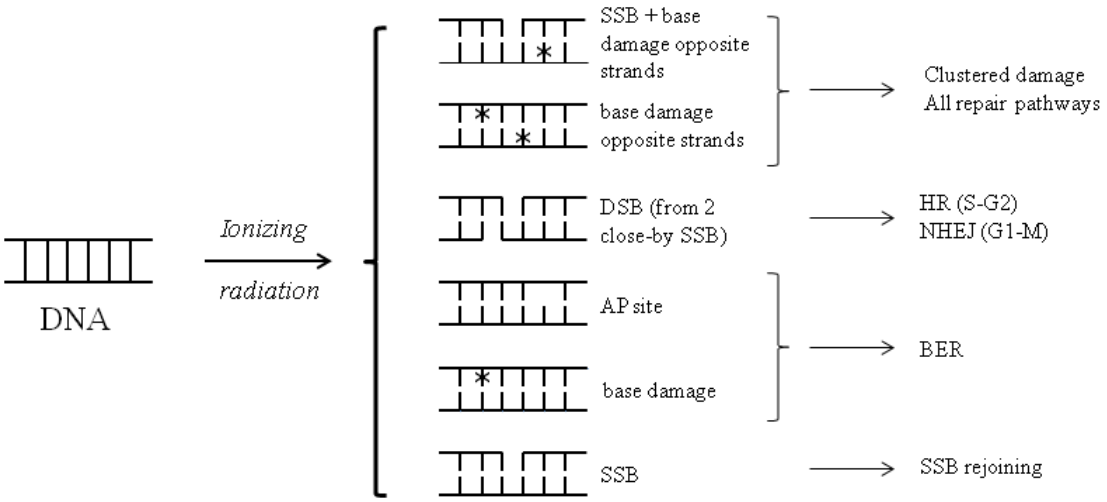

Figure 1-7 Some of the different types of DNA bistranded clustered damage sites and isolated lesions which can occur following ionizing radiation and the DNA repair pathways common to the different types of damage. Successful repair retains DNA integrity and cell survival, unsuccessful repair or mis-repair can lead to e.g. cell death, mutations and cancer. (HR, homologous recombination; NHEJ, non-homologous end joining; BER, base excision repair).

The mechanisms by which DNA damage is repaired, a process termed the DNA damage response (DDR), is highly complex and involves many different proteins. The pathways which are initially utilised during DDR depend upon the type and severity of the damage induced, and the position the cell is within the cell cycle when the damage is induced (Figure 1-7). The area of DNA repair is a huge topic, which is constantly evolving and for brevity only simple descriptions of the most common processes which occur in mammalian cells are described below.

1.5.1 Base damage and single strand breaks

Base damage and SSB are major lesions that occur endogenously throughout the daily insult of oxidative stress and are also common following exposure of cells to IR. Isolated lesions are repaired within less than 1 h (Ward 1988), whereas clusters of base lesions are repaired less efficiently and may involve additional repair pathways (Eccles *et al.* 2011).

The majority of the enzymes involved in *base excision repair (BER)* are also involved in the repair of AP sites and SSB. In mammalian cells, the process of BER detects and removes a single modified base from damaged DNA and then inserts a nucleotide followed by ligation (short patch). If the strand ends are not appropriate for ligation (3′-OH and 5′-phosphate), then repair proceeds by long patch repair (reviewed in (Robertson *et al.* 2009)). Long patch repair involves incorporation of up to six nucleotides and the removal of the resulting flap by FEN1 followed by ligation. Short patch repair is the most commonly used pathway and for simplicity only this process is described here. BER is initiated by chemical or radiation-induced alteration to a base; this alteration is recognized by a DNA glycosylase specific to the particular lesion (e.g OGG1 and NEIL 1 detect FaPyG and 8oxoG, and Nth removes oxidised pyrimidines in mammals). The damaged base is excised by cleaving the N-glycosidic bond, forming an AP site. Cleavage of the sugar-phosphate phosphodiester bond and removal of the remainder of the nucleotide utilises an AP-endonuclease (e.g. APEX 1) forming a single nucleotide gap (SSB). DNA polymerase β removes the 2′-deoxyribose phosphate and incorporates the appropriate single nucleotide into the gap followed by ligation utilising DNA ligase III and X-ray repair cross complementing 1 (XRCC1) to join the nick. Simple SSB, where base damage is not present, are repaired following the same ligation step following PARP recognition (termed SSB repair).

Nucleotide excision repair (NER) removes in particular bulky pyridine dimers which cause a distortion in the DNA helix and can result from UV damage of DNA (Nouspikel 2009). Unlike BER, a common set of enzymes recognize the distortion and remove a short sequence of oligonucleotides around the distortion. The gap is then filled by polymerases. NER is generally not utilised by the cell machinery to repair IR-induced damage.

1.5.2 Double strand breaks

Double strand breaks are the most deleterious type of DNA damage that is induced by IR. The majority of DSB generated by radiation doses relevant to radiotherapy using low LET

are rejoined within 30-60 min (Gulston *et al.* 2004), but ~20% breaks remain after this time and even at >24 h, as they are more difficult to repair (Schmid *et al.* 2010; Reynolds *et al.* 2012). These longer lifetime breaks may contribute to cell death. Even a single DSB can lead to chromosomal instability and death. During repair of DSB, the process of cell division is delayed or stopped. Additionally, cell cycle checkpoints between the G1/S (P53, Chk 2) and G2/M (Chk 1) phases of the cell cycle (Figure 1-8) are activated by phosphorylation by ataxia telangiectasia mutated (ATM) and ataxia telangiectasia related (ATR) proteins respectively, stopping progression through the cell cycle. There are two major pathways involved in DSB repair which are generally followed; dependent upon the position of the cell in the cell cycle, but some cross-talk is thought to occur between the two pathways; non-homologous end joining and homologous recombination.

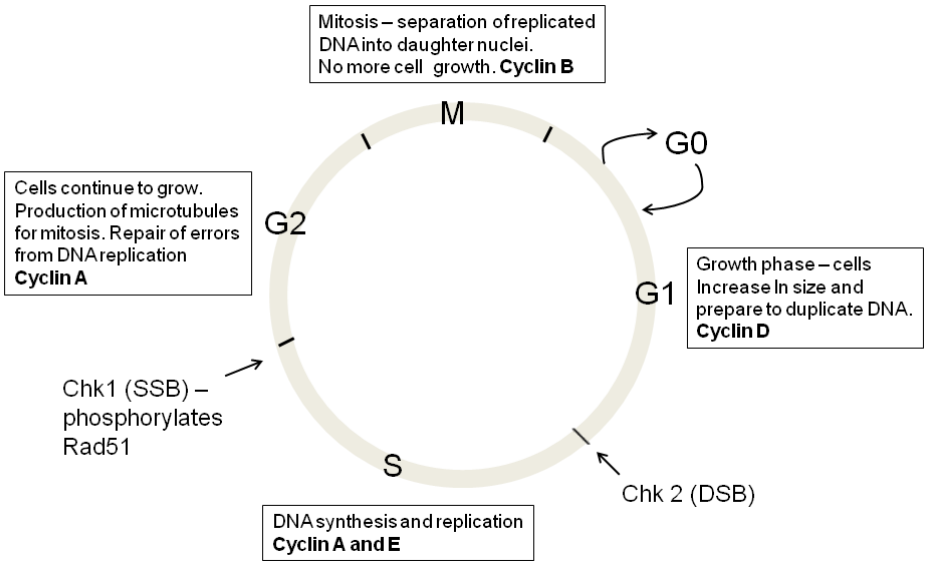

Figure 1-8 Schematic to show the cell cycle and involvement of cyclins and checkpoint protein.

Non-homologous end joining (NHEJ) is the major repair pathway in mammalian cells (reviewed in (Mladenov and Iliakis 2011)) and active throughout the cell cycle from G0 to M phases but can be error prone, for example through the insertion of incorrect bases. Although

very complex, the process can be described in simple terms. DSB termini are recognized and encircled by Ku70/80 heterodimers and then ATM-mediated phosphorylated DNA-PKcs bind, but only to those which are complex DSB (Peddi *et al.* 2008; Reynolds *et al.* 2012). This association allows the ends of the DSB to be held together prior to ligation. In the classical pathway, DNA polymerases can fill in the gaps between compatible ends with oligonucleotides. When DNA-PKcs is present to allow additional processing of complex DSB prior to ligation, lengths of the DNA strands close to the break are removed by the endonuclease Artemis, leaving 3′ and 5′ overhangs on adjacent strands and other lesions close to the ends may be removed. Polymerases fill in the gaps using the microhomology between the two strands. For all types of DSB processed, the complex of DNA ligase IV/XRCC4/XLF, hold the blunt ends of the DNA together for re-joining.

Homologous recombination (HR) in mammalian cells involves a complex assortment of proteins (reviewed in (Helleday 2003)) and it is slower but less likely to result in repair errors, including the insertion of incorrect bases, than NHEJ. HR only occurs during S and G2 phases of the cell cycle, as the process requires an identical DNA sequence on a sister chromatid to repair a damaged strand of DNA. In a simplified model involving an ATM-dependent process, the MRN complex (MRE11, RAD50, Nbs1) binds to the two ends of the break and processes the DNA by end resection to form a 3′ single stranded overhang. The overhang is recognised by replication protein A (RPA), a single strand binding protein; before ATR activated Chk1 (checkpoint protein 1) slows progression through S-phase and activates RAD51 and RAD52 to associate with the overhang in exchange with RPA and hold the damaged and undamaged sister chromatids together. Sister chromatid exchange then occurs through the action of BRACA1, BRACA2, RAD52 and RAD54, before polymerases join the missing nucleotides and ligation occurs to repair the break.

Following IR damage, there is an increased demand for HR from lesions occurring within the replication fork and from collapsed replication forks following SSB. Apart from

those DSB which arise directly from IR or through endogenous processes, some can also arise through *stalling of a replication fork or fork collapse*. Although the majority of IR-induced SSB are generally repaired in < 1 h (Dikomey and Franzke 1986) when base modifications occur close (within one to two turns of the DNA helix) to sites of SSB in clusters of damage (Figure 1-5), repair can be difficult (Eccles *et al.* 2011). These clustered damage sites account for ~30% of damage induced by low LET radiation (Nikjoo *et al.* 1998) and ~90% from high LET radiation (Goodhead 1994) and can be simple or complex. Complex damage comprises different lesions including SSB and DSB and is most noticeable following high LET radiation. A major feature of clustered damage is their difficulty to repair (Jenner *et al.* 1993; Eccles *et al.* 2011). If lesions or SSB within a clustered site are not repaired before they encounter a replication fork, they may develop into replication-induced DSB (Figure 1-9) (Saleh-Gohari *et al.* 2005; Harper *et al.* 2010) and lead to enhanced levels of mutations (Eccles *et al.* 2011).

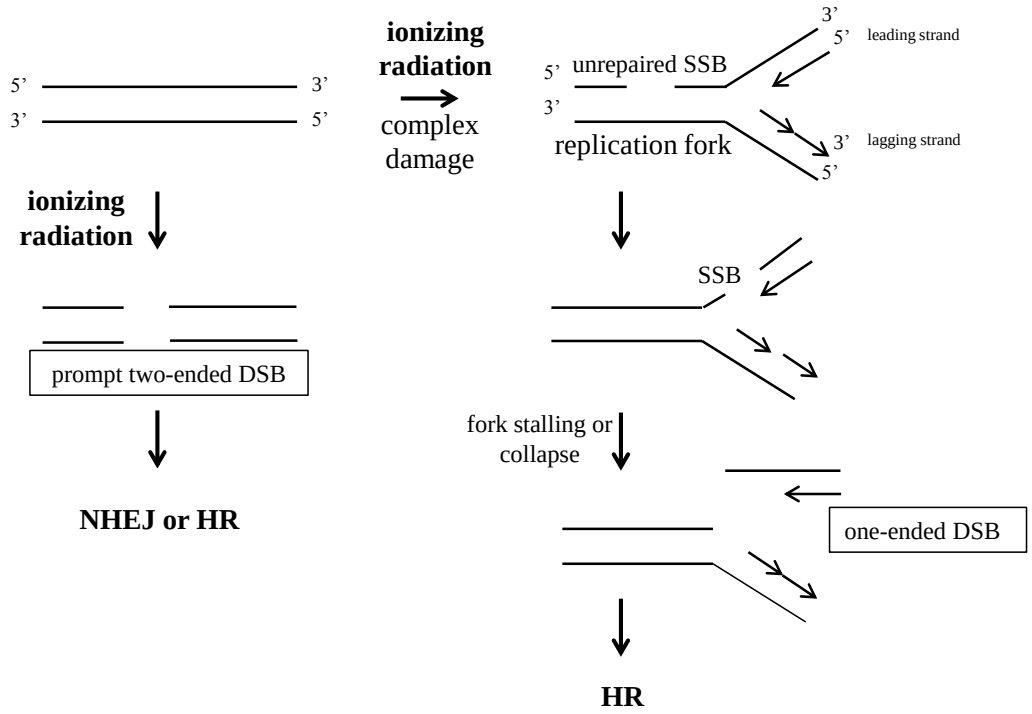

Figure 1-9 Schematic to show the formation of radiation-induced prompt two-ended and replication-induced one-ended double strand breaks in DNA.

The synthesis and replication of double stranded DNA occurs at particular regions of the DNA in replication bubbles. Within these replication bubbles there are regions of single-stranded DNA termed replication forks, where DNA is synthesised in a 5′-3′ direction (Figure 1-9) on the leading strand by polymerase ε. The opposite lagging strand utilises polymerase α and δ and a series of smaller regions of DNA termed Okasaki fragments to ensure 5′-3′ synthesis. Replication forks continually move down the parental DNA during DNA replication.

Clustered lesions created close to a replication fork are difficult to repair and may induce stalled or collapsed replication forks and one-ended DSB (Figure 1-9). HR involving RAD51 is then predominately required for the repair process (Jeggo *et al.* 2011; Jones and Petermann 2012). The DNA binding protein RPA binds to the single-stranded region of the collapsed replication fork and activates ATR to phosphorylate Chk 1. This slows progression through S-phase allowing time for the cell to restart, repair or arrest the replication fork.

1.5.3 Markers for cellular double strand break formation and repair

Even one DSB can lead to chromosomal instability and death, and therefore the ability to measure the extent of IR-induced DSB in cells is a strong indicator of radiosensitivity. The ability of a cell to repair these breaks efficiently is also an important factor to understand. Following damage the cell responds by targeting the MRN complex to the damaged site (Lavin 2004; Borde and Cobb 2009) which then activates the phosphorylation of the kinases ATM, ATR and DNA PKcs. These kinases are involved in the phosphorylation and localization of H2AX and 53BP1 to the sites of DSB, which then provide a scaffold structure for DNA repair. It is these scaffold proteins which are commonly identified as markers of DSB. Antibodies against the phosphorylated and non-phosphorylated forms of the proteins have been developed which can be used for Western blotting, flow cytometry and immunofluorescence and can be used as indicators for the formation and repair of DSB.

H2AX is a gene which encodes for a histone H2A family member present in association with DNA in the cell nucleus. Within several minutes following DNA damage by IR the protein becomes phosphorylated by the action of cellular kinases including ATM and DNA PKcs forming γH2AX (Stiff *et al.* 2004). Hundreds to thousands of H2AX are phosphorylated, up to mega base pairs from the actual break, following the formation of DSB (or replication-induced DSB). Following sparsely ionizing radiation, these sites of γH2AX formation can be detected by immunofluorescence microscopy as discrete foci within the cell nucleus, through the use of fluorophores conjugated to antibodies against the phosphorylated protein. Numbers of foci generally reach a maximum at about 30 min following IR (Rogakou *et al.* 1998) and are proportional to the numbers of DSB present (Rogakou *et al.* 1998; Rothkamm and Löbrich 2003) but numbers are only qualitative markers of the numbers of DSB, as many are rejoined before the level of γH2AX foci reaches a maximum (Reynolds *et al.* 2012). The numbers of foci are reduced as DSB are repaired (Leatherbarrow *et al.* 2006; Lobrich *et al.* 2010). Following DSB repair, dephosphorylation occurs and foci are generally no longer visible. Phosphorylation of H2AX by ATR also occurs at single stranded regions of DNA associated with stalled replication forks (Figure 1-9) and therefore γH2AX can also mark these one-ended DSB (Lobrich *et al.* 2010; Jones and Petermann 2012).

53BP1 (human tumour suppressor P53 binding protein 1) concentrates at, and binds to, methylated histone H3 and H4 residues within a few minutes of IR-induced DNA damage, in response to binding of the MRN complex to the break. Following localization, 53BP1 is phosphorylated and in a complex mechanism, it mediates checkpoint activation and repair through the Chk proteins (Lee *et al.* 2009; Harding and Bristow 2012). Effector proteins like p53 are then activated and direct the cell to repair, induce cell cycle arrest or cause cell death through apoptosis or senescence (FitzGerald *et al.* 2009).

The numbers of 53BP1 foci peak 30 min following irradiation and are proportional to the number of DSB (Schultz *et al.* 2000). Numbers of foci per cell are reduced as DNA repair

progresses (Schultz *et al.* 2000) and in most cases, 53BP1 foci co-localise with γH2AX where the level of co-localisation is dependent upon the irradiation dose and time following irradiation (Marková *et al.* 2007).

Antibodies against *RAD51* can also be used as markers of DSB which undergo repair by HR in S and G2 phases of the cell cycle. RAD51 is involved in strand-pairing of the homologous chromatids for repair by HR, by forming DNA-protein filaments. It binds to RPA which itself binds to the single stranded regions of resected DNA next to the DSB (§1.5.2).

HR is also involved in repair of replication-induced one-ended DSB which occur through the collapse of replication forks (Figure 1-9). As in HR, RAD51 binds to RPA bound to the single stranded region of the DNA and is then involved in donor duplex (D-loop) formation and reformation of a replication fork (Jones and Petermann 2012). Observation of RAD51 foci may therefore also identify the presence of these types of breaks in addition to those DSB generated directly by IR.

1.5.4 Markers of the cell cycle and DNA replication

Cells progress through their cell cycle with the length of time in each phase dependent upon the cell type. Cyclin proteins control progression through the cell cycle (Figure 1-8) by activation of cyclin dependent kinases (cdk). Cyclin A in particular is involved in initiating and completing cell replication through binding to cdk2 (Pagano *et al.* 1992). Cyclin A levels decrease as cells enter mitosis and the levels are re-established as cells re-enter S-phase. Antibodies against cyclin A can therefore be used as markers for cells in a population undergoing replication in S and G2 phases of the cell cycle.

Another marker for S-phase cells is 5-bromo-2′-deoxyuridine (BrdU) which is a synthetic analogue of thymidine. Cells can be pulse labelled with BrdU (15-30 min) where it is incorporated into S-phase genomic DNA during its replication. Antibodies against BrdU are then used to mark S phase cells containing incorporated BrdU in the DNA. BrdU is

particularly useful in flow cytometry studies to measure the percentage of cells in S-phase, but it can also be used in immunohistochemistry studies (e.g. described in (Harper *et al.* 2010)).

1.6 Nitric oxide

Nitric oxide ($^{\bullet}$NO) gained significant and extensive interest in the research world following its identification over 20 years ago as endothelium derived relaxing factor (Palmer *et al.* 1987). However, it has many other biological effects which are dependent upon its microenvironment, concentration and lifetime (Sonveaux *et al.* 2009). In addition to its role as a vasodilator, it has roles in inflammation, thrombosis, immunity and neurotransmission but has also been shown to be implicated in cancer, diabetes, Parkinson's disease and Alzheimer's disease (Ignarro 2000).

1.6.1 Biological reactivity of nitric oxide

$^{\bullet}$NO is an endogenous, small gaseous molecule, which exists as a free radical with a single unpaired electron. It is a colourless gas at room temperature and has a solubility of ~2 mmol dm^{-3} (at 1 atm partial pressure, 25 °C) in water with solubility 6-7 times higher in lipid membranes than in water (Koppenol 1998) and is therefore able to enter cell membranes effectively. Unlike other free radicals it has a low reduction potential ($E°(^{\bullet}NO/^{3}NO^{-}) = -0.8$ V (Bartberger *et al.* 2002) and is not a good oxidant, cannot abstract H-atoms, nor react with unsaturated bonds unlike $^{\bullet}$OH. However, due to its unpaired electron, it reacts extremely rapidly with other radical species and as such has antioxidant properties, inhibiting lipid peroxidation for example, by reacting with lipid peroxyl radicals ($LOO^{\bullet}$) (Eq. 1-8) (Hummel *et al.* 2005).

$$^{\bullet}NO + LOO^{\bullet} \rightarrow LOONO. \qquad (1\text{-}8)$$

The molecule has a strong affinity for Fe^{2+} ions and readily binds to haem-containing proteins (e.g cytochrome P450, oxyhaemoglobin and soluble guanylate cyclase (Ignarro 2000)). The

physiological concentration of $^{\bullet}NO$ in normal tissue is thought to range from <100 pM to ~5 nM but it is a very difficult compound to quantitate (Hall and Garthwaite 2009). The half-life of $^{\bullet}NO$ in normoxic tissue is estimated to be ~0.1 s (Thomas *et al.* 2001) where lifetime is proportional to 1/[$^{\bullet}NO$], as reaction of $^{\bullet}NO$ with O_2 is second order in $^{\bullet}NO$ (Wink *et al.* 1993). Lack of availability of oxyhemoglobin, O_2 or $O_2^{\bullet-}$ for reaction with $^{\bullet}NO$ can increase the lifetime and diffusion distance of $^{\bullet}NO$ to hundreds of microns. Reactivity of $^{\bullet}NO$ is also enhanced and altered by reaction with O_2 or $O_2^{\bullet-}$, converting it to highly reactive nitrogen species (RNOS) including nitrogen dioxide ($^{\bullet}NO_2$), dinitrogen trioxide (N_2O_3) and peroxynitrite ($ONOO^-$) (Eq. 1-(9-12)).

$$2\ ^{\bullet}NO + O_2 \rightarrow 2\ ^{\bullet}NO_2 \rightarrow N_2O_4 \qquad (1\text{-}9)$$

$$^{\bullet}NO_2 + {}^{\bullet}NO \leftrightharpoons N_2O_3 \qquad (1\text{-}10)$$

$$N_2O_3 + H_2O \rightarrow 2NO_2^- + 2H^+ \qquad (1\text{-}11)$$

$$O_2^{\bullet-} + {}^{\bullet}NO \rightarrow ONOO^-. \qquad (1\text{-}12)$$

In comparison to $^{\bullet}NO$, $^{\bullet}NO_2$ has a reduction potential of ($E°(NO_2^{\bullet}/NO_2^-)$ = 1.04 V (Stanbury 1989) and is a strong oxidant, and it is reactions with $^{\bullet}NO_2$ which are sometimes mistakenly attributed to $^{\bullet}NO$. Auto-oxidation of $^{\bullet}NO$ in tissues is therefore critical to the specific actions of the molecule.

Peroxynitrite, a product of the reaction between $^{\bullet}NO$ and $O_2^{\bullet-}$ (Eq. 1-12) is also highly reactive. Its reactivity is generally thought to involve a free-radical based mechanism (Lehnig 1999). At neutral pH (pK_a 6.8) it rapidly decomposes ($t_{½}$ = 1 s, pH 7.4, 37 °C (Beckman *et al.* 1990)), with ~30% of peroxynitrite forming the highly oxidising radicals, $^{\bullet}NO_2$ and $^{\bullet}OH$ through homolysis (Gerasimov and Lymar 1999; Hodges and Ingold 1999). Peroxynitrite also rapidly reacts with CO_2 (k = 5.8 x 10^4 mol^{-1} dm^3 s^{-1}) to form a transient nitrosoperoxocarboxylate adduct ($ONOOCO_2^-$) where ~35% decomposes into the highly oxidising radicals $^{\bullet}NO_2$ and $CO_3^{\bullet-}$ (Lymar and Hurst 1998; Bonini *et al.* 1999; Goldstein *et al.*

2001) (Eq. 1-(13-14)). Following the identification of this mechanism, reactions of $CO_3^{\bullet-}$ with biological molecules have been studied with interest.

$$ONOO^- + CO_2 \rightarrow ONOOCO_2^- \quad (1\text{-}13)$$

$$ONOOCO_2^- \rightarrow {}^{\bullet}NO_2 + CO_3^{\bullet-}. \quad (1\text{-}14)$$

1.6.2 Biological synthesis of nitric oxide

$^{\bullet}$NO is endogenously formed from the action of nitric oxide synthases (NOS) with L-arginine (Eq. 1-15). These reactions are dependent on NADPH and O_2 and also require tetrahydrobiopterin, flavin adenine dinucleotide (FAD) and flavin mononucleotide (FMN) as cofactors (Ignarro 2000).

$$\text{L-arginine} \rightarrow N^{\omega}\text{-hydroxy-L-arginine} \rightarrow \text{L-citrulline} + {}^{\bullet}NO + H_2O. \quad (1\text{-}15)$$

There are 3 major isoforms of NOS which regulate the biological effect of $^{\bullet}$NO in tissues, by controlling the location and concentration produced. Endothelial (eNOS) and neuronal NOS are constitutively activated and produce low concentrations of $^{\bullet}$NO for short periods of time, whereas inducible NOS (iNOS) can be activated by cytokines and can produce much higher concentrations of $^{\bullet}$NO for sustained periods of time (Sonveaux *et al.* 2009). For the sake of brevity, only the functions of eNOS and iNOS will be discussed further.

Endothelial NOS is a constitutive enzyme located in the endothelium of blood vessels at the smooth muscle interface. Activity is controlled through the release of free calcium ions from intracellular stores binding to calmodulin. Within seconds, $^{\bullet}$NO is produced at concentrations ranging from pM to nM for short periods of time (seconds to minutes). eNOS activity is particularly associated with regulating vasodilation. $^{\bullet}$NO can diffuse and stimulate soluble guanylate cyclase in the smooth muscle vascular cells, catalysing the formation of cyclic guanosine monophosphate (cGMP) from guanosine triphosphate to cause transient vascular relaxation (Ignarro 2000). eNOS can also be activated by a vascular endothelial growth factor (VEGF) stimulated pathway and can have a pro-angiogenic effect (Duda *et al.*

2004) and may be involved in tumour invasion. Hence eNOS expression has been correlated with poor prognosis in gastric cancer (Wang *et al.* 2005). Activation of eNOS is proposed to be particularly relevant in tumours a few days following radiotherapy, when angiogenesis can be very prevalent (Sonveaux *et al.* 2009). It is therefore a potentially important enzyme which warrants investigations into drug-induced inhibition, for preventing continued cancer growth, both pre- and post-radiotherapy.

Inducible NOS is of particular interest in the area of cancer research. Upon stimulation by cytokines, it can produce high (up to several micromolar) $^{\bullet}NO$ for sustained periods (hours to days) and is particularly associated with inflammation. Although produced by most cell types, it is particularly associated with macrophages. Release of $^{\bullet}NO$ from macrophages infiltrating irradiated tumours within a few hours of initial treatment can induce vasodilation which could aid subsequent radiosensitization (Sonveaux *et al.* 2009). Cytokine activation of iNOS (Jiang *et al.* 2010) and radiation-induced promoters of iNOS (Worthington *et al.* 2004) also show a radiosensitizing effect. High concentrations of $^{\bullet}NO$ produced by macrophage iNOS during inflammation can be sustained for days and be cytotoxic to cells (Sonveaux *et al.* 2009). However, if O_2 availability is reduced, as is seen in chronic inflammation, NOS activity is reduced (Singh *et al.* 2009) and production of $^{\bullet}NO$ can drop (apparent K_m = 130 µM O_2 (Stuehr *et al.* 2004)). Maintenance of these lower levels for sustained periods is potentially damaging to tissue. Nitrosative stress through secondary reactions of $^{\bullet}NO$ forming RNOS (Eq 1-(9-12)) can cause deamination (loss of $–NH_2$ groups) of nucleophiles, mutations, DNA strand breaks and nitrosothiol and nitrosamine formation; this can be associated with mutagenic and carcinogenic processes (Nguyen *et al.* 1992; Tannenbaum *et al.* 1994). Indeed many human malignant tumours express high levels of iNOS (reviewed in (Singh and Gupta 2011)) and poor prognosis has been correlated with iNOS expression (Ekmekcioglu *et al.* 2006; Glynn *et al.* 2010).

Despite much research into localization and activity of NOS enzymes, •NO itself is notoriously difficult to measure effectively in biological systems (Bryan and Grisham 2007), and therefore a difficult molecule to associate reliably with particular damaging processes.

1.6.3 Nitric oxide and cancer – a 'double-edged sword'

Nitric oxide can have pro- and anti-tumorogenic effects, dependent upon its concentration, lifetime and location (reviewed in (Fukumura *et al.* 2006)). Exposure of normal tissues to •NO can lead to angiogenesis, mutations and cancer. However, •NO-exposure to tumours can also inhibit tumour growth and enhance radiosensitization and chemosensitization. The diverse functions, reactivities and diffusibility of •NO, means that numerous normal and tumour tissue systems will be affected by the manipulation of •NO, and close consideration must therefore be placed on the pro- and anti-tumorogenic effects.

1.6.3.1 *DNA damage by reactive nitrogen species*

•NO is unreactive towards DNA in the absence of O_2 but damage can occur by reactive nitrogen species (RNOS) formed from •NO in aerobic tissue (Tannenbaum *et al.* 1994) and as a consequence •NO has been related to carcinogenesis (Nguyen *et al.* 1992). Primary amines (R-NH_2) common to cytosine, adenine and guanine are deaminated to R-OH/R=O on exposure to RNOS. Deamination has been reported to occur in bases, nucleotides, nucleosides and in calf thymus DNA (Wink *et al.* 1991; Nguyen *et al.* 1992; Caulfield *et al.* 1998; Suzuki *et al.* 2000; Suzuki *et al.* 2009). Reaction of RNOS with secondary amines (R_2-NH) in comparison, form N-nitroso derivatives (R_2-NNO) which can have mutagenic consequences by alkylating DNA (Tannenbaum *et al.* 1994). In addition, peroxynitrite (Eq. 1-12) can also induce DNA damage, for example forming 8-nitroguanine and 8oxoG modifications by reaction with guanine residues (Yermilov *et al.* 1995; Burney *et al.* 1999). •NO_2 (Eq. 1-9) reacts with guanosine radicals to form 8-nitroguanine and 5-

guanidino-4-nitroimidazole lesions in oligonucleotides (Joffe *et al.* 2003) suggesting a further potential DNA damaging role for oxidised •NO.

1.6.3.2 *Nitric oxide and HIF-1α - hypoxia and angiogenesis*

Hypoxia is present in many tumours and causes a poor prognosis for radiotherapy as discussed earlier (§1.3.1). Hypoxia inducible factor (HIF-1) is involved in enabling cells to adapt to changes in oxygen concentrations. These processes can involve angiogenesis, activated through the up-regulation of HIF-1 and expression of VEGF (Harris 2002). HIF-1 can be highly expressed in solid tumours where there can be high degrees of hypoxia so angiogenesis is essential to allow further growth. The activity of HIF-1 is determined by intracellular concentrations of HIF-1α, a subunit of HIF-1. HIF-1α is over-expressed in many cancer cells (Zhong *et al.* 1999) but is virtually undetectable in normoxic cells as it is rapidly degraded in aerobic conditions, through ubiquitylation and proteasome degradation. Oxygen is essential for the enzymatic hydroxylation of HIF-1α which signals destruction of HIF-1α. •NO is also able to stabilise HIF-1α in normoxia through the inhibition of the oxygen-activated prolyl hydroxylases which signal the sub-unit for destruction (Metzen *et al.* 2003). It may therefore have a modulatory role in controlling hypoxia. In addition, stabilisation of HIF-1α may occur through •NO-induced S-nitrosylation (Li *et al.* 2007; Chowdhury *et al.* 2012). •NO may stabilise HIF-1α following radiotherapy and it could be a major factor which contributes to angiogenesis in tumours following radiotherapy (Li *et al.* 2007; Sonveaux *et al.* 2009). Macrophage invasion into irradiated tumours could lead to high levels of iNOS-induced •NO; this could then stabilise HIF-1α and promote post-radiotherapy angiogenesis. Inhibition of NOS post-radiotherapy by, for example, L-NNA (which is a non-specific NOS inhibitor (Ng *et al.* 2007)), could potentially inhibit this angiogenesis and has been suggested to be a potential therapy worth considering (Li *et al.* 2007; Sessa 2007).

1.6.3.3 *Nitric oxide and vascular effect*

Nitric oxide has a vascular effect in tissue. Activation of tumour specific eNOS or administration of a •NO donor may promote tumour blood flow to a hypoxic tumour leading to better radiotherapy responses and drug delivery for tumour suppression. However, enhancement of tumour •NO levels and the subsequent increase of tumour vascular flow can result in a reduction of pO_2 in the tumour through the phenomenon of 'vascular steal'. Maximum dilation of a blood vessel can result in the surrounding tissue 'stealing' the oxygen from these vessels (described in (Sonveaux *et al.* 2009)). Unfortunately, due to the heterogeneity of tumour blood vessels it is difficult to predict the effect of tumour oxygenation resulting from administration of a •NO donor (Shan *et al.* 1997) and results are therefore variable (see Sonveaux, Jordan *et al.* 2009)). •NO donors such as isosorbide dinitrate, S-nitrosocaptopril and S-nitrosohaemoglobin all increase tumour blood flow through vasodilation (see references in (Jordan and Sonveaux 2012)). The stimulation of eNOS by insulin is reported to induce tumour oxygenation non-specifically, through inhibiting tumour cell respiration (Jordan *et al.* 2002). Nitrite has also been used to deliver •NO to tumours (Frérart *et al.* 2008), a process which is potentially safe and non-toxic. As many tumours exhibit lower pH because of increased metabolism and glycolysis, •NO levels increase in these tumours for ~30 min when nitrite is delivered as a bolus.

In contrast to the possibility of treating tumours through increasing blood flow, reducing blood flow can also be beneficial. A recent clinical trial administering L-NNA, a NOS inhibitor, led to a decrease in tumour blood flow which was sustained for 24 h (Ng *et al.* 2007). As a single agent this treatment is unlikely to result in cancer cure; however, the trial is important in showing that inhibition of NOS in patients induces a vasoactive tumour response despite the inhibitor not being specific for tumour NOS.

Timing of delivery of •NO as a vasoactive agent in combination with other therapies, especially radiotherapy, could be crucial to outcome. Hypoxic tumour tissue can become re-

oxygenated and angiogenesis initiated within a few hours of radiotherapy (Sonveaux *et al.* 2009). This process could in part be due to a pathway involving •NO. Re-oxygenation of a hypoxic tumour will increase its radiation response on repeated radiotherapy fractions but stimulation of angiogenesis is a problem which could be targeted by administration of NOS inhibitors post radiation.

1.6.4 Nitric oxide and radiotherapy

Although oxygen is a well known radiosensitizer in radiobiology (Gray *et al.* 1953), •NO was also reported over 60 years ago to act as a radiosensitizer. Anoxic bacteria and mammalian cells were radiosensitized by high levels of •NO (>15 μM) at high radiation doses (5 – 45 Gy) (Howard-Flanders 1957; Gray *et al.* 1958). Later, hypoxic mammalian cell radiosensitization was observed at doses below 5 Gy and at concentrations of •NO <2 μM (Wardman *et al.* 2007). Elevated radiation response by •NO in hypoxic cells and tumours could be attributed to many factors including an increase in tumour oxygenation through the ability of •NO to act as a vasodilator (Jordan *et al.* 2003; Ning *et al.* 2012); the induction of apoptosis through activation of p53 (Cook *et al.* 2004); inhibition of DNA repair enzymes (Chien *et al.* 2004); the ability of •NO to induce bystander effects (Shao *et al.* 2003) and apoptosis (Portess *et al.* 2007); and enhanced radiation-induced DNA damage seen through increased formation of DSB, detected as γH2AX foci (Wardman *et al.* 2007; Stewart *et al.* 2011).

DNA damage is thought to contribute to the lethal effects of IR, and so the effects which •NO might have on modifying the types of radiation-induced DNA damage and on the repair of this damage are important to understand. It has been reported that the yields of SSB and DSB in mammalian cells under hypoxia are enhanced by •NO following IR (Wardman *et al.* 2007; Stewart *et al.* 2011). The DSB formed, as measured by γH2AX foci, under hypoxia but in the presence of •NO, repair more slowly than those induced when in aerobic or anaerobic conditions (Wardman *et al.* 2007). However, the mechanisms and types of DNA

damage formed in the presence of •NO under anaerobic conditions are largely unknown. One proposal is that •NO may react with DNA radicals formed by IR (Mitchell *et al.* 1993; Keefer and Wink 1996; Jordan *et al.* 2004) and in doing so, form modified bases (e.g. Scheme 1-5), although no evidence exists at present to support this reaction mechanism. Whether potential base lesions produced could be repaired by BER is also unknown, as the modified bases may not be recognised by cellular glycosylases.

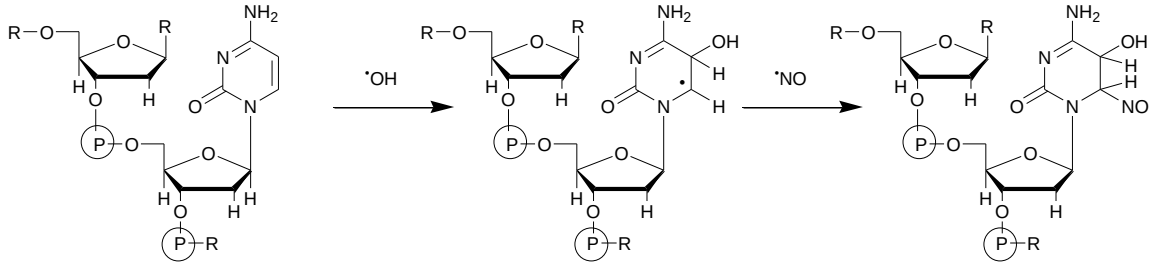

Scheme 1-5 Proposed mechanism for the reaction of •NO with an •OH-adduct of a cytosine base in DNA.

Ionizing radiation induces DNA damage by direct ionization of DNA or by reaction of the bases (Pouget *et al.* 2002) with radiolytically formed •OH to form products, both via intermediate base radicals. •NO reacts rapidly (k ~10^9 M^{-1} s^{-1}) with the •OH-adducts of uracil and 2′-deoxyguanosine monophosphate (dGMP) in anoxia (Wardman *et al.* 2007), so that identifying the reactions and products with DNA bases may offer some understanding as to how •NO radiosensitizes cells via modification of DNA damage.

Oxygen reacts with nucleobase •OH-adduct radicals with similar rate constants (Willson 1970) as •NO, and can increase radiosensitivity of cells, typically by a factor of 2-3 (Hall 2000). However, unlike •NO when O_2 reacts with base radicals in DNA, long-lived peroxyl radicals are formed. Some of these peroxyl radical adducts may interact with adjoining sugars in the DNA strand, and abstract a H-atom forming a SSB (von Sonntag 2006) (Scheme 1-4). In addition, SSB are formed by the direct reaction of •OH with the sugar

moiety (Scheme 1-2) (von Sonntag 2006). In contrast to the observations with O_2, the DNA products resulting from DNA radical interactions with •NO would be diamagnetic e.g. nitroso adducts (Scheme 1-5) and may protect against the formation of SSB. The exact identity and nature of these potential •NO-induced products and how they may initiate cell death are as yet unknown.

1.6.5 Delivery of nitric oxide to hypoxic tumours

•NO in tissue at low O_2 concentration is stable and should be able to penetrate into tumours, as it is readily soluble in lipid membranes with a high diffusion coefficient in water (Wise and Houghton 1968). Apart from the cytotoxic properties that it may exhibit at high concentrations, toxicity could be enhanced by its radiosensitizing properties. The potential of •NO to modify the types of DNA damage produced under hypoxia remains to be examined in detail as a possible mechanism involved in radiosensitization of hypoxic cells in tumour tissue. However, delivery of •NO to tumour tissue is potentially very challenging. Methods and techniques which have been investigated involve chemical agents such as: NONOates (see below) (Mitchell *et al.* 1993); S-nitroso-N-acetylpenicillamine (SNAP) (Janssens *et al.* 1999); •NO-donating non-steroidal anti-inflammatory drugs (Stewart *et al.* 2011); dinitroazetidines (Ning *et al.* 2012); insulin stimulated eNOS release of •NO (Jordan *et al.* 2002); gene therapy using a radiation-induced promoter of inducible nitric oxide synthase (iNOS) (Coulter *et al.* 2008) and induction of iNOS with cytokines (Singh *et al.* 2009; Jiang *et al.* 2010).

Development of a pro-drug which releases •NO only in hypoxia could therefore be a strategic target for radiotherapy, where the drug could release •NO in these radioresistant regions. Diazeniumdiolates, also called NONOates, release •NO in acidic conditions and at physiological pH but are stable in alkali (Maragos *et al.* 1991; Keefer *et al.* 1996). The release rate and yield of •NO from these molecules varies with the structure of the NONOate (Davies *et al.* 2001). NONOates have been investigated for treatment of many disorders including

heart problems and tissue- or tumour-specific release of •NO from a NONOate by conjugation with a targeting group have been investigated. For example conjugation to glioma specific peptides allows targeting of •NO to glioblastoma multiforme for therapy (Safdar and Taite 2012). Tumour specific release of •NO has also been achieved by harnessing elevated levels of glutathione transferase in tumours (Shami *et al.* 2003; Kizlitepe *et al.* 2007). Synthesis of pro-drugs which release NONOates in hypoxia may therefore allow targeting of •NO to these difficult to treat regions, based on the principles developed over many years for hypoxia activated bioreductive area (reviewed in (Wilson and Hay 2011) and as has recently been described for a indolequinone-diazeniumdiolate pro-drug (Sharma *et al.* 2013). Similar compounds (*ortho*-nitrobenzyl-substituted diazeniumdiolates) have also been identified which release •NO in photochemical systems (Makings and Tsien 1994; Ruane *et al.* 2002).

Although •NO can be considered a 'double-edged sword' for cancer, delivery of low concentrations of •NO to hypoxic regions of a tumour for short periods of time during therapy could radiosensitize hypoxic cells, both through the direct reactions of •NO with DNA radicals and through an •NO-induced increase in tumour blood flow. Following radiotherapy, subsequent addition of NOS inhibitors to reduce the radiation-induced release of •NO could offer benefits to therapy (Li *et al.* 2007).

1.7 Free radical chemistry of tyrosine

Tyrosine (tyr) is an important component of many proteins and some enzyme active sites. The one-electron oxidation of tyr residues to phenoxyl radicals (tyr•) is critical to some enzyme functions. For example, ribonucleotide reductase (RR), involved in the conversion of ribonucleotides to deoxyribonucleotides for DNA synthesis, has an essential tyr in its active site (Fontecave 1998). •NO inhibits the activity of RR in a reversible reaction (Kwon *et al.* 1991; Lepoivre *et al.* 1992; Roy *et al.* 1995) but the mechanism for its action is not clear. RR is a very attractive target for cancer therapy as inhibition of the enzyme could prevent DNA

synthesis, and tumour growth rate can be associated with the activity of RR. Understanding the mechanism involved in the free radical reactions of •NO with tyr radicals could help in future developments of drugs which may act through the release of •NO.

1.7.1 Ribonucleotide reductase and reaction with nitric oxide

Ribonucleotide reductase is an essential enzyme involved in the synthesis of DNA and its activity can be rate limiting during cell replication. RR is required for the NADPH dependent reduction of ribonucleotides into deoxyribonucleotides (dNTPs) (Scheme 1-6).

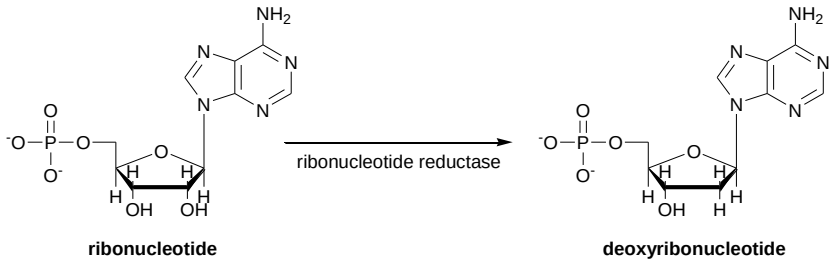

Scheme 1-6 Reduction of ribonucleotides by ribonucleotide reductase.

Mammalian RRs consist of two different dimeric subunits, R1 and R2. R2 carries a stable protein tyr• essential for catalysis and it undergoes complex free-radical chemistry in a non-haem di-iron containing active site (reviewed in (Stubbe and van der Donk 1995; Fontecave 1998)).

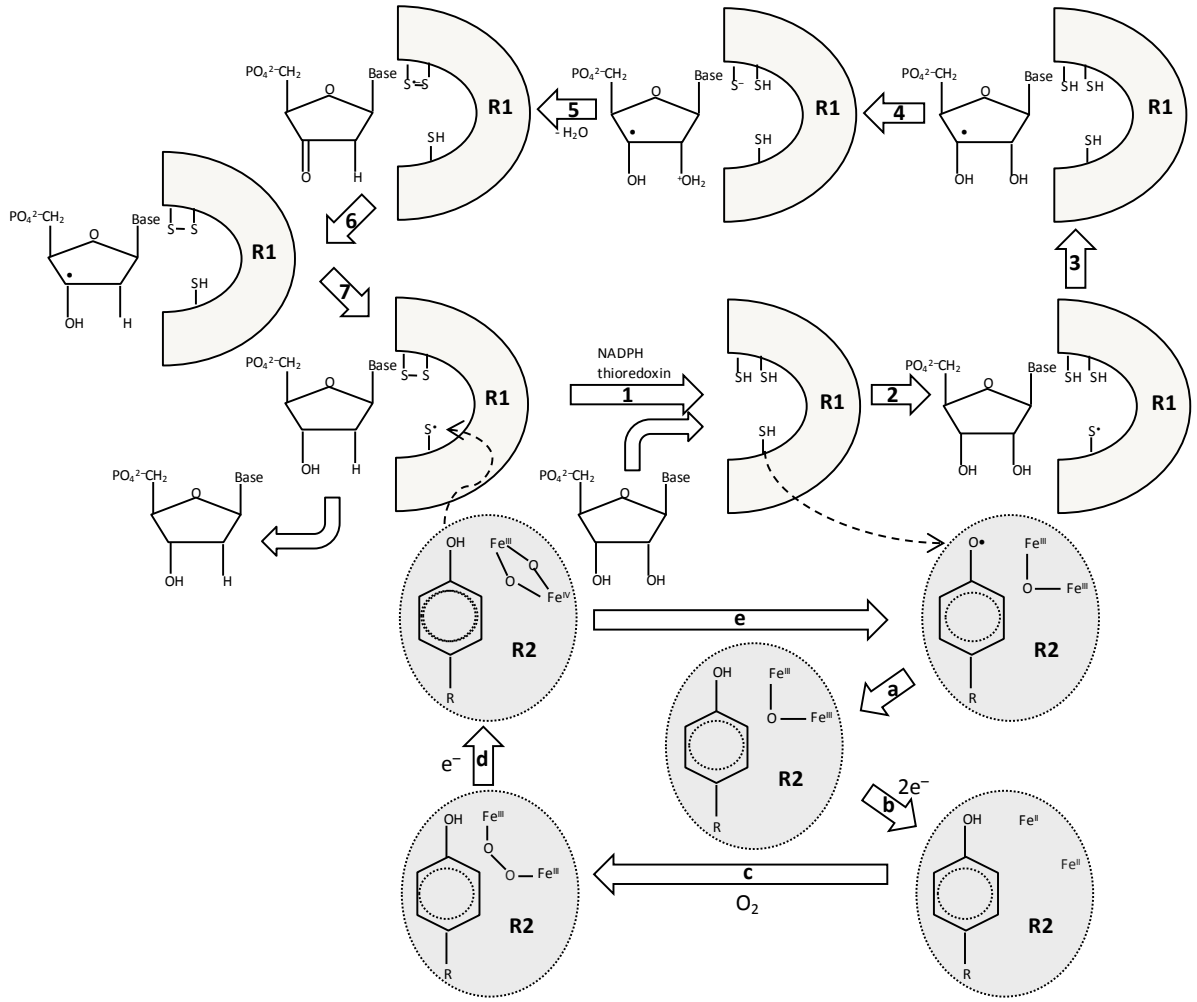

Scheme 1-7 Schematic to show some of the possible free radical reactions between R1 and R2 subunits involved in the activity of ribonucleotide reductase (adapted from (Stubbe and van der Donk 1995; Fontecave 1998)).

The tyrosyl radical abstracts an H-atom from a cysteine residue in the active site on R1, which is then involved in the dehydroxylation of ribonucleotides through complex free radical steps (Scheme 1-7) also involving thioredoxin reductase-thioredoxin electron transfer chains. Oxygen is an essential cofactor for the reduction reactions and hypoxia inhibits the activity of RR, reducing the dNTP pools in cells (Zhang *et al.* 2011) until O_2 levels are replenished (Pires *et al.* 2010). Hydroxyurea (HU) also inhibits the activity of RR (for example (Zhang *et al.* 2011)) and depletes dNTP pools. The drug is used as a treatment for sickle cell anaemia and has also been studied as a radiosensitizer for head and neck and cervical cancer treatment (Navarra and Preziosi 1999; Candelaria *et al.* 2006). HU is also a source of $^{\bullet}NO$ (King 2004),

for example oxidation of HU by peroxidases (Huang *et al.* 2002) and calalase (Huang *et al.* 2004) produce $^{\bullet}NO$. It is therefore possible that $^{\bullet}NO$ may be involved in the actions of HU, contributing to the radiosensitizing effects.

1.7.2 Reaction of tyrosine with oxidizing radicals – repair and reactivity of tyrosine radicals

The presence of modified tyr residues in tissue is often used as an indicator of enhanced nitrosative and oxidative stress (reviewed in (Radi 2004)). In particular 3-nitrotyrosine ($3NO_2$tyr) and 3,3′-dityrosine (dityr) are commonly detected using ELISA assays. The kinetics involved in the formation of these modified tyr residues have been well characterised in aqueous solution with free tyr. However, reaction of the intermediate tyr$^{\bullet}$ with O_2 and $^{\bullet}NO$ have not been fully elucidated.

The microenvironment may have a large effect on tyr reactivity (Zhang *et al.* 2001): in membrane proteins, diffusion of oxidants into lipid bilayers may be hindered (Bartesaghi *et al.* 2006) and lateral movement of tyr units within the membrane to allow dimerization to occur may be severely restricted. Also lipid radicals themselves may be able to oxidise tyr (Bartesaghi *et al.* 2010; Folkes *et al.* 2012). Further investigations into the free radical chemistry involved in these reactions will expand knowledge of how these tyr biomarkers are formed and help to explain biochemical variation in tissues and tumours.

$^{\bullet}OH$ are strong one-electron oxidants but they mainly react with tyr through addition/elimination reactions with the aromatic ring forming $^{\bullet}OH$ adduct intermediates (k = 1 x 10^{10} M^{-1} s^{-1} (Solar *et al.* 1984)) as is observed with DNA bases. Oxygen reacts rapidly with the $^{\bullet}OH$ adduct of tyr forming 3-hydroxytyrosine/L-Dopa (3OHtyr) (k = 1.7 x 10^{9} M^{-1} s^{-1} (Cudina and Josimovic 1987)). In addition, a phosphate (HPO_4^{2-}) catalyzed reaction (k = 5.8 x 10^{7} M^{-1} s^{-1} (Mvula *et al.* 2001)) causes the radical to dehydrate forming tyr$^{\bullet}$, the same radical as is produced directly by one-electron oxidants including $^{\bullet}NO_2$, (k = 2.9 x 10^{7} M^{-1} s^{-1}, pH 12 (Alfassi 1987)) and $CO_3^{\bullet-}$ (k = 4.5 x 10^{7} M^{-1} s^{-1}, pH 7 (Chen and Hoffman 1973)).

The fate of tyr$^{\bullet}$ depends upon the balance between the availability and concentration of antioxidants and reactants. Thiols and ascorbate can repair tyr$^{\bullet}$ regenerating tyr. $^{\bullet}NO_2$ (generally formed through the decomposition of peroxynitrite) reacts forming $3NO_2$tyr (k ~3 x 10^9 M^{-1} s^{-1} (Prütz *et al.* 1985)), which is used as a marker of nitrosative stress and the presence of peroxynitrite. Other reactions may also occur, including reactions with $^{\bullet}NO$. All of these reactions are in competition with dimerization to form dityr ($2k$ = 2.5 x 10^8 s^{-1} (Hunter *et al.* 1989)) and the formation of dityr reflects oxidative damage.

Reduced glutathione (GSH) reacts with tyr$^{\bullet}$ (k = 2 x 10^6 M^{-1} s^{-1} at pH 7.5, Eq. 1-16, (Folkes *et al.* 2011)), in competition with the formation of dityr (Eq. 1-17), to form thiyl radicals (GS$^{\bullet}$) and ultimately oxidised glutathione (GSSG) (Folkes *et al.* 2011) (Eq. 1-18):

$$tyr^{\bullet} + GSH \leftrightarrows tyr + GS^{\bullet} \quad (1\text{-}16)$$

$$2tyr^{\bullet} \rightarrow dityr \quad (1\text{-}17)$$

$$GS^{\bullet} + GS^{\bullet} \rightarrow GSSG. \quad (1\text{-}18)$$

In addition to repair of tyr$^{\bullet}$, a conjugate with GSH has also been identified, but the fate of this molecule in cells is as yet unknown (Folkes *et al.* 2011). Under physiological conditions, where both ascorbate and GSH are present, it is likely that GSH is not involved in the 'repair' of tyrosyl radicals and one-electron reduction by ascorbate (k = 4.4 x 10^8 M^{-1} s^{-1} (Hunter *et al.* 1989)) would be favoured when GSH and ascorbate are present in physiological concentrations, a reflection of the faster rate of reaction for reaction 1-19.

$$tyr^{\bullet} + AscH \rightarrow tyr + Asc^{\bullet -} + H^{+}. \quad (1\text{-}19)$$

$^{\bullet}NO$ shows antioxidant properties and reacts with tyr$^{\bullet}$ very rapidly (k = 10^9 M^{-1} s^{-1} (Eiserich *et al.* 1995; Goldstein *et al.* 2000)). These reactions may be one of the reasons why $^{\bullet}NO$ is able to inhibit tyrosine-containing enzymes such as RR (Kwon *et al.* 1991; Lepoivre *et al.* 1992; Roy *et al.* 1995). It is thought that reversible radical-radical combinations form a nitroso species (Scheme 1-8) as tyr$^{\bullet}$ is regenerated, as detected by electron spin resonance

following removal of •NO (Roy *et al.* 1995). The authors suggested that the C-nitroso or O-nitroso species exist in equilibrium with tyr•. A nitroso product has not as yet been identified, although debate is ongoing as to the reaction mechanisms involved in the reaction of tyr• and •NO.

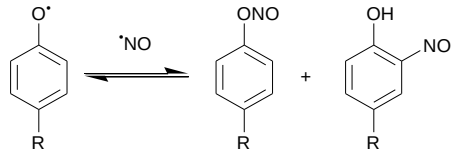

Scheme 1-8 Proposed mechanism for the reversible inhibition of ribonucleotide reductase by reaction of tyrosine radicals with nitric oxide.

In comparison to •NO, the rate of reaction of O_2 with tyr• is extremely slow (k ~10^3 M^{-1} s^{-1} (Hunter *et al.* 1989; Jin *et al.* 1993) as observed with other phenolic radicals (Janzen *et al.* 1993). Questions remain as to why the reaction of tyr• with •NO is so much faster compared to equivalent reactions with O_2 and as a consequence how •NO may specifically be beneficial to tumour therapy in terms of preventing DNA synthesis and repair through the inhibition of RR.

1.8 Aims of the project

The aim of this project is to investigate the radiobiology of •NO in hypoxia, in association with cancer growth and therapy. In particular the project concentrates on the mechanisms by which •NO may increase tumour response to radiotherapy under hypoxia. The focus is on gaining an understanding of the •NO-induced DNA damage and the resultant repair following IR under hypoxia. DNA damage will be measured using γ-radiolysis of DNA bases, nucleosides, nucleotides and single-stranded oligonucleotides following reaction with •OH, where products will be detected using high performance liquid chromatography. DNA damage will also be detected in irradiated double stranded plasmid DNA using electrophoresis and in mammalian cells, including hamster fibroblasts and human foetal lung

fibroblast cells, using markers for DSB. Studies will also be carried out into the development of novel hypoxia specific pro-drugs of •NO as potential radiosensitizers, in an attempt to understand if hypoxic tumour tissue could be targeted by •NO for radiotherapy. These studies will utilise radiation chemistry techniques, reduction of pro-drugs with cytochrome P450 and reduction of pro-drugs by human hepatocyte carcinoma cells. In addition, reactions between •NO and tyrosine radicals, an essential component of many proteins, membrane receptors and particularly ribonucleotide reductase, will be investigated using radiation chemistry techniques, in order to gain a greater understand into the role which •NO may have in the modulation of the nucleotide pool essential for DNA synthesis and repair. A consequence of the depletion of the cellular dNTP pool may add to the radiosensitizing properties of nitric oxide. The work will increase our knowledge into the potential for the modification of levels of •NO in tumours for anti-cancer therapeutics.

2 Materials and Methods

2.1 Sources of chemicals and materials

Tris-HCl, dipotassium or disodium orthophosphate, potassium or sodium dihydrogen orthophosphate, sodium citrate, sodium formate, sodium hydroxide, sodium azide, ethanol, dichloromethane, isopropanol, tetrabutyl ammonium hydroxide (TBAOH), acetonitrile and methanol (LCMS grade) were obtained from Fisher Scientific, UK. Eagle's modified medium (EMEM), Dulbecco's modified eagles medium (DMEM), non-essential amino acids, L-glutamine, pencillamine/streptomycin, trypsin-EDTA (0.25%), metaphosphoric acid (MPA), agarose (Type IV-A), ethidium bromide, propidium iodide (PI), RNase IV, calf thymus DNA, DNA bases, nucleosides and nucleotides, 8-azaguanine, nuclease P1, zinc chloride, potassium bromide (AnalaR grade), sodium chloride, glutathione (GSH), glutathione-S-transferase (45.7 units/mg protein), hydrochloric acid (HCl), ethidium bromide, tyrosine, 3-hydroxytyrosine, 3-nitrotyrosine, low melting point agarose, normal melting point agarose and horseradish peroxidase (HRP) were obtained from Sigma-Aldrich (Poole, UK). 8-Azaadenine was obtained from MP Biomedicals, UK. Oligonucleotides were obtained from Eurogentec, Belgium. PUC18 Plasmid DNA (PUC18, 2686 base pairs, 1.746 x 10^6 Da, 2.07 µg/µl in 0.1 mM Tris) was a kind gift from Dr. Elzbieta Jagielska (University of Oxford), and was prepared as previously described (Hodgkins *et al.* 1996). Formamidopyrimidine-DNA glycosylase (Fpg) was a kind gift from Murat Saparbev, (Institut Gustave Roussy, France) and Serge Boiteaux (CEA, Departement de Radiobiologie et Radiopathologie, France). Monobromobimane was obtained from Molecular Probes, UK. Foetal calf serum (FCS) was obtained from Biosera, East Sussex, UK and Gibco, UK. Phosphate buffered saline (PBS) from Oxoid, UK and one tablet was dissolved in 100 ml water. P450 reductase + cytochrome b_5 insect cell supersomes (5 mg/ml protein) in 100 mM potassium phosphate (pH 7.4) were

obtained from BD Biosciences (Oxford, UK) and stored in small aliquots at –80 °C. SyBr Gold was obtained from Invitrogen, UK. Synthesis of 1-[(5′-nitrofuryl)methoxy]-2-oxo-3,3-diethyl-1-triazene (NF-DEANO) was kindly carried out by Dr. Matthew Naylor (Gray Cancer Institute, Northwood, UK) and Geoff Lynn (University of Oxford). Synthesis of 1-[(4′-nitrophenyl)methoxyl]-2-oxo-3,3-diethyl-1-triazene (NB-DEANO) was also carried out by Dr. Matthew Naylor. Synthesis of 1-[(2′-nitroimidazol-5-yl)methoxyl]-2-oxo-3,3-diethyl-1-triazene (NI-DEANO) was kindly carried out by Cindy Körner (University of Oxford). All compounds were confirmed by NMR and MS.

Antibody	**Supplier**	**Dilution**	**Method**
anti phospho histone H2AX (200 µg /200 µl), mouse monoclonal	Upstate, USA Millipore, UK	1 : 300 1 : 3000	flow cytometry confocal microscopy
anti 53BP1 (1 mg/l ml) rabbit monoclonal	Abcam, UK	1 : 500	confocal microscopy
anti cyclin A, mouse monoclonal	Vector Laboratories	1 : 50	confocal microscopy
anti RAD51, (1mg/ml) mouse monoclonal	GeneTex (Bioscience UK)	1 : 1000	confocal microscopy
Alexa Fluor 488, (2 mg /ml) goat anti mouse IgG	Invitrogen, UK	1 : 300 1 : 3000 1 : 1500	flow cytometry confocal microscopy (+ cyclin A)
Alexa Fluor 633, (2mg/ml) goat anti rabbit	Invitrogen, UK	1 : 3000	confocal microscopy

Table 2-1 Table showing the primary and secondary antibodies used for immunofluorescence studies.

Cell lines were obtained from the European Collection of Cell Cultures, Salisbury, UK. Vectashield containing DAPI was obtained from Vector Laboratories, UK. Antibodies were obtained from the suppliers shown in Table 2-1 and diluted as described (Table 2-1). Zero grade nitrous oxide (N_2O) and nitrogen (N_2) were supplied by the British Oxygen Company (BOC) (Guildford, UK) and 1% nitric oxide ($^{\bullet}NO$) balance N_2, 1% oxygen (O_2) balance N_2 and 20% O_2 balance N_2O were supplied by BOC special gases (Guildford, UK).

2.2 Handling of nitric oxide

$^{\bullet}NO$ in a pressurised cylinder can be contaminated with the highly oxidizing species nitrogen dioxide ($^{\bullet}NO_2$) from the disproportionation of $^{\bullet}NO$ under pressure (Eq. 2-1).

$$3\ {}^{\bullet}NO \rightarrow N_2O + {}^{\bullet}NO_2 \qquad (2\text{-}1)$$

Although concentrations of pressurized $^{\bullet}NO$ did not exceed 10000 ppm in experiments described in these studies, as a precaution the gas was purified. In all cases $^{\bullet}NO$ was bubbled through two 500 ml deoxygenated Dressler bottles containing glass sinters to maximize gas solubility, and equipped with metal neck braces and springs to prevent the bubbling heads from popping up and allowing O_2 into the system. The first bottle contained 50 ml 1 M NaOH, to remove any contaminating $^{\bullet}NO_2$ (Eq. 2-2) and the second contained 50 ml Millipore Synergy water to remove any NaOH spray (Figure 2-1).

$$^{\bullet}NO + {}^{\bullet}NO_2 + {}^{-}OH \rightarrow 2NO_2^{-} + H^{+}. \qquad (2\text{-}2)$$

Anaerobic conditions were maintained throughout the experimental procedure to prevent the formation of $^{\bullet}NO_2$ (Eq. 1-9).

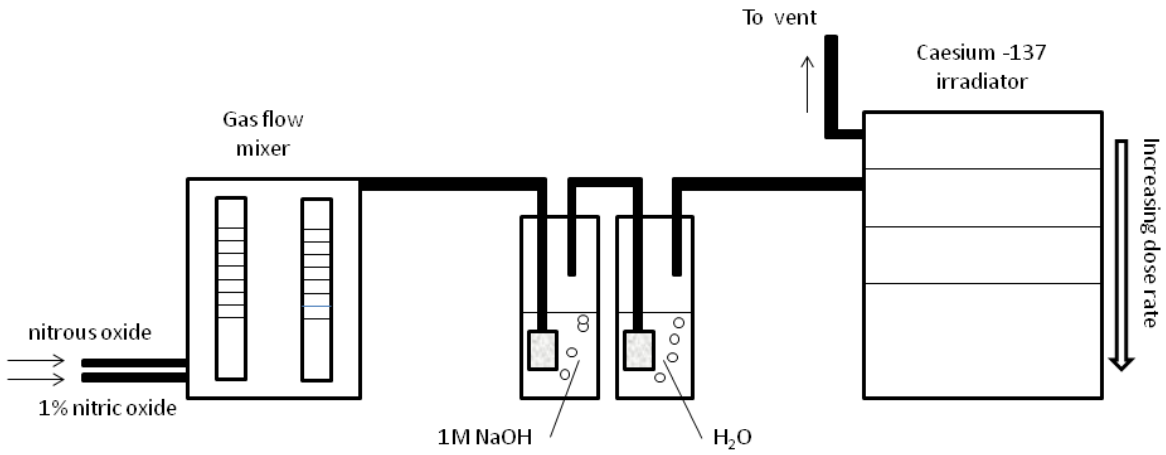

Figure 2-1 Apparatus for mixing and purifying nitric oxide for γ-radiolysis experiments.

Glass tubing with ball and socket joints, stainless steel and PEEK tubing and stainless steel hypodermic needles were used wherever possible, with Tygon® rubber tubing for joining kept to a minimum, as butyl rubber is permeable to nitric oxide, and may lead to the formation of nitrogen oxides (Ishibashi *et al.* 2000). Where necessary, gases were mixed (v/v) in a flow mixer, with flow rates of ~50 - 200 ml/min (Figure 2-1). Saturated solutions of 1% $^{\bullet}NO$/99% N_2 in PBS are ~18 µM $^{\bullet}NO$ at 25 °C (Zacharia and Deen 2005).

2.3 Gamma irradiation

Radiation chemistry is a very useful tool for understanding and measuring free radical reactions in biological systems. The radiolysis of water generates oxidising and reducing reactive species; hydroxyl radicals ($^{\bullet}OH$), hydrated electrons (e_{aq}^-) and protons (H^+) along with low yields of hydrogen atoms ($H^{\bullet}$), hydrogen peroxide (H_2O_2) and hydrogen (H_2). Yields of these reactive species can be expressed in terms of *G* value. This value is the chemical yield in µM Gy^{-1}, where 1 Gy is the absorption of 1 joule of radiation energy by one kilogram of matter (1 Gy = 1 J/kg = 100 rad). Total free radical generation from water is in the range of 0.6 - 0.7 µM Gy^{-1} with $^{\bullet}OH$ (oxidising) and e_{aq}^- (reducing) being the major products having *G* values of 0.28 and 0.27 µM Gy^{-1} respectively. These species can be selectively scavenged

to allow for reaction of the other radicals to be studied independently. The dose to an experimental system is calculated using Fricke dosimetry.

2.3.1 Fricke dosimetry

Fricke dosimetry (Spinks and Woods 1976) is used to measure the absorbed dose to a solution. The process involves the measurement of ferric ions from an oxic, acidic, aqueous ferrous sulphate solution exposed to IR (Eq. 2-(3-8)).

$$H_2O \rightarrow {}^{\bullet}H + {}^{\bullet}OH + H_2O_2 \quad (2\text{-}3)$$

$${}^{\bullet}OH + Fe^{2+} \rightarrow OH^- + Fe^{3+} \quad (2\text{-}4)$$

$${}^{\bullet}H + O_2 \rightarrow {}^{\bullet}HO_2 \quad (2\text{-}5)$$

$${}^{\bullet}HO_2 + Fe^{2+} \rightarrow HO_2^- + Fe^{3+} \quad (2\text{-}6)$$

$$HO_2^- + H^+ \rightarrow H_2O_2 \quad (2\text{-}7)$$

$$H_2O_2 + Fe^{2+} \rightarrow {}^{\bullet}OH + OH^- + Fe^{3+}. \quad (2\text{-}8)$$

Reagent	Concentration
$FeSO_4.7H_2O$	1 mM
H_2SO_4	0.4 M
NaCl	1 mM

Table 2-2 Components of dosimeter solution for Fricke dose determination.

Samples were irradiated in a Caesium-137 GSR D1 irradiator (Gamma-service Medical GmbH, Leipzig, Germany) at room temperature (RT). Dosimetry was carried out for each irradiation vessel and volume of solution to be used in an experiment. Dosimeter solution (Table 2-2) was irradiated, and at regular intervals a sample was removed and the optical density at 304 nm and 25 °C was measured using a Hewlett-Packard 8453 diode array spectrophotometer. Un-irradiated solution was used as a blank. A graph of optical density was plotted against irradiation time (min) and the slope of this line used to calculate the dose rate.

The molar extinction coefficient (ε) of Fe^{3+} at 25 °C is 2197 M^{-1} cm^{-1} (± 0.7% / °C) therefore the concentration of Fe^{3+} produced per min is:

(OD / min (slope)) / 2197 mol dm^{-3} min^{-1}

A dose of 10 Gy produces a *G* (Fe^{3+}) of 15.5 x 1.036 µmol dm^{-3}/Gy in water; 0.4 M H_2SO_4 has a density of 1.024 therefore:

$$\text{Dose rate} = \frac{\text{OD / min (slope) x 10}}{2197 \times 15.5 \times 1.024 \times 1.036 \times 10^{-6}} \quad \text{Gy min}^{-1}$$

2.3.2 Generation of oxidizing radicals by ionizing radiation

Saturating solutions with N_2O before irradiation allows for e_{aq}^- generated through the ionization of water to be converted into $^{\bullet}OH$ (Eq. 2-9) increasing the *G* value of $^{\bullet}OH$ to 0.57 µmol Gy^{-1}. $^{\bullet}OH$ then either reacts directly with the solute under study or with the salts such as Br^-, NO_2^- or N_3^- when present, to generate one-electron oxidizing radicals (Eq. 2-(10-13)). These oxidizing radicals can then react with the compound under study forming one-electron oxidized radical species.

$$e_{aq}^- + N_2O + H^+ \rightarrow {}^{\bullet}OH + N_2 \quad (2\text{-}9)$$

$$^{\bullet}OH + Br^- \rightarrow {}^-OH + Br^{\bullet} \quad (2\text{-}10)$$

$$Br^{\bullet} + Br^- \rightarrow Br_2^{\bullet -} \quad (2\text{-}11)$$

$$^{\bullet}OH + NO_2^- \rightarrow {}^{\bullet}NO_2 + {}^-OH \quad (2\text{-}12)$$

$$^{\bullet}OH + N_3^- \rightarrow N_3^{\bullet} + {}^-OH. \quad (2\text{-}13)$$

2.3.3 Generation of reducing radicals by ionizing radiation

Formate in solution scavenges the oxidizing $^{\bullet}OH$ radicals and allows reductive reactions to be studied. The resulting formate radical is a strong one-electron reductant with a reduction potential of -2.0 V vs. normal hydrogen electrode (NHE) (Wardman 1989) and is produced from $^{\bullet}OH$ and $^{\bullet}H$-oxidation of formate ions (Eq. 2-(14-15)).

$$^{\bullet}OH + HCO_2^- \rightarrow H_2O + {}^{\bullet}CO_2^- \quad (2\text{-}14)$$

$$^{\bullet}H + HCO_2^- \rightarrow H_2 + {}^{\bullet}CO_2^-. \quad (2\text{-}15)$$

Formate solutions saturated with N_2 produce a reducing environment (e_{aq}^- + $CO_2^{\bullet-}$) with a reducing radical chemical yield of G = 0.62 µM Gy^{-1}. Solutions saturated with N_2O produce $CO_2^{\bullet-}$ radicals alone with a G value = 0.69 µM Gy^{-1} (Naylor *et al.* 1994).

2.3.4 γ-Irradiation in the presence of nitric oxide

For irradiation studies using $^{\bullet}NO$, concentrations of each component were calculated to ensure that >95% primary radicals reacted with the sample and not with $^{\bullet}NO$. Secondary radicals generated can then react with $^{\bullet}NO$. In procedures using <18 µM $^{\bullet}NO$, or radiation doses which would deplete $^{\bullet}NO$ by direct reaction with $^{\bullet}OH$ (k = 1 x 10^{10} M^{-1} s^{-1} (Seddon *et al.* 1973)) or other oxidants, gas flow was maintained throughout the irradiation period using ports in the side of the irradiator (Figure 2-1). The dose rate varies significantly in the z-plane of the irradiator and bubbling helps to average out the dose rate throughout the sample, especially at the higher dose rates. In some studies, following γ-radiation, $^{\bullet}NO$ was flushed out of the solutions by bubbling with N_2 to ensure that the highly oxidising species $^{\bullet}NO_2$ could not be formed from any remaining $^{\bullet}NO$ reacting with O_2 post-irradiation.

2.4 HPLC analysis

Samples were analysed by high performance liquid chromatography (HPLC) (Waters 2695, Watford, UK) equipped with a photodiode array detection (Waters 2996), fluorescence spectroscopy detection (Waters 474) or mass spectrometry detection (Waters micromass ZQ) (LCMS) operating in electrospray positive (ES^+) or negative (ES^-) mode. For liquid chromatography with mass spectrometry (LCMS) analysis a flow splitter, constructed of a short length of 0.007 inch i.d. PEEK tubing attached to a T-fitting on the mass spectrometer (MS) inlet, diverted approximately half of this to waste, the remainder going to the MS detector. A divert valve (Rheodyne MX7900, Hichrom, Reading, UK) was used to divert flow

away from the MS at the beginning and end of each chromatogram. Mass spectra were recorded at 3 kV, extractor lens 1 V, RF lens 0.1 V, source temperature 120 °C, desolvation temperature 450 °C, desolvation gas flow 500 l/h and cone gas flow of 130 l/h with the cone voltage varied dependent upon the analyte.

2.5 Maintenance of cell lines

V79-4 hamster fibroblast cells were grown in Eagle's modified medium (EMEM) containing 10% FCS, 2 mM L-glutamine, pencillamine (100 U), streptomycin (0.1 mg/ml) and sodium bicarbonate (2.2 g/l) in a humidified incubator at 37 °C in air containing 5% CO_2. HF-19 human foetal lung fibroblast cells were grown in EMEM as above containing 15% FCS. HepG2 human Negroid hepatocyte carcinoma cells were grown in Dulbecco's modified Eagle's medium (DMEM) containing 10% FCS with 1% non-essential amino acids and 4 mM L-glutamine. Unless otherwise stated, cells were harvested by trypsin-EDTA (0.25%) digestion. The medium was removed, cell monolayers were washed with PBS (2 x 10 ml) and trypsin-EDTA added for ~5 min at 37 °C to detach the cells. The enzyme was inhibited by the addition of 10 ml medium containing FCS and the cells spun (200 g, 4 min, 20 °C), the supernatant removed and the cells resuspended as required.

2.5.1 Measurement of cell cycle status

The proportion of cells in G1, S and G2/M phases of the cell cycle was monitored by staining cellular DNA with PI. 0.5 ml of ~3 x 10^5 cells in PBS was spun in 1.5 ml polypropylene tubes for 5 min (200 g, 20 °C), the cell pellet was then fixed in 0.5 ml ice cold 70% ethanol and stored at –20 °C. Samples were warmed to RT then spun as above to remove the ethanol. 0.5 ml PI (20 µg/ml) containing RNase (4 µg/ml) were added to each sample, mixed and incubated at 37 °C for 30 min.

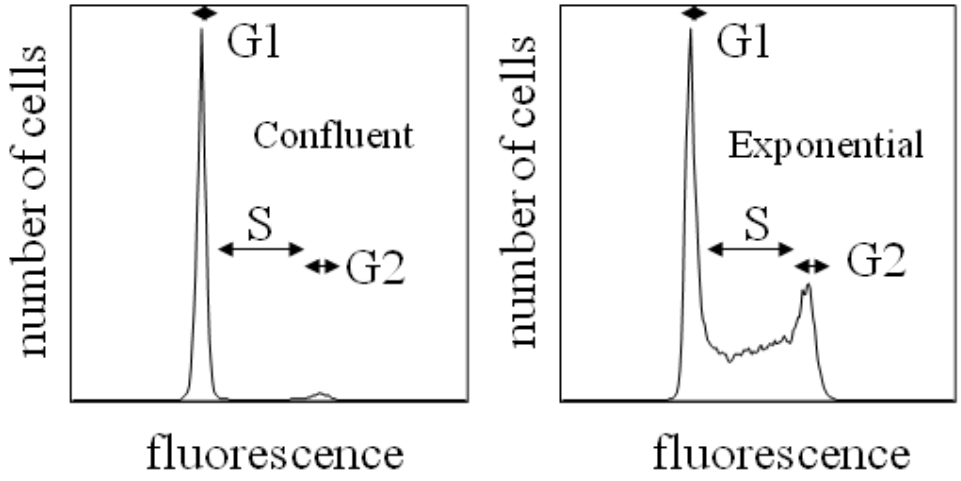

Figure 2-2 Histograms to show the proportion of cells in G1/S/G2 phases of the cell cycle in confluent and exponentially growing V79-4 cells.

Analysis was carried out on a FACScan flow cytometer (Becton Dickinson, UK) running CellQuest software with 10,000 events counted. Using a dot plot of forward scatter against side scatter, single cells in G1-G2 phase were gated and the gated cells were used to create a histogram of PI fluorescence against number of cells. The proportion of cells in G1, S and G2 phases were calculated by using a ModFit program (Verity Software House). Cells were regarded as approaching confluency if the proportion of cells in G1 phase was >65% and the proportion of cells in S phase <22% (Figure 2-2).

2.5.2 Procedure for irradiating cell suspensions

Cell suspensions in PBS were de-oxygenated at RT by bubbling slowly with N_2 or 1% O_2 (~13 µM O_2)/balance N_2 for 30 min in glass bubbling towers equipped with 25 ml glass syringes. The N_2 gas supply was then changed to 1% $^{\bullet}NO$ (~18 µM $^{\bullet}NO$) where required, for a further 20 min, as described previously (Wardman *et al.* 2007). The cells were then drawn slowly into the syringes that were removed from the apparatus, sealed with a glass cap and irradiated at RT.

2.6 Measurement of DNA modifications following oxidation by •OH in the presence of •NO

2.6.1 HPLC and LCMS analysis of bases, nucleosides and nucleotides

Samples were analysed by LCMS operating in electrospray positive (ES^+) or negative (ES^-) mode equipped with photodiode array detection. Chromatography used a Hichrom RPB column (3.2 x 250 mm, 5 µm particle size). Separation was achieved using gradients or isocratic elution, with flow rates of 0.5 ml/min, and mixtures of 10 mM formic acid, 10 mM ammonium formate, methanol and acetonitrile depending on the analyte.

2.6.2 Reaction of •NO with guanine radicals

Guanine was dissolved in a small volume of NaOH (0.5 ml, 0.5 M) before diluting with potassium phosphate buffer (10 mM, pH 8) and the pH adjusted to 8.1 with perchloric acid ($HClO_4$) to give a 0.3 mM solution. In a 4 ml glass vial, equipped with a re-sealable septa cap, 3 ml solution was first saturated with N_2O then with ~1.8 µM •NO/~ 22.5 mM N_2O which was supplied throughout radiolysis (13 Gy/min) at RT (§2.2). Samples (100 µl) were removed every 2 min for analysis by HPLC. Chromatographic separation was achieved using 10 mM formic acid, and methanol with a gradient of 3-8% methanol, in 7 min, 8-20% methanol in 2 min and returning to starting conditions over 0.1 min. Formation of xanthine (X) and 8-azaguanine (8azaG) were confirmed and quantitated by co-elution with commercially available standards.

2′-Deoxyguanosine-5′-monophosphate (dGMP, 1 mM) was dissolved in sodium phosphate buffer (10 mM, pH 7.4) or at 3 mM with the addition of potassium bromide (KBr, 50 mM). Reaction of $Br_2^{\bullet-}$ with dGMP is ~100-fold slowler than reaction with •OH and therefore the concentration of dGMP was increased to reduce competitive reactions of $Br_2^{\bullet-}$ with •NO (see Table 2-3).

reaction	k (M^{-1} s^{-1})	[reactant] (M^{-1})	k (s^{-1})	%	rate constant reference
$Br_2^{\bullet-}$ + $^{\bullet}NO$	4.8×10^9	1.8×10^{-6}	8.6×10^3	7	(Czapski *et al.* 1994)
$Br_2^{\bullet-}$ + dGMP	4.0×10^7	3×10^{-3}	1.2×10^5	93	(Willson 1974)

Table 2-3 Table to show the competition reactions between dGMP and $^{\bullet}NO$ for reaction with $Br_2^{\bullet-}$.

To investigate the effect of pH on the reactions of dGMP radicals with $^{\bullet}NO$, dGMP was dissolved in 10 mM sodium phosphate buffer at pH 4.8 – 7.8 without (1mM dGMP) or with (3 mM dGMP) the addition of 50 mM KBr. To investigate the effect of phosphate concentration, dGMP was dissolved as above in sodium phosphate buffer (0.1 – 20 mM) at pH 7.4. Solutions were saturated with N_2O (~25 mM) then bubbled with $^{\bullet}NO$ (~1.8 µM)/N_2O (~22.5 mM) where required and irradiated up to 260 Gy (13 Gy/min) at RT with constant bubbling. Chromatographic separation was achieved using 10 mM formic acid, 10 mM ammonium formate and methanol with a gradient of 3-8% methanol, 97% formic acid – 92% ammonium formate in 8 min, 8-20% methanol, 92-80% ammonium formate in 2 min, 20-50% methanol, 80-50% ammonium formate in 0.5 min and returning to starting conditions over 0.1 min. Mass spectra were obtained in ES^+ or ES^- mode with a cone voltage of 22 – 30 V.

2.6.2.1 *Reaction of 2′-deoxyguanosine monophosphate with acidified nitrite solution*

dGMP (5 mM) was dissolved in sodium acetate solution (100 mM, pH 3.7) containing sodium nitrite (50 mM) and incubated at 37 °C for 2 h as described previously (Suzuki *et al.* 1996; Suzuki *et al.* 2000). Mixtures of the products from the reaction of dGMP with HNO_2 and dGMP with $^{\bullet}OH$ in the presence of $^{\bullet}NO$ were separated by chromatography using isocratic elution with 97% 10 mM ammonium formate and acetonitrile, monitoring at 258 nm.

2.6.2.2 *Formation of 2′-deoxy-8-azaguanosine monophosphate (8azadGMP) for analysis*

dGMP (100ml, 1 mM) was dissolved in sodium phosphate buffer (10 mM, pH 7.4) and saturated with N_2O in a Dressler bottle then irradiated on the base of the irradiator (~13 Gy/min) for 90 min at RT whilst bubbling with ~1.8 µM •NO (§2.6.2). The irradiated solution was freeze-dried overnight. The solid residue was dissolved in 3 ml 50% acetonitrile/water (v/v) and 8azadGMP was purified by HPLC. Separation was achieved using isocratic elution with 5% methanol, 95% 10 mM formic acid. Accumulated injections were collected and freeze-dried and the dry product stored at -20 °C. Accurate mass was determined using a MicroTOF mass spectrometer operating in ESI mode with a negative polarity (Chemistry Department, University of Oxford).

2.6.3 Reaction of adenine radicals with •NO

Adenine (0.5 mM) was dissolved in potassium phosphate buffer (10 mM, pH 7.6) with or without the addition of KBr (50 mM) and saturated with N_2O for 10 min at RT. Samples were then irradiated at 13 Gy/min for 2 min intervals with and without •NO (~1.8 µM) (§2.6.2). HPLC chromatographic separation was achieved using 10 mM formic acid and methanol with a gradient of 3-10% methanol in 9 min and returning to starting conditions over 0.1 min. Mass spectrometry was used in ES^+ or ES^- mode with a cone voltage of 22 or 20 V respectively.

2′-deoxyadenosine (dA, 0.4 mM) and 2′-deoxyadenosine monophosphate (dAMP, 1 mM) were dissolved in potassium phosphate buffer (10 mM, pH 7.6) with and without the presence of 50 mM KBr and irradiated at RT (§2.6.2). HPLC chromatographic separation was achieved using a flow rate of 0.6 ml/min, 10 mM formic acid and methanol with a gradient of 3-10% methanol in 8 min, 10-20% in 2 min, 20-50% in 2 min and returning to starting conditions over 0.1 min.

2.6.4 *Reaction of thymine and cytosine radicals with nitric oxide*

Thymine, thymidine (dT), cytosine and 2′-deoxycytidine (dC) (0.5 mM) were dissolved in sodium phosphate buffer (10 mM, pH 7.4). Solutions were saturated with N_2O and then irradiated at a dose rate of 13 Gy/min with and without continuous bubbling with ~1.8 μM $^{\bullet}NO$ (§2.6.2) at RT. Chromatographic separation of products was achieved with a flow rate of 0.5 ml/min, 10 mM formic acid and methanol with a gradient of 3-8% methanol in 7 min and 8 – 20% in 2 min for thymine; 8-25% methanol in 7 min for dT; and 3-8% methanol in 7 min and 8-25% in 3 min for dC, all then returning to starting conditions over 0.1 min. Products arising from the oxidation of cytosine were separated by isocratic elution with 3% methanol, 97% 10 mM formic acid. Mass spectrometry was used in ES^+ mode with a cone voltage of 22 or 30 V.

Thymidine monophosphate (dTMP) and 2′-deoxycytidine monophosphate (dCMP) (1 mM) were dissolved in sodium phosphate buffer (10 mM, pH 7.4). Solutions (1 ml, 1 mM) were irradiated up to 260 Gy in the presence of ~1.8 μM $^{\bullet}NO$ at RT (§2.6.2). Separation of products used a gradient of 3 – 8% methanol in 7 min, 8 – 20% in a further 2 min and then returning to starting conditions in 0.1 min with a flow rate of 0.5 ml/min. Mass spectra were recorded in ES^+ mode with a cone voltage of 20 or 25 V and ES^- mode with a cone voltage of 16 V.

2.6.5 *Reaction of oligonucleotide radicals with nitric oxide*

Oligonucleotides (GCGCGC) were dissolved in water (300 μM) and aliquots were stored at –20 °C. Solutions were defrosted just before irradiation and diluted further in water (90 μl, 100 μM) and saturated with N_2O before irradiation. Where required, a mixture of ~0.9 μM $^{\bullet}NO$/~24.5 mM N_2O was passed over the top of the solution throughout the irradiation period (20 min, 13 Gy/min). Following irradiation, samples were split into 2 x 45 μl; one was mixed with 50 μl 10 mM formic acid for immediate HPLC analysis and one was retained for enzymatic digestion. Micrococcal nuclease P1 (≥ 200 U/mg protein) was dissolved in sodium

acetate (50 mM) and zinc chloride (5 mM) at pH 5.5 to give a 150 µg/ml solution (~30 U/ml). Aliquots were stored at –80 °C. Oligonucleotide solutions (45 µl, 100 µM) pre- or post-irradiation were mixed with nuclease P1 (3.45 µl, 150 µg/ml) and incubated for 40 min at 50 °C. Samples were then placed on ice and the enzyme inhibited by the addition of 50 µl 10 mM formic acid. Chromatographic separation of products from a 10 µl injection volume was achieved with a flow rate of 0.5 ml/min and 10 mM ammonium formate, 10 mM formic acid and methanol with a gradient of 97-62% ammonium formate/0-31% formic acid/3-7% methanol in 6 min, 62-0% ammonium formate, 31-50% formic acid/7-50% methanol in 7 min and returning to starting conditions over 0.1 min. Retention times were compared to those obtained from the reaction of single nucleotides with •OH in the presence of •NO.

2.6.6 *Measurement of the melting temperature of duplex DNA*

Calf thymus DNA was dissolved in water (0.5 mg/ml). Unbuffered solutions were saturated with N_2O or •NO (~3.6 µM)/N_2O (~20 mM) and irradiated (260 Gy, 13 Gy/min) at RT with continuous bubbling. •NO was then removed by bubbling with N_2. DNA solutions were diluted 10 fold with 15 mM sodium chloride/1.5 mM sodium citrate at pH 7. The differential optical absorption (260 nm–(800-820 nm)) was measured using a photodiode array spectrophotometer (Hewlett Packard, 8453) equipped with a Peltier cell heater with a slow increase in temperature (30-90 °C, ~2 °C/min). Temperature was plotted against optical absorption at 260 nm normalised to the absorbance at RT and the melting curve of duplex DNA (T_m) calculated from a sigmoidal fit of the data.

2.6.7 *Measurement of plasmid strand breaks under anoxic conditions in the presence and absence of •NO*

Conditions were established so that 99% •NO reacted with •OH-induced DNA radicals. DNA concentration was calculated based upon single nucleotides. The stock concentration of plasmid in µg/µl was initially determined using the optical absorbance at 260 nm where an

OD of 1 is equivalent to a concentration of 50 µg/ml of double stranded DNA (Sambrook and Russell 2001). The molar concentration of plasmid single nucleotides was then calculated using the function:

$$[\text{PUC18 (M)} = \left(\frac{\text{mass plasmid (g)}}{(\text{vol solution (l)} \times \text{Mwt PUC18 } (1.746 \times 10^6))} \right) \times (\text{number of bases (5372)})$$

Taking into account known rate constants, the ratio of reactivity of $^{\bullet}OH$ with all the components of the irradiation solutions could be calculated as shown (Table 2-4).

reactant	k ($^{\bullet}OH$) ($M^{-1}\ s^{-1}$)	[reactant] (M^{-1})	k (s^{-1})	%	rate constant reference
plasmid	8.0×10^8	1×10^{-3}	8.0×10^5	88	(Scholes *et al.* 1969)
$^{\bullet}NO$	1.0×10^{10}	9×10^{-7}	9×10^3	1	(Seddon *et al.* 1973)
Tris	1.5×10^9	1×10^{-4}	1×10^5	11	(Hicks and Gebicki 1986)

Table 2-4 Competition reactions between plasmid DNA, $^{\bullet}NO$ and Tris buffer for reaction with $^{\bullet}OH$.

PUC18 was diluted in Tris buffer (0.1 mM, pH 8) just before irradiation to give a concentration of 0.32 µg/µl (0.98 mM). Solutions in glass inserts in 2 ml glass vials fitted with re-sealable caps were saturated with N_2O for 5 min at RT before passing $^{\bullet}NO$ (~0.9 µM) balanced with N_2O over the top of the samples where required. Following irradiation at increasing doses (1 Gy/min), 3 µl was removed with a gas tight syringe, added to 9 µl of 10 mM Tris at pH 8 and maintained on ice. Irradiated samples were diluted with Tris buffer (10 mM) to a concentration of 0.3 mM PUC18. To a 9 µl sample, 2.4 µl loading buffer (40% sucrose, 0.025% bromophenol blue, 0.025% xylene cyanol, 5 mM EDTA, pH 8) was added. 6 µl was loaded onto an agarose gel (1%) and electrophoresed (Bio-Rad mini-gel) at RT (8

V/cm, 2 h) in running buffer (89.2 mM Tris base, 89 mM boric acid, 2 mM EDTA, pH 8). Following electrophoresis, gels were stained with ethidium bromide (10 µg/ml in running buffer) for up to 1 h at RT and visualized by fluorescence over a UV lamp. Bands in the gel were quantified using Quantity One software (Bio-Rad). In order to account for variations in gel loading, each lane was quantified individually. The intensities of supercoiled DNA bands were adjusted to account for the fact that ethidium bromide binds to this form of DNA with only 70% efficiency of that for the other forms (Hodgkins *et al.* 1996). The percentage of supercoiled DNA was plotted on a logarithmic scale against a linear scale of dose and data analyzed by non-linear least squares and the fitting function $y = Ae^{-bx}$ (A = intercept, b = slope).

2.6.8 *Detection of 2′-deoxy-8-azaguaaosine monophosphate (8azadGMP) following irradiation of plasmid DNA*

PUC18 (0.27 µg/µl, 0.83 mM) was diluted in 0.1 mM Tris-HCl at pH 8 and saturated with N_2O. Solutions were irradiated at RT in the presence of a constant flow of ~1.8 µM •NO (§2.6.2) for 60 min (13 Gy/min). Following irradiation, an equal volume of buffer was added (5 mM $ZnCl_2$, 50 mM sodium acetate, pH 5.5) along with nuclease P1 (1.5 U/ml) and incubated at 50 °C for 50 min. The reaction was stopped by placing the mixture on ice. 8AzadGMP was detected using HPLC equipped with fluorescence detection. Chromatography used a Gemini column (150 x 3 mm, 3 µm, 35 °C) with a flow rate of 0.5 ml/min. Separation was achieved using 10 mM potassium dihydrogen orthophosphate, 5 mM TBAOH, 10% methanol at pH 9 with a linear gradient of 0–55% of 75% acetonitrile in 7 min, 55-100% in 1 min, returning to starting conditions over 0.1 min. 8AzadGMP was detected by fluorescence (Ex 280, Em 390 nm) using a 5 µl flow cell and identified by co-elution with that prepared from the irradiation of dGMP in the presence of •NO.

2.6.9 Conversion of •NO-associated DNA products into SSB by enzymatic excision

Formamidopyrimidine-DNA glycosylase (Fpg protein) identifies and excises 8oxoG, FaPyG, possibly FaPyA and 5,6-dihydropyrimidine base modifications and breaks the adjoining nucleotide bond to form a SSB. Fpg protein was tested to see if it could excise •NO-induced DNA modifications. PUC18 plasmid (1 mM) was γ-irradiated (~5 Gy) in N_2O-saturated solution (~25 mM) or in the presence of •NO (~0.9 µM)/N_2O (~24 mM) (~10 Gy) in Tris buffer (0.1 mM, pH 8) at RT. Following irradiation, samples were placed on ice and diluted to 47 ng/µl plasmid in 10 mM Tris, pH 8. 10 µl plasmid solutions were precipitated with 1 µl 3 M sodium acetate in 30 µl ice cold ethanol for 30 min at –20 °C. Samples were spun (17760 g, 30 min, 4 °C) and the pellet air dried for 30 min at RT. DNA was resuspended in activation buffer (20 µl, 0.5 mM EDTA, 0.1 M KCl, 40 mM Hepes, 0.5 mM dithiothreitol, 0.2 mg/ml BSA, pH 8 with KOH) with or without the addition of 1 µl of Fpg (21 ng/µl). Samples were incubated with Fpg at 37 °C for 1 h then enzyme activity was stopped with 3 µl 0.5 M EDTA and placed on ice. Loading buffer was added (5 µl) and 15 µl samples electrophoresed as above. The percentage supercoiled DNA was calculated as described above and the slope of the dependence of the relative amount of supercoiled DNA on dose, calculated assuming linearity, was used to determine the ratio of enzyme induced SSB to prompt SSB (Gulston *et al.* 2002).

$$\text{Base damage : SSB} = \frac{\text{yield SSB (enzyme-induced)} - \text{yield SSB (heat)}}{\text{yield SSB (heat)}}$$

2.7 Radiosensitization by nitric oxide - DNA damage and repair

2.7.1 Clonogenic survival assay

V79-4 cells were grown to confluence or harvested in exponential growth and suspended in PBS at ~5 x 10^5 cells/ml. Small samples were fixed in 70% ethanol and stored at

–20 °C for measurement of cell cycle status (§2.2.5). Following gas saturation, cell suspensions were irradiated at 0.5 Gy/min for up to 5 Gy at RT. Approximately 2 ml samples were removed after each dose and placed on ice. Irradiated cells were kindly counted by Mick Woodcock (University of Oxford) using a FACS Vantage flow cytometer equipped with a Sort Enhancement Module (Becton Dickinson, UK) into triplicate 25cm^2 tissue culture flasks (~250–750 cells) containing EMEM. Cells were grown for 7 days at 37 °C. Colonies were fixed with 75% methanol and stained with methylene blue (1% w/v in water). Surviving fraction (SF) was calculated by counting the number of colonies (>50 cells) and dividing by the number of cells plated. SF were then corrected by dividing by the plating efficiency (calculated by measuring the SF of un-irradiated but gas bubbled cells).

2.7.2 *Irradiation of cells for measurement of γH2AX staining by flow cytometry*

V79-4 cell suspensions (15 ml PBS at 3-5 x 10^5 cells/ml) were deoxygenated and irradiated (5 Gy, 0.5 Gy/min) at RT in sealed glass syringes (§2.5.2). Samples were placed on ice and spun (5 min, 1500 g, 4 °C). Pellets were resuspended in EMEM at RT (3.2 ml) and plated (0.5 ml, ~7 x 10^5 cells) with EMEM (2 ml) into 6 well plates at 37 °C. Between 30 min and 4 h after plating, cells were scraped into the medium in a single well and spun as above. Cell pellets were fixed in 70% ethanol and stored at –20 °C.

Fixed cells were warmed to RT then spun (200 g, 5 min) to remove the ethanol and washed with 2% FCS in PBS (0.5 ml). The cell pellet was then incubated with anti-phospho histone H2AX (100 µl, Table 2-1) in 2% FCS/PBS) for 1 h at RT. Cells were washed as above then the secondary antibody Alexa Fluor 488 (100 µl, Table 2-1) in 2% FCS/PBS was added (1 h, RT) and kept out of the light. Cells were washed once more and DNA stained with PI containing RNase as described above. Cells were analysed within 24 h using a FACScan flow cytometer (Becton Dickinson) running CellQuest software. 10,000 cells were counted and analyzed using WinMDI software (http://facs.scripps.edu/software.html), gated for G1 – G2 cell cycle status. A histogram was created from a dot plot of PI fluorescence

against γH2AX fluorescence, and the average green fluorescence, indicating γH2AX foci formation, was measured and normalized to control levels.

2.7.3 *Irradiation of cells for measurement of γH2AX foci using confocal microscopy*

V79-4 cell suspensions (15 ml PBS at 3-5 x 10^5 cells/ml) were deoxygenated and irradiated (2 Gy) in sealed glass syringes (§2.5.2). Samples were placed on ice before centrifuging (5 min, 200 g, 4 °C). Pellets were resuspended in 0.5 volumes of EMEM and plated plated onto glass cover slips attached to glass sided dishes at 37 °C for 30 min to 24 h. Attached cells were washed with PBS and fixed in 1 ml cold 3% paraformaldehyde (PFA) in PBS and stored at 4 °C for up to 2 weeks. Fixed cells on glass dishes were washed with 1 ml PBS (3 x 5 min) and lysed with 1% Triton X-100 in PBS (0.5 ml x 10 min). Cells were washed again (1 ml PBS 3 x 5 min) and the non-specific protein binding was blocked with 1 ml 1% bovine serum albumin (BSA), 1% fish skin gelatin (FSG) in PBS for 1 h at RT before incubation with anti-phospho histone H2AX (200 µl) (Table 2-1) in 1% BSA/1% FSG, 4 °C, overnight or 1 h RT. Cells were washed again and incubated with Alexa Fluor 488 (150 µl in 1% BSA/1% FSG) (Table 2-1) for 1 h in the dark at RT. Cells were then washed with a further 1 ml PBS (3 x 5 min). Cells were mounted under glass coverslips with a drop of Vectashield containing DAPI to stain the nuclei and stored at 4 °C in the dark. Foci were measured within a few days using a Biorad confocal microscope equipped with a x40 oil objective. Foci were counted using ImageJ software (http://rsbweb.nih.gov/ij/).

2.7.4 *Irradiation of cells for staining with anti-RAD51 antibodies*

V79-4 cell suspensions (15 ml PBS ~5 x 10^5 cells/ml) were deoxygenated and irradiated (10 Gy, 1.6 Gy/min) in sealed glass syringes (§2.5.2). Following irradiation, samples were placed on ice then centrifuged (5 min, 200 g, 4 °C). Pellets were resuspended in 5 ml EMEM and 1 ml plated onto glass cover slips attached to glass sided dishes in 2 ml EMEM at 37 °C for 4 - 24 h. Cells were then washed with PBS and fixed in cold (0.5 ml) 3%

PFA/0.1% Triton X-100 in PBS for 15 min. Cells were then washed once again with PBS (3 x 10 min) and stored in 1 ml PBS at 4 °C for up to 2 weeks before staining. Cells were incubated in PBS/0.3% Triton X-100 (0.5 ml, 10 min) then non-specific protein binding was blocked with 3% BSA (0.5 ml, 40 min). Cells were incubated with the primary antibody, mouse anti-RAD51 (Table 2-1) (200 µl) in 3% BSA, 4 °C, overnight or 1 h at RT. Cells were washed again and incubated with the secondary antibodies (Table 2-1) (200 µl, in 3% BSA 1 h, RT). Cells were then washed with a further 1 ml PBS (3 x 5 min) and mounted, stored and analysed (§2.7.3).

2.7.5 Irradiation of HF-19 cells for co-staining with anti-53BP1 and anti-cyclin A

HF-19 cell suspensions (15 ml PBS ~3 x 10^5 cells/ml) were deoxygenated and irradiated (2 Gy) in sealed glass syringes (§2.5.2). Cells were spun (5 min, 200 g) and the pellet resuspended in EMEM to a cell density of ~9 x 10^5/ml. 1 ml cell suspension was added to 2 ml medium, pre-warmed to 37 °C in glass dishes and incubated for 4-6 h at 37 °C. Cells were then washed with 1 ml PBS and fixed in 3% PFA and kept at 4 °C for up to a week before antibody incubation.

Fixed cells were washed with 1 ml PBS (3 x 5 min) and lysed with 1% Triton X-100 in PBS (0.5 ml x 10 min) then washed again (1 ml PBS, 3 x 5 min). Non-specific protein binding was blocked with 1 ml 1% BSA/1% FSG in PBS for 1 h at RT. Cells were incubated with primary antibodies against 53BP1 and cyclin A (Table 2-1) (200 µl in 1% BSA/1% FSG, 4 °C, overnight). Cells were washed with 1 ml PBS (3 x 5 min) and incubated with secondary antibodies (Table 2-1) (150 µl in 1% BSA/1% FSG, 1 h, RT) and then washed once more. Cells were mounted, stored and analysed as described above (§2.7.3).

2.7.6 Measurement of cellular glutathione after bubbling cells in suspension

V79-4 cells in suspension in PBS (~5 x 10^5/ml) were bubbled slowly for 30 min with N_2 as described above (§ 2.5.2). Where required the gas was then changed to 1% (~18 µM)

•NO balance N_2 for 20 min. N_2 flow was then replaced for a further 5 min to ensure that •NO_2 could not be formed upon reoxygenation of the cell suspensions, which would deplete the cells of GSH. Following gas bubbling, cells were placed in a 15 ml conical tube and counted using a haemocytometer. Samples of ~5 x10^5 cells were spun (200 g, 5 min) and resuspended in metaphosphoric acid (MPA) (5% w/v) containing EDTA (1 mM) and stored at 4 °C for up to 24 h or at -20 °C for longer periods. Cell suspensions were thawed where required, spun (5 min, 1500 g) and 2 x 0.2 ml placed in Eppendorf tubes. To each sample was added 12.5 µl 0.1 mM mercaptoethanol, 12.5 µl 10 mM monobromobimane and 0.125 ml 2 M Tris base/1 mM EDTA, mixed and left for 15 min in the dark. Reactions were stopped by the addition of 25 µl 6 M HCl and potential contaminating HPLC peaks removed by extracting in 0.25 ml dichloromethane. Chromatography used a 250 x 4.6 mm Hypersil 5ODS column (Hichrom, Reading, UK). Separation used a linear gradient comprising A: 40 mM ammonium phosphate, 10 mM phosphoric acid, 5 mM octane sulphonic acid and B: 75% acetonitrile and B was varied from 10-40% over 10 min with a flow rate of 2 ml/min. GSH was measured by quantifying with authentic GSH using fluorescence spectroscopy equipped with a 16 µl flow cell at excitation wavelength 398 nm, emission wavelength 476 nm.

2.7.7 Effect of glutathione depletion on cellular radiosensitivity

Buthionine sulphoxide (BSO) (0.1 mM) was added to exponentially growing V79-4 cells for 16 h. The following day cells were harvested by trypsin digestion (§2.5) and resuspended in PBS (5 x 10^5/ml) and a 1 ml sample removed, spun down (5 min, 17600 g), fixed in 5% MPA/1mM EDTA and stored at –20 °C for analysis (§2.7.6) to check that GSH levels had been depleted. The cell suspensions were saturated with N_2 (§2.5.2) and irradiated (5 Gy, 0.5 Gy/min). Cells were plated (§ 2.7.2) for 0.5, 1, 2, 4 and 6 h and then processed for γH2AX analysis by flow cytometry as described above (§ 2.7.2).

2.7.8 Alkaline comet assay for determination of frank and repair-induced SSB

To ensure that cellular SSB were not induced by trypsin, V79-4 cells were removed from flasks by scraping. Cells were spun (5 min, 200 g) and re-suspended in PBS (~1 x 10^5/ml) and degassed by bubbling slowly with N_2 and then with 1% (~18 µM) $^{\bullet}NO$ where required. Cells were irradiated in glass capped glass syringes (1 Gy) at RT then immediately placed on ice. Samples were spun (200 g, 4 min) and resuspended in an equal volume of EMEM (1 x 10^5/ml) and kept on ice to prevent DNA repair. Samples (0.25 ml) were mixed with 1% low melting point agarose (1 ml) and 1 ml was added to pre-prepared frosted slides. (The slides were prepared by pre-coating with 0.8 ml 1% normal melting point agarose, a coverslip added and the slides placed on a tray on ice to set, the coverslip was then removed and the slides left to dry overnight). To the cells in agarose on the slides a coverslip was added and the slides placed on a metal tray on ice to set. For cell samples used for Fpg glycosylase digests, 100 µl cell suspensions was mixed with 80 µl normal melting point agarose and placed on ice to set. For DNA repair studies slides were placed in a humidified box at 37 °C with coverslips and after 0-1 h were placed on ice, the coverslip removed and the cells lysed in lysis buffer (2.5 M NaCl, 100 mM EDTA, 10 mM Tris base, 1% DMSO, 1% Triton X-100, pH 10.5) for at least 1 h at 4 °C. Alternatively, for studies of dose effect or glycosylase digests the coverslips were immediately removed from the slides once the agarose was set and the cells lysed as above. For the glycosylase digestion the slides were then washed in 3 x 1 ml for 5 min in enzyme activation buffer (§2.6.9) and 50 µl 1.05 ng/µl Fpg added, and the coverslip replaced. Slides were incubated in a humidified box for 30 min at 37 °C then removed, placed on ice and washed (3 x 1 ml PBS). All slides once prepared were placed in an electrophoresis tank and the DNA allowed to unwind for 30 min in cold electrophoresis buffer (300 mM NaOH, 1 mM EDTA, 1% DMSO) out of light. Samples were then electrophoresed for 25 min (25 V, 300 mA) and washed (1 ml, 3 x 5 min) in neutralization buffer (500 mM Tris-HCl, pH 8), washed with Millipore Synergy water (1 ml)

and left to dry overnight. Slides were rehydrated with Millipore Synergy water (1 ml) for 30 min before staining with SyBr Gold (1 ml, 1:10000) in Millipore Synergy water for 30 min. Excess stain was removed by washing briefly in water. Slides were dried overnight before analysis using a comet detection system developed by the Technology Development Group, University of Oxford. Results were expressed as comet tail moment (Kent *et al.* 1995).

2.8 Release of nitric oxide from bioreductively activated pro-drugs

2.8.1 Measurement of the reaction of pro-drugs with reducing radicals

NONOate pro-drugs (50 µM) were dissolved in sodium formate (0.1 M) containing sodium phosphate buffer (5 mM, pH 7.4). Solutions (10 ml) were saturated with N_2 or N_2O for 15 min and irradiated in glass syringes at various dose rates determined using Fricke dosimetry (§2.3.1). At regular intervals samples were removed into vials for HPLC analysis. Separation was achieved with a RPB column (100 x 3.2 mm, 5 µm) (Hichrom, Reading) with a flow rate of 1 ml/min and a linear gradient comprising 10 mM formic acid and methanol. The products from the reduction of NF-DEANO were separated with a gradient of 15 - 70% methanol in 7 min returning to starting conditions over 0.1 min and detected at 314 nm. The products from the reduction of NB-DEANO were separated with a gradient of 30 – 80% methanol in 5 min returning to starting conditions over 0.1 min and detected at 262 nm. The products from the reduction of NI-DEANO were separated with a gradient of 20 – 70% methanol in 7 min returning to starting conditions over 0.1 min and detected at 314 nm.

2.8.2 Release of •NO following reduction of pro-drugs by reducing radicals

Pro-drugs (10 mM) were dissolved in DMSO and stored at 4 °C. Solutions of the pro-drugs (50 µM containing ± ~70 mM DMSO) were made in sodium formate (0.1 M) containing sodium phosphate buffer (5 mM, pH 7.4). Samples (1.5 ml) were saturated with N_2 in 2 ml brown vials with re-sealable septa. Solutions were irradiated at 14.1 Gy/min at 1 min

intervals up to 5 min at RT. Samples were removed from the irradiator carefully to ensure that minimal disruption of the solution and head space in the vial occurred and left for 30 min before measuring dissolved •NO by chemiluminescence and loss of the pro-drugs by HPLC (§ 2.8.1).

•NO was measured using a chemiluminescence detector (Sievers Model 280 nitric oxide analyzer; Analytix Ltd., UK) as described previously (Folkes and Wardman 2004). Calibration of the detector used the formation of •NO from the reaction of sodium nitrite with potassium iodide (Eq. 2-16).

$$2\,KI + 2NaNO_2 + 2H_2SO_4 \rightarrow 2^{\bullet}NO + I_2 + 2H_2O + 2Na_2SO_4. \qquad (2\text{-}16)$$

Potassium iodide (KI, 5 ml, 0.1 M) in sulphuric acid (0.1 M) was placed in a glass vessel equipped with a Perspex cap containing a small hole. The solution was gassed with N_2 for 5 min to remove O_2 and then the cap pushed down into the solution to remove the headspace. Sodium nitrite (5 µl of 5 mM) was injected through the hole into the KI solution which was mixed with a glass magnetic flea. After ~1 min 50 µl of the solution was removed with a gas-tight syringe and injected into the •NO analyzer into a glass bubbler containing PBS (5 ml) bubbled with N_2. Dissolved •NO in the solutions was displaced and carried into the detector by the stream of inert N_2. The reaction of gaseous •NO with ozone forms excited state $^{*}NO_2^{\bullet}$ (Eq. 2-17), which decays to ground state emitting light (Eq. 2-18).

$$^{\bullet}NO + O_3 \rightarrow {}^{*}NO_2^{\bullet} + O_2 \qquad (2\text{-}17)$$

$$^{*}NO_2^{\bullet} \rightarrow NO_2 + h\nu. \qquad (2\text{-}18)$$

Infra-red (~1100 nm) emission from $^{*}NO_2^{\bullet}$ is detected by a thermoelectrically cooled, red-sensitive photomultiplier tube. Sensitivity of the technique is ~1 pmole in liquid samples. The signal is recorded in mV and the area under the curve is linearly proportional to •NO concentration. Sodium nitrite was re-injected a further 4 times to generate a calibration curve and the curve was repeated 3 times and calibration performed on a daily basis. An average of

the areas under the curves was calculated, and a linear regression fitted. Following calibration of the detector, samples of the irradiated pro-drugs (50 µl) were injected to measure the concentration of radiation-released •NO.

2.8.3 Reduction of NF-DEANO by sodium dithionite

NF-DEANO (50 µM) in potassium phosphate buffer (10 mM, pH 7.6) was placed in a glass vial equipped with a re-sealable septa and saturated with N_2 through a stainless steel needle. Sodium dithionite was prepared in N_2-saturated Millipore Synergy water (~3-6 mM) and N_2-flow was continued in all solutions throughout the studies. The stock concentration of sodium dithionite solid was measured using $\varepsilon_{315\ nm}$ = 8043 M^{-1} cm^{-1} (Yousafzai and Eady 2002). Sodium dithionite solution (~0-70 µM) was added to anaerobic NF-DEANO and samples removed for HPLC analysis (§2.8.1) using a gas-tight syringe.

2.8.4 Reduction of NF-DEANO by P450 reductase supersomes

NADPH dependent supersomes containing P450 reductase were used to study the enzymatic reduction of NF-DEANO. Supersomes were stored in aliquots at -80 °C, thawed in a 37 °C water bath, then immediately placed on ice. A solution of sodium phosphate buffer (1.5 ml, 0.25 M, pH 7.4) containing EDTA (100 µM) and NADPH (80 µM) was deoxygenated by gassing with N_2 for 15 min at 37 °C in a 4 ml vial equipped with a re-sealable septum. Supersomes (30 µl) were added and N_2 flow continued over the top of the solution for a further 2 min. NF-DEANO (8 µl of a 10 mM stock in DMSO) was then injected to give a final concentration of 50 µM and solutions were left to incubate at 37 °C. Every 5 min 50 µl was removed with a gas tight syringe for •NO analysis and a further 50 µl removed and mixed with the same volume of acetonitrile for HPLC analysis. The precipitated protein was removed (5 min, 11450g) and NF-DEANO measured as described above (§ 2.8.1).

2.8.5 Effect of oxygen on the reduction of pro-drugs by HepG2 cells

HepG2 cells contain reductase enzymes and they were used to study cellular reduction of the pro-drugs. Cells were harvested by trypsin digestion and suspended in PBS at ~9 x 10^6 cells/ml. The cells were passed through a 19G needle to encourage the formation of single cells as HepG2 cells have a tendency to clump. Cell suspensions (1 ml) were placed in 10 ml glass vials fitted with Suba Seal rubber septa. Cell suspensions were deoxygenated by flowing N_2, N_2/0.25% O_2, N_2/0.5% O_2 or N_2/1% O_2 or 0.2% O_2, 5% CO_2/N_2 over the top of the solutions for 15 min on ice with occasional swirling to help the gas exchange. The pro-drug was then added (5 µl of a 10 mM stock in DMSO), mixed and 50 µl removed with a gas-tight syringe onto ice for HPLC analysis, and the remaining cells placed at 37 °C. Gas flow was continued and every 10 min a further 50 µl was removed. An equal volume of acetonitrile was added to each sample before centrifuging (5 min, 11450 g). The supernatant was analysed by HPLC as described above (§ 2.8.1).

2.8.6 Radiosensitization of V79-4 cells following reduction of NF-DEANO by supersomes

V79-4 cells (~3.5 x 10^5/ml) were suspended in PBS and saturated with N_2 for 30 min at RT in glass bubbling towers equipped with 25 ml glass syringes. DMSO (20 µl) was added to control and supersome control cells with a gas tight syringe and NF-DEANO (20 µl, 10 mM stock in DMSO) was added to drug control and drug + supersomes cells. NADPH (80 µl, 10 mM) and supersomes (50 µl, 1300 nmole/(min x mg) protein) were finally added and the cells bubbled slowly with N_2 for a further 5 min. Cells were then drawn into glass syringes, a small sample removed onto ice, the syringes sealed with glass caps and placed at 37 °C in a humidified incubator for 30 min. A further sample was then removed for measurement of the loss of NF-DEANO by HPLC. Cell suspensions were irradiated at 0.5 Gy/min for up to 5 Gy at RT. Following irradiations ~2 ml samples were removed and placed on ice. Irradiated cells were plated for clonogenic assays (§2.7.1).

To show that the reduction of NF-DEANO by P450 reductases produces •NO and it is this which adds to the radiosensitizing effects of NF-DEANO, V79-4 cells (2 x 3 x 10^5/ml) were saturated with N_2 and incubated with supersomes for 30 min as described above. Following incubation, one sample of the cells were re-bubbled with N_2 for 10 min to remove any generated •NO and then both samples were irradiated. An additional 2 ml sample was removed into polypropylene tubes after 2 Gy for DNA damage measurements. Irradiated cells (0-5 Gy) were plated for clonogenic survival assays (§2.7.1). The 2 Gy samples were spun (200 g, 5 min) and resuspended in 4 ml EMEM. 1 ml (~1.5 x 10^5 cells) was plated onto glass cover slips attached to glass sided dishes for 2-6 h. Cells were washed with PBS (1 ml) and fixed in 3% PFA (1 ml). Cells were stained and counted for γH2AX (§2.7.3).

2.8.7 Radiosensitization of HepG2 cells by NF-DEANO

HepG2 cells were suspended in PBS (~1 x 10^7/ml). Samples (1.5 ml) were saturated with N_2 in 10 ml glass vials fitted with Suba Seal rubber caps by passing a flow of N_2 over the surface of the cell suspension for 15 min at RT. NF-DEANO or DMSO (6 µl, 10 mM stock to give a 40 µM solution) were then added with a gas-tight syringe.

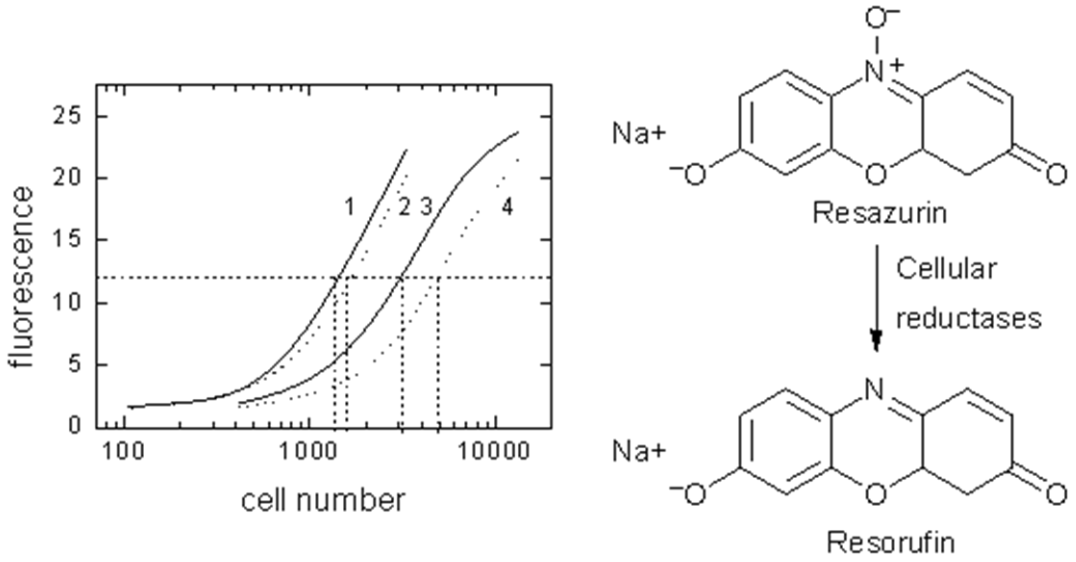

Figure 2-3 Representation of the method used to calculate relative survival from number of cells plated to give ~50% proliferation, where 1 – control 0 Gy, 2 – drug 0 Gy, 3- control 8 Gy, 4-drug 8 Gy. Also shown is the molecular change which occurs when non-fluorescent resazurin is reduced to fluorescent resorufin by viable cells.

A small sample was removed for HPLC analysis, gas flow was stopped and the cell suspensions placed at 37 °C for 30 min. A further 50 µl sample was then removed for measurement of the loss of NF-DEANO by HPLC. Cell suspensions were irradiated up to 10 Gy at 0.5 Gy/min and 100 µl samples removed onto ice after each dose. Cells were plated into 96 well plates (200 µl) in DMEM at serial dilutions of maximum ~3 x 10^4 cells/well (8-10 Gy) and ~4 x 10^3 cells/well (0-6 Gy).Cells were grown for 9 days, medium removed and viability measured using a resazurin assay. 100 µl resazurin (10 µg/ml in DMEM) was added for up to 3 h at 37 °C before measuring the fluorescence (Ex 544, Em 590 nm) of the reduced resazurin (resorufin) in the wells using a plate reader (POLARstar Omega, BMG Labtech). Relative proliferation was calculated by measuring the number of cells which had been plated to give the mid-point fluorescence intensity of the curve relative to the number of cells plated for the control cells at 0 Gy (Figure 2-3).

2.9 Reactions of tyrosine radicals

2.9.1 Analysis of tyrosine metabolites

Samples were analysed by HPLC. Chromatography used a Hydro RP column (Phenomenex, 3.0 x 150 mm, 4 µm). Separation was achieved with 10 mM formic acid and methanol, with a gradient of 0 - 20% methanol over 5 min or 0% for 3 min then 0 – 80% methanol over 3 min returning to starting conditions over 0.1 min with a 0.8 ml/min flow rate. Products were monitored at 280 nm and dityr was detected using fluorescence at Ex 294 Em 401 nm with a 5 µl flow cell. Dityrosine standard was prepared as described previously (Bartesaghi *et al.* 2010). It was purified by HPLC from 100 µl injections and the combined extracts freeze-dried overnight. The dried solid was redissolved in 20 mM sodium phosphate buffer, pH 7.4 and the concentration determined using ε_{315} = 5700 cm M^{-1}.

2.9.2 Oxidation of tyrosine using γ-radiolysis

Tyr (0.5 mM) was dissolved in a small volume of NaOH (0.5 M), diluted in phosphate buffer alone (1-10 mM, pH 7.4) (for reactions with $^{\bullet}OH$), with the addition of sodium azide (50 mM) (for reactions of $N_3^{\bullet}$), sodium nitrite (5 mM) (for reactions of $^{\bullet}NO_2$) or potassium bromide (50 mM) (for reactions of $Br_2^{\bullet-}$). The pH of solutions was adjusted to 7.4 with $HClO_4$. Solutions (3 ml) were saturated with N_2O ± 20% or 10% O_2 (~20 mM N_2O/~260 µM O_2 or ~22.5 mM N_2O/~130 µM O_2) or N_2O (~25 mM). For reactions involving $^{\bullet}NO$, solutions were bubbled with N_2O (~24.5 mM)/$^{\bullet}NO$ (~1.8 µM) throughout the irradiation period (§2.2). All solutions were irradiated (13 Gy/min) up to 70 Gy at RT. Data were plotted against radical input approximating that in N_2O-saturated solutions ~0.6 µM radicals are generated/Gy.

2.9.3 Measurement of nitrite formation

Following irradiations, tyr solutions which had been irradiated in the presence of $^{\bullet}NO$, were bubbled with N_2 to remove remaining $^{\bullet}NO$. The loss of tyr and formation of dityr were measured as described above (§2.9.1). Nitrite was then measured in the same solutions by HPLC with absorption at 214 nm, calibrated with authentic sodium nitrite. Chromatography utilized an ACE column (3 µm, 3.0 x 125 mm) maintained at 35 °C with analytes separated with isocratic elution using 10 mM potassium dihydrogen phosphate, 5 mM TBAOH and 4% acetonitrile and a flow rate of 0.5 ml/min.

2.10 Measurement of the reaction of hydroxyurea with horseradish peroxidase

Reactions between hydroxyurea (HU) and horseradish peroxidase (HRP) were performed using a double mix stopped-flow spectrophotometer (HiTech Scientific) maintained at 25 or 37 °C. Initially HRP (1.7 µM, determined using $\varepsilon_{402} = 1.02 \times 10^5\ M^{-1}\ cm^{-1}$ (Dunford 1999)) was mixed with an equal concentration of H_2O_2 (determined using $\varepsilon_{240} = 39.4\ M^{-1}\ cm^{-1}$(Nelson and Kiesow 1972)) for 1 s before HU was sequentially added (final

concentration 50-250 µM) in potassium phosphate buffer (10 mM, pH 7) and the rate of formation and decay of HRP compound II measured at 418 nm. An average of 5 transients was obtained and a first order exponential fit made to the data using Kinetic Studio software. A second order rate constant was obtained by fitting linear regression to the observed first order rate constants obtained for each concentration of HU.

2.11 Measurement of the oxidation of hydroxyurea with hydroxyl radicals

Hydroxyurea (1 mM) was dissolved in potassium phosphate buffer (10 mM, pH 7.6) and 20 ml solutions were saturated with N_2O. Solutions were irradiated (13.9 Gy/min) and samples periodically removed for LCMS analysis. Samples (25 µl) were mixed with acetonitrile (75 µl) and analysed for hydroxyurea concentration using LCMS monitoring in single ion mode at *m/z* 77.1 (M+H). Separation used a SeQuant ZIC-HILIC column (3.5 µm, 100 Å, 100 x 2.1 mm, Hichrom, UK) with a flow rate of 0.25 ml/min and isocratic elution with 15% 10 mM formic acid/85% acetonitrile.

3 Reaction of nitric oxide with radiation-induced DNA base radicals

3.1 Introduction

Ionizing radiation induces a plethora of damage to cellular DNA. The types, abundance and proximity of lesions to other sites of damage, which include base damage, AP sites, SSB and DSB, determine the ultimate outcome for the cell, be it death by apoptosis, mitotic cell death or necrosis, survival or mutation. Apart from direct damage resulting from IR, and indirect effects involving reactions of DNA with $^{\bullet}OH$, the surrounding microenvironment can change the types and severity of damage occurring (as discussed in §1.3). In particular O_2, a long established radiosensitizer, can increase DNA damage. The vast majority of $^{\bullet}OH$ induce damage to the bases, and a recent review describes the types of chemistry occurring with and without the presence of O_2 (Dizdaroglu and Jaruga 2012). Some base damage induced in the presence of O_2 is different to that induced in its absence. The reaction of O_2 with base $^{\bullet}OH$-adduct radicals formed during IR forms peroxyl radicals which may abstract protons from adjoining sugar molecules causing strand breaks (Bamatraf *et al.* 1998) and these reactions may be partially responsible for the radiosensitizing effects of O_2. $^{\bullet}NO$ radiosensitizes cells at least as efficiently as O_2 and reacts with uracil and dGMP $^{\bullet}OH$-adducts at near diffusion controlled rates (Wardman *et al.* 2007), similar to equivalent reactions with O_2. However, unlike O_2, as $^{\bullet}NO$ is a free radical with one unpaired electron, its reaction with radiation-induced radicals forms diamagnetic non-radical species, thus preventing further chain reactions and may in some instances protect against the formation of radiation damage in DNA. Potential products formed on reaction of $^{\bullet}NO$ with base radicals have not as yet been identified.

The aim of this project was to identify, using HPLC with mass spectrometry and UV-visible spectroscopy, some of the base modifications of nucleobases, nucleosides, nucleotides and short oligonucleotides arising from γ-radiation in N_2O-saturated solutions in the presence of •NO. The identification of specific modifications to these DNA components may help to understand in part, how •NO acts as a hypoxic cell radiosensitizer.

Unless otherwise stated, in all of the studies discussed in this project, samples were saturated with N_2O with or without the presence of a constant supply of ~1.8 μM •NO during irradiations, the latter by continuously bubbling samples with 10% (of 1%) •NO mixed with 90% N_2O. Sections 3.2 and 3.7 are largely described in (Folkes and O'Neill 2013a); section 3.3 is largely described in (Folkes and O'Neill 2013b).

3.2 Reaction of nitric oxide with •OH-induced guanine radicals

It has previously been shown using pulse radiolysis that •NO reacts with •OH-induced dGMP radicals in N_2O-saturated solution extremely rapidly, with a second order rate constant of 2×10^9 M^{-1} s^{-1} at pH 5.1 (Wardman *et al.* 2007), although the identity of the products from the reaction was not established. Knowledge of the modifications which occur may offer some insight into the mechanisms by which •NO may modify any guanine radicals induced during radiosensitization.

Guanine is rather insoluble in water and so the majority of studies in this project were carried out using 2′-deoxyguanosine monophosphate (dGMP). The products which were identified from the oxidation of dGMP by •OH in N_2O-saturated solutions in 10 mM phosphate buffer at pH 7.4 (Figure 3-1A) include 2,6-diamino-4-hydroxy-5-formaidopyrimidine monophosphate (FaPydGMP) identified by *m/z* 366.0 (M+H) and its UV-visible spectrum (Figure 3-1C, (Hems 1958)), guanine and 7,8-dihydro-8-oxoguanine (8oxodGMP), identified by its UV-visible spectrum (Figure 3-1C) (Kasai and Nishimura 1984) and *m/z* 364.1 (M+H). The presence of ~1.8 μM •NO during γ-radiation at pH 7.4

significantly reduced the yields of 8oxodGMP and FaPydGMP to the limits of detection, whereas the yield of guanine was unaffected (Figure 3-1B). However, two new major products were observed (Figure 3-1B, products **1** and **2**), both of which show *m/z* 346.9 (M-H), but their UV-visible spectra are significantly different (Figure 3-1D).

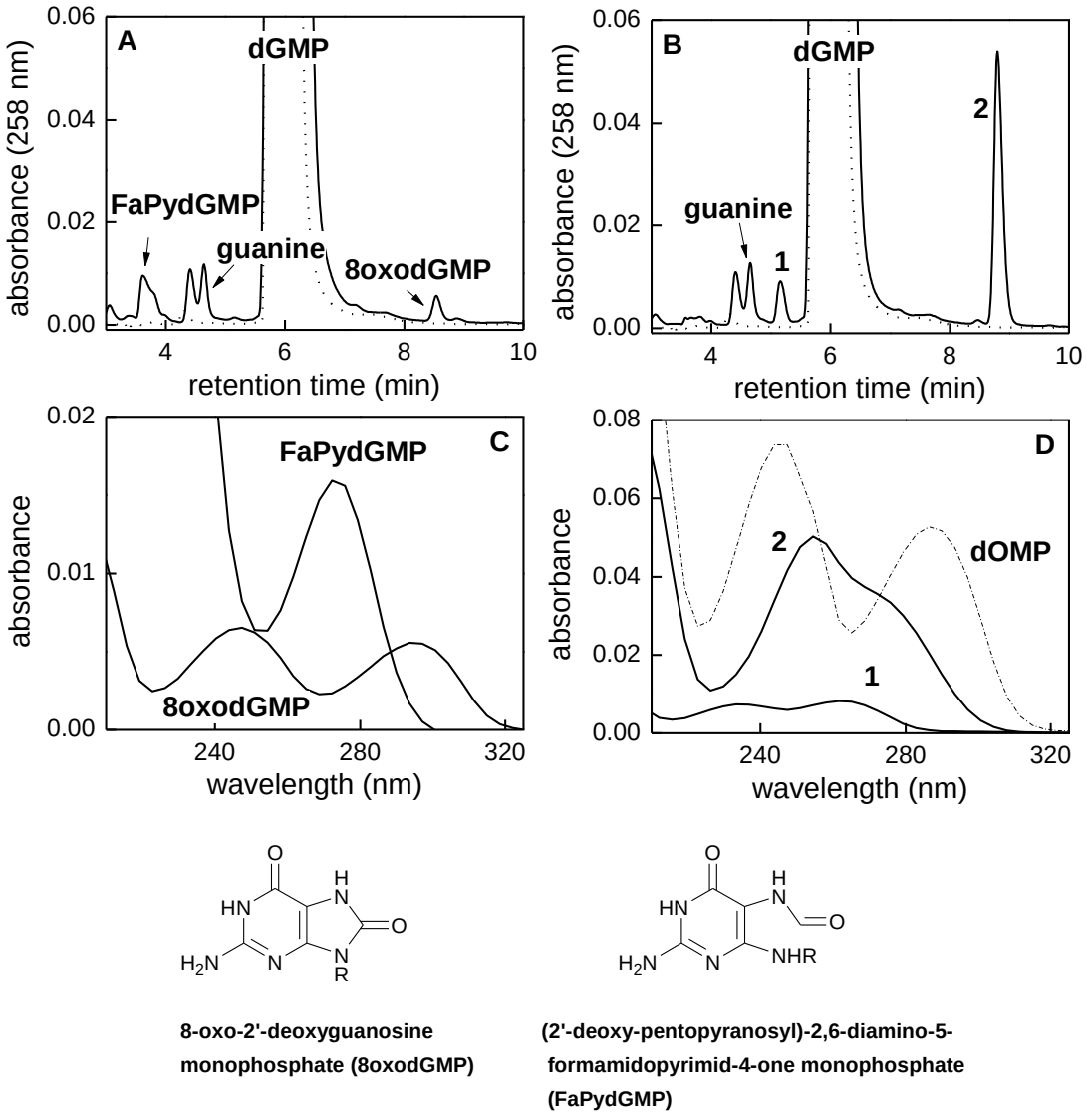

Figure 3-1 (A) HPLC chromatogram showing the oxidation of 1mM dGMP by •OH in N_2O-saturated 10 mM phosphate buffer at pH 7.4, after 260 Gy (dotted line 0 Gy); (B) in the presence of 1.8 µM •NO; (C) optical absorption spectra of the major •OH-induced oxidation products of dGMP and (D) in the presence of 1.8 µM •NO, together with the UV-visible spectra of 2'-deoxyoxanosine (dOMP) shown for comparison to product 2. Chromatography comprised a gradient of 3-8% methanol, 97% 10 mM formic acid-92% 10 mM ammonium formate over 8 min, 8-20% methanol, 92-80% ammonium formate in 2 min, 20-50% methanol, 80-50% ammonium formate in 0.5 min, returning to starting conditions over 0.1 min. Reprinted (with minor modification) from *Free Radical Biology & Medicine*, Vol 58, Lisa K. Folkes and Peter O'Neill, Modification of DNA damage mechanisms by nitric oxide during ionizing radiation, 14-25, Copyright (2013), with permission from Elsevier.

3.2.1 Identification of product 1

Product **1**, formed from the reaction of •OH with dGMP in the presence of •NO, elutes with the same retention time as 2′-deoxyxanthosine monophosphate (dXMP) which formed from the reaction of dGMP with nitrous acid, a deamination reaction known to produce 2′-deoxyxanthosine from 2′-deoxyguanosine (Suzuki *et al.* 1996). Product **1** has a *m/z* of 346.9 (M-H) which corresponds to a molecular weight of 347.9, the same as for dXMP. The UV-visible spectrum (Figure 3-1D) has similar λ_{max} values as those reported for 2′-deoxyxanthosine (Vongchampa *et al.* 2003).

The structure of the xanthine moiety of dXMP (2′-deoxyxanthosine monophosphate) is shown in Figure 3-2. Xanthine is a deamination product of guanine moieties, induced through nitrosation reactions (Nguyen *et al.* 1992; Caulfield *et al.* 1998). It is a commercially available compound and the knowledge that it can be formed from guanine in nitrosating conditions helped to further confirm the identity of product **1** as dXMP (see §3.2.3).

3.2.2 Identification of product 2

Product **2** formed from the oxidation of dGMP by •OH in the presence of •NO was a more challenging compound to identify. It has been reported that reaction of dG with acidified nitrite in aerated solution (pH 3.7), where the primary oxidant is likely to be NO^+, $•NO_2$ or N_2O_3, forms two major products, dX and 2′-deoxyoxanosine (dO) (Suzuki *et al.* 1996). Both dX and dO have a molecular weight of 348 Da, so it was initially thought that these are also the two products (but the phosphorylated forms) formed from the reaction of dGMP-•OH adducts with •NO. However, despite product **2** and 2′-deoxyoxanosine monophosphate (dOMP) being extremely difficult to separate by chromatography and exhibiting the same molecular weight, they have different UV-visible spectra (Figure 3-1D).

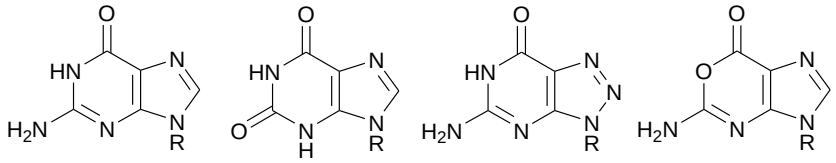

Figure 3-2 Structures of 2′-deoxyguanosine monophosphate (dGMP), product 1 (2′-deoxyxanthosine monophosphate (dXMP)), product 2 (8-aza-2′-deoxyguanosine monophosphate (8azadGMP)) and 2′-deoxyoxanosine monophosphate (dOMP). R = 2′-deoxyribose monophosphate.

Initial thoughts without considering the chemistry which might occur to form product **2** from dGMP-•OH adducts reacting with •NO, were that a N to O substitution at N-3 may occur, in a similar manner as is seen for dOMP, where N to O substitution occurs at N-1 (Figure 3-2). With the kind help of Dr. Robert Paton (University of Oxford), calculations were carried out to predict the UV-visible spectrum of this molecule if this transformation had indeed happened. The predicted spectrum was very different to the actual spectrum of **2** and therefore the identity remained unclear. Generation of **2** in higher yields by irradiating 100 ml of dGMP in 10 mM phosphate buffer at pH 7.4 in the presence of a constant flow of ~1.8 µM •NO/~24.5 mM N_2O for 1 h at ~13 Gy/min, concentrating by freeze drying and purifying by HPLC was carried out. An accurate mass of *m/z* 347.0525 (M-H) was obtained from the purified solid, which has a close correlation to a theoretical isotope model of $C_9H_{12}N_6O_7P_1$ (347.0505) and compatible with 8-aza-2′-deoxyguanosine monophosphate (8azadGMP) (Figure 3-2). Conversion of a benzimidazole to a benzotriazole has been identified through nitration by $•NO_2$ (Kaiya *et al.* 2004). The mechanism was suggested to proceed through the formation of 1-nitrobenzimidazole; however, the details were unclear. The authors suggested that conversion of guanine to 8-azaguanine may occur in cells following reaction with peroxynitrite. The proposal for the conversion occurring by reaction of •NO with guanine-•OH adducts has not previously been discussed.

3.2.3 Reaction of guanine radicals with nitric oxide

8-Azaguanine (8azaG) and xanthine (X) are both commercially available compounds. If guanine radicals react with •NO in the same way as they react with dGMP radicals, then the products from the reaction should co-elute with the standard compounds. Guanine base is not very soluble, so solutions were made by initially dissolving guanine in a small volume of NaOH before adjusting the pH to 8.1 with $HClO_4$. The pH could not be lowered below 8.1, or the concentration of guanine increased above 0.3 mM, without it coming out of solution.

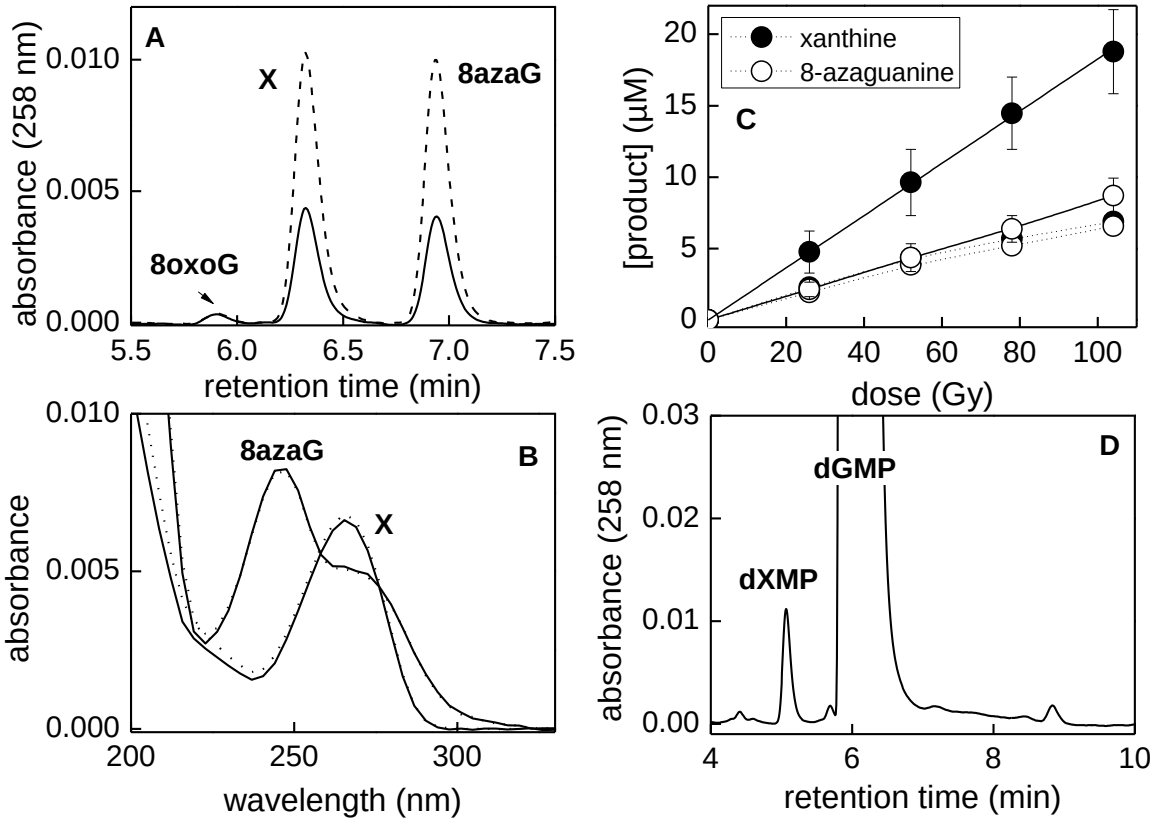

Figure 3-3 (A) Chromatogram showing the oxidation of guanine (0.3 mM) by •OH in the presence of ~ 1.8 μM •NO (~ 104 Gy) (solid line) spiked with xanthine (X) and 8-azaguanine (8azaG) (dashed line). Chromatography conditions used a gradient of 10 mM formic acid with 3-8% methanol in 7 min, 8-20% in 2 min and, returning to starting conditions after 0.1 min; (B) UV-visible spectra of X and 8azaG formed from above with the spectra of the authentic compounds superimposed (dotted lines). (C) Yield of xanthine and 8-azaguanine from the oxidation of guanine (0.3 mM) by •OH in 10 mM phosphate buffer in the presence of ~1.8 μM •NO; dotted line pH 8.1, solid line pH 8.4; (D) Chromatogram showing the formation of dXMP from the oxidation of dGMP (1 mM) by $Br_2^{\bullet-}$ in 10 mM phosphate buffer, pH 7.4 (260 Gy). Chromatography conditions were as described in Figure 3-1. A, B and D reproduced (with minor modification) from *Free Radical Biology & Medicine*, Vol 58, Lisa K. Folkes and Peter O'Neill, Modification of DNA damage mechanisms by nitric oxide during ionizing radiation, 14-25, Copyright (2013), with permission from Elsevier.

The products formed in the reaction of G with •OH at pH 8.1 in the presence of •NO co-elute with xanthine and 8azaG standards (Figure 3-3A) and exhibit identical UV-visible spectra with the respective standards (Figure 3-3B). The product which co-elutes with 8-azaguanine exhibits a *m/z* of 153.04 (M+H), indicative of a structural change of guanine from (C-8(H)) to N. The yields of both X and 8azaG increase with dose with ~6.5 µM being formed after a dose of 100 Gy in N_2O-saturated solution at pH 8.1 (Figure 3-3C). At pH 8.4, the yield of 8azaG was not significantly changed but the yield of X increased to ~18.7 µM for 100 Gy (Figure 3-3C). The mechanisms for formation of these products from •OH-adducts of G/dGMP in the presence of •NO are discussed in §3.2.5.

3.2.4 Studies into the conditions required for the formation of 2′-deoxyxanthosine monophosphate and 2′-deoxy-8-azaguanosine monophosphate

It became apparent during the studies described in this thesis that pH and the presence of inorganic phosphate in radiolysis experiments had an effect on the products observed. When dGMP is oxidised by •OH in the presence of •NO at pH 7.4 in 10 mM phosphate, dXMP and 8azadGMP are formed (Figure 3-1). However, when $Br_2^{\bullet-}$ was used as the oxidant in the same conditions, but also in the presence of 50 mM KBr, only dXMP was identified (Figure 3-3D). These results suggest that dXMP and 8azadGMP are formed from the reaction of •NO with different radical intermediates, but that dXMP forms through a common intermediate of the oxidation of dGMP by either •OH or $Br_2^{\bullet-}$. The yield of dXMP from reactions of dGMP with •OH and $Br_2^{\bullet-}$ in the presence of ~1.8 µM •NO in N_2O-saturated solution was inversely proportional to phosphate concentration at pH 7.4 (Figure 3-4A, B and D), although the yield of dXMP in 1 mM phosphate from oxidation by $Br_2^{\bullet-}$ was ~60% less than that formed from the same reactions with •OH (Figure 3-4D). In addition, when dGMP was oxidised by •OH in the presence of •NO, the yield of dXMP (HPLC peak area) was unchanged from pH 5-6.5 but rapidly rose at higher pH (Figure 3-4C).

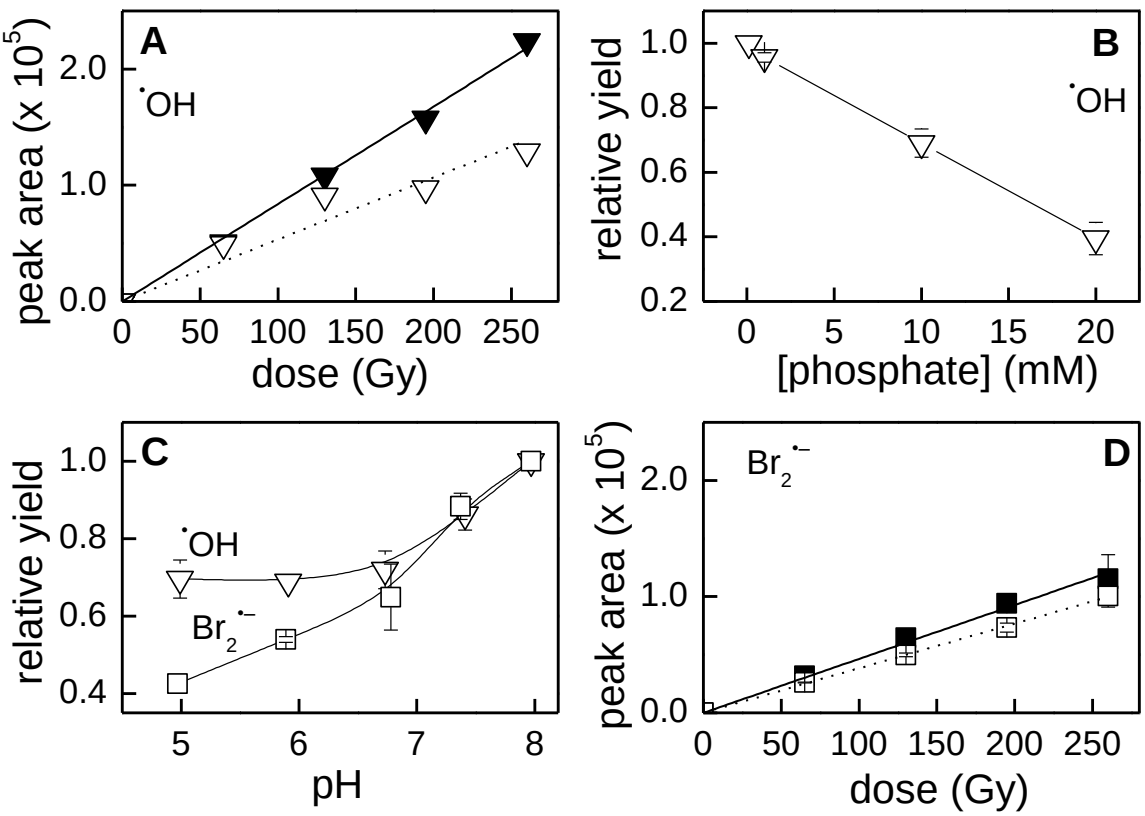

Figure 3-4 Yield of dXMP following the **o**xidation of dGMP by •OH (1mM dGMP) or $Br_2^{\bullet-}$ (3 mM dGMP) at pH 7.4 in the presence of ~ 1.8 µM •NO (13 Gy / min) A: dose dependence from •OH oxidation in 1mM (▼) or 10 mM (▽) phosphate; B: effect of phosphate concentration on •OH-induced formation (normalized to 0.1 mM phosphate) (260 Gy); C: effect of pH (195 Gy); D: dose dependence from $Br_2^{\bullet-}$ oxidation in 1mM (■) or 10 mM (□) phosphate. Relative yield is expressed as peak area of each product divided by the maximum peak area for that product.

When $Br_2^{\bullet-}$ was used as the primary oxidant, the yield of dXMP also increased with a rise in pH, although the response was more gradual over the pH range (Figure 3-4C). Reaction of dGMP with •OH, but not $Br_2^{\bullet-}$, in N_2O-saturated solution forms 8oxodGMP and FaPydGMP, and both of these products are derived from the C-8(•OH) adduct (Dizdaroglu and Jaruga 2012). In the presence of •NO during oxidation of dGMP by •OH, the yields of both 8oxodGMP and FaPydGMP were reduced and 8azadGMP was observed, but the identity of the intermediate radical which may react with •NO is unclear. Phosphate concentration (0.1 – 20 mM) had no effect on the yield of 8azadGMP (Figure 3-5A and B), suggesting once again that 8azadGMP is not formed through the same radical intermediate as dXMP. The

radiolytic yield of 8azadGMP decreased in a pH dependent manner from pH 7.8-4.5 in 10 mM phosphate (Figure 3-5C). In comparison, the yields of 8oxodGMP and FaPydGMP decreased as pH was increased, especially above pH 7 (Figure 3-5D).

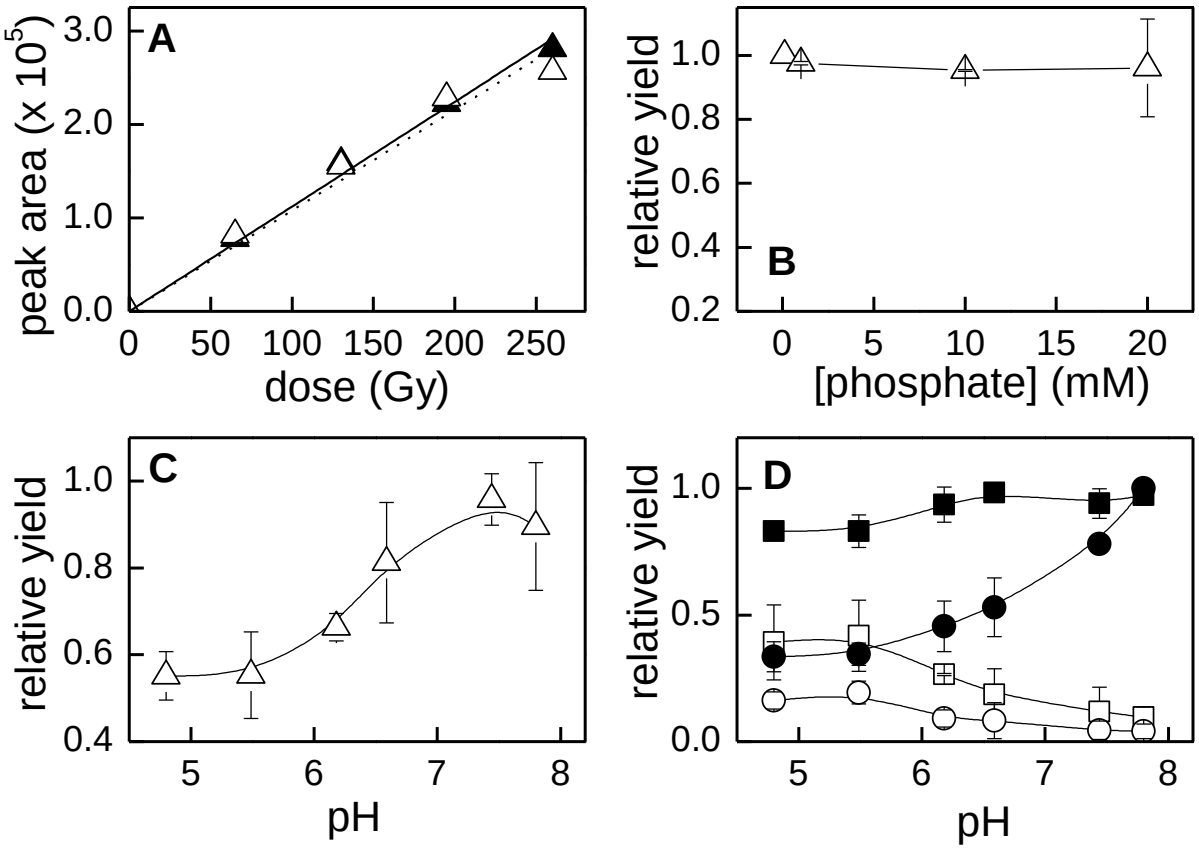

Figure 3-5 Yield of 8azadGMP following the **o**xidation of dGMP (1mM) by •OH at pH 7.4 in the presence of ~1.8 µM •NO (13 Gy / min) A: dose dependence in 1mM (△) or 10 mM (▲) phosphate; B: effect of phosphate concentration (normalized to 0.1 mM phosphate) (260 Gy); C: effect of pH in 10 mM phosphate (195 Gy); D: Effect of pH on the yield of 8oxodGMP (●,○), and FaPydGMP (■, □) in the absence (closed symbol) and presence of •NO (open symbols) (195 Gy) in 10 mM phosphate. Reproduced (with minor modification) from *Free Radical Biology & Medicine*, Vol 58, Lisa K. Folkes and Peter O'Neill, Modification of DNA damage mechanisms by nitric oxide during ionizing radiation, 14-25, Copyright (2013), with permission from Elsevier.

3.2.5 Proposals for the mechanisms involved in the formation of 2′-deoxyxanthosine monophosphate and 2′-deoxy-8-azaguanosine monophosphate

Reactions of dG/dGMP with •OH have been investigated over many years, but the mechanisms involved are still not completely understood. First investigated by pulse radiolysis (O'Neill 1983; O'Neill and Chapman 1985), reaction of dG/dGMP with •OH

produces radical adducts, with ~65% forming a mildly oxidising radical on C-4 and ~17% of ˙OH on C-8 to form a reducing radical (Candeias and Steenken 2000). Despite the low yield, it is the C-8(˙OH) intermediate which is responsible for the formation of the major products, (FaPyG and 8oxoG), observed from the reaction of G/dG/dGMP with ˙OH (Scheme 3-1) (Dizdaroglu and Jaruga 2012).

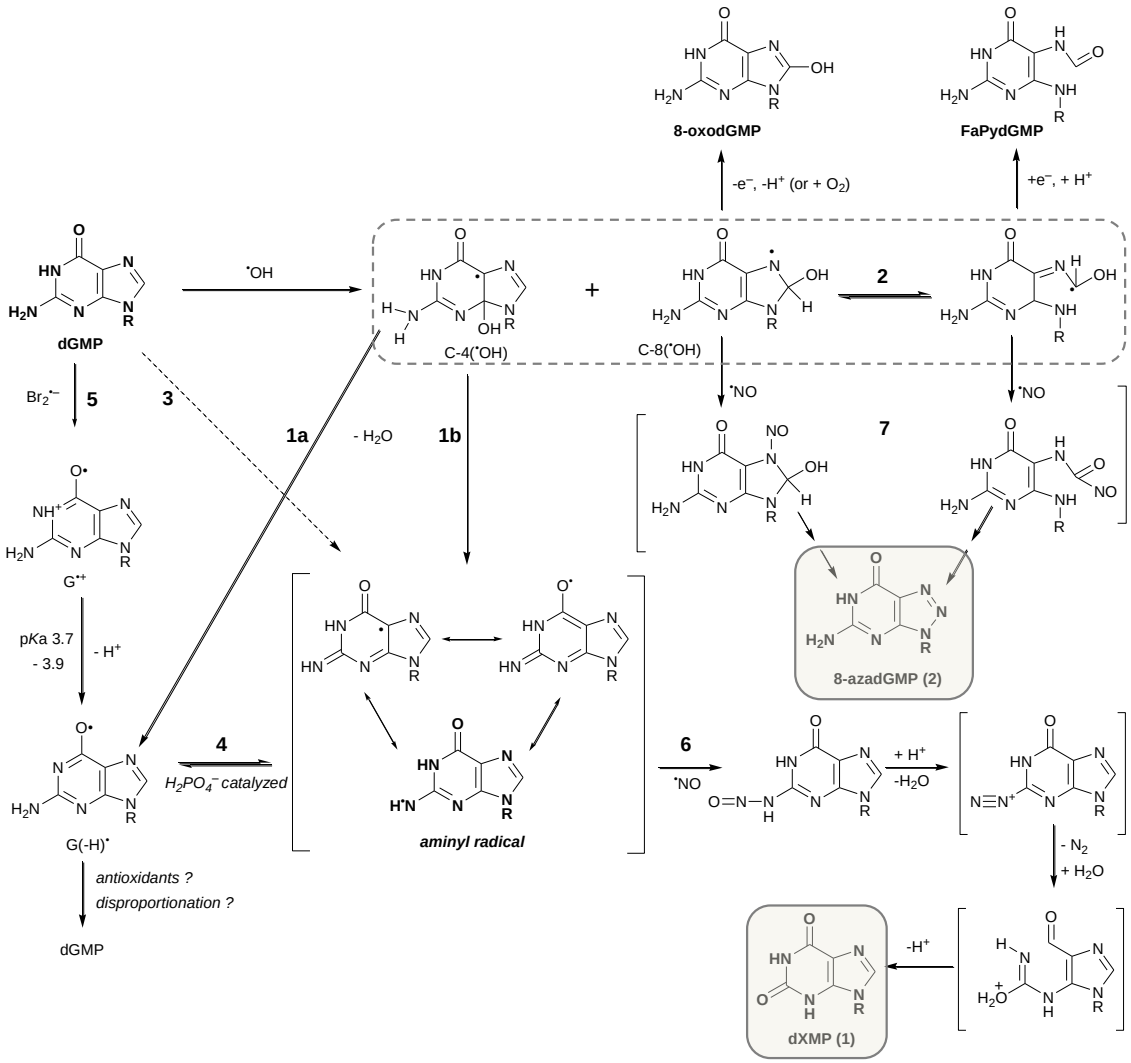

Scheme 3-1 Proposed mechanisms for the oxidation of dGMP by $Br_2^{\bullet-}$ or ˙OH and the formation of dXMP (1) and 8azadGMP (2) from the presence of nitric oxide. The various mesomeric forms of the aminyl radical are shown but other radicals have been drawn in one form only for simplicity.

Dehydration of the C-4(˙OH) adduct was originally thought to lead to a more strongly oxidising radical G(-H)˙ (Scheme 3-1, reaction 1) (Candeias and Steenken 2000). Recently it

was suggested from re-evaluation of the formation of G(-H)• (Chatgilialoglu *et al.* 2009; Chatgilialoglu *et al.* 2011), that •OH may abstract a H-atom from the primary amine on C-2 of guanosine/dG (Scheme 3-1, reaction 3), rather than forming an •OH-adduct at C-4. An aminyl radical, identified by the broad absorption centred at 610 nm, was suggested to form, which in a water-catalysed reaction tautomerises to G(-H)• (Scheme 3-1, reaction 4), shown by the loss in absorption at 610 nm. However, H-atom abstraction from an aromatic amine by •OH is widely disputed (Adhikary *et al.* 2006; Naumov and von Sonntag 2008; Phadatare *et al.* 2011; Dizdaroglu and Jaruga 2012). The mechanism under dispute may reflect the consequences of phosphate present in the reaction solutions.

Previously it has been proposed that dGMP C-4(•OH) adducts, monitored by pulse radiolysis, absorb with a broad band between ~500 and 680 nm in water. The decay of this absorption monitored at 600 nm was dependent on phosphate concentration at pH 7.3 with a second order rate constant of $k = 2 \times 10^7$ M^{-1} s^{-1} (Wardman and Clarke 1985), although the reasons for this phosphate effect were not established at the time. In other studies it was found that the C-4(•OH) adduct of dG, monitored at 620 nm and with a similar broad absorption, also decays in a phosphate dependent manner with a second order rate constant of $k = 6.7 \times 10^7$ M^{-1} s^{-1} (pH 7) (Candeias and Steenken 2000). However, in more recent studies, the loss of absorbance at 620 nm following the reaction of the guanine moiety of guanosine with •OH was attributed to the tautomerisation of the aminyl radical to G(-H)•, and assigned a rate constant of $k = 2.3 \times 10^4$ s^{-1} in water (Chatgilialoglu *et al.* 2009).

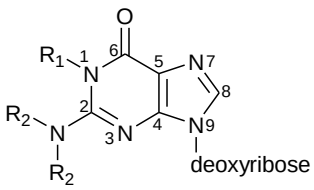

Figure 3-6 Figure to show the numbering of atoms in guanine moieties.

When C-2 of guanosine (Figure 3-6) was substituted with a diethylamino group (R_2 = CH_3CH_2), where the aminyl radical is not formed as proton abstraction can not occur, the broad absorption centred around 620 nm was not observed (Chatgilialoglu *et al.* 2009). However, substitution of dG at C-1 with a methyl group (R_1 = CH_3) showed absorption at 615 nm following oxidation of dG by $Br_2^{\bullet-}$ in 1 mM phosphate at pH 7.4 (Candeias and Steenken 1989) or by $N_3^{\bullet}$ in 5 mM phosphate at pH 7 (Faraggi *et al.* 1996). This type of substitution will form an aminyl radical on C-2 through the inductive effect of the methyl group. It is proposed that the radical absorption centred around 620 nm (Candeias and Steenken 2000), which was observed from pulse radiolysis studies with dG/dGMP, may be attributed to the aminyl radical rather than the C-4($^{\bullet}$OH) adduct. In the presence of phosphate, the absorption at 620 nm is shorter lived, if seen at all, adding evidence to the proposal that an equilibrium exists between the aminyl radical and G(-H)$^{\bullet}$ which favours formation of G(-H)$^{\bullet}$ in the presence of $H_2PO_4^-$. The aminyl radical is unlikely to arise through direct H-atom abstraction by $^{\bullet}$OH from the amine group as previously discussed (Phadatare *et al.* 2011; Dizdaroglu and Jaruga 2012) but through a rapid dehydration of the C-4($^{\bullet}$OH) adduct, which in pulse radiolysis studies may occur within the time of the electron pulse. Loss of water through reaction 1a or 1b (Scheme 3-1) will give G-(H)$^{\bullet}$ and the aminyl radical, which depending upon phosphate ($H_2PO_4^-$) concentration leads to tautomerisation. This tautomerisation accounts for the presence of the aminyl radical, following oxidation of dGMP by $Br_2^{\bullet-}$ proceeding initially through the formation of G(-H)$^{\bullet}$ (Scheme 3-1, reaction 4). In low phosphate and high pH, the equilibrium favours the aminyl radical. It is hypothesised that the previous rate constant attributed to the dehydration of the C-4($^{\bullet}$OH) adduct (k = 6 x 10^3 s^{-1}, pH 7.6 in water (Candeias and Steenken 2000)) can now be assigned to the equilibrium 4 between G(-H)$^{\bullet}$ and the aminyl radical. The rate constant is similar to that proposed for the tautomerisation reaction of guanosine (Chatgilialoglu *et al.* 2009).

Previously it was shown that 2′-deoxyxanthosine (dX) is formed through the reaction of acidified nitrite with dG (Suzuki *et al.* 1996). A mechanism was proposed where the deamination of dG is through the formation of a diazonium intermediate on the primary amine (Suzuki *et al.* 2000). This type of mechanism was also proposed for the formation of xanthine from the reaction of 1-nitro-3-acetonitrile with DNA (Lucas *et al.* 2001) Theoretically, combination of •NO with the aminyl radical could progress through the same type of diazonium intermediate, leading to deamination and formation of xanthine (X) (Scheme 3-1, reaction 6). The ability of •NO to 'fix' the aminyl radical, forming X/dXMP in a pH- and phosphate-dependent manner has allowed this new hypothesis of phosphate-catalysed tautomerisation between the aminyl radical and G(-H)• to be proposed. As phosphate reduces the radiolytic yield of dXMP, it is proposed that only the aminyl radical reacts with •NO to form dXMP (Scheme 3-1, reaction 6). With a pK_a of 6.9 for the $H_2PO_4^-/HPO_4^{2-}$ equilibrium (Candeias and Steenken 2000) the data obtained in this study show a good dependence upon yield of dXMP with $H_2PO_4^-$ availability; the increase in yield of dXMP with a decrease in phosphate concentration at pH ~7 (Figure 3-4B) and decrease in yield with a decrease in pH at a fixed concentration of 10 mM phosphate (Figure 3-4C) is consistent with the reduced efficiency of the phosphate-catalysed tautomerisation of the aminyl radical by HPO_4^{2-} (3.5 x 10^7 M^{-1} s^{-1} (Candeias and Steenken 2000)) compared with $H_2PO_4^-$ (1.8 x 10^8 M^{-1} s^{-1} (Candeias and Steenken 2000)). The increase in yield of X but not 8azaG from the oxidation of G with •OH in the presence of •NO in N_2O-saturated solution at pH 8.4 compared to pH 8.1 (Figure 3-3C) also supports the results observed with dGMP.

dGMP is oxidised by both •OH and $Br_2^{\bullet-}$ radicals, forming the same highly oxidising G(-H)• radical, but through different radical intermediates (Scheme 3-1, reactions 1 and 5). dGMP is oxidised by $Br_2^{\bullet-}$ (k = 4 x 10^7 M^{-1} s^{-1}, pH 7, (Willson 1974)) initially forming the radical cation, $G^{\bullet+}$, which then decays to G(-H)• (Scheme 3-1, reaction 5). In comparison, reaction with •OH leads mainly to C-4(•OH) adducts to form either G(-H)• or aminyl radicals

through dehydration (Scheme 3-1 reaction 1a and 1b respectively), which is now proposed to occur within <1 μs, in contrast to previous assignments to the dehydration through loss of absorption at around 620 nm where k = 6 x 10^3 s^{-1}, pH 7.6 in water (Candeias and Steenken 2000) .

As 8oxoG and FaPyG arise from the C-8(•OH) adduct following 1-electron oxidation or ring opening and one-electron reduction respectively (Scheme 3-1, reaction 2) they are not observed when $Br_2^{\bullet-}$ is used as the oxidant, as has been observed previously (Candeias and Steenken 2000). In the same manner 8azadGMP is only observed from the oxidation of dGMP by •OH in the presence of •NO and not from $Br_2^{\bullet-}$ in the presence of •NO, therefore it is also likely to result from the C-8(•OH) adduct. Without further analysis it is difficult to be certain mechanistically how 8azaG arises from G (Scheme 3-1, reaction 7); however, the pH curve for the formation of 8azadGMP is very similar to that of 8oxodGMP, which suggests that the ring closed form may be more reactive towards •NO, although ring-opening must occur at some point to allow the structural changes. Conversion of a benzoimidazole to a benzotriazole has previously been investigated as a possible structural modification of guanine following reaction with peroxynitrite (Kaiya *et al.* 2004). Synthesis was by a free radical based mechanism comprising nitrogen dioxide and ozone (*Kyodai* nitration), but mechanisms were not proposed in the study. Whether this modification to guanine occurs in polynucleotides or cellular DNA is unknown but this matter will be addressed in Chapter 4.

3.3 Reaction of nitric oxide with •OH-induced adenine radicals

3.3.1 Adenine base

Adenine (A) has a greater solubility in water than guanine and so studying radiation-induced radical oxidation reactions with the base itself were easier. As with G, the majority of evidence for free-radical mechanisms which occur with A has been established using pulse radiolysis (O'Neill *et al.* 1985; Steenken 1989; Vieira and Steenken 1990). Adenine reacts

with •OH in a similar way to G with adducts formed at various sites on the molecule (Scheme 3-2). The majority of •OH (~50%) yield adducts at C-4 forming a weak oxidant which dehydrates to a neutral, strongly oxidising N-centred radical (k = 1.9 x 10^4 s^{-1} (Vieira and Steenken 1990)). In addition, ~37% of •OH-adducts reside on C-8 to form a reducing radical. In similar mechanisms to those proposed for G, oxidation of this C-8(•OH) adduct by the loss of an electron forms 7,8-dihydro-8-oxoadenine (8oxoA), but also ring-opening can occur followed by reduction, to form 4,6-diamino-5-formamidopyrimidine (FaPyA) (Scheme 3-2).

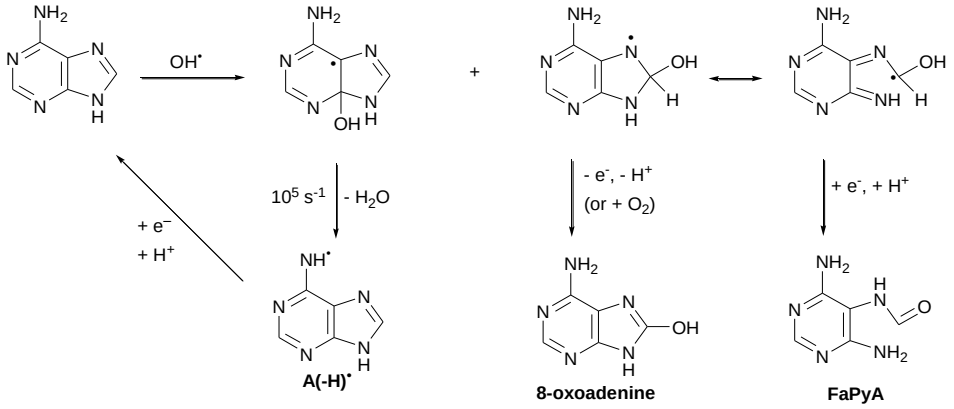

Scheme 3-2 Proposed major mechanisms for the reaction of •OH with adenine base.

When A (0.5 mM) was oxidised by •OH in N_2O-saturated 10 mM phosphate buffer at pH 7.6, using doses of up to 130 Gy, two major products were observed (Figure 3-7A). The first product eluted with a retention time of 2.8 min and could be extracted from a total ion count spectrum with *m/z* of 152.0 (M-H) and is tentatively assigned to FaPyA. The second product, with a retention time of 6.7 min and *m/z* 152.0 (M+H), is assigned to 8oxoA. The presence of ~1.8 µM •NO at pH 7.6 significantly reduced the yield of the peaks tentatively assigned to FaPyA and 8oxoA (Figure 3-7A). In addition, two new products (**3** and **4**), both with molecular weights 1 Da greater than A, were formed.

The chemistry which occurs following reaction of G and A with •OH is very similar (Breen and Murphy 1995; Dizdaroglu and Jaruga 2012); therefore it is likely that reactions

which occur with guanine-•OH adducts and •NO (§3.2) would also occur between •NO and adenine-•OH adducts. If this prediction is correct then hypoxanthine (HX) and 8-azadenine (8azaA) would be expected to be formed. As these compounds are commercially available this concept could be readily tested.

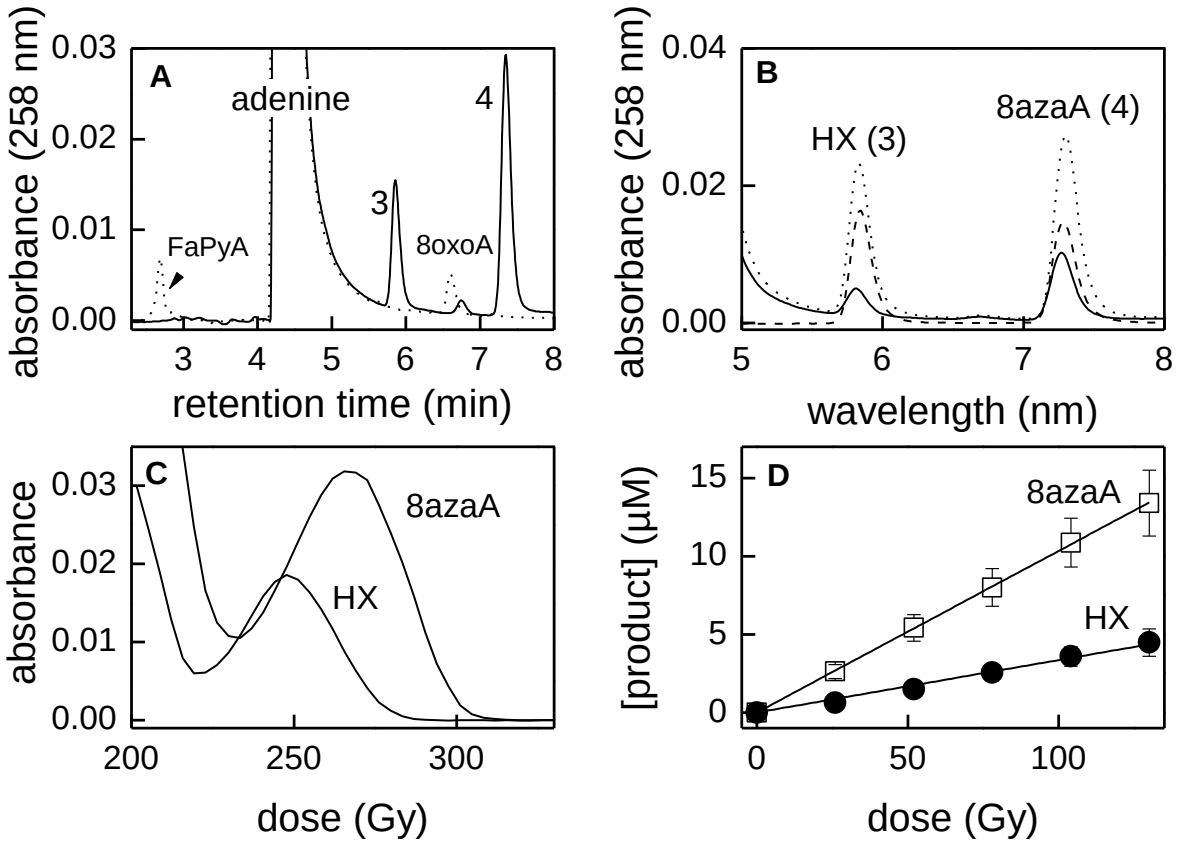

Figure 3-7 (A) Chromatogram monitoring at 258 nm showing oxidation of adenine (0.5 mM) at pH 7.6 in 10mM phosphate buffer by •OH in the absence (…) or presence of ~1.8 µM •NO (---) after 130 Gy. Chromatography conditions used a gradient of 10 mM formic acid with 3-10% methanol in 9 min, returning to starting conditions after 0.1 min; (B) chromatograms showing the co-elution of standards of HX and 8azaA with product 3 and 4. (C) UV-visible spectra of products 3 (hypoxanthine, HX) and 4 (8-azaadenine, 8azaA); (D) Yield of HX and 8-azaA with dose. Reproduced (with minor modification) from *Nitric Oxide*, Lisa K. Folkes and Peter O'Neill, Vol 34, DNA damage induced by nitric oxide is enhanced at replication, 47-55, Copyright (2013), with permission from Elsevier.

3.3.2 Formation of hypoxanthine from •OH reaction with adenine in the presence of •NO

The earlier eluting peak (product **3**, retention time 5.9 min) observed following oxidation of A by •OH in the presence of •NO, exhibits *m/z* of 137.0 (M+H). The product co-elutes with the deaminated form of A, hypoxanthine (HX) (Figure 3-7B), and exhibits the

same UV-visible spectrum as commercially available HX with λ_{max} 250 nm (Figure 3-7C). In addition, product **3** co-elutes with the HX formed when A is treated with acidified nitrite (pH 3.7), a reaction which induces deamination of A. Product **3** is therefore assigned to HX and its yield following γ-radiolysis of A (0.5 mM) in the presence of •NO is linear with dose with a *G* value of 0.034 ± 0.001 μM/Gy (Figure 3-7D). Notably the yield of HX was ~10-fold less following the oxidation of A by $Br_2^{\bullet-}$ in the presence of •NO at pH 7.6, compared to that observed when •OH-induced oxidation occurred (Figure 3-8). The mechanism by which HX is formed in the reaction of •NO with A(-H)• will be discussed further (§3.3.6).

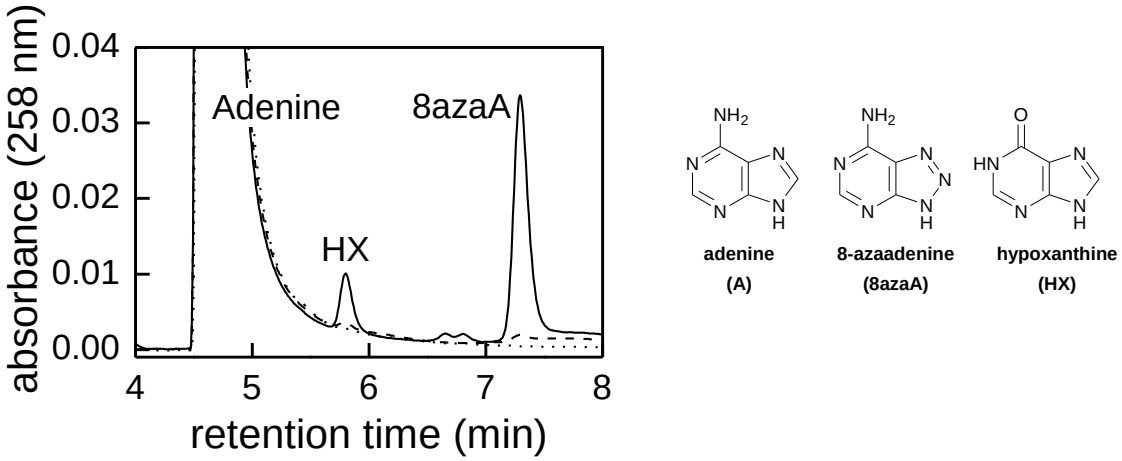

Figure 3-8 Chromatogram to show the formation of HX and 8azaA following the oxidation of adenine (0.5 mM) with •OH (—) or $Br_2^{\bullet-}$ (…) in 10 mM phosphate, pH 7.6 in the presence of ~1.8 μM •NO (195 Gy). Chromatography conditions used a gradient of 10 mM formic acid with 3-10% methanol in 9 min, returning to starting conditions after 0.1 min. Also shown are the structures of adenine and •NO-modified products (R = H).

3.3.3 Formation of 8-azaadenine from •OH reaction with adenine in the presence of •NO

The second eluting peak, (product **4**, retention time 7.3 min) observed following •OH-oxidation of A in the presence of •NO exhibits *m/z* 137.0 (M+H). The UV-visible spectrum of this product is similar to A with λ_{max} 267 nm (Figure 3-7C). The product was not observed when A was treated with acidified nitrite (pH 3.7) or when A was oxidised by $Br_2^{\bullet-}$ in the presence of •NO (Figure 3-8). Product **4** co-elutes with an authentic sample of 8azaA (Figure 3-7B) confirming its identity as 8azaA, in agreement with the corresponding chemistry which

also occurs when G is irradiated in N_2O-saturated solution in the presence of •NO. The yield of 8azaA is linear with dose, with a *G* value of 0.100 ± 0.001 μM/Gy (Figure 3-7D) and is 3-fold greater than the yield of HX.

3.3.4 2′-Deoxyadenosine (dA)

Sugar damage to nucleosides and nucleotides by hydroxyl radicals has been reported to account for only ~20% of total radical damage (von Sonntag 1987). It was therefore assumed that in the main, modifications following irradiation of dA in the presence of •NO will involve interactions with the base. When dA was oxidised by •OH in anoxia at pH 7.6, A, 8oxodA and 8oxoA were observed (Figure 3-9A). The peak assigned to A elutes with the same retention time (3.8 min) and exhibits the same UV spectrum and *m/z* 136 (M+H) as a standard sample of A. The peak assigned to 8oxoA elutes with the same retention time (5.5 min) as observed with 8oxoA following oxidation of A by •OH. The product also exhibits *m/z* 152 (M+H). The peak with a retention time 13.6 min is assigned to 8oxodA with *m/z* 268 (M+H), corresponding to an increase of 16 Da compared to dA. In addition, a fragment value of *m/z* 151 (M+H) was obtained, indicative of the loss of the deoxyribose sugar (- *m/z* 116) upon ionization. A product with a retention time of 3.2 min was also observed which has a *m/z* 270 (M+H) and is tentatively assigned to FaPydA. In the presence of •NO, but in the absence of O_2 at pH 7.5, the yields of A for a dose of ~390 Gy (Figure 3-9A) compared with that when irradiated in anoxia alone are similar, in agreement with the corresponding observations with dGMP (Figure 3-1). The yields of 8oxodA and 8oxoA are reduced to the limits of detection when •NO is present (Figure 3-9A).

The reactions of •NO with the •OH-adducts of dA are expected to be similar to those observed with A, based on the similar reactions seen with G and dGMP (§3.2). 2′-Deoxyinosine (dI) and 2′-deoxy-8-azaadenine (8azadA) would therefore be expected to be formed. HPLC analysis with a gradient of 10 mM formic acid and methanol at a pH of ~2.3 showed the formation of three major products (Figure 3-9A, products **5**-**7**) which increased in

area with increasing doses from 0-130 Gy (Figure 3-9B). None of these products correspond with dI or 8azadA, although a small peak, which represents 8azaA, was observed (Figure 3-9A).

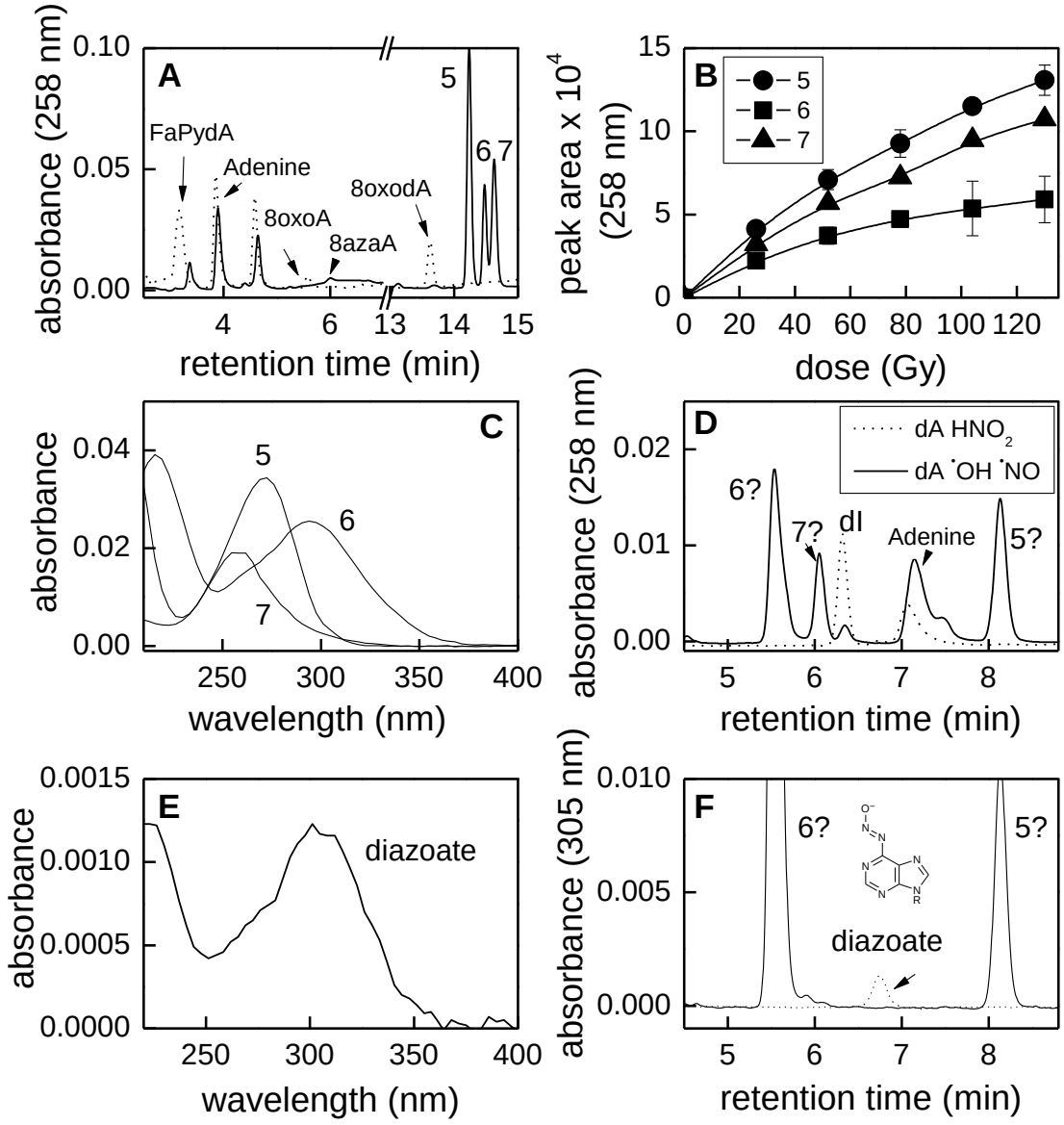

Figure 3-9 (A) Chromatogram obtained using a 10 mM formic acid eluent (3-10% methanol in 8 min, 10-20% in 2 min, 20-50% 2 min, returning to starting conditions after 0.1 min) monitoring at 258 nm shows the formation of products 3-5 following oxidation of 2′-deoxyadenosine (0.5 mM) at pH 7.6 by •OH (dotted line) with a dose of 390 Gy under anoxia in the presence of ~ 1.8 µM •NO (solid line) and (B) the dose dependent yields of products 5-7. (C) UV-visible spectra of products 3-5 (pH 2.8) following radiolysis of dA; Chromatograms obtained using a 10 mM ammonium formate eluent (10% methanol 2 min, 10-15% 8 min, 15-50% 2 min, returning to starting conditions in 0.1 min) monitoring at (D) 258 nm and (F) 305 nm show oxidation of 2′-deoxyadenosine as above after 130 Gy in the presence of ~1.8 µM •NO (solid line) or following reaction with HNO_2 for 20 min at room temperature (dotted line); (E) UV-visible spectra of 2′-deoxyadenosine diazoate (pH 6.9).

Products **5** and **6** both exhibit *m/z* values of 279 (M-H)/281 (M+H) and product **7** exhibits a *m/z* value of 190 (M+H) but does not ionize in ES^- mode. All three have very different UV spectra (Figure 3-9C). Authentic commercially available dI co-eluted with dA using formic acid/methanol as eluent and as a consequence the eluent was changed to 10 mM ammonium formate (pH ~6)/methanol to ensure separation. Even under these conditions, there was little evidence for the formation of significant levels of dI following the reaction of •OH with dA in the presence of •NO (Figure 3-9D). Products **5-7** appear to elute earlier in the higher pH eluent than the low pH eluent, suggesting that they may contain acidic groups. In an attempt to identify the products, further tests were carried out.

As products **5** and **6** show a *m/z* increase of 29, compared with that of dA, there is a possibility that they represent •NO-adducts of dA. It has previously been reported that dI is formed following reaction of dA with acidified sodium nitrite (pH 3.7). The reaction proceeds through the formation of 2′-deoxyadenosine diazoate, which was has a *m/z* of 279.2 (M–H) (Suzuki *et al.* 2009). Following incubation of nitrous acid with dA for 20 min at RT, the product which is likely to represent the diazoate identified by Suzuki *et al*, does not co-elute with any of the products resulting from reaction of •OH with dA in the presence of •NO (Figure 3-9F) ruling out its formation in this reaction. It is possible that nitrosylation may have occurred at an alternative site to the primary amine, which would give a product with the same mass as the diazoate described above.

Since nucleosides can be deglycosylated by heating with formic acid, solutions of dA, which had been irradiated (260 Gy) in the presence of •NO, were subsequently heated for 30 min at 60 °C in the presence of 0.5 M formic acid. As well as the expected increase in the peak area corresponding to A from deglycosylation of dA, HX and 8azaA were also observed, while the peak areas of products **5** and **6** were significantly reduced (Figure 3-10). Neither HX nor 8azaA were seen upon heating un-irradiated dA; however, A was released to a similar

extent independent of irradiation. Notably the peak area of product **7** did not change upon heating in acid, suggesting that it is already deglycosylated.

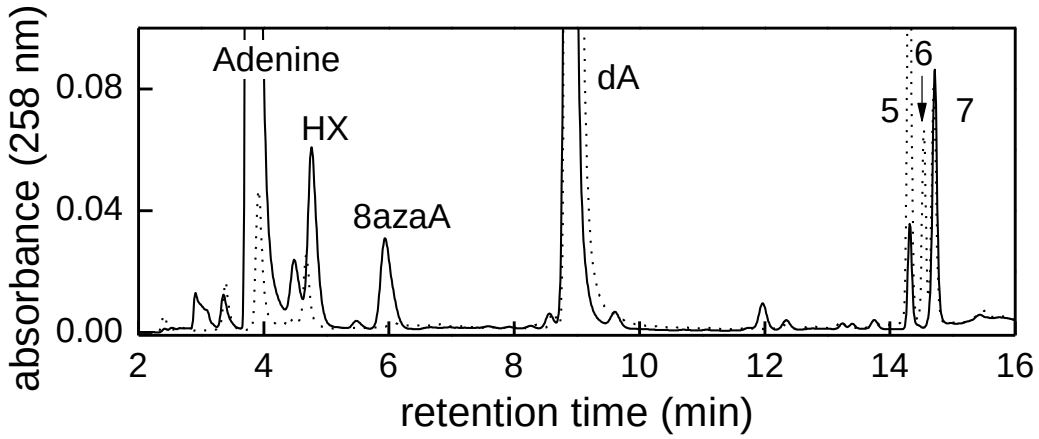

Figure 3-10 Chromatogram showing the products obtained following the oxidation of dA (0.4 mM) with •OH in the presence of ~1.8 µM •NO after 260 Gy at pH 7.6 in 10 mM phosphate immediately (…) or after heating with 0.5 M formic acid for 30 min at 60 °C (—). Chromatography conditions are 10 mM formic acid, 3-10% methanol in 8 min, 10-20% in 2min, 20-50% in 2 min, returning to starting conditions after 0.1 min.

The identification of all of the three products obtained shortly after the oxidation of dA by •OH in the presence of •NO are as yet unknown, although deamination does not seem to be a major pathway. Products **5** and **6** exhibit the same *m/z* of 279.2 (M-H) as that reported for the diazoate modification of dA but only product **6** has a similar UV-visible spectrum as reported by Suzuki *et al* (Figure 3-9C and E). Re-analysis of the products of the reaction between dA-•OH radicals and •NO by HPLC a few days following radiolysis, showed complete absence of product **5** with formation of 8azaA. It is suggested that **5** may be a nitroso adduct of dA which rearranges and depurinates slowly to release 8azaA. In comparison, HX was still not observed. Products **5** and **7** are base sensitive and disappear on addition of ~5 mM NaOH, forming two earlier eluting products (11.4 and 13.5 min) with *m/z* 253 (M+H). Both products have similar UV-visible spectra with λ_{max} 276 nm. It is possible that one of these products may represent 8azadA but further analysis is required to be certain.

When dA was oxidized by $Br_2^{\bullet-}$ in the presence of $^{\bullet}NO$ at pH 7.6, the yields of **5**, **6** and **7** were significantly reduced but product **6** predominated. Oxidation of dA by $Br_2^{\bullet-}$ does not lead to the formation of $^{\bullet}OH$-adducts but proceeds directly to d(A-H)$^{\bullet}$ which may then react with $^{\bullet}NO$. The small yields of products **5-7** may be formed if a low level of unavoidable competing $^{\bullet}OH$ radicals react with dA. 8azaA was not observed even after heating in formic acid, but a small peak which may represent HX was observed without heating. Products **5-7** therefore most probably arise from reactions of $^{\bullet}NO$ with $^{\bullet}OH$ adducts of dA, but this will be discussed later (§3.3.6).

3.3.5 2′-Deoxyadenosine monophosphate (dAMP)

The reaction of dAMP with $^{\bullet}OH$ follows similar pathways as seen with dA. When dAMP was oxidised by $^{\bullet}OH$ in the presence of $^{\bullet}NO$ two major products were observed (Figure 3-11A, products **8** and **9**). The earlier eluting peak, with a retention time of 12.1 min, has *m/z* of 359.1 (M-H), an increase in molecular weight of 29 over dAMP, and a UV-visible spectrum with λ_{max} 272 nm (Figure 3-11B) very similar to product **5** observed from similar reactions with dA. It was difficult to obtain a mass for **9** but the UV-visible spectrum (Figure 3-11B) is very similar to **6** observed from similar reactions with dA. In addition, **7** was also formed, in similar yields to that from corresponding reactions of dA. There was no evidence for the formation of 2′-deoxyinosine monophosphate or 2′-deoxy-8-azaadenosine monophosphate immediately following radiolysis. However, upon heating in the presence of 0.5 M formic acid, 8azaA and HX were observed and products **8** and **9** disappeared (Figure 3-11A), whilst 7 remained unchanged, as observed with dA (Figure 3-10). None of these late eluting products were observed in any significant amounts when dAMP was oxidised by $Br_2^{\bullet-}$ in the presence of $^{\bullet}NO$, suggesting that as with dA, they arise from $^{\bullet}OH$-induced products.

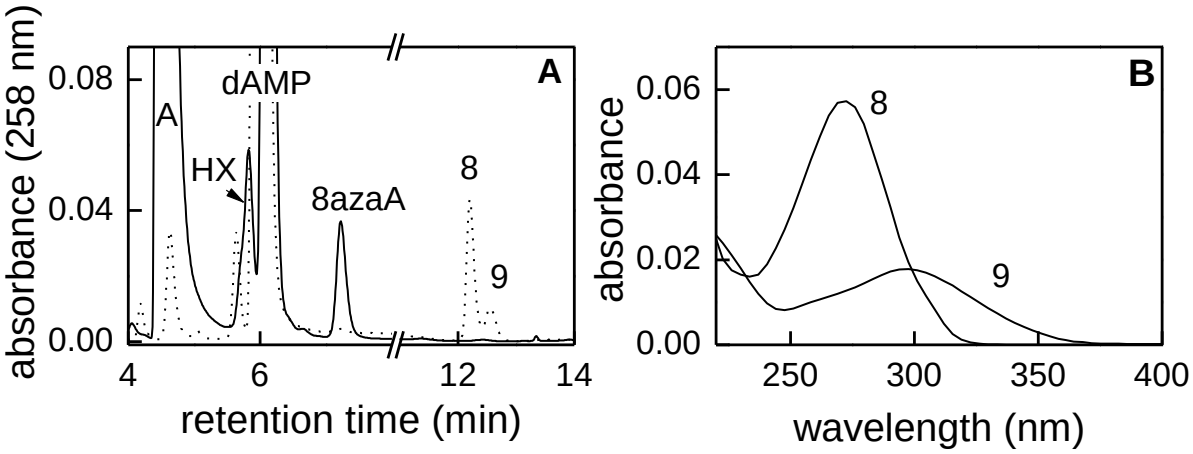

Figure 3-11 (A) Chromatogram showing the products obtained following the oxidation of dAMP with •OH in the presence of ~1.8 µM •NO after 260 Gy at pH 7.6 in 10 mM phosphate immediately (…) or after heating with 0.5 M formic acid for 30 min at 60 °C (—); (B) UV-visible spectra of products 8 and 9. Chromatography conditions are 3-7% methanol/10 mM formic acid in 4 min, 7-10% methanol/10 mM ammonium formate in 4 min, 10–20% methanol/10 mM ammonium formate in 2 min, 20-50% methanol/10 mM ammonium formate in 2 min and returning to 10 mM formic acid starting conditions after 0.1 min.

3.3.6 Discussion of reactions of •OH with adenine compounds in the presence of •NO - possible mechanisms involved in the formation of hypoxanthine and 8-azaadenine

Considering the chemistry which occurs in the formation of X from G following radiolysis of G/dGMP in N_2O-saturated solution in the presence of ~1.8 µM •NO (Scheme 3-1), HX was initially thought to form through reaction of A(-H)• with •NO. The intermediate C-4(•OH) adduct of A dehydrates to form A(-H)• (k = 1.3 x 10^5 s^{-1}) (Vieira and Steenken 1987). The presence of the ribose sugar on N-9 in dA reduces the rate of dehydration of the C4-(•OH) adduct to ~2.9 x 10^4 s^{-1} (O'Neill *et al.* 1985). The slower rate of decay of C-4(•OH) increases the probability of reaction of •NO with the hydrated intermediate approximately 4-fold. If •NO reacts with the C-4(•OH) radical before dehydration occurs, then dI would be expected to be formed in lower yields with dA than HX is formed from A. In addition, if the rate constant for reaction of •NO with A-•OH radical adducts is ~10^9 M^{-1} s^{-1}, similar to that of G-•OH radicals, then at ~1.8 µM •NO, the rate will be ~1.8 x 10^3 s^{-1}, ~20-fold slower than the

rate of dehydration of the dA-•OH adduct and therefore unlikely to be the major reaction pathway, suggesting that •NO reacts predominately with A(-H)•.

Potentially the C-4(•OH) adduct of A could dehydrate by two different pathways to form radical intermediates **Y** and **Z** (Scheme 3-3). The fact that the C-4(•OH) adduct of A dehydrates faster than that of dA suggests that dehydration should favour the formation of radical **Y** relative to **Z** since dehydration may involve the proton at N-9. It was initially thought that HX would be formed through reaction of the N-centred radical (**Z**) of A/dA/dAMP with •NO followed by deamination (Scheme 3-3). However, HX is not formed to any significant extent when A is oxidized by $Br_2^{\bullet-}$ in the presence of •NO, where the radical formed would primarily be **Z** (Scheme 3-3). In addition, dI was not observed when dA was oxidized by either •OH or $Br_2^{\bullet-}$ in the presence of •NO. Since dehydration of the C-4(•OH) adduct of dA to form radical **Y** is not possible when deoxyribose is attached at N-9, radical **Z** would predominate. It is likely that •NO reacts with radical **Y** of adenine to form a nitroso adduct, which rearranges and breaks down to form HX (Scheme 3-3). This would be consistent with the lack of formation of HX from dA/dAMP, as radical **Y** is not formed with dA/dAMP. However, •NO may also be able to react with radical **Z** of dA/dAMP and the products of this reaction may account for the observation of products **5-9**, which as yet have not been identified. This reaction may also occur with radical **Z** of adenine but yields may be too low to observe.

The effect of ribose attached to N-9 of guanine on the dehydration rate of the C-4(•OH) adduct of dGMP is not significantly different to that of G even though it has a removable proton on N-9 (Steenken 1989). It was proposed earlier in this chapter that the C-4(•OH) adduct of G/dGMP dehydrates at a significantly faster rate than previously reported (§3.2.5), to yield the dehydrated radical products (G-H)• and the aminyl radical of both G and dGMP. The relative yields of these two products depend upon pH and phosphate concentration (§3.2.4). Therefore the presence of deoxyribose on N-9 does not affect the rate

of dehydration reactions of G or dGMP radicals following reaction with •NO and both the free base and nucleotide may form X/dXMP. Similar to the guanine system, the use of •NO in adenine systems has allowed new perspectives to be considered on the •OH-induced radical chemistry of purines.

Formation of 8azaA would also have been expected to arise by similar mechanisms, as was suggested earlier for the formation of 8azaG from the C-8(•OH) adduct of G/dGMP (Scheme 3-1). Certainly when considering reactions of A, mechanisms may well follow a similar pathway as observed for G, with the formation of 8azaA. However, once the deoxyribose sugar is attached to the base, 8azadA/8azadGMP do not appear to be formed during or soon after radiolysis at pH 7.6. This is very much in contrast to reactions seen with dGMP. However, at least one of the products which are formed from reactions of dA/dAMP-•OH adduct intermediates with •NO releases 8azaA upon heating in formic acid and also several days following radiolysis without heating. Interestingly, 8azadGMP is very insensitive to the release of 8azaG upon heating in formic acid, which implies that 8azadGMP is relatively stable to deglycosylation. The formation of the benzotriazole may stabilize the glycolytic bond. In the case of dA/dAMP, benzotriazole formation does not seem to occur quickly, but a relatively stable nitroso adduct may exist which may be attached on N-7 and/or C-8 of the ring-opened form (Scheme 3-3).

The presence of the deoxyribose sugar on N-9 of dA/dAMP may stabilise potential nitroso adducts to rearrangement, reducing the rate of formation of 8azaA compared to similar reactions with A, which may reflect the slower rate of ring-opening of the C-8(•OH) adduct for dA compared to A (O'Neill *et al.* 1985; Vieira and Steenken 1987), a mechanistic change which must occur to allow a C-N exchange at atom position 8.

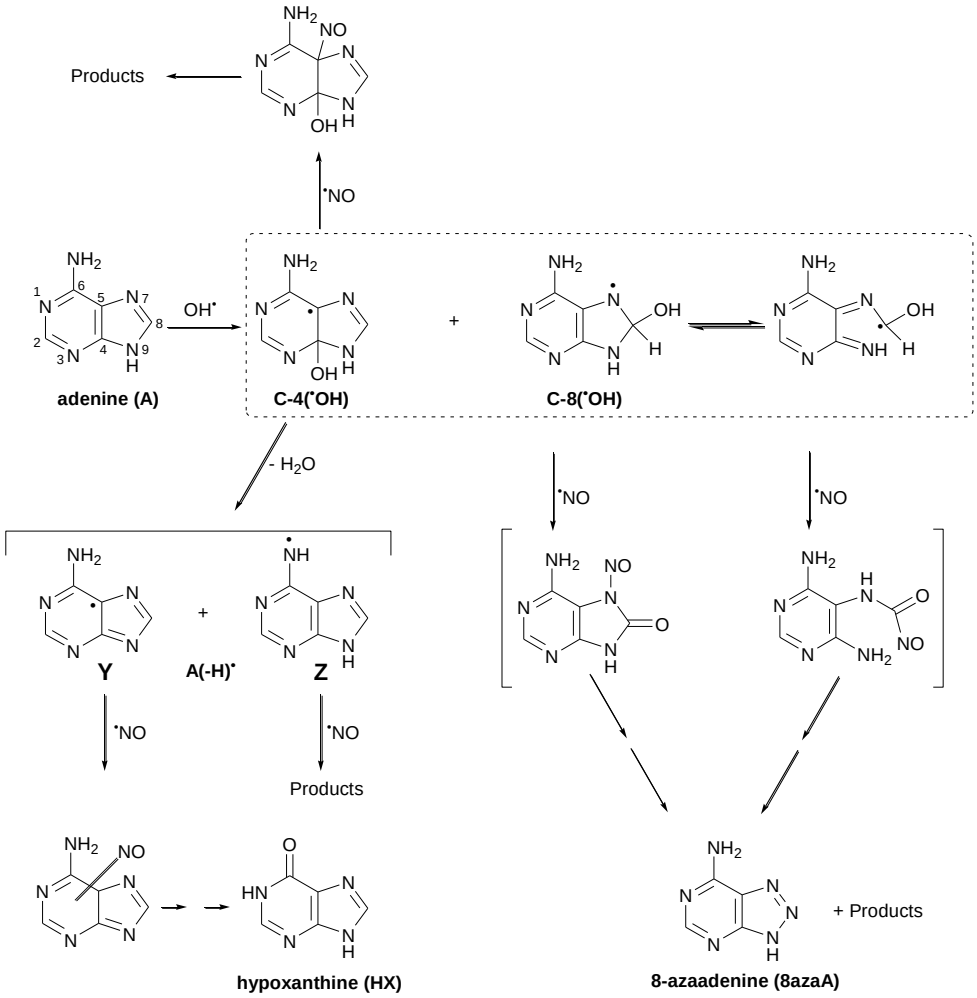

Scheme 3-3 Mechanisms which may be involved in the reaction of •NO with the •OH-induced radicals of adenine. Reproduced (with minor modification) from *Nitric Oxide*, Lisa K. Folkes and Peter O'Neill, Vol 34, DNA damage induced by nitric oxide is enhanced at replication, 47-55, Copyright (2013), with permission from Elsevier.

3.4 Reactions of nitric oxide with •OH-induced thymine radicals

3.4.1 Thymine base

Oxidation of thymine (T) by •OH (k = 6.4 x 10^{10} dm^3 mol^{-1} s^{-1} (Buxton *et al.* 1988)) produces •OH adducts with ~60% of •OH moieties residing on C-5, forming a reducing radical, and ~30% residing on C-6, forming a strongly oxidizing radical. In addition ~10% of radicals arise from H-atom abstraction from the methyl group (described in (von Sonntag 2006; Dizdaroglu and Jaruga 2012)) (Scheme 3-4).

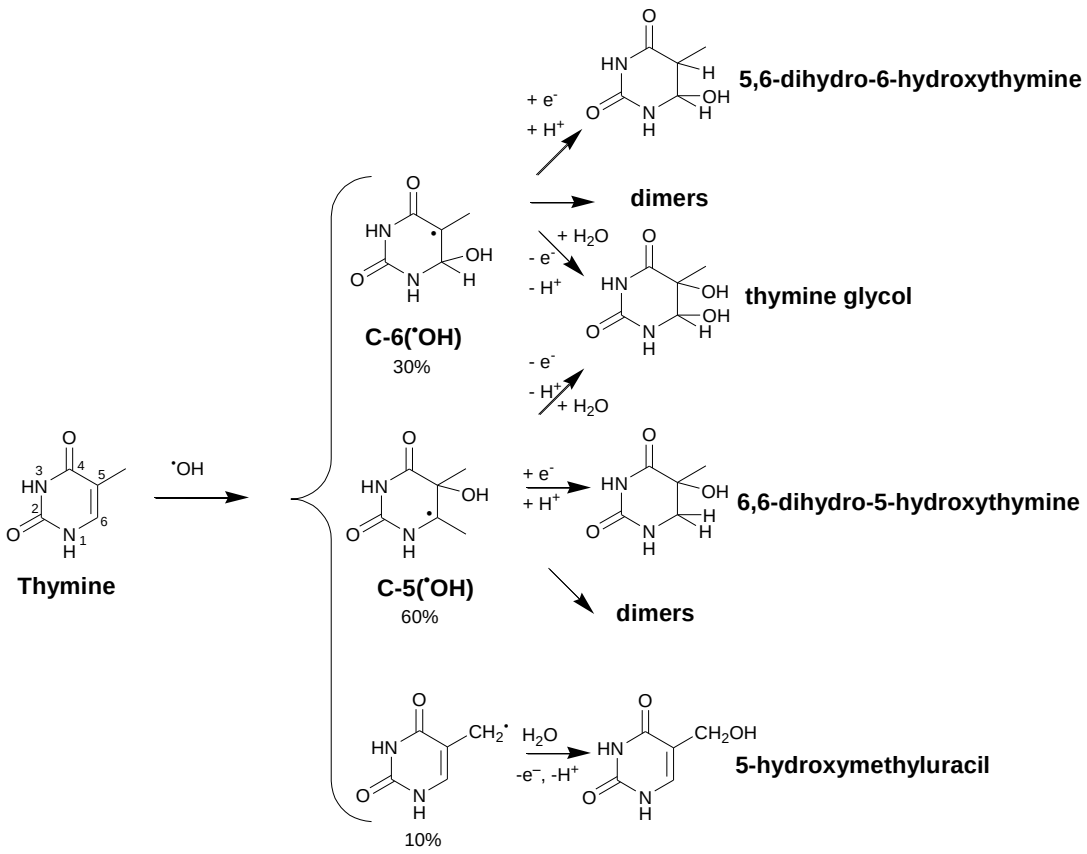

Scheme 3-4 Major mechanisms involved in the formation of products following reactions of thymine with •OH in anoxia.

In addition, water can add to the exocyclic carbon-centred radical in anoxic conditions to form 5-hydroxymethyluracil and to the 6-yl and 5-yl radicals to form thymine glycol (Scheme 3-4). Thymine glycol particularly dominates in oxygenated systems and is one of the most widely studied of DNA lesions in irradiated DNA. However, dimers are also some of the most abundant products arising from these reactions with free thymine (Idriss Ali 1979; Idriss Ali and Scholes 1979).

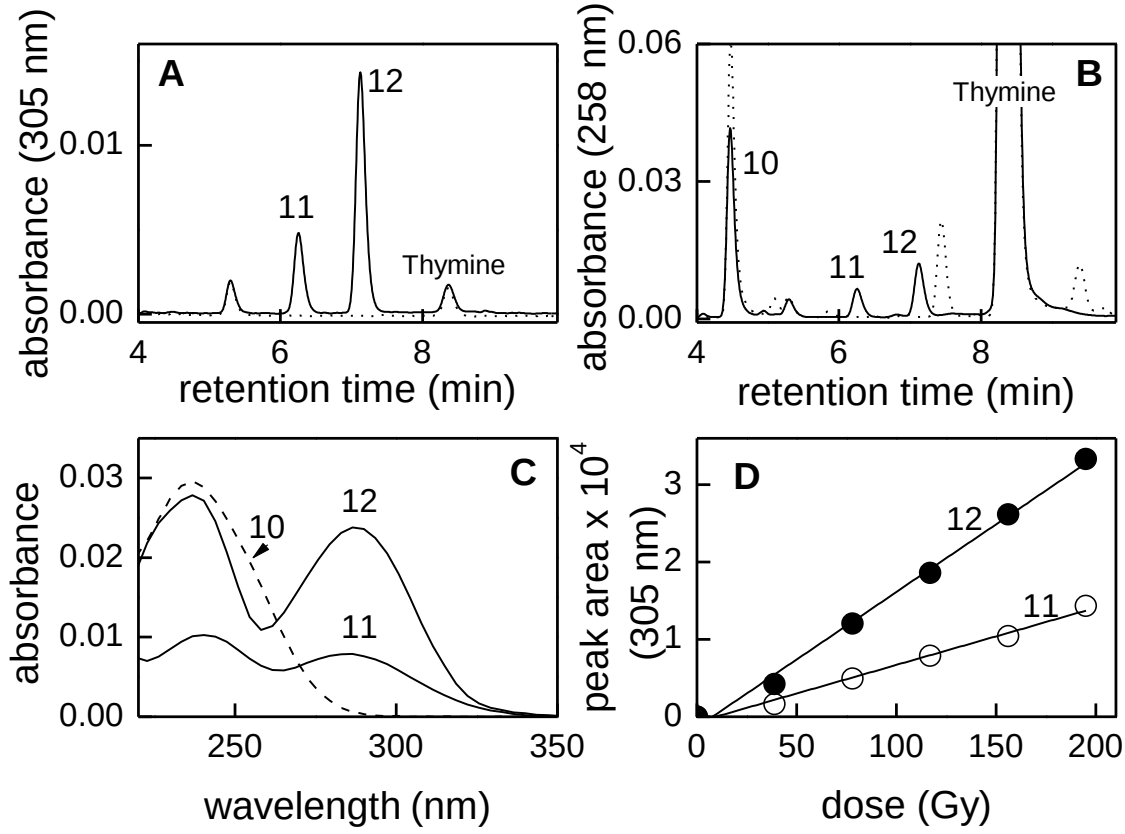

Figure 3-12 Chromatograms showing the formation of products following oxidation of thymine (0.5 mM) with •OH (…) in the presence of 1.8 μM NO (—) at pH 7.4 after 130 Gy monitoring at (A) 305 nm and (B) 258 nm; (C) UV-visible spectra of products; (D) radiochemical yield of products 11 and 12 monitoring at 305 nm. Chromatography conditions are 10 mM formic acid 3-8% methanol in 7 min, 8-20% methanol in 2 min and returning to starting conditions in 0.1 min.

γ-Radiolysis of T in N_2O-saturated solution at pH 7.4 showed the formation of three products by HPLC (Figure 3-12B). The earliest eluting peak has *m/z* of 143.0 (M+H) and is likely to be 5-hydroxymethyluracil based on previous studies (discussed in (von Sonntag 2006)) but could potentially be 6-hydroxythymine. The latter two products both show *m/z* of 269.0 (M+H) and are likely to be mono hydroxylated dimers of T (Idriss Ali 1979). In the presence of •NO these products were no longer observed, but three alternative products were seen (Figure 3-12A and B, peaks **10**-**12**). Product **10** has *m/z* of 174.0 (M+H) and a UV-visible spectrum with λ_{max} 237 nm (Figure 3-12C). The mass increase above T suggests the addition of –OH and –NO (126 + 17 + 30). A reduction in λ_{max} compared to T also suggests a

loss of conjugation within the molecule. The product is tentatively assigned to 6-hydro-6-hydroxy-5-nitrosothymine or 6-hydro-5-hydroxy-6-nitrosothymine (Scheme 3-5). Products **11** and **12** have *m/z* of 155 (M+H) suggestive of the addition of -NO to form 6-nitrosothymine or 5-nitrosomethyluracil (Scheme 3-5).

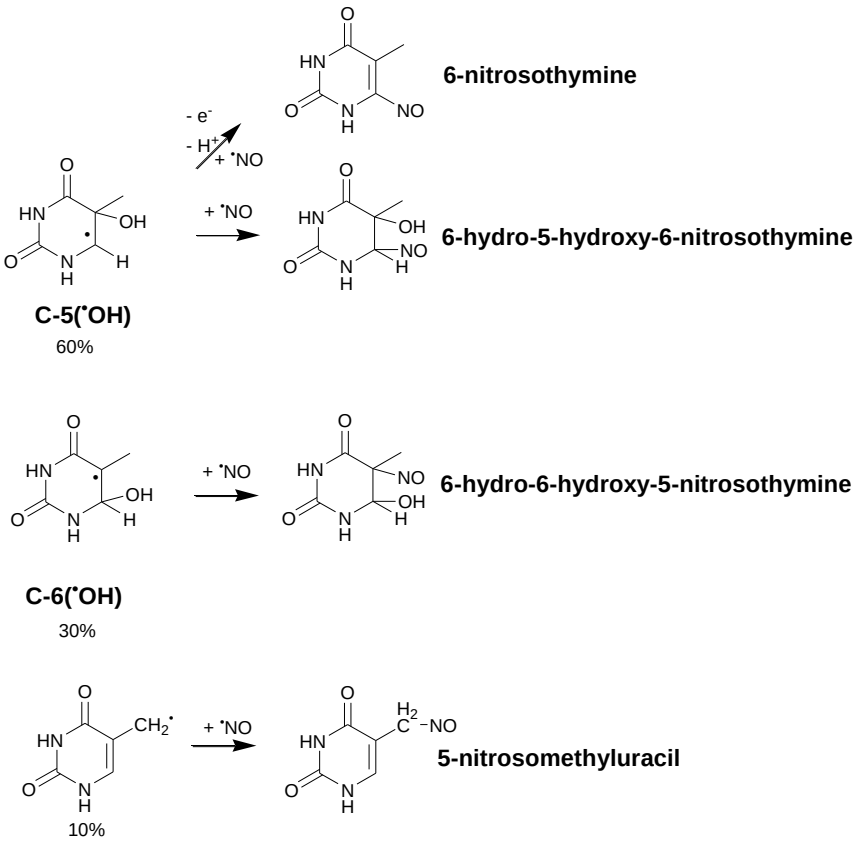

Scheme 3-5 Proposed mechanisms for the reaction of •NO with •OH-induced radicals of thymine.

3.4.2 Thymidine (dT)

•OH-induced modifications to thymine in thymidine (dT) are similar to those shown in Scheme 3-4 with additional thymine release also occurring possibly following H-atom abstraction from C-1′ of the deoxyribose sugar. When reactions of dT with •OH were carried out in the presence of ~1.8 µM •NO, T release was increased slightly compared to solutions irradiated in N_2O alone. In addition three new products were observed which were not seen in

the absence of •NO (Figure 3-13A, products **13-15**). Products **13** and **14** have *m/z* of 272 (M+H) and UV-visible spectra akin to **11** and **12** seen from similar reactions with T (Figure 3-12). They are tentatively assigned to •OH/•NO adducts, 5-nitrosomethyluridine and 6-nitroso-5-hydroxy-6-hydrothymidine (Scheme 3-5).

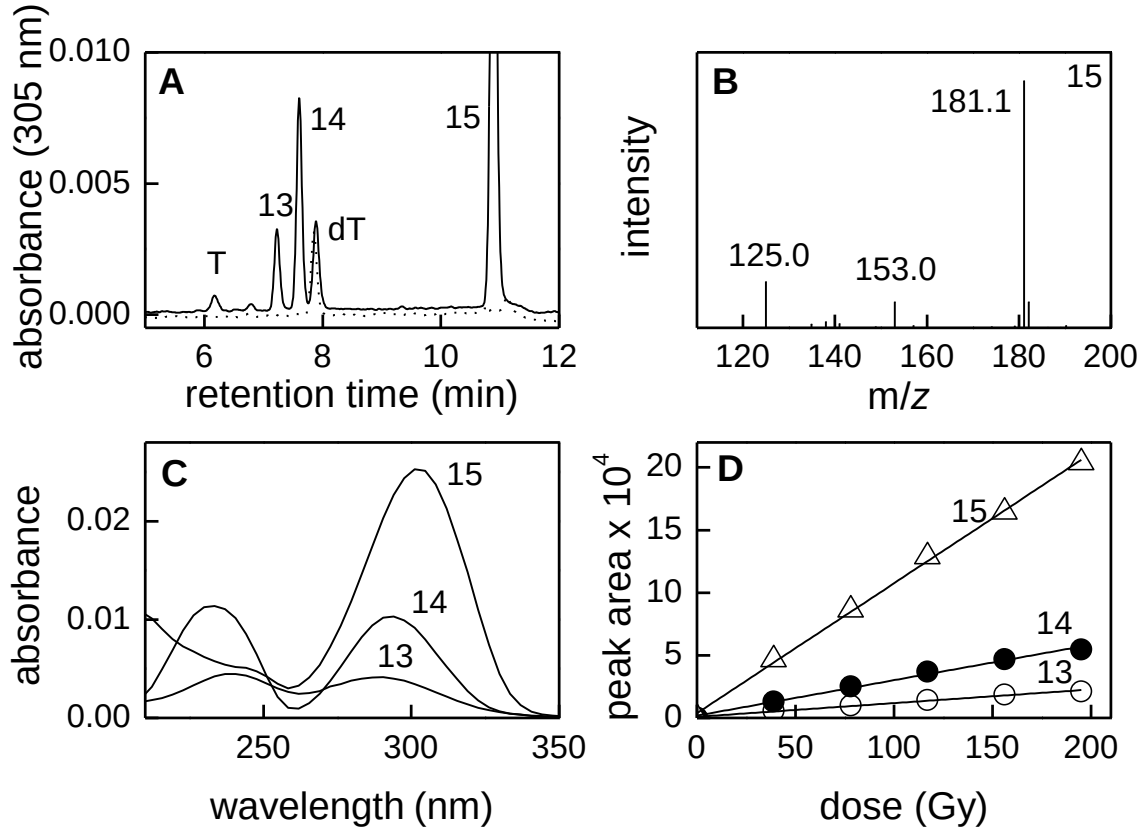

Figure 3-13 (A) Chromatograms showing formation of products after oxidation of thymidine (dT) (0.5 mM) by •OH (…) in the presence of ~1.8 µM •NO (—) after 130 Gy in 10 mM phosphate buffer, pH 7.4; (B) Mass spectrum of product 15; (C) UV-visible spectra of products 13-15; (D) Radiochemical yields of products 13-15 monitoring at 305 nm. Chromatography conditions are 10 mM formic acid with 8-25% methanol in 7 min returning to starting conditions after 0.1 min.

Product **15** has a *m/z* of 181 (M+H) and a UV-visible spectrum with λ_{max} 305 nm (Figure 3-13C). The mass is too small to be an adduct of dT so some fragmentation of dT must have occurred, although there is a possibility that the product is fragmenting within the mass spectrometer (but reducing the ionisation voltage used and ionising in ES^+ or ES^- mode has no effect upon the highest mass fragment observed). In an attempt to identify **15**, a larger

volume of dT (100 ml) was irradiated (1 h, ~13 Gy/min) in the presence of a constant supply of ~1.8 μM •NO/24.5 mM N_2O at pH 7.4. Product **15** was purified using HPLC chromatography and freeze-dried. By LCMS operating in ES^+ mode with a cone voltage of 20 V the product with *m/z* 181.0 (M+H) fragments into *m/z* 153.0 and 125.0 (M+H) (Figure 3-13B). The smaller fragments may indicate loss of N_2^+ and CO^+ respectively from the parent ion. The peak area of **15** is unchanged following heating in 0.5 M formic acid which suggests that it probably does not contain a glycosidic bond; however, some retention of a deoxyribose fragment in the molecule may remain to explain the molecular weight increase of 54 Da over thymine.

3.4.3 Thymidine monophosphate (dTMP)

The oxidation of thymidine monophosphate (dTMP) by •OH at pH 7.4 released T (Figure 3-14A). In the presence of •NO a product formed (Figure 3-14A, peak **16**) with a *m/z* of 350.0 (M-H) at a cone voltage of 25 V (a mass could not be obtained in ES^+ mode suggesting that the phosphate group is still attached) and a UV-visible spectrum with a λ_{max} of 295 nm (Figure 3-14B), similar to that observed with N_2O-saturated solutions of T and dT in the presence of •NO. Product **15** was also observed, which suggests that it only arises from the reactions of •NO with thymine when it is attached to a deoxyribose sugar, or from reactions with the deoxyribose sugar radicals themselves. Preliminary attempts to scale up and purify **15** from dTMP were unsuccessful. The dried product, which had been purified by solid phase extraction, decomposed somewhat to release T when redissolved in water containing 10% acetonitrile and further decomposition occurred overnight.

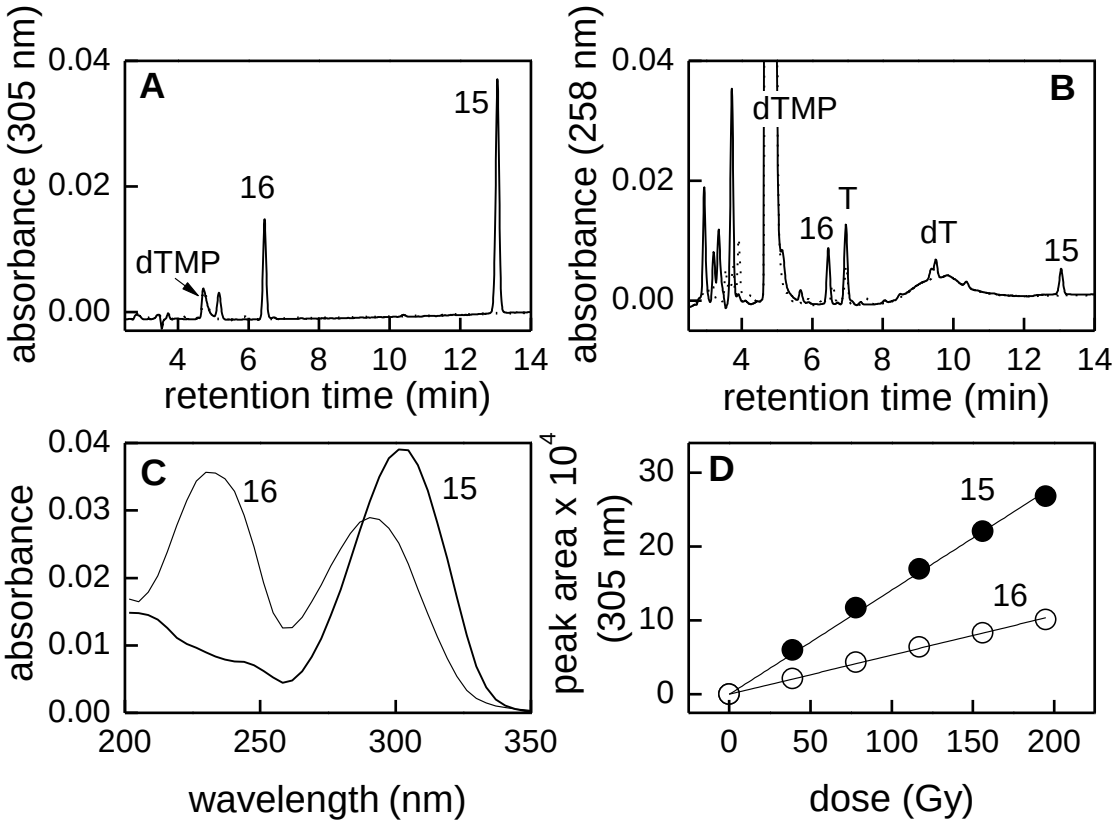

Figure 3-14 Chromatograms showing the oxidation of thymidine monophosphate (dTMP) (1 mM) by ˙OH (…) in the presence of ~1.8 µM ˙NO (—) in 10 mM phosphate buffer at pH 7.4 after 195 Gy at (A) 305 nm; (B) 258 nm; (C) UV visible spectra of products 15-16; (D) yields of products 15-16. Chromatography conditions are; 5% methanol/95% 10 mM ammonium formate to 25% methanol/75 % 10 mM formic acid in 10 min, returning to start in 0.1 min.

3.5 Reactions of nitric oxide with ˙OH-induced cytosine radicals

3.5.1 Cytosine base

As with the other purines and pyrimidines, oxidation of cytosine (C) by ˙OH (k = 6.3 x 10^9 dm^3 mol^{-1} s^{-1}, pH 7 (Michaels and Hunt 1973)) generates ˙OH adducts, with ~87% conjugating at C-5, the most electron rich site in C, to form a reducing radical and ~10% at C-6 to form a weakly oxidizing radical (Dizdaroglu and Jaruga 2012). γ-Radiolysis of N_2O-saturated solutions of C at pH 7.4 formed a product with a UV-visible spectrum with λ_{max} 320 nm and *m/z* of 238 (M+H) (Figure 3-15A). This product is tentatively assigned to a dimer of

the type shown in Scheme 3-6. Dimers of cytosine-•OH adducts account for >50% of all products in anaerobic conditions, using a dose rate of 110 Gy/min (Dizdaroglu and Simic 1984). Interaction of cytosine radicals through disproportionation and dimerisation is fast (k = 6.5 x 10^8 $M^{-1}s^{-1}$ (Hayon and Simic 1973)) and may include water elimination. •OH-adducts at C-6 are thought to dehydrate more easily than those at C-5 (Dizdaroglu and Simic 1984) with deamination also observed with some dimers. The second most common product (~25%) from the reaction of •OH with cytosine base in anoxia is 5-hydroxycytosine (Dizdaroglu and Simic 1984) (Scheme 3-6), although this product was not identified following radiolysis studies described in this project. This may reflect the hydrophilic nature of the product which would show little column retention with the chromatography conditions utilised.

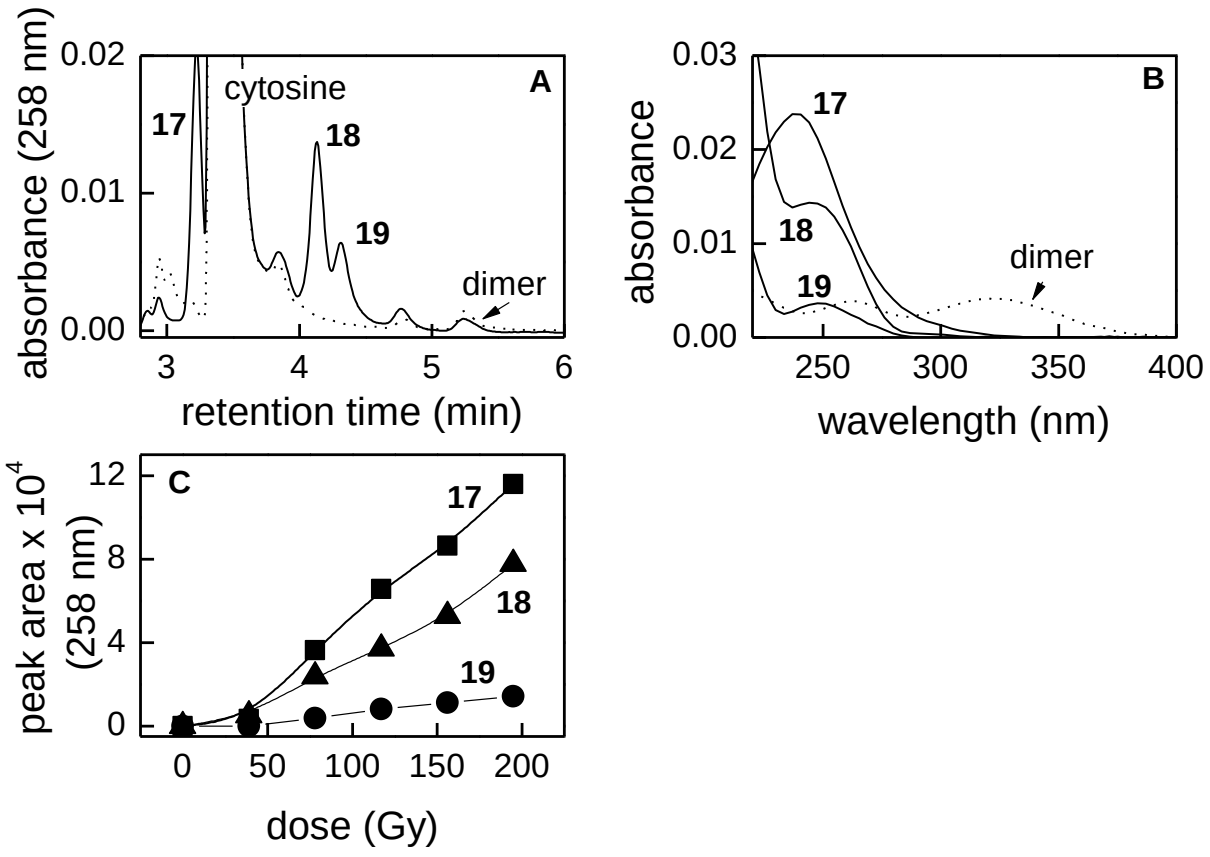

Figure 3-15 (A) Chromatogram showing oxidation of cytosine (0.5 mM) by •OH (…) in the presence of ~1.8 µM •NO (—) in 10 mM phosphate buffer at pH 7.4 after 130 Gy; (B) UV visible spectra of products 17-19; (C) yields of products 17-19. Chromatography conditions are 0-3% methanol/10 mM formic acid in 10 min.

It has previously been reported that O_2 inhibits the formation of cytosine dimers (Dizdaroglu and Simic 1984); however, the presence of •NO during γ-radiolysis does not significantly affect the yield of the proposed dimer. Other products were also observed, which formed in a dose-dependent manner (Figure 3-15A and C, products **17-19**). Product **18**, the highest yielding product, ionizes by mass spectrometry with *m/z* of 159 (M+H) and a UV-visible spectrum with λ_{max} 245 nm. It is tentatively assigned to 5,6-dihydro-5-hydroxy-6-nitrosocytosine as was proposed for similar reactions using uracil (Wardman *et al.* 2007). •NO may react with the major C-5(•OH) adduct forming a nitroso adduct on C-6 (Scheme 3-6). It has not been possible to identify any of the other products but they are likely to represent other nitroso adducts as has been suggested for thymine.

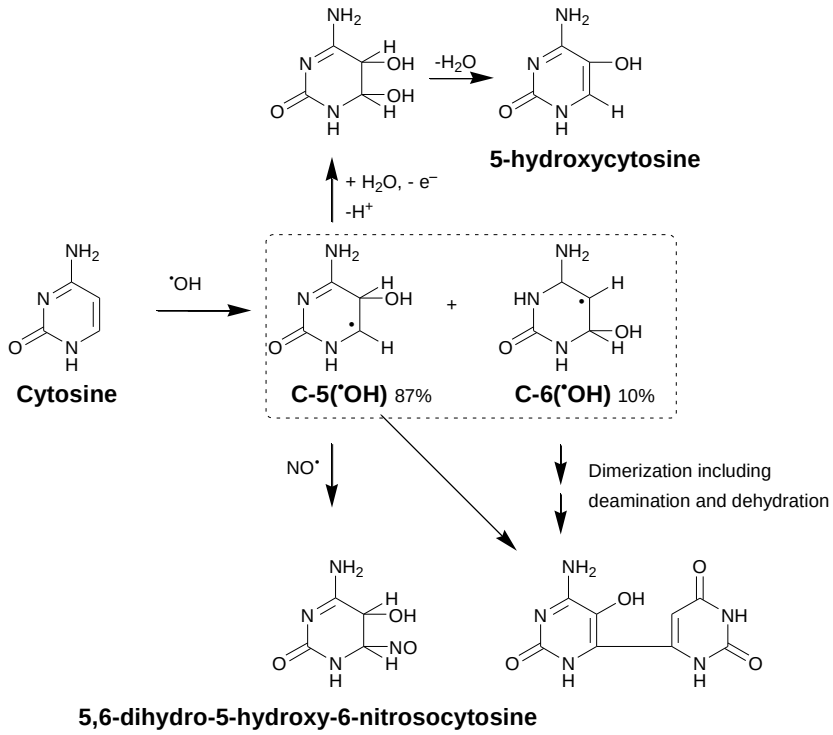

Scheme 3-6 Proposed mechanisms for the most common modifications of cytosine following oxidation by •OH in anoxia with or without the presence of •NO.

Notably, uracil was not observed following the oxidation of C with •OH with or without the presence of •NO, whereas •NO reacts with C in aerated solution to form uracil

(Caulfield *et al.* 1998). In those studies up to 1.8 mM •NO was used and systems were oxygenated, therefore deamination is likely to occur through reaction with higher nitrogen oxides. Earlier in this chapter it was described how •NO may react with the N-centred radical of G to induce deamination to xanthine. Cytosine is unlikely to form a N-centred radical on its primary amine following reaction with •OH, which might explain why uracil was not observed as a product when •NO is present during radiolysis.

3.5.2 2′-Deoxycytidine (dC)

The reaction of dC with •OH was expected to be similar to that observed with C but may also include those products which occur through reactions with the deoxyribose sugar. Oxidation of dC by •OH in the presence of •NO at pH 7.4 formed two major products which were specific to the presence of •NO (Figure 3-16, products **20**-**21**). Product **20** has a UV-visible spectrum with λ_{max} at 237 nm and *m/z* 257.0 (M+H) corresponding to a molecular weight of 256.0, which suggests the addition of •NO (and loss of H) to dC (227 + 30 – 1) at some site on the molecule. Product **21** has a UV-visible spectrum with λ_{max} of 310 nm, very similar to **15** from dT/dTMP, and also shows the same mass change as was seen above T, with the addition of 54 Da to C to give *m/z* 165 (M+H). The product was not observed when C was irradiated in the presence of •NO; therefore it must contain a component from the deoxyribose sugar. A larger volume of dC was irradiated in the presence of •NO and **21** was purified by HPLC, freeze-dried overnight and an accurate mass obtained (with thanks to Colin Sparrow, University of Oxford) with *m/z* 166.0607 (M+H). A molecular formula of $C_7H_8N_3O_2$ is proposed for this mass. In addition to this ion, an additional larger mass with *m/z* 301.1372 (M+H) was also observed which comprises a far larger proportion of the total ions observed. This mass has never been observed using LCMS. A molecular formula of $C_9H_{17}N_8O_4$ is proposed for this high mass ion (M+H) but it could be an artefact formed through ionisation reactions. As yet the identities of **20** and **21** remain unknown.

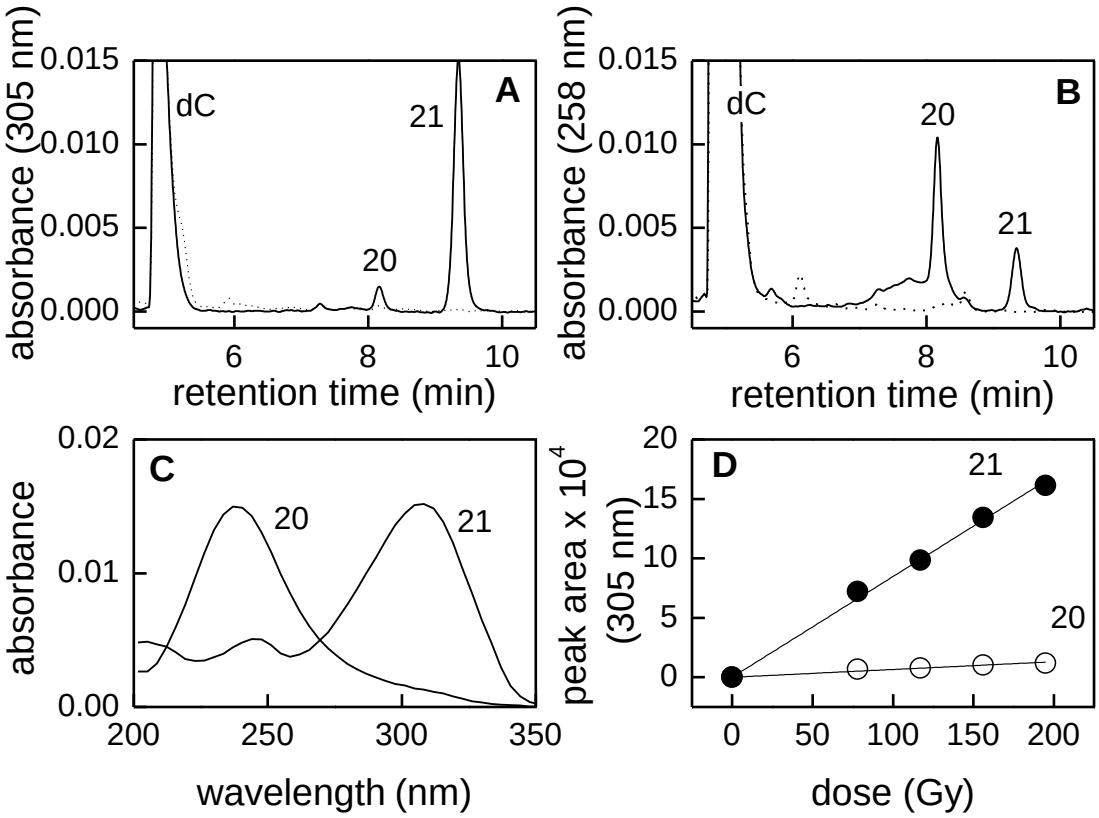

Figure 3-16 Chromatograms showing oxidation of 2′-deoxycytidine (0.5 mM) by •OH (…) in the presence of ~1.8 µM •NO (—) in 10 mM phosphate buffer at pH 7.4 after 195 Gy at (A) 305 nm; (B) 258 nm; (C) UV visible spectra of products 20-21; (D) yields of products 20-21. Chromatography conditions are; 3-8% methanol/10 mM formic acid in 7 min, 8-25% in 3 min, returning to start in 0.1 min.

3.5.3 2′-Deoxycytidine monophosphate (dCMP)

Oxidation of dCMP by •OH in the presence of •NO formed products different to those formed by •OH alone (Figure 3-17). In particular, the major product formed co-elutes with **21** formed from γ-radiolysis of N_2O-saturated dC in the presence of 1.8 µM •NO. Mass spectral analysis with a cone voltage of 25 V showed fragments of *m/z* 122.0 and 138.1 (M+H) corresponding to losses of ions of 44 and 28. This fragmentation pattern was also observed when **15** from dT/dTMP was ionized in ES^+ mode. Neither **15** nor **21** can be ionised in ES^- mode suggesting the absence of a phosphate group.

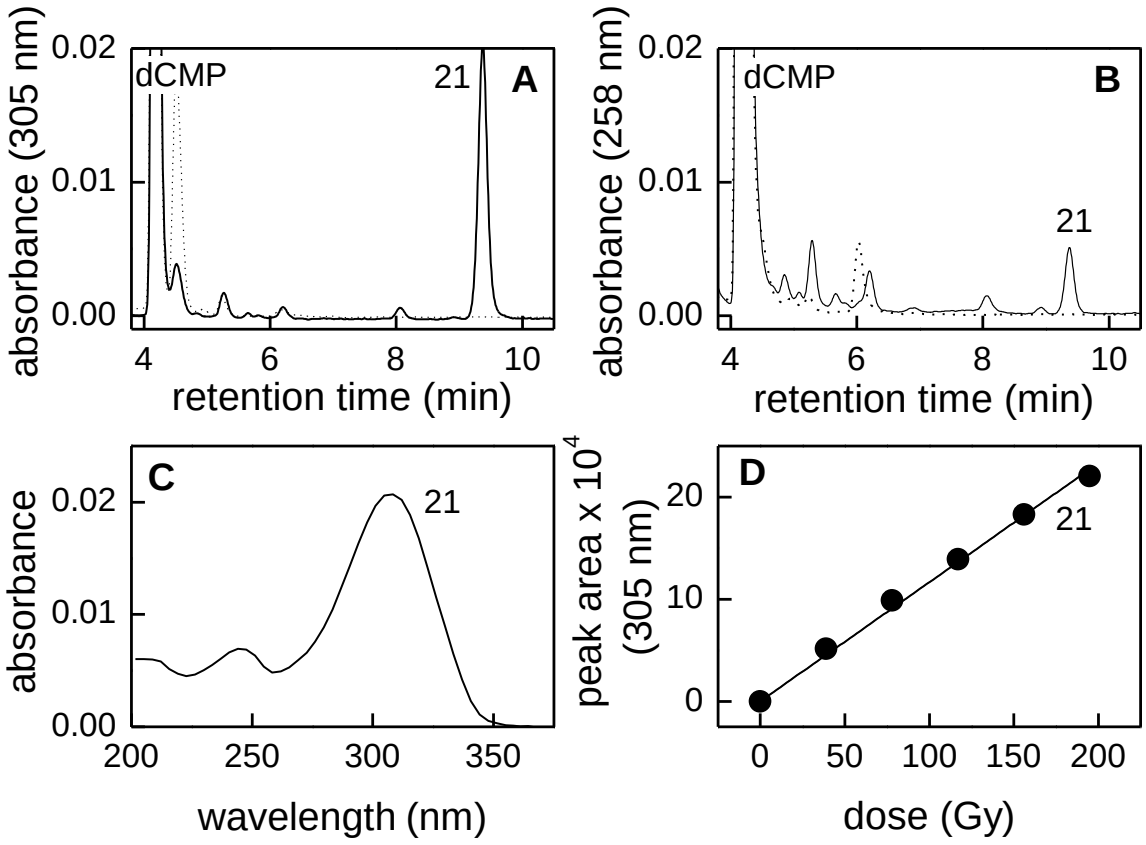

Figure 3-17 Chromatograms showing oxidation of 2′-deoxycytidine monophosphate (1 mM) by •OH (…) in the presence of ~1.8 µM •NO (—) in 10 mM phosphate buffer at pH 7.4 after 195 Gy at (A) 305nm; (B) 258 nm; (C) UV visible spectra of product 21; (D) yield of products 21. Chromatography conditions are; 3-8% methanol/10 mM formic acid in 7 min, 8-25% in 3 min, returning to start in 0.1 min.

3.6 Reaction of nitric oxide with •OH-induced oligomer radical adducts

Products which arise from reaction of •OH with free bases or nucleotides can vary in their abundance and type compared to the same reactions with DNA. In preliminary studies to investigate whether •NO reacts with polynucleotide radicals compared with single nucleotide •OH-adducts, short oligomers were utilised. A 6-mer of single-stranded GCGCGC or ATATAT were irradiated in N_2O-saturated solutions with and without the presence of •NO. Irradiated solutions were analysed shortly after radiolysis, or they were subjected to digestion of the phosphodiester bonds by nuclease P1 to release the free nucleotides.

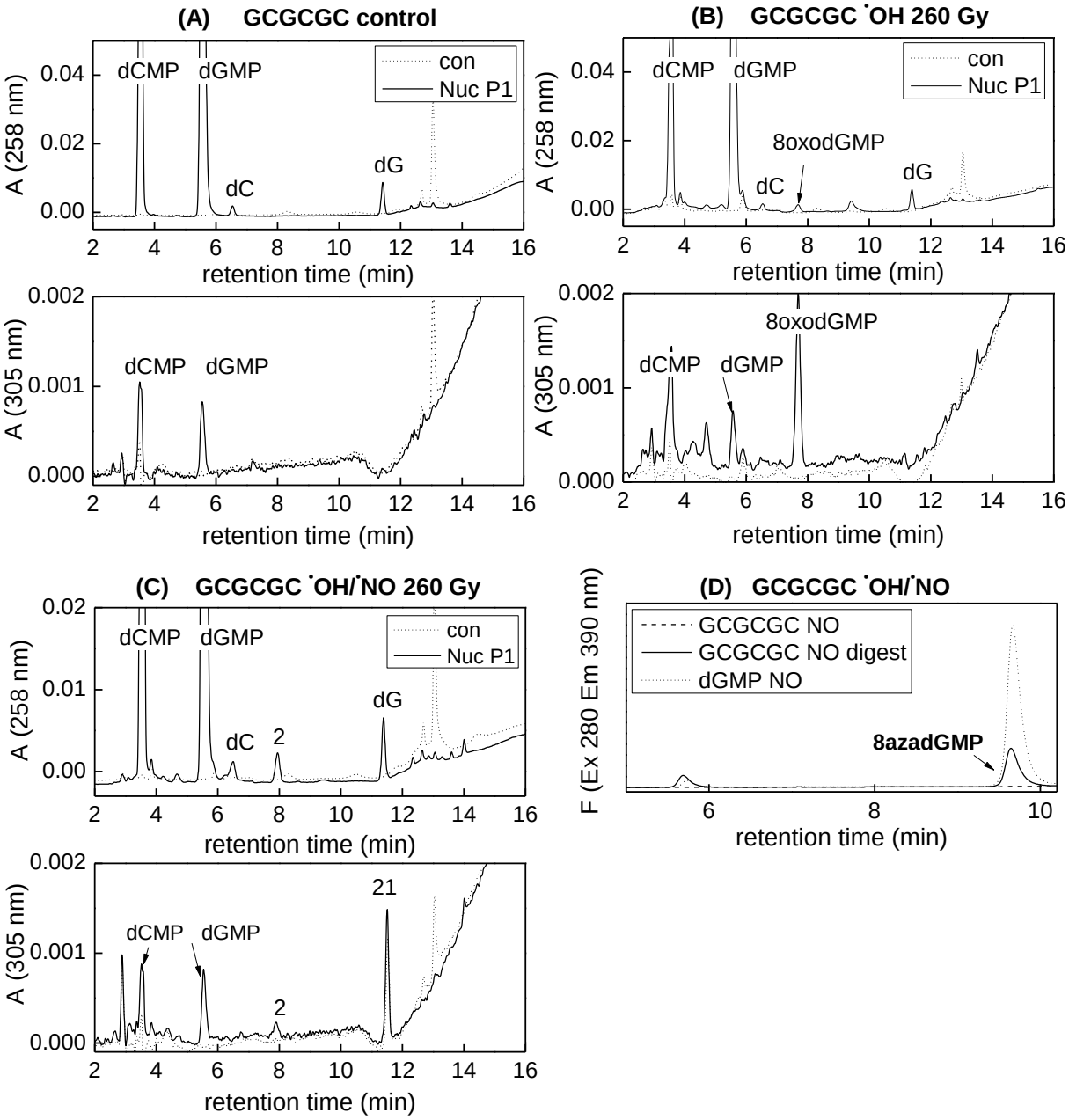

Figure 3-18 Chromatograms of GCGCGC oligomers before (…) or after digestion with nuclease P1 (—) detected at 258 nm and 305 nm; (A) control unirradiated oligomer; formation of products from the γ-radiolysis (260 Gy) of GCGCGC in N_2O-saturated solution without (B) and with (C) the presence of ~1.8 μM ˙NO. Chromatography conditions are 97-62% 10 mM ammonium formate, 0-31% 10 mM formic acid/methanol in 6 min, 31-50% 10 mM formic acid/7-50% methanol in 7 min, returning to starting conditions in 0.1 min. (D) Chromatograms showing the detection of 8azadGMP in GCGCGC oligomers following γ-irradiation (260 Gy) in N_2O-saturated solution in the presence of 1.8 μM ˙NO. Chromatography conditions used a Gemini column and comprised an eluent of 10 mM potassium dihydrogen orthophosphate, 5 mM TBAOH, 10% methanol at pH 9 with a linear gradient of 0–55% of 75% acetonitrile in 7 min, 55-100% in 1 min, returning to starting conditions over 0.1 min.

HPLC analysis of control GCGCGC showed the presence of dCMP, dGMP, dC and dG following nuclease P1 digestion of the oligomer but no significant peaks were observed without digestion (Figure 3-18A). Irradiation of the oligomer in N_2O-saturated solution showed the additional formation of 8oxodGMP, especially obvious at 305 nm, but only following nuclease P1 digestion (Figure 3-18B). Irradiation of GCGCGC in the presence of •NO, without digestion, showed evidence for the formation of **21** at 305 nm (Figure 3-18C), which was observed when dC or dCMP were oxidised by •OH in the presence of •NO (Figure 3-16 and Figure 3-17). As **21** is seen without digestion and the molecular weight is less than dCMP, it is likely that it is no longer part of the oligomer (see §3.5.2 and 3.5.3). Following digestion of irradiated GCGCGC, product **2**, 8azadGMP, was also observed but 8oxodGMP was not. To obtain further evidence of the formation of 8azadGMP in irradiated GCGCGC oligomer, the irradiated sample was digested with nuclease P1 and chromatographed with a high pH eluent. 8azadGMP is fluorescent at pH >9 and therefore it can be identified through its fluorescence. The product from the digestion of GCGCGC irradiated in the presence of •NO co-eluted with 8azadGMP obtained from the irradiation of dGMP under the same conditions confirming its identity (Figure 3-18D). Similar studies using ATATAT showed the presence of dTMP, dAMP, dT and dA in nuclease P1 digested control unirradiated oligomer (Figure 3-19A). Irradiation of the oligomer with or without the presence of •NO had little effect on the yields of these compounds. In N_2O-saturated solution in the absence of •NO, an additional unidentified product was seen eluting closely after dAMP, but only following digestion (Figure 3-19B).

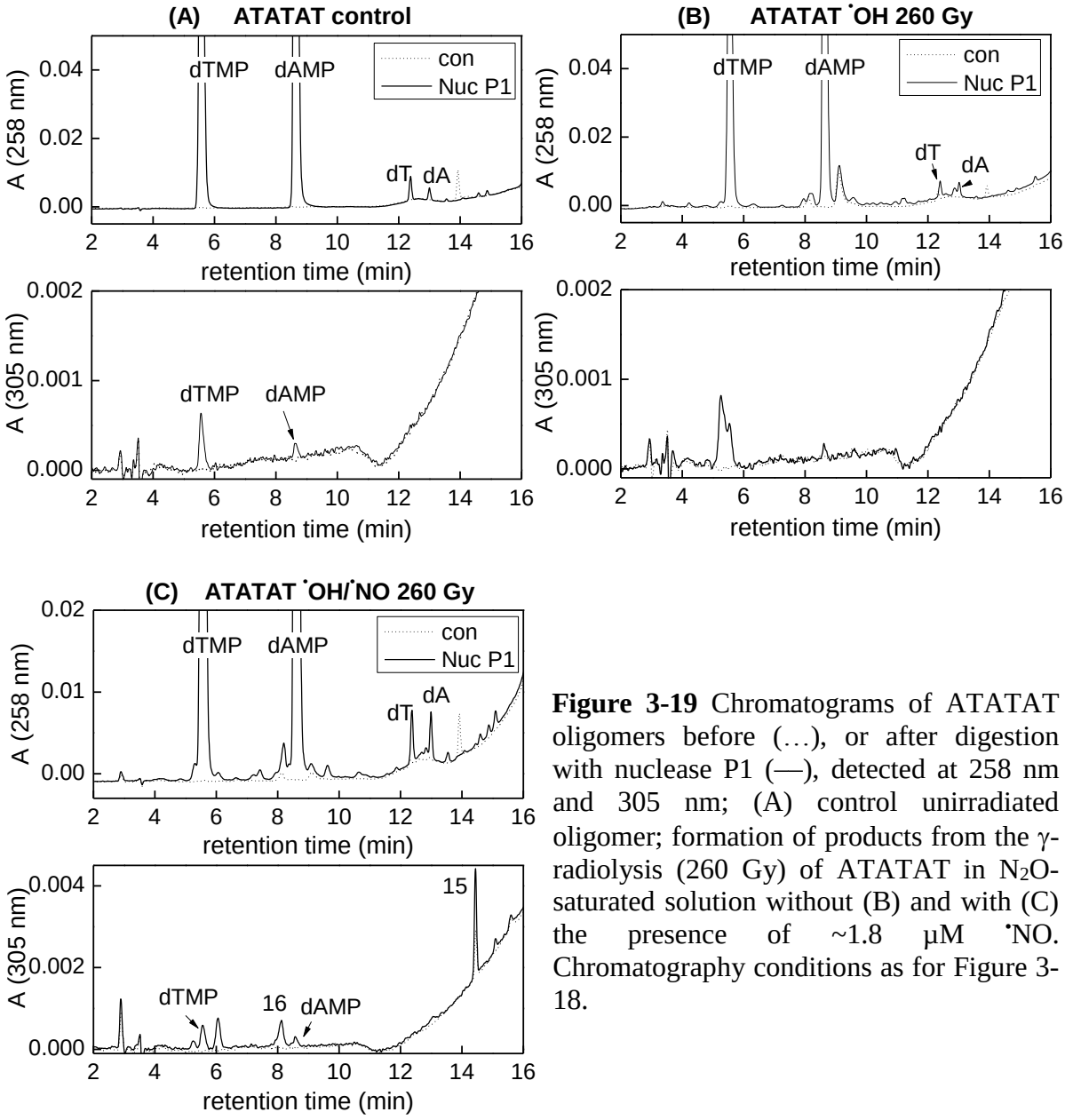

Figure 3-19 Chromatograms of ATATAT oligomers before (…), or after digestion with nuclease P1 (—), detected at 258 nm and 305 nm; (A) control unirradiated oligomer; formation of products from the γ-radiolysis (260 Gy) of ATATAT in N_2O-saturated solution without (B) and with (C) the presence of ~1.8 μM •NO. Chromatography conditions as for Figure 3-18.

When •NO was also present, **15** was observed immediately following radiolysis and digestion with nuclease P1 did not affect the peak area. Digestion also showed the presence of **16** which is observed when dTMP is oxidised by •OH in the presence of •NO (Figure 3-19C). None of the products which were identified following γ-radiolysis of dAMP in the presence of •NO were identified in these studies. However, the products observed from dAMP were quite hydrophobic (§3.3.5) and may not elute in the chromatography conditions used for the oligomer studies.

3.7 Measurement of calf-thymus DNA melting temperature

The temperature at which double-stranded DNA unwinds (melting temperature T_m) is an indication of DNA integrity. Upon heating, the absorbance of DNA in solution increases as the average absorption per base is highest in free nucleotides and is lowest in double stranded DNA. An increase in temperature breaks the hydrogen bonds between the base pairs allowing the DNA to unwind and hence increases its absorbance in solution (Sambrook and Russell 2001). Changes induced in DNA following γ-radiolysis, which will include base modifications and SSB, will reduce the temperature required to unwind the DNA. Calf thymus DNA exhibited a T_m of 71.1 ± 0.2 °C in 15 mM NaCl, 0.15 mM sodium acetate at pH 7 (Figure 3-20). γ-Radiolysis of N_2O-saturated calf-thymus DNA (260 Gy) decreased the T_m (57.3 ± 0.8 °C) and changed the curve shape as observed previously (Rafi and Wheeler 1973), indicating partial helix unwinding due to the presence of radiation-induced SSB. Irradiation of solutions of N_2O-saturated DNA in the presence of $^{\bullet}NO$ (~3.6 μM)/N_2O (~20 mM) also reduced the T_m (63.2 ± 0.3 °C) but the curve shape was more similar to that of the control unirradiated DNA. This indicates that in the presence of $^{\bullet}NO$ fewer SSB are formed but base modifications may occur which may change the hydrogen bonding between some base pairs and hence reduce T_m. γ-Radiolysis studies with dGMP (Figure 3-1) and GCGCGC oligomers (Figure 3-18) have shown that 8azadGMP is formed following the reaction of dGMP with $^{\bullet}OH$ in N_2O-saturated solutions in the presence of $^{\bullet}NO$. It is shown in Chapter 4 that 8azadGMP is also formed in plasmid DNA irradiated in similar conditions. It has previously been reported that the incorporation of 8azadGMP into oligonucleotides demonstrated little change to DNA duplex stability with no significant changes in T_m. The strength of hydrogen bonding between G-C and 8azaG-C is not significantly affected by the replacement of C-8 with N-8, although geometry of the DNA helix and solvation are expected to be affected (Seela and Lampe 1994; Seela *et al.* 1998; Contreras and Madariaga 2003). The addition of dX within a duplex oligonucleotide reduced the T_m by 5 °C compared to the dG control

oligonucleotide (Vongchampa *et al.* 2003) suggesting weaker hydrogen bonding. Other •NO-associated base modifications described earlier in this chapter may have additional effects upon hydrogen bonding between base pairs. In particular, the formation of products **15** and **21**, as yet uncharacterised, are indicative of the possible formation of an AP site resulting in reducing the strength of hydrogen bonding in the DNA molecule.

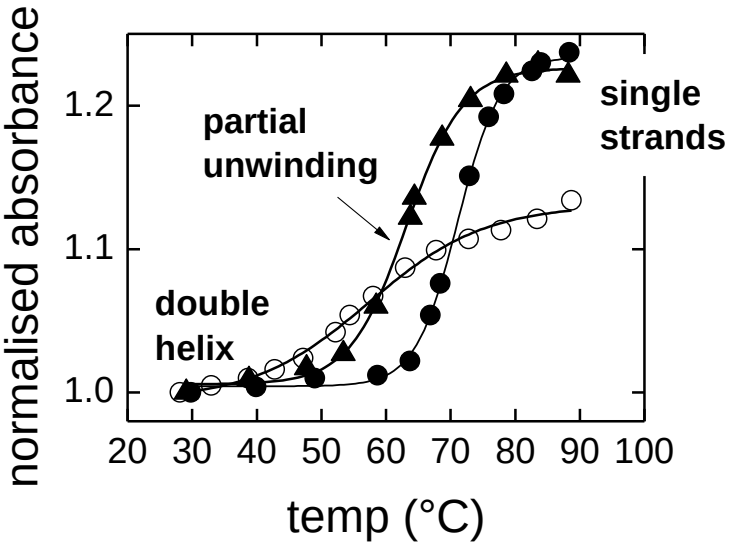

Figure 3-20 Effect of temperature on the melting of calf thymus DNA (50 µg/ml) in 0.015 M NaCl and 15 mM sodium acetate, pH 7 monitored at 260-820 nm: control un-irradiated DNA (●), N_2O-saturated (~25 mM) (○) and N_2O (~20 mM)/•NO (~3.6 µM) saturated DNA (▲) both after γ-radiolysis (260 Gy). Curves are representative of replicative experiments. Reproduced (with minor modification) from *Free Radical Biology & Medicine*, Vol 58, Lisa K. Folkes and Peter O'Neill, Modification of DNA damage mechanisms by nitric oxide during ionizing radiation, 14-25, Copyright (2013), with permission from Elsevier.

Formation of •NO-modified sites in close proximity to each other through clusters of DNA lesions which are known to be formed through ionizing radiation (§1.4.2) would also change the geometry of the DNA double helix and the T_m. These effects are discussed further in Chapter 4.

3.8 General discussion

Nitric oxide has been shown to be an effective radiosensitizer of hypoxic cells in many separate studies, for example, (Mitchell *et al.* 1993; Mitchell *et al.* 1996; Wardman *et al.*

2007; Singh *et al.* 2009; Stewart *et al.* 2011) but the mechanisms by which it elicits its effect are unclear. One way by which •NO may radiosensitize is thought to be due to fixation of radiation-induced DNA carbon-centred radicals by •NO to form diamagnetic C-nitroso adducts. As shown in some of the results in this chapter, DNA-derived products are different to those formed in the absence of •NO. These products, if formed in genomic DNA, may be difficult to repair and as a consequence could lead to cell death. However, apart from one study which shows some evidence for the formation of such an adduct with uracil (Wardman *et al.* 2007), no other investigations have been carried out into identification of the radiation-induced products formed in the presence of •NO under anoxic conditions.

It is well known that the addition of •NO in aerated solutions to G, A and C and their respective nucleosides and nucleotides forms xanthine (X), hypoxanthine (HX) and uracil respectively (and their corresponding nucleosides and nucleotides) through deamination of the primary amines in these bases (Wink *et al.* 1991; Nguyen *et al.* 1992; Caulfield *et al.* 1998). In addition, reaction of dG with acidified nitrite at pH 3.7 forms dO and dX (Suzuki *et al.* 1996) and dA reacts to form dI, where the mechanisms are thought to involve a diazonium intermediate (Suzuki *et al.* 2009). Similar reactions occur in single and double stranded DNA where xanthine derived from G is formed at twice the yield of uracil (from C) (Caulfield *et al.* 1998) and dXMP is formed at three times the yield of dOMP in oligonucleotides (Suzuki *et al.* 1997). The reactions described above generally involve reaction of nucleobases with oxidised states of •NO such as $•NO_2$, N_2O_3 and NO^+, rather than direct reactions with •NO, so that the chemical pathways involved in initiating DNA damage would be very different to those occurring during γ-radiolysis.

In the radiolysis studies described in this chapter, the concentrations of reactants are adjusted to ensure that ~95% of •OH react directly with the bases/nucleosides/nucleotides and not with •NO (which would form nitrite), and that by supplying a constant source of a low concentration of •NO in the absence of O_2, the radicals formed on the nucleobases can then

react with •NO. Although in the presence of •NO the deamination products, X and HX, are formed from γ-radiolysis of G and A respectively, additional novel products have also been identified: 8azaG and 8azaA. In contrast, C does not undergo deamination during γ-radiolysis in anaerobic conditions in the presence of •NO. These differences between the purines and pyrimidines may in part reflect the respective intermediate radicals formed through reaction of the nucleobases with •OH and the subsequent reaction of the base radicals with •NO. The present work has suggested that deamination of G and A occurs through direct reaction of N-centred radicals with •NO. Equivalent radicals of C are unlikely to occur from reaction with •OH, which might explain why uracil is not observed in the presence of •NO. The formation of oxanine was not observed in any of the studies with G moieties, giving further evidence for the different chemistry which exists between reacting high concentrations of •NO with G in aerated solutions ($•NO_2/N_2O_3$) and γ-radiolysis of G in the presence of •NO in anaerobic conditions. In the case of A, the chemistry which occurs with the free base radicals is not the same when the proton on N-9 is substituted by deoxyribose. These differences suggest that HX and 8azaA modifications to A may not occur directly in DNA, although other modifications may occur.

Apart from •NO-induced deamination reactions which may or may not occur to the nucleotides in DNA, the repair efficiency of any of the products described in this chapter, if formed in genomic DNA, is as yet not known in detail. In addition, if these products are formed within radiation-induced clusters, changes in cell toxicity may also occur. This will be discussed further in Chapter 4. 8azaG has been investigated as an anti-cancer therapeutic (Kidder *et al.* 1951; Colsky *et al.* 1955; Dourado *et al.* 2007) and it is readily incorporated into cellular RNA. If 8azadGMP is formed in irradiated cellular DNA, or indeed RNA, then it may be partially responsible for the radiosensitization effects seen with •NO.

dXMP is stable to depurination in single and double stranded oligonucleotides at neutral pH (Vongchampa *et al.* 2003) and therefore is unlikely to be responsible for the

formation of spontaneous AP sites. The DNA repair enzyme, *E.Coli* endonuclease V, is able to repair X and HX lesions (Schouten and Weiss 1999; He *et al.* 2000) and 3-methyladenine DNA glycosylase II (AlkA) and endonuclease VIII in *E.coli* are also able to recognize X lesions (Terato *et al.* 2002) and are effective for the removal of X from X:C base pairs. In mammalian cells the AlkA homologue, methylpurine glycosylase, shows specificity for X in X:C pairs but not in other base pairings (Wuenschell *et al.* 2003). In comparison HX is recognized and removed more readily by human methylpurine glycosylase (Saparbaev and Laval 1994). The incorporation of any lesion within mammalian DNA may also have mutagenic potential if repair is delayed and the lesion carried through to replication where mis-pairing can occur (Eccles *et al.* 2011). Alternatively, deficiency of repair of damaged bases which might exist close to other damaged bases or SSB in clusters generated through IR may lead to deleterious cytotoxic replication-induced DSB; this is discussed further in Chapter 4.

To be able to study the potential for repair of the lesions generated during ionizing radiation in the presence of •NO, identification of all of the damaged bases formed in free nucleotides, oligonucleotides and DNA is necessary. Generation of sufficient quantities of the products and purification (for nmr, accurate mass and elemental analysis) of the many products arising from just one type of nucleotide reacting with •OH in the presence of •NO is in itself problematic, and mixed nucleotides in DNA even more challenging. As a constant supply of a low concentration of •NO is required throughout the irradiation period to generate the products and a maximum available dose rate of ~13 Gy/min available in the Institute's irradiator, increasing the product yield to the 5-10 mg required for these tests is not a straightforward task and a higher dose rate may be preferred. Alternatively, chemical synthesis of the predicted products could be carried out to confirm their identity. These base modifications could then be incorporated in DNA oligonucleotides to study their DNA repair mechanisms.

The ability of •NO to 'fix' radiation-induced free radicals to form non-radical species has helped to explain some uncertainties existing in the •OH-mediated mechanisms involved with nucleobases. Whether the modifications observed in these studies exist in genomic DNA following radiosensitization by •NO and what effect they might have on DNA strand break formation, repair and cell survival is addressed in Chapter 4.

4 Radiosensitization by nitric oxide – DNA damage and repair

4.1 Introduction

Previous findings have shown that micromolar concentrations of •NO sensitizes hypoxic mammalian cells to low LET radiation both through reduced cell survival and increased levels of γH2AX foci (Wardman *et al.* 2007), although the mechanisms of its action are largely unknown. The effects in cells are thought to involve in part the formation of some different types of DNA damage (Keefer and Wink 1996). As shown in Chapter 3, •NO induces specific lesions to DNA bases in hypoxia which are not normally formed by IR. These modifications may be difficult to repair, particularly if formed in clustered damage sites specific to radiation (§1.4.2). It is thought that processing of clusters containing •NO-modified DNA bases may lead to potentially lethal replication-induced DSB.

The aim of the investigations in this chapter was to determine if the types of DNA damage induced in the presence of •NO in anoxia compared to those generated in the same conditions in its absence (as described in Chapter 3), may be involved in the mechanisms by which •NO acts as a hypoxic cell radiosensitizer. The quantitation of radiation-induced DNA strand breaks in plasmids in the presence of •NO, before and after treatment with a glycosylase, to convert lesions into detectable SSB, should give an insight into if •NO modifies the level of prompt SSB and whether some of the damage sites are converted into SSB through repair processes. In addition, the measurement of •NO-induced DNA damage in irradiated hypoxic mammalian cells and the processing of any radiation-induced DNA lesions modified by •NO should determine if repair and/or replication are involved in the formation of additional DSB or SSB, other than those induced directly by radiation.

Section 4.2 is largely described in (Folkes and O'Neill 2013a); sections 4.4 and 4.5 are largely described in (Folkes and O'Neill 2013b).

4.2 Effect of •NO on the levels of SSB induced in plasmid DNA by γ-radiation

It has been previously been shown that the rate of reaction of •NO with the base-•OH adduct radicals of dGMP and uracil occurs at near diffusion controlled rates (Wardman *et al.* 2007). In Chapter 3 it was shown that •NO reacts with DNA base radicals in anoxia to form novel products which differ to those generated in anoxia alone. Some of the products identified through reactions with free 2′-deoxynucleotides were also seen to occur with short oligonucleotides (§3.6). It was important to establish whether these modifications generated by •NO may also occur in plasmid double-stranded DNA and how these lesions, if formed, may affect the formation of strand breaks.

Plasmid DNA is a good model system to follow SSB formation when exposed to IR. The reaction of •OH with PUC18 DNA (~1 mM) in N_2O-saturated Tris buffer (10 mM), which also acts as a scavenger, showed a loss in the intensity of the supercoiled plasmid DNA band with increasing dose (Figure 4-1A), and an increase in intensity in the band corresponding to the relaxed form of the plasmid due to SSB formation. The additional presence of ~1.8 μM •NO reduced the level of SSB per unit with dose by approximately 3-fold (Figure 4-1A). The protection which •NO has on the formation of SSB may reflect the ability of •NO to 'fix' radical damage (Scheme 1-5). However, fast reactions of •NO with •OH ($k \sim 10^{10}$ M^{-1} s^{-1} (Seddon *et al.* 1973) could also contribute to the lower levels of SSB observed, by •NO potentially competing with DNA and Tris for reaction with •OH. By comparing the relevant rate constants, •OH has a 50-fold greater reactivity with the plasmid DNA than with •NO, at the concentrations used so is unlikely to react directly with •NO (Table 4-1).

reactant	k (•OH) (M^{-1} s^{-1})	[solute] (M^{-1})	k (solute) (s^{-1})	%
PUC18	8×10^{8}	1×10^{-3}	8×10^{5}	5.1
•NO	1.0×10^{10}	1.8×10^{-6}	1.8×10^{4}	0.1
Tris	1.5×10^{9}	1×10^{-2}	1.5×10^{7}	94.8

Table 4-1 Table to show the relative reactivity of solution components with •OH in N_2O-saturated solutions.

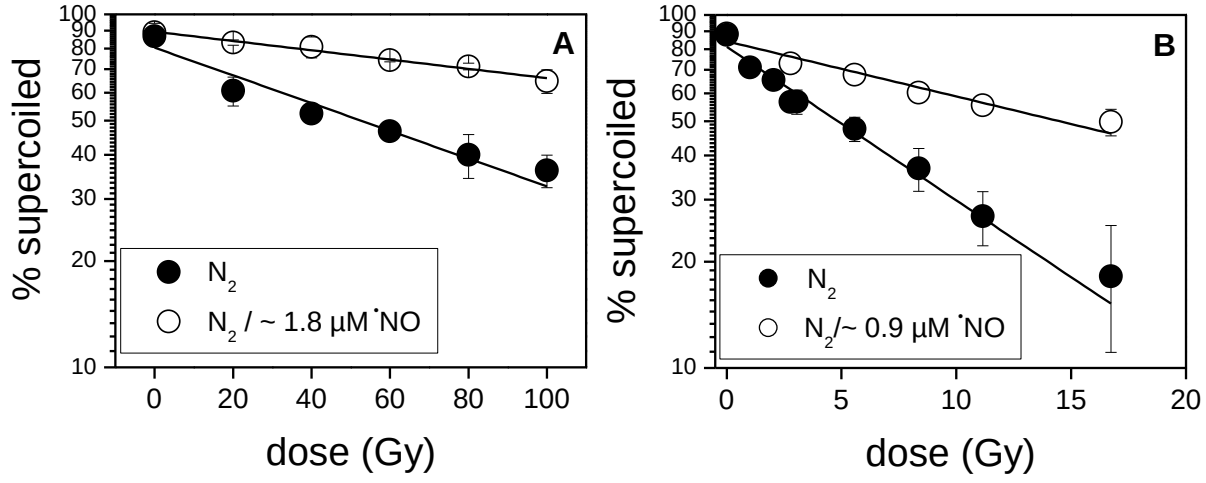

Figure 4-1 Measurement of SSB from the γ-irradiation of N_2O-saturated solutions containing PUC18 (~1 mM) in the presence of a constant supply of A: 1.8 µM •NO, 10 mM Tris HCl and a dose rate of 13 Gy/min B: 0.9 µM •NO, 0.1 mM Tris HCl and a dose rate of 1.2 Gy/min. results represent mean and s.e.m of at least 3 independent experiments. (B Reprinted (with minor modification) from *Free Radical Biology & Medicine*, Vol 58, Lisa K. Folkes and Peter O'Neill, Modification of DNA damage mechanisms by nitric oxide during ionizing radiation, 14-25, Copyright (2013), with permission from Elsevier.

The concentration ratio between DNA and •NO was varied by changing the DNA concentration from 0.3-10.3 mM and •NO from 0.9–9 µM. These changes in ratio were found to have little or no effect on the protection which •NO had on the yield of SSB following 100 Gy, shown by the relatively parallel lines (Figure 4-2A). The level of SSB (determined as the loss in the % of supercoiled DNA) increased slightly as the DNA concentration increased, which may reflect the reduced scavenger effect. In these types of experiments, the scavenger concentration of Tris is usually used at 100 mM, to ensure constant biomimetic conditions

(scavenging capacity), so that the mean •OH-diffusion distance is ~4 nm (Roots and Okada 1975), the mean diffusion distance for •OH in cells. Under these conditions the majority of the •OH produced react with the Tris scavenger (Table 4-1). However, reaction of Tris with •OH produces Tris radicals (Hicks and Gebicki 1986) and •NO reacts rapidly with most carbon-centred radicals ((k ~10^9 M^{-1} s^{-1}) (Czapski *et al.* 1994)). •NO could become depleted by reactions with •OH-induced Tris radicals in competition with its reaction with DNA-•OH adducts, especially at lower concentrations of DNA (although the samples are continually exposed to a stream of ~0.9-1.8 µM •NO). Although a rate constant for reaction of •NO with Tris radicals was not determined in this study, a stable Tris-NO derived product was identified by HPLC following γ-radiolysis of 10 mM Tris in the presence of ~0.9 µM •NO/~24 mM N_2O (Figure 4-2B).

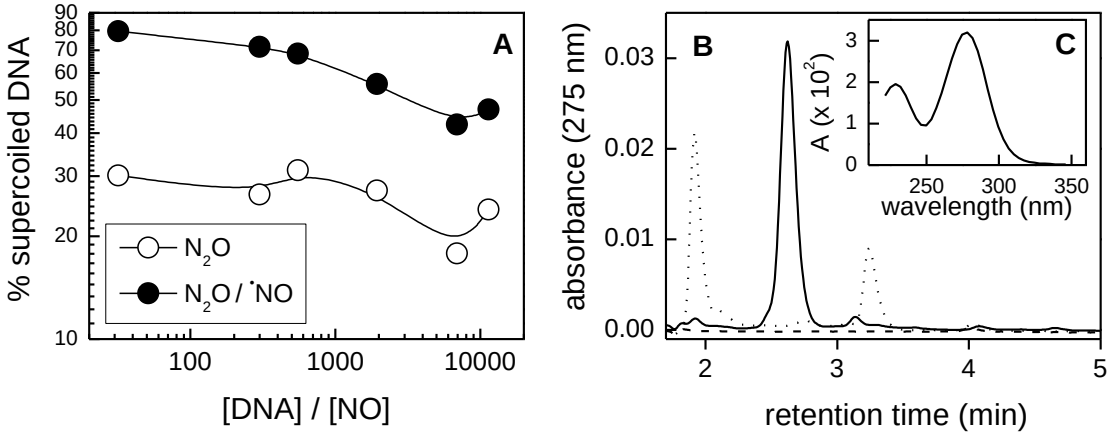

Figure 4-2 (A) Effect of the ratio of PUC18 DNA to •NO concentration on the formation of SSB following γ-radiolysis (~100 Gy) in N_2O saturated solutions with 10 mM Tris, 1mM EDTA, pH 8; (B) Chromatograms showing the formation of absorbing products at 275 nm following the γ-radiolysis (~195 Gy) of N_2O-saturated Tris (10 mM) (…) in the presence of ~0.9 µM •NO (—),un-irradiated Tris (---); (C) Absorption spectrum for the •NO-modified product (retention time 2.7 min).

Although •NO has an ~3-fold protective effect on the formation of SSB in solutions containing 1 mM plasmid, 1.8 µM •NO and 10 mM Tris (Table 4-2), it was decided in further studies to use a concentration of 0.1 mM Tris, at a fixed concentration of PUC18 of 1 mM, at

[•NO] (μM)	[Tris] (mM)	slope	•NO effect
0	10	0.009 ± 0.0002	
1.8	10	0.003 ± 0.0002	3.0
0	0.1	0.119 ± 0.004	
0.9	0.1	0.036 ± 0.004	3.3

Table 4-2 Effect of scavenger (Tris) and •NO concentration on the yield of SSB in PUC18 plasmid following γ-irradiation.

doses up to 10 Gy, to reduce the probability of reaction of •OH-induced Tris radicals with •NO. Constant bubbling throughout the irradiation time also minimizes the depletion of •NO. From the comparison of the slopes of dose dependence for formation of SSB under N_2O in the presence or absence of •NO in 0.1 mM Tris, •NO has an ~3 fold protective effect on the fractional loss of supercoiled DNA (Figure 4-1B, Table 4-2), similar to that determined with 10 mM Tris present. The results are indicative of fewer prompt SSB being formed in the presence of •NO under anaerobic conditions. From these findings it is inferred that •NO protects against prompt radiation-induced SSB in the absence of O_2. However, it has previously been reported that •NO promotes the formation of SSB (detected by alkaline comet analysis) and DSB (detected by γH2AX foci) in irradiated anoxic mammalian cells (Wardman *et al.* 2007). The plasmid results were therefore surprising. One explanation for the differences observed between cells and plasmid DNA is that DNA damage repair processes occur in cells, which may convert some types of DNA damage into further strand breaks, in addition to those formed immediately upon irradiation. To investigate this possibility, digestion of irradiated plasmids by a glycosylase involved in base excision repair was studied.

4.2.1 Enzymatic excision of base lesions in irradiated plasmid DNA

Since •NO reduces the number of radiation-induced SSB in anoxia and base excision repair (BER) is believed to be a major repair pathway for protecting cells from •NO-induced damage (Richardson *et al.* 2009), it was investigated whether some of the radiation-induced

damage in plasmid DNA in the presence of •NO could be converted into additional SSB, termed enzyme sensitive SSB, by enzymatic digestion. Glycosylases are the first step in BER, cleaving the N-glycosidic bonds of the damaged bases from the remaining DNA chain leaving an abasic site. The *E.coli* glycosylase Fpg, identifies and removes some radiation-induced purine modified bases in plasmid DNA as described previously (Fulford *et al.* 2001). Plasmid DNA which had been irradiated with and without the presence of •NO was treated post-irradiation with Fpg. Any additional SSB were measured by a decrease in the percentage of supercoiled DNA, with a concomitant increase in the formation of relaxed and linear forms of the plasmid. Since additional SSB are formed, it is inferred that some of the damaged bases present in the plasmid DNA are converted into enzyme sensitive SSB by Fpg. Quantitation of the glycosylase-induced increase in the yield of SSB (assuming a linear response from the single dose studies which were carried out), indicates that •NO doubles the yield of Fpg sensitive SSB relative to that of prompt SSB when compared with the finding using •OH alone (Table 4-3).

γ-radiolysis conditions	**% supercoiled DNA remaining**	**extrapolated fractional loss/Gy**	**prompt SSB: glycosylase induced SSB**
•OH control	54.3 ± 2.1	0.10	
•OH + heat	58.1 ± 2.0	0.08	
•OH + Fpg	36.3 ± 3.9	0.18	1 : 1.0 ± 0.1
•OH + •NO control	71.6 ± 3.9	0.02	
•OH + •NO + heat	60.4 ± 4.2	0.04	
•OH + •NO + Fpg	25.3 ± 2.1	0.12	1 : 2.0 ± 0.2

Table 4-3 Measurement of SSB and Fpg-sensitive SSB in PUC18 plasmid DNA following either 5 Gy irradiation of 1 mM PUC18 in N_2O-saturated solutions or 10 Gy γ-irradiation of 1 mM PUC18 in aqueous solutions containing ~0.9 μM •NO (balance N_2O). Reproduced (with minor modification) from *Free Radical Biology & Medicine,* Vol 58, Lisa K. Folkes and Peter O'Neill, Modification of DNA damage mechanisms by nitric oxide during ionizing radiation, 14-25, Copyright (2013), with permission from Elsevier.

The yield of enzyme sensitive SSB in the presence of •NO also includes any products coming from DNA radicals which are not reactive to •NO. These results give strong evidence that •NO may induce cellular DNA strand breaks damage through base excision repair processes.

4.2.2 Detection of 2′-deoxy-8-azaguanosine monophosphate in irradiated plasmid DNA

It was shown in Chapter 3 that •NO reacts with guanine-•OH adducts to from 8-azaguanine. This chemistry occurs with the free base, nucleotide and a short single-stranded oligomer. As the formation of radiation-induced SSB in PUC18 plasmid DNA is protected by the presence of •NO, and Fpg, a glycosylase which recognizes some purine modifications, creates further SSB after incubation with irradiated plasmid, it is possible that 2′-deoxy-8-azaguanosine (8azadGMP) is also formed in the irradiated plasmid DNA which may be recognized by Fpg.

When solutions of PUC18 plasmid (1mM) were irradiated with up to ~800 Gy in anoxia in the presence of ~1.8 μM •NO, a product was formed which following nuclease P1 digestion, was measured by HPLC analysis with fluorescence detection at pH 9. As this product co-elutes with 8azadGMP formed from •OH-oxidation of dGMP in anoxia in the presence of •NO (Figure 4-3), it is likely that 8azadGMP is generated in plasmid DNA irradiated in anoxia in the presence of •NO.

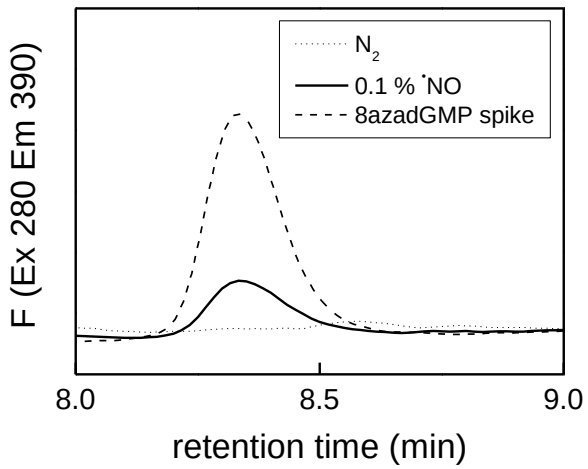

Figure 4-3 Chromatogram to show the formation of 8azadGMP (detected using fluorescent spectroscopy at excitation 280 nm and emission 390 nm, pH 9) in plasmid DNA digested with nuclease P1 following γ-radiolysis (~780 Gy) with (—) or without (---) the presence of ~1.8 μM •NO. Also shown is a sample spiked with 8azadGMP (generated through the oxidation of dGMP by •OH in the presence of •NO) (…). Chromatography conditions as for Figure 3-18D.

It is not known whether 8azadGMP is a substrate for Fpg and therefore whether it contributes to the formation of Fpg sensitive SSB. However, modifications to other nucleotides induced by •NO during IR are also likely, which may or may not be recognized by repair enzymes. At present no other modifications of any of the bases in irradiated plasmid, other than 8azadGMP, have been identified at the doses used.

4.3 Effect of •NO on the formation of DNA SSB in irradiated anoxic cells

The protective effect which •NO has on the formation of γ-radiation-induced SSB in double-stranded plasmid DNA may not necessarily be translated to cellular systems, where the DNA is packaged within the nucleus in histone protein bound nucleosomes. The alkaline comet assay can be utilized to measure SSB in genomic DNA. The level of SSB in V79-379A cells immediately following 1–2 Gy γ-radiation in the presence of ~18 μM •NO were found to be slightly higher than those induced in anoxia alone (Wardman *et al.* 2007). Other studies showed that the formation of SSB in prostate PC-3 cells in normoxia in the presence of a •NO-donating non-steroidal anti-inflammatory was significantly increased over levels in control cells after 4 Gy but not at 0 or 2 Gy. The rate of repair of SSB following 8 Gy in cells exposed to the •NO-donating drug was also significantly reduced up to 60 min compared to that in un-exposed irradiated cells (Stewart *et al.* 2011).

The formation of radiation-induced prompt SSB (measured using the alkaline comet assay) in V79-4 cells, saturated with N_2, with and without the presence of 18 μM •NO increased with dose (0-2 Gy), with no observable differences seen between the two conditions (Figure 4-4A). Incubation of the irradiated cells at 37 °C for up to 1 h on agarose slides, showed no differences in SSB yield between cells irradiated in the presence of •NO and cells irradiated in anoxia alone (Figure 4-4B), suggesting that in V79-4 cells, if DNA repair enzymes recognize •NO-associated base modifications, they do not convert damage into additional and detectable SSB within 60 min. It should be noted that 1 h at 37 °C is sufficient

time to repair the majority of radiation-induced SSB in aerobic conditions (Dikomey and Franzke 1986). The levels of deoxyribose nucleotide pools (dNTPs) in cells are significantly decreased by exposure to hypoxia (Pires *et al.* 2010), so a depleted dNTP pool may reduce the rate of repair of radiation-induced SSB in anoxia.

As the repair studies suggest that glycosylases present in V79-4 cells do not recognize •NO-modified base lesions and convert them into detectable SSB, Fpg, which was used for digestion of irradiated plasmids (§4.2.1) was incubated with post-lysis nucleoids embedded in agarose post-irradiation. The comet tail moments were increased in cells irradiated in both anoxia and in the presence of •NO following incubation with Fpg; however, no observable differences were seen between the two conditions (Figure 4-4C). Some of the lesions formed under these conditions are therefore converted into SSB by Fpg but these may be due to oxidized purine lesions which are formed independently of the presence of •NO.

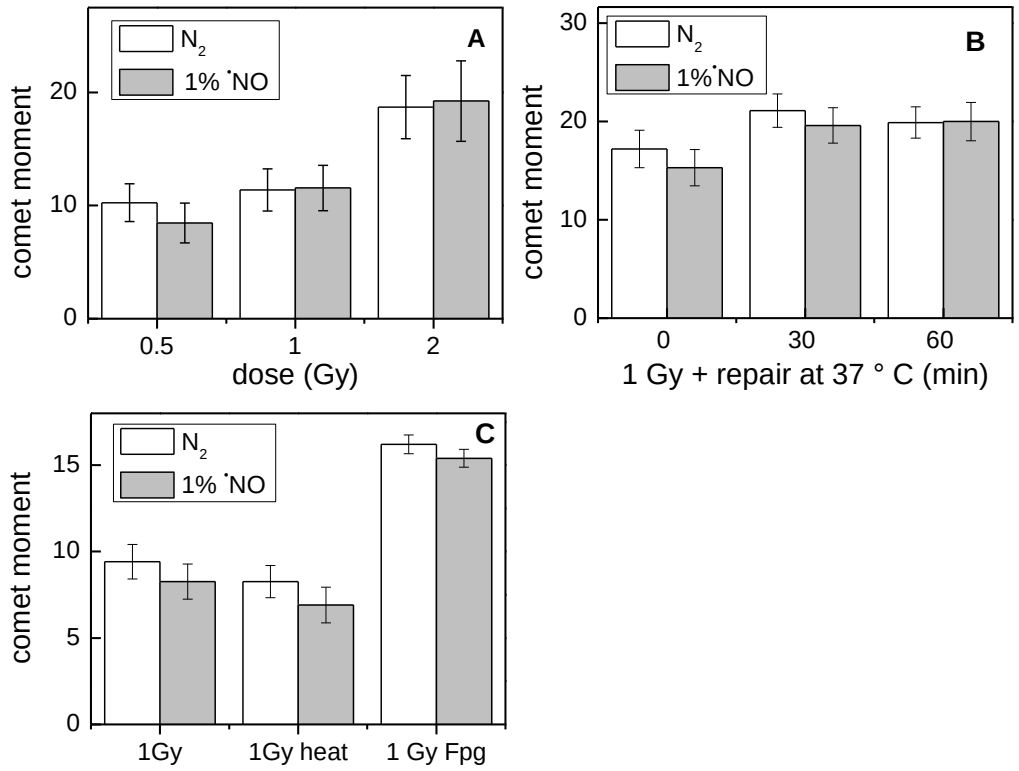

Figure 4-4 Measurement of SSB by alkaline comet assay in exponentially growing V79-4 cells γ-irradiated in anoxia (N_2) or in 18 μM •NO; (A) effect of dose on the comet moment; (B) effect of time of incubation at 37 °C following 1 Gy; (C) effect of incubation at 37 °C for 1 h with Fpg glycosylase (1.05 ng/μl) following 1 Gy. Results represent the mean and s.e.m. of at least 3 independent experiments.

4.4 Effect of •NO on induction of DNA DSB in irradiated mammalian cells

It has previously been reported that anoxic hamster fibroblast (V79-379A) and human breast cancer cells (MCF-7) γ-irradiated in anoxia in the presence of •NO result in more DSB than cells irradiated in anoxia alone, and that repair of DSB is delayed (Wardman *et al.* 2007). Having shown earlier that the presence of •NO led to a specific base modification (8azadGMP) in γ-irradiated plasmid DNA (§4.2.2), and that some additional modifications may also be recognised and removed by Fpg (§4.2.1), it is proposed that if repair of DNA damage induced in the presence of •NO is inefficient, then •NO-enhanced DSB in irradiated cells may be due to increased probability of base lesions encountering a replication fork. As a consequence, un-repaired lesions may result in replication-induced DSB through the collapse of replication forks (§1.5.2). Some of the base modifications may occur close to SSB or other lesions to give clusters of lesions, which can also lead to replication-induced DSB. The effect of cell cycle or growth phase on radiation cell survival was initially studied following irradiation under anoxia in the presence of •NO.

4.4.1 Effect of cell replication on nitric oxide-induced radiosensitization

In order to investigate whether cells undergoing replication in S and G2 phases of the cell cycle are more radiosensitive in the presence of •NO than those cells in G1, V79-4 cells either in mid-exponential growth or approaching confluency were studied. A clonogenic assay was utilised and the surviving fraction (SF) measured as a function of dose from 0-5 Gy. V79-4 cells in both growth conditions were radiosensitized by ~18 μM •NO compared to cells exposed to anoxia alone. Confluent cells irradiated in the presence of •NO showed a decrease in cell survival with dose, with a survival enhancement ratio (SER) of 1.4 at 0.4 SF (Figure 4-5A). Exponentially growing cells showed a higher SER of 2.0 at 0.4 SF (Figure 4-5B). Although radiosensitization in the presence of •NO was similar in both growing conditions, in its absence exponentially growing cells were more resistant to radiation than their largely non-replicating confluent counterparts, as has been shown previously (Berry *et al.* 1970).

4.4.2 *Measurement of γH2AX formation and repair by flow cytometry*

By measuring the levels of DSB, detected as γH2AX staining, in cells irradiated in either exponential growth or when approaching confluency, it was possible to address whether replication-induced DSB are formed which may then contribute to cytotoxicity. Following γ-irradiation (5 Gy), cells in both exponential growth and in a state of confluency, showed increased levels of fluorescence (representative of γH2AX foci formation), detected using flow cytometry, when exposed to ~18 μM •NO compared to cells irradiated in anoxia alone. Histograms of fluorescence intensity against number of cells showed a shift towards the right when cells were irradiated, indicating that more cells stained for γH2AX compared to un-irradiated cells. This is particularly noticeable in the presence of •NO (Figure 4-5C). From the histogram plots for each treatment, the mean fluorescence was calculated and divided by the mean control fluorescent levels to calculate relative fluorescence. Replicating cells exhibited higher fluorescence following IR than confluent cells, especially when •NO was present (Figure 4-5D and E). Under both growth conditions, anoxic cells reached maximum labeling ~90 min after plating at 37 °C. However, cells exposed to ~18 μM •NO did not reach a maximum level of staining until 2-3 h after plating. This effect was particularly apparent in the exponentially growing cells.

Studies were continued with exponentially growing cells only, incubated up to 24 h following 5 Gy. Repair of cellular DSB could be detected by the loss of fluorescence over time of incubation at 37 °C. At 3 h post-irradiation, cells which had been irradiated in the presence of •NO showed significantly higher levels of fluorescence over those cells which had been irradiated in anoxia alone; however, by 4 h the differences were not significant but still higher for •NO-exposed cells. The rate of repair of DSB (shown by the loss in fluorescence over time) is broadly similar for cells irradiated in both anoxia and in ~18 μM •NO. By 24 h there are no apparent differences in fluorescence levels between the two growth conditions (Figure 4-6A).

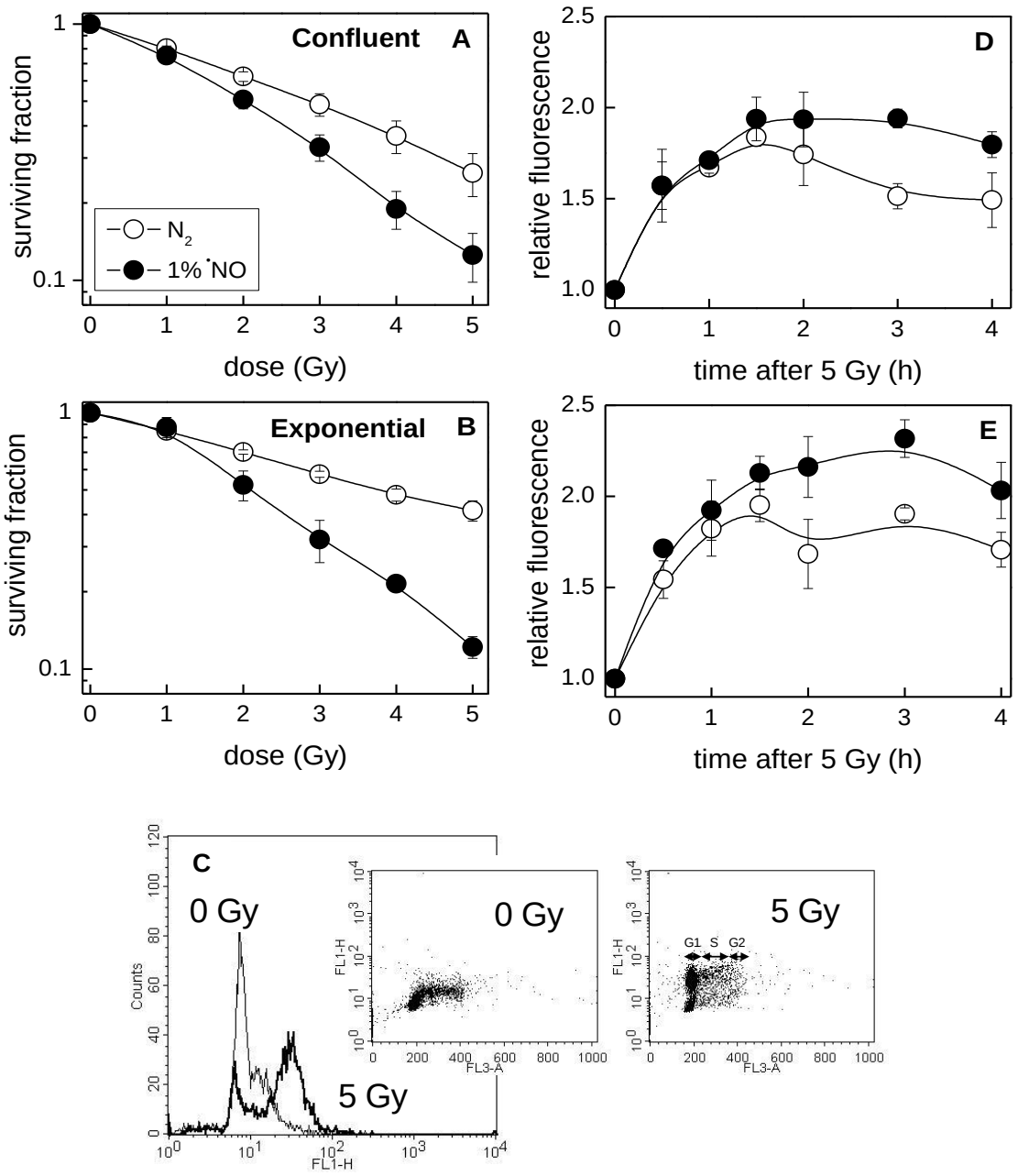

Figure 4-5 Cell survival of V79-4 cells with dose following γ-radiation in N_2 (○) or ~18 μM •NO/N_2 (●) saturated cell suspensions in (A) confluent and (B) exponential growth cells; (C) Flow cytometry histogram and dot plots gated for G1-G2 status showing the increase in fluorescence with radiation in exponential cells 2 h following γ-irradiation with 0 or 5 Gy when saturated with ~18 μM •NO/N_2; effect of time on the formation of γH2AX foci in (D) confluent and (E) exponential growth cells. Results represent the mean and s.e.m. of at least 3 independent experiments. Reproduced (with minor modification) from *Nitric Oxide*, Lisa K. Folkes and Peter O'Neill, Vol 34, DNA damage induced by nitric oxide is enhanced at replication, 47-55, Copyright (2013), with permission from Elsevier.

Re-analysis of the flow cytometry data with additional gating for each phase of the cell cycle (G1, S, G2) shows evidence for differences observed in γH2AX staining in cells

irradiated in anoxia and those irradiated in the presence of •NO (Figure 4-6A) to be most evident in cells in G2, at times 4-6 h following irradiation (Figure 4-6B and C). Cells are most radiosensitive to •NO in exponential growth (Figure. 4-5B) where S-phase cells can represent ~55% of the total cell population.

Measurement of DSB by flow cytometry is relatively simple and quick to analyse. However, values only give an indication of γH2AX levels in an average population and do not account for the number of foci per cell. Measurements could also be prone to apparent high fluorescence levels which could occur from pan-nuclear staining of apoptopic cells for example. Confocal microscopy gives a more specific indication of DSB through detection of γH2AX foci in each cell and so studies were also undertaken using this technique.

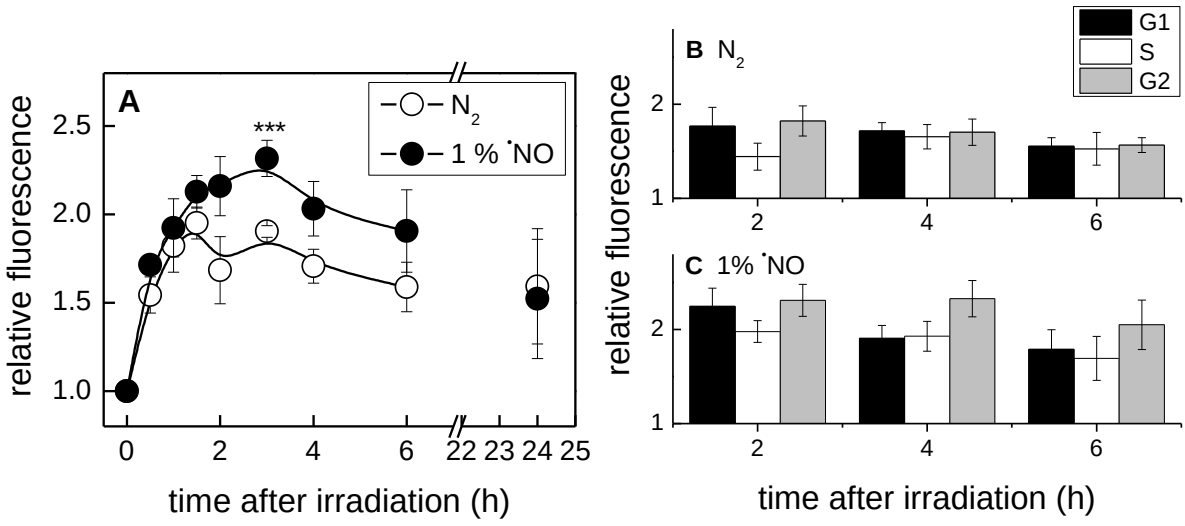

Figure 4-6 Effect of time of incubation at 37 °C following γ-radiolysis (5 Gy) of exponentially growing V79-4 cells in N_2 or ~18 μM •NO saturated cell suspensions on (A) the formation of γH2AX staining in the total cell population and the relative fluorescence in G1, S and G2 cells irradiated in (B) N_2 and (C) ~18 μM •NO, all measured by flow cytometry. Results represent the mean and s.e.m of at least 3 independent experiments. *** $p < 0.001$.

4.4.3 Measurement of γH2AX foci formation and repair by confocal microscopy

Irradiation (up to 2 Gy) of V79-4 cells saturated with N_2 or in the presence of ~18 μM $^{\bullet}NO$ (balance N_2) produced γH2AX foci within 30 min of plating of the irradiated cells at 37 °C.

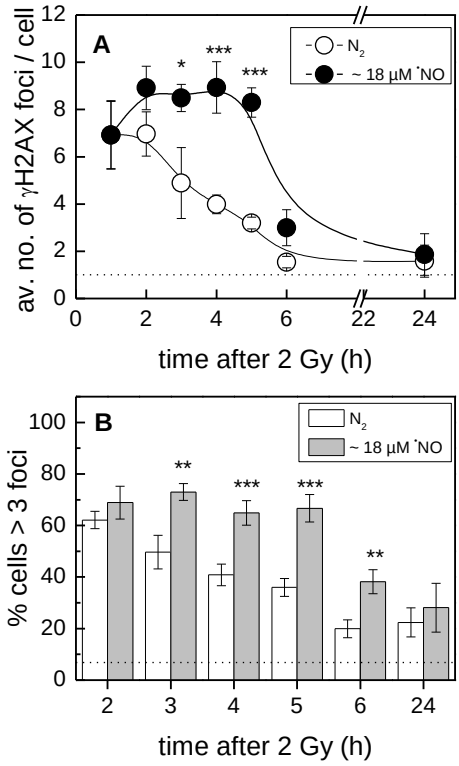

Figure 4-7 Effect of incubation time at 37 °C on (A) the formation and repair of γH2AX foci and (B) the percentage of cells containing >3 foci in exponentially growing V79-4 cells γ-irradiated (2 Gy) in anoxia (N_2) or in ~18 μM $^{\bullet}NO$. Dotted lines show the numbers of foci/cell for sham treated cells 24 h after plating. Results represent the mean and s.e.m. of at least 3 independent experiments. * $p < 0.05$, ** $p < 0.01$, *** $p < 0.001$. (A) reproduced (with minor modification) from *Nitric Oxide*, Lisa K. Folkes and Peter O'Neill, Vol 34, DNA damage induced by nitric oxide is enhanced at replication, 47-55. Copyright (2013), with permission from Elsevier.

Flow cytometry analysis of the formation of γH2AX staining in V79-4 cells irradiated in the presence of $^{\bullet}NO$ showed that maximum staining was observed ~2 h later than for those cells irradiated in anoxia alone (Figure 4-5E). Measurement of γH2AX foci in attached irradiated cells using confocal microscopy also showed a delay in the maximum staining levels for those cells irradiated in the presence of $^{\bullet}NO$. Highest numbers of foci were observed in cells which had been irradiated with 2 Gy in anoxia, 1 h after incubation at 37 °C with ~7 foci/cell. The

numbers of foci/cell then decreased with time and by 6 h numbers were close to control levels of γH2AX, indicating that repair of most DSB had occurred (Figure 4-7A). In contrast, those cells irradiated in the presence of ~18 μM •NO in anoxia showed γH2AX foci which continued to increase in number to a maximum of ~9 foci/cell after 2 h at 37 °C. Foci numbers remained high up to 5 h following irradiation, when numbers subsequently decreased and were not significantly different to the levels observed at 6 h in those cells which had been irradiated in anoxia alone (Figure 4-7A). Apart from the increase in foci number observed in cells which had been irradiated in the presence of •NO, significantly more cells expressed > 3 foci per cell, 3-6 h following irradiation of •NO-exposed cells, than those irradiated in anoxia alone (Figure 4-7B). The delay in reaching maximum numbers of γH2AX foci in cells which had been irradiated in the presence of ~18 μM •NO and the slow rate of repair of DSB observed 2-5 h post-irradiation is suggestive of additional DSB being formed at replication. To investigate further whether replication-induced DSB contribute to the enhancement of DNA damage associated with •NO, RAD51 was used as a marker for homologous recombination (Harper *et al.* 2010; Groth *et al.* 2012) which repairs replication-induced DNA DSB during S and G2 phases of the cell cycle (§1.5.3).

4.4.4 Measurement of RAD51 foci in V79-4 cells by confocal microscopy

V79-4 cells were γ-irradiated (10 Gy) in anoxia or in the presence of ~18 μM •NO and the number of cells which formed RAD51 foci were counted as well as the number of foci per positive cell. Similar numbers of RAD51 foci per positive cell were observed 4-6 h post-irradiation in both anoxia and •NO-treated cells (Figure 4-8A). However, after 24 h incubation at 37 °C, those cells which were irradiated in the presence of •NO exhibited about double the number of foci/positively stained cell than those irradiated in N_2 alone (Figure 4-8A). This effect was also reflected in the percentage of cells which showed foci (Figure 4-8B); however, the difference here was not significant.

Since the numbers of RAD51 foci are higher 24 h after γ-radiolysis in V79-4 cells irradiated in the presence of •NO than those irradiated in anoxia alone, this suggests that •NO-associated DNA damage may lead to replication-induced DSB during S-phase through encountering a replication fork.

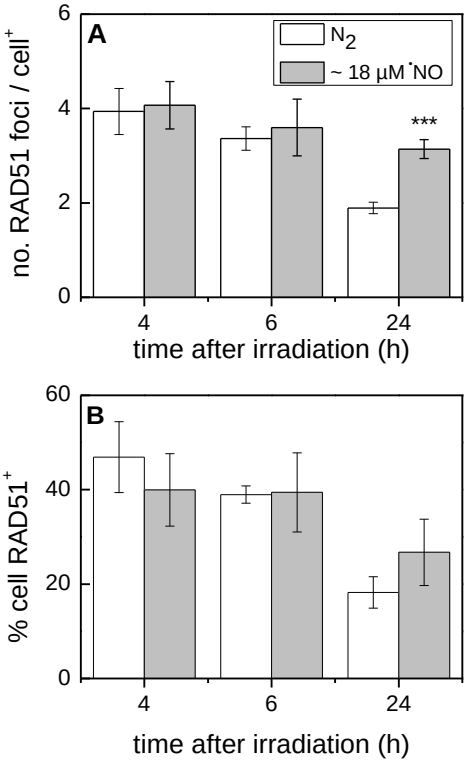

Figure 4-8 Effect of time after plating in EMEM ~15 min following γ-radiolysis (10 Gy) of suspensions of V79-4 cells saturated with N_2 or 1% •NO (~18 µM)/N_2 on; (A) the number of RAD51 foci per cell positive for RAD51 staining and (B) the percentage of cells expressing RAD51 foci. Results represent data from at least 3 independent experiments. *** p <0.001. Reproduced (with minor modification) from *Nitric Oxide*, Lisa K. Folkes and Peter O'Neill, Vol 34, DNA damage induced by nitric oxide is enhanced at replication, 47-55, Copyright (2013), with permission from Elsevier.

To investigate further whether replication may be involved in the enhanced DNA damage induced by •NO in irradiated cells, human HF-19 cells were used which could be co-stained for cyclin A, a marker for cells in S and G2 phase, and also 53BP1, an alternative marker to γH2AX for radiation-induced DSB. The antibody against γH2AX could not be used for these studies as it requires the same secondary antibody as the cyclin A primary antibody.

4.4.5 *Detection of DNA double strand breaks in relation to cell cycle*

HF-19 cells irradiated with 2 Gy in the presence of ~18 μM •NO in anoxia showed an ~2-fold increase in the level of 53BP1 foci/cell, 4 h after plating at 37 °C, compared with cells irradiated in anoxia alone. The majority of the increased numbers of foci were observed in cells also expressing cyclin A, a marker of cells in S and G2 phases of the cell cycle (Figure 4-9).

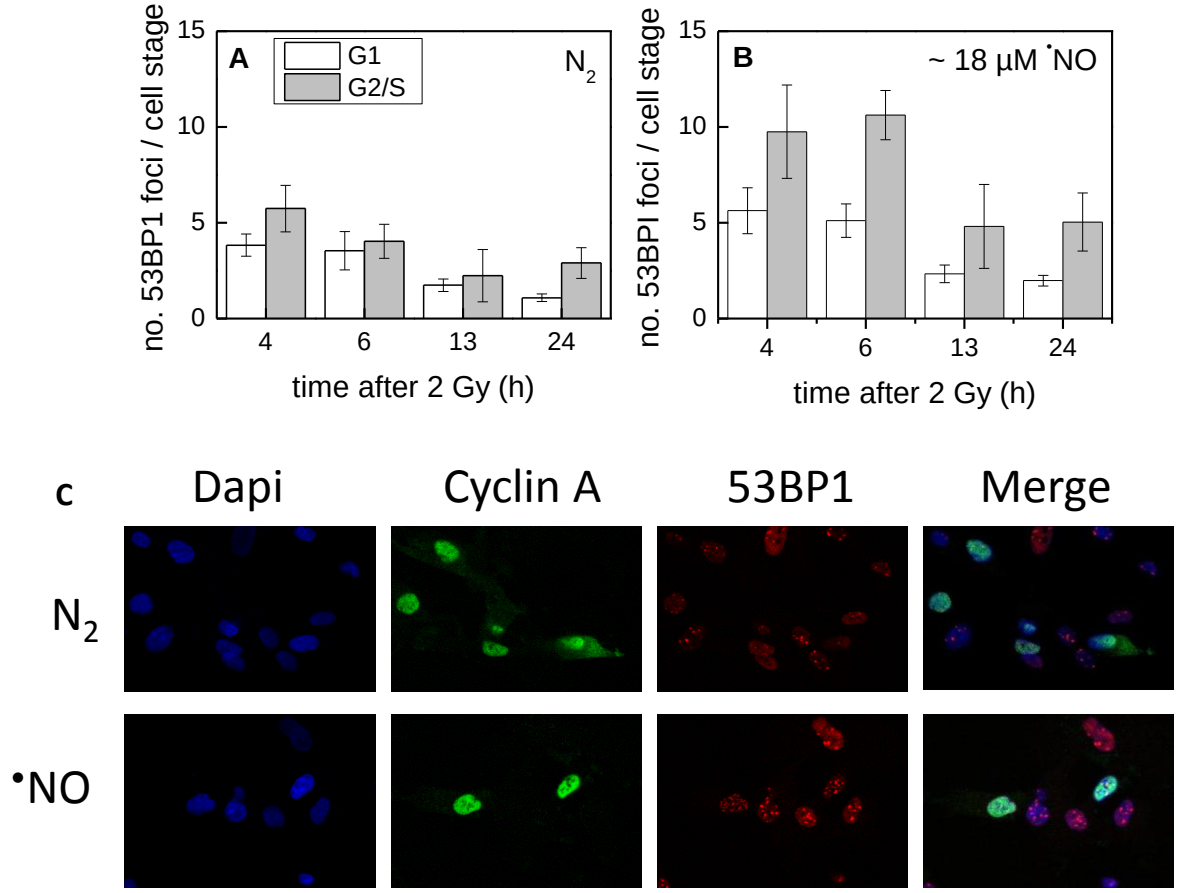

Figure 4-9 Effect of time after plating on the number of 53BP1 foci in G1 or S/G2 (cyclin A positive) phases of the cell cycle after γ-radiolysis (2 Gy) of HF-19 cells in; (A) N_2-saturated cell suspensions; (B) •NO (~18 μM) saturated cell suspensions; (C) Confocal images (x40) 6 h following radiolysis, DAPI identifies the nucleus. Reproduced (with minor modifications) from *Nitric Oxide*, Lisa K. Folkes and Peter O'Neill, Vol 34, DNA damage induced by nitric oxide is enhanced at replication, 47-55, Copyright (2013), with permission from Elsevier.

HF-19 cells which had been irradiated (2 Gy) in anoxia with or without the addition of ~18 μM •NO were also stained independently for γH2AX. In agreement with the findings using V79-4 cells, HF-19 cells irradiated in the presence of •NO exhibited more γH2AX foci

per cell than those treated in anoxia alone (Figure 4-10A). Although fewer time points were taken using HF-19 cells, the results indicate that the loss of foci is similarly slow when •NO is present during γ-radiolysis. Further, a greater proportion of cells also exhibit >3 γH2AX foci compared to those cells irradiated in anoxia alone (Figure 10B).

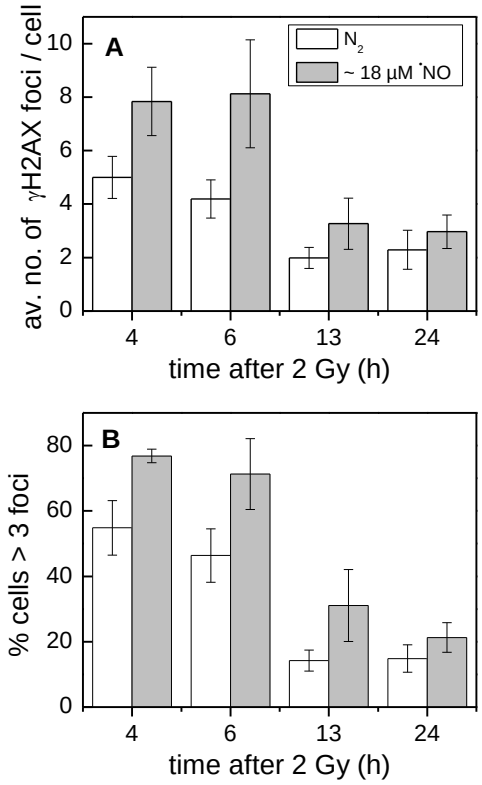

Figure 4-10 Effect of time after plating ~15 min following γ-radiolysis (2 Gy) of suspensions of HF-19 cells saturated with N_2 or 1% •NO (~18 µM)/N_2 on; (A) the number of γH2AX foci per cell and (B) the percentage of cells expressing >3 γH2AX foci. Results represent the mean and s.e.m of at least 3 independent experiments.

4.5 Radiosensitization of cells in hypoxia

The data described above were obtained in anoxic cells because of the difficulties of preventing interaction of •NO with O_2, where the resulting products may complicate the findings (§1.6.3). In tumours, anoxic regions are likely to contain necrotic non-viable cells which are not a target for radiotherapy. It is the hypoxic regions (O_2 <1%) of tumours where the cells are particularly difficult to kill (§1.3.1). As discussed earlier, one mechanism by which O_2 enhances radiation-lethality is due to the induction of DNA strand breaks and modified bases (§1.4.4). Preliminary investigations were undertaken using similar concentrations of the two gases to radiosensitize V79-4 cells, and study whether the time-dependent changes in the formation of γH2AX and 53BP1 foci reflected differences in

survival and DNA repair. Exponentially growing V79-4 cells were saturated with 1% O_2/N_2 (~13 µM O_2) or 1% $^{\bullet}NO/N_2$ (~18 µM $^{\bullet}NO$) and irradiated with doses up to 5 Gy for cell survival studies and 2 Gy for foci measurements.

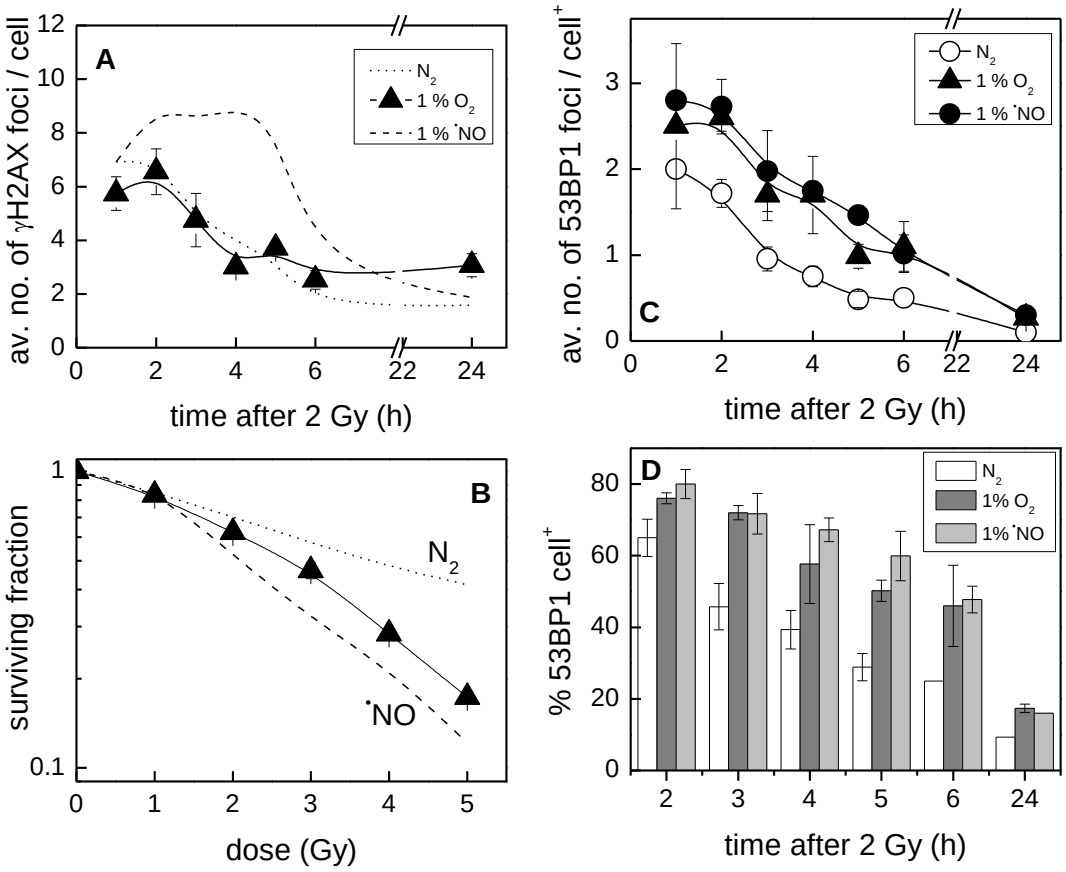

Figure 4-11 Effect of incubation time following 2 Gy γ-rays in N_2, 1% O_2/N_2 or 1% $^{\bullet}NO/N_2$ saturated cells on the formation and repair of DSB measured by γH2AX (A) and 53BP1 (C) in V79-4 cells. (B) Radiosensitization of V79-4 cells by ~13 µM O_2; (D) percentage of cells expressing 53BP1 foci. All results represent the mean and s.e.m of at least 3 independent experiments. A and B reproduced (with minor modification) from *Nitric Oxide*, Lisa K. Folkes and Peter O'Neill, Vol 34, DNA damage induced by nitric oxide is enhanced at replication, 47-55, Copyright (2013), with permission from Elsevier.

Differences were seen between O_2 and $^{\bullet}NO$-exposed cells in the numbers of γH2AX foci per cell. Cells irradiated in 1% O_2 exhibited less foci than those irradiated in the presence of 1% $^{\bullet}NO$, most significantly 2-5 h post-irradiation (Figure 4-11A). The loss of γH2AX foci with time indicate that DSB are repaired more efficiently after irradiation in 1% O_2 or under anoxia compared to in 1% $^{\bullet}NO/N_2$. In addition, exponentially growing V79-4 cells irradiated

in the presence of 1% O_2 were radiosensitized with a SER of 1.6 at a survival fraction of 0.4 compared to 2.0 for 1% •NO (~18 μM) (Figure 4-11B). It has also previously been reported that at lower concentrations, •NO (~70 nM) is a much more efficient radiosensitizer than equivalent concentrations of O_2 (Wardman *et al.* 2007).

Both O_2 and •NO induce more 53BP1 foci/cell than cells irradiated in anoxia. However, the delay in repair of DSB, seen as a loss of radiation-induced γH2AX foci, in the presence of •NO is different to that for loss of radiation-induced 53BP1 foci in the presence of •NO (Figure 4-11C). Following IR many of the DSB are repaired within 1 h as shown by pulsed field gel electrophoresis (Rothkamm and Löbrich 2003; Leatherbarrow *et al.* 2006). 53BP1 foci are thought to represent the presence of DSB but γH2AX foci may be a better indicator for stalled replication forks, as 53BP1 foci were not formed following replication arrest by hydroxyurea (Schultz *et al.* 2000).

4.6 Effect of antioxidants on the radiosensitization of cells in vitro

Antioxidants are chemicals which react rapidly with reactive oxygen species and free radicals and are efficient radioprotectors. In tissue the levels of antioxidants (which include the hydrophilic chemicals urate, ascorbate and glutathione (GSH)) are well regulated; however, in cultured cells, ascorbate in particular is usually absent. GSH is the major antioxidant present in cells in culture and therefore variation in its concentration may change the radiosensitivity of cells.

4.6.1 Measurement of glutathione in cells bubbled with N_2 or •NO in suspension

GSH is a particularly effective radioprotector in hypoxia (Bump *et al.* 1982), but must be present at the exact time of radiation to react with •OH generated by IR, and also with the secondary short-lived biomolecule free radicals which are generated by IR. The concentration of GSH in cells is also important, as reactivity with radiation-induced free radicals is determined by competitive reactions with other reactants such as O_2. GSH itself also reacts

slowly with •NO with an apparent second order rate constant of 0.08 ± 0.008 $M^{-1}s^{-1}$ at pH 7.4, 37 °C (Folkes and Wardman 2004) but the reaction kinetics are complex. The presence of •NO in experimental systems could therefore deplete cells of thiols and hence increase cell radiosensitization indirectly through the loss of antioxidants.

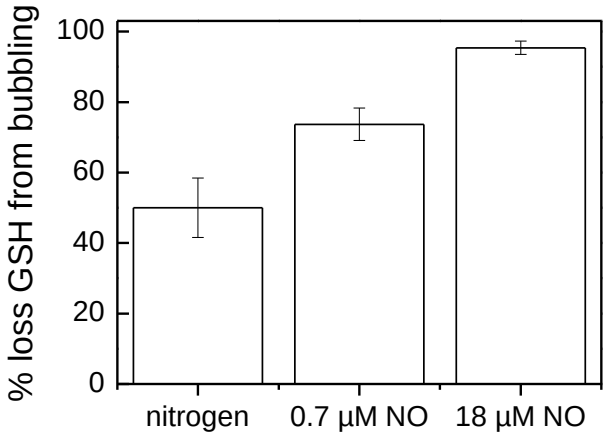

Figure 4-12 Effect of gentle bubbling of V79-4 cell suspensions (~5 x 10^5/ml) in PBS for 30 min with N_2 or •NO/N_2 at room temperature on cellular GSH concentrations. Concentration of GSH in control un-bubbled cells was 1.6 ± 0.1 pmoles/cell. Results represent the mean and SD of 2-3 experiments (n=3 0.7 µM •NO).

Suspensions of V79-4 cells in PBS were bubbled gently with N_2 for ~30 min. The anoxic cells were then continued to be bubbled with N_2 or the gas changed to 1% •NO/N_2 (~18 µM) for a further 20 min. Finally the cells were saturated with N_2 to ensure that •NO_2 could not be formed on re-exposure of the cells to air. Despite the reported slow rate of reaction of GSH with •NO, in V79-4 cells bubbled with a constant supply of ~18 µM •NO, GSH is almost completely depleted. However, bubbling with N_2 alone also decreases cellular GSH by ~50% (Figure 4-12). Using the experimental set-up, GSH cannot be measured without exposing the anoxic cells to O_2 before analysis of the GSH. As after ischemia reperfusion, a rapid re-oxygenation of anoxic cells can cause a sudden burst of reactive oxygen species, GSH may be depleted by reaction with these free radicals. The subsequent formation of oxidized GSH (GSSG) may be an indicator of this occurring and perhaps worth investigating further. Even if

this effect is partially responsible for depletion of cellular GSH, those cells exposed to •NO, even at 0.7 µM, are most sensitive to the loss of GSH.

The reasonably rapid loss of GSH observed is in contrast to previous studies where a bolus addition of 18 µM •NO was seen to reduce cellular GSH by about half after 1 h at 37 °C (Folkes and Wardman 2004). In other studies where •NO was formed directly in cells in aerobic conditions through the induction of iNOS, GSH levels were not seen to be depleted (Singh *et al.* 2009). In the methods used in these current studies, diffusion of •NO out of solution is not possible. •NO (18 µM) is supplied constantly to cells in suspension for ~30 min by bubbling slowly with 1% •NO. The rate of reaction between GSH and •NO is therefore not limited by a low and depleting concentration of •NO. It is also possible that the reaction rate measured previously (Folkes and Wardman 2004) is lower than what might occur in cells where the rate may be increased through the action of glutathione S transferase (GST) which catalyses the conjugation of glutathione with other molecules.

Sample	***k* (mol^{-1} dm^3 s^{-1})**
GSH + •NO	2.22 ± 0.13
GSH + •NO + 4 U GST	2.79 ± 0.03

Table 4-4 Table to show the second order rate constants for the reaction of GSH (5 mM) with •NO (~ 18 µM) in anoxia at room temperature, pH 7.2 with or without the addition of 4 U glutathione S transferase.

The rate of reaction of GSH (5 mM) with 18 µM •NO was measured at RT using a chemiluminescence •NO analyser to measure the exponential rate of loss of •NO, as described previously (Folkes and Wardman 2004). The addition of 4 U GST shows a small (~20%) increase in the rate of loss of •NO at pH 7.2 compared to in the presence of GSH alone, which

suggests that GST may catalyze the reaction between GSH and •NO but not to any significant level (Table 4-4).

4.6.2 Measurement of the formation of γH2AX in cells depleted of glutathione

As •NO-exposure depletes V79-4 cells of GSH, the radiosensitizing effects seen on cell survival and DSB formation may be at least partially associated with loss of this radioprotecting antioxidant in cells in culture. GSH is synthesised from the amino acids cytosine, glycine and glutamate by the enzyme glutathione synthetase. Buthione sulfoxide (BSO) inhibits this enzyme and cells can be depleted of GSH 16 h after incubation with 0.1 mM BSO. The effect of BSO on radiation-induced γH2AX staining following IR in anoxia was therefore measured to see if the delay in DSB repair seen with •NO is also observed in GSH depleted cells which had not been exposed to •NO.

Using flow cytometry to measure time-dependent γH2AX staining induced by radiation in anoxic V79-4 cells depleted of GSH, results were found to be similar to those for anoxic cells without BSO treatment (Figure 4-13). In addition, no delay in the rate of repair of DSB was observed, which suggests that the radiosensitizing effects of •NO cannot be due to the loss of GSH only.

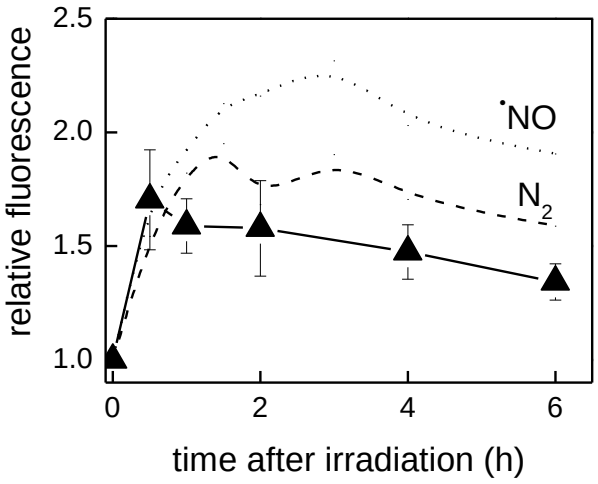

Figure 4-13 Formation and repair of γH2AX foci measured using flow cytometry, in V79-4 cells depleted of GSH by incubation with BSO. Results represent means and s.e.m. of 3 independent experiments. (dotted and dashed lines are reproduced from Figure 4-5E).

4.7 General discussion

Nitric oxide is an efficient radiosensitizer of cells and this effect can in part be explained by the formation of novel DNA damage, including the generation of nucleobase modifications. IR induces prompt SSB in plasmid DNA. In the absence of O_2 SSB are mainly due to H-atom abstraction from C-4′ of the deoxyribose sugar, the major radical produced from 2′-deoxyribose in DNA (scheme 1-2)(Miaskiewicz and Osman 1994). Plasmid DNA irradiated in anoxia in the presence of •NO shows a 3-fold protective effect on the formation of SSB compared to those irradiated in anoxia alone. This suggests that •NO may react with and 'repair' any sugar radicals formed. However, the majority of •OH-induced damage occurs to the bases in DNA forming •OH-adducts. These adducts may then be able to abstract a H-atom from the sugar and generate a SSB. If •NO reacted with these •OH adducts then SSB formation would be inhibited but a base modification would remain. These modifications could be recognized by DNA repair enzymes. Incubation of irradiated plasmid with Fpg glycosylase shows an approximate 2-fold increase in detectable SSB in those plasmids irradiated in the presence of •NO compared to those irradiated in anoxia alone, suggesting that purine modifications induced by •NO in these conditions exceed those in the absence of •NO. Indeed, the guanine modification, 8-azadGMP is observed in plasmid DNA following γ-radiolysis in the presence of •NO. However, in anoxic V79-4 cells, the presence of •NO did not show any effect upon the generation of SSB either immediately following irradiation (1 Gy) or up to 1 h following incubation at 37 °C. As neither condition shows a reduction in the comet moment over this time, this suggests that DNA repair may be slower than expected when the cells are incubated in agarose. Attached cells in medium may show faster repair kinetics but the nature of the experimental set-up for studying the effects of •NO radiosensitivity makes it difficult to investigate this possibility.

Extremely hypoxic Chinese hamster cells show slower repair kinetics of SSB after exposure to X-rays compared to moderately hypoxic cells (Koch and Painter 1975). The slow

repair of SSB in cells irradiated in anoxia, with or without the presence of •NO may reflect a reduction in the cellular dNTP pool which occurs upon exposure to anoxia (Pires *et al.* 2010), so that BER is delayed until dNTP levels are restored upon reoxygenation. Some damaged bases formed during γ-radiolysis of V79-4 cells in anoxia with or without the presence of •NO, are recognized by Fpg, reflected by an increase in the tail moment following incubation of the cells with the glycosylase, but the presence of •NO has no significant effect on the numbers of detectable SSB.

Detection of 8azadGMP in genomic DNA following IR in the presence of •NO would add evidence for the hypothesis that •NO causes novel base damage in irradiated cells. Measurement of DNA changes which occur to nucleotides in cells is difficult, as large doses are required to induce enough damage to detect by HPLC or LCMS. In addition, the DNA must be extracted from the cells and digested to release free nucleotides, a process which can potentially alter the original radiation-induced modifications. The large dose requirement is particularly difficult when using •NO, as the concentration needs to be kept low to ensure that •NO only reacts with radiation-induced DNA radicals. Cells need to be constantly exposed to the gas throughout long irradiation times, but if a higher dose rate of γ-radiation were to become available, then these studies may be more achievable.

Although •NO does not enhance the formation of prompt SSB during radiation treatment, it does enhance the number of detectable DSB in cells following γ-radiolysis, where repair of DSB is delayed compared to those DSB generated in cells irradiated in anoxia alone. Prompt DSBs are thought to be the critical damage in a cell even though the number of DSB in a cell following IR is far less than the number of SSB (Goodhead 1994). Prompt DSB arise through the phenomenon of radiation inducing clusters of DNA damage. Lesions within the clusters, which can include SSB, DSB, AP sites and base modifications are generally slower to repair than non-clustered damage (Jenner *et al.* 1993; Eccles *et al.* 2011). If radiation-induced DNA lesions are not repaired efficiently, the possibility exists that damage

is carried through to replication and when it meets a replication fork, it is then recognized and may develop into the late onset of replication-induced DSB (Harper *et al.* 2010). When cells are dividing in exponential growth, the S-phase cells exhibit replication forks in their DNA and so replication-induced DSB may be more prominent than in non-dividing cells. V79-4 hamster fibroblasts are more sensitive to radiosensitization by •NO when in exponential growth compared to confluent cells. It is proposed therefore that •NO-associated radiation-induced genomic damage (fixation of damage) in exponential growth cells has a greater probability of encountering a replication fork, particularly if present in a cluster, to give replication-induced DSB

Phosphorylation of histone H2AX to give γH2AX, which identifies both frank and replication-induced DSB, is used as a marker of DNA damage in cells (Rogakou *et al.* 1998). The loss of foci has been shown to be related to the repair of DSB (Leatherbarrow *et al.* 2006; Lobrich *et al.* 2010), both for prompt and replication-induced DSB (Harper *et al.* 2010), although how soon after repair dephosphorylation of γH2AX occurs is unknown. Radiosensitization of V79-4 cells by •NO increases the average number of γH2AX foci in irradiated cells but this enhancement is not obvious until ~3 h following irradiation when the majority of DSB will have been rejoined (Jenner *et al.* 1993). Although DSB are repaired after this time, even after 24 h, cells irradiated with 2 Gy in the presence of ~18 μM •NO express twice as many foci as cells irradiated in anoxia alone. Long-lived foci are indicative of unrepaired DSB which are generally more complex (Jenner *et al.* 1993; Reynolds *et al.* 2012), replication-induced DSB or those induced in heterochromatin (Goodarzi *et al.* 2008). Flow cytometry analysis of γH2AX stained cells suggests that the enhancement seen in the •NO-treated cells may reside particularly in G2/M cells. •NO-associated damage following IR incurred in genomic DNA during S phase, if not repaired, may be carried through to G2 where ultimate demise of the cell occurs through the enhanced formation of DSB. This hypothesis is supported by previous findings that cells in G2/M phase are most sensitive to

radiosensitization by •NO (Su *et al.* 2011). In addition, colon cancer cells were found to be most sensitive to •NO in the absence of radiation in G2/M phase (Jarry *et al.* 2004). Indeed co-staining of irradiated HF-19 cells with cyclin A for cell cycle status and 53BP1 foci for DSB formation shows a correlation between foci number and cells in S/G2 phase. This suggests that processing of base damage, particularly if present in clustered damage sites, results in late onset replication-induced DSB and cell death during replication. Further evidence for the formation of late onset replication-induced DSB in the presence of •NO is through the enhanced formation of the average numbers of RAD51 foci compared to in cells irradiated in anoxia alone, 24 h following IR. RAD51 is a protein involved in homologous recombination and persistent γH2AX foci co-stain with RAD51, which correlates with loss of clonogenicity (Banath *et al.* 2010), although this may indicate apoptosis rather than stalled replication forks.

DSB formation can also occur if replication forks are stalled due to low dNTP pools, which can occur in response to the presence of hydroxyurea (HU). •NO is released following the reaction of HU with peroxidases and other oxidants, so it may be possible that part of the effects of HU, including its radiosensitizing properties are due to •NO. This will be discussed further in Chapter 6.

There is no doubt that •NO is a very efficient radiosensitizer (Oronsky *et al.* 2012), but data obtained in cells in culture may reflect in part, changes which occur in cellular GSH levels. GSH is an antioxidant with radioprotective properties in hypoxia, and is present in many cells, in its reduced form, at concentrations of ~1-10 mM. Depletion of GSH in hypoxic cells increases radiosensitization (Bump *et al.* 1982); also early DNA damage (SSB, DSB and oxidised bases) is increased in oxygenated radioresistant cells and genomic instability is improved in further progeny, particularly in cells irradiated with high LET radiation (Hanot *et al.* 2012). GSH may therefore also be involved in modulating the DNA damage response (reviewed in (Chatterjee 2013)). •NO reacts slowly with GSH with complex

kinetics (Folkes and Wardman 2004), but it is conceivable that bubbling cells in suspension for 20 min with ~18 μM •NO, as was carried out for experiments described in this chapter, would radiosensitize those cells, simply through the loss of the radioprotector. Despite GSH levels being depleted during exposure to 1% •NO, even bubbling cells with N_2 alone depletes the cells of half of their GSH pool. In addition, cells depleted of GSH by exposure to BSO did not show the same time profiles in the loss in the levels of γH2AX staining following radiation compared to those cells exposed to •NO. These differences may be explained through competition kinetics. As •NO reacts much more efficiently with DNA radicals than GSH ($k \leq 10^7$ M^{-1} s^{-1} (O'Neill 1983), even at a concentration of 1 mM, GSH is unlikely to compete with •NO for 'repair' of the DNA radicals and hence novel base lesions which result directly from •NO would still occur.

Although the mechanisms by which •NO radiosensitizes anoxic cells are still not fully understood, it seems extremely likely that specific DNA damage is involved. Future work should focus on identifying this damage in irradiated cells. In addition, delivery of •NO to hypoxic tissue should be addressed if its role as a radiosensitizer is to be progressed. The concept of hypoxia activated bioreductive drugs as agents which could conceivably be used to deliver •NO to hypoxic tumours for therapy is discussed in Chapter 5.

5 Hypoxia activated pro-drugs of nitric oxide

5.1 Introduction

Many tumours contain regions of hypoxia distal from blood vessels and areas which are transiently oxygenated by the nature of irregular tumour vessels which open and close uncontrollably. Hypoxic tumours can be very resistant to chemo- and radiotherapy treatment, and survival following treatment is closely linked to tumour oxygenation. Radiosensitizers and drugs which are selective to low oxygen conditions are able to enhance the effectiveness of treatment in these hypoxic tumours by reducing the effective radiation dose necessary to kill the cells. Pro-drugs which are activated by cellular reductases in hypoxia to release a drug have been developed and were first described by the group in New Zealand (Denny *et al.* 1996) (§1.3.3). There have been many studies into the design of these pro-drugs both in terms of effector molecule, linker and drug. Recently, the bioreductive release of •NO from indolequinone pro-drugs has been described (Sharma *et al.* 2013).

The aim of this study was to investigate whether pro-drugs based on nitroaromatic molecules could be developed, which release a NONOate in a reductive environment in hypoxia. Reducing radicals generated by radiolysis, supersomes containing NADPH-dependent P450 reductases, sodium dithionite and hepatoma G2 cells would be investigated for their ability to reduce these pro-drugs. NONOates are stable in alkaline pH but once protonated spontaneously decompose in a temperature dependent manner to release •NO, with specific half lives ($t_{½}$) dependent upon the structure of the NONOate (Davies *et al.* 2001). The possibility of radiosensitization of hypoxic cells by the subsequent formation of •NO from a bioreductively activated pro-drug would also be investigated.

5.2 Measurement of the reduction of pro-drugs by reducing radicals

The pro-drugs tested in this study comprised a 5-nitrofuran (NF), a 4-nitrobenzyl ether (NB) and a 2-nitro-5-methylimidazole (NI) all linked to diethylamine diazeniumdiolate **(**DEANO), termed NF-DEANO, NB-DEANO and NI-DEANO respectively (Figure 5-1). The reduction potential of a molecule determines the likelihood of that molecule to be reduced through the uptake of an electron. The more positive its reduction potential is, the greater the tendency to acquire an electron, with couples written as (oxidant/reductant). $CO_2^{\bullet-}$ is a strong reductant (E_o ($CO_2/CO_2^{\bullet-}$) = –2000 mV) (Wardman 1989), and reduces all of the pro-drug effector molecules under study with high efficiency as the reduction potentials ($RNO_2/RNO_2^{\bullet-}$) for all of the nitroaromatics are above that of $CO_2^{\bullet-}$. With a difference in potentials of ~1600 mV the compounds will readily accept an electron from $CO_2^{\bullet-}$. Typical reduction potentials of similarly-substituted 5-nitrofurans are (~ – 300 mV), 2-nitroimidazoles (~ – 400 mV) and 4-nitrobenzyl alcohol (~ – 480 mV) (Wardman 1989)).

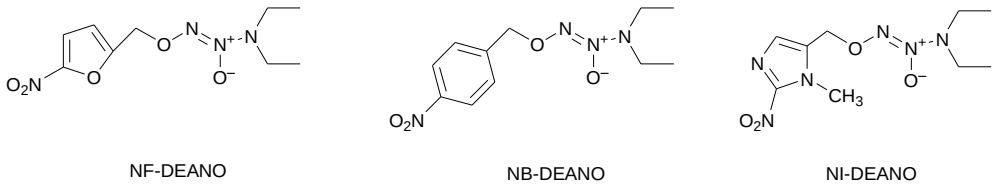

Figure 5-1 Structures of the bioreductive NONOate pro-drugs studied.

All of the pro-drugs investigated reacted with reducing radicals ($CO_2^{\bullet-}$ + e_{aq}^- (§ 2.3.3)) with loss of the pro-drug. NF-DEANO is reduced by $CO_2^{\bullet-}$ in N_2O-saturated solutions at pH 7.4 with a second order rate constant of ~9 x 10^8 M^{-1} s^{-1} (K. B. Patel, unpublished results) and radical absorption centred at ~440 nm (with a lifetime of >1 ms) suggestive of the formation of a nitro radical anion ($R\text{-}NO_2^{\bullet-}$) (Everett *et al.* 1999). In the same conditions NB-DEANO reacts with a second order rate constant of 7.1 x 10^8 M^{-1} s^{-1} (K. B. Patel, unpublished results).

Reaction is expected to proceed through R-$NO_2^{\bullet-}$ (Eq. 5-1), with subsequent release of DEANO, presumably by electron-transfer reactions. The efficiency of release of a drug from a nitroheterocyclic pro-drug in anoxia is dependent upon competing reactions of R-$NO_2^{\bullet-}$ with each other (Eq. 5-(2-4)) and further reduction (Eq. 5-5). These competitions vary with the specific nitroheterocycle. It has been shown that NF-$NO_2^{\bullet-}$ radical anions decay with dose-rate dependent second order kinetics. At low dose rates, decay of the radical anions will be predominately by Eq. 5-2 but at higher dose rates the radicals are more likely to react with each other by disproportionation, regenerating half of the parent pro-drug (Eq. 5-3) or possibly by dimerization (Eq. 5-4). In comparison NB-$NO_2^{\bullet-}$ radicals decay by first order kinetics (Eq. 5-2) with rates independent of dose rate and NI-$NO_2^{\bullet-}$ radicals decay by predominately first order kinetics at low dose rates (Wardman 1985).

$$\text{R-NO}_2 + \text{CO}_2^{\bullet-} \rightarrow \text{R-NO}_2^{\bullet-} + \text{CO}_2 \qquad (5\text{-}1)$$

$$\text{R-NO}_2^{\bullet-} \rightarrow \text{products} \qquad (5\text{-}2)$$

$$2\ \text{R-NO}_2^{\bullet-} + \text{H}^+ \rightarrow \text{R-NO}_2 + \text{R-NO} + \text{H}_2\text{O} \qquad (5\text{-}3)$$

$$2\ \text{R-NO}_2^{\bullet-} \rightarrow \text{dimers.} \qquad (5\text{-}4)$$

5.2.1 Effect of dose rate on reduction of pro-drugs

The dose rate at which N_2-saturated solutions of the pro-drugs in sodium formate were irradiated was varied by placing the solutions at different distances from the Caesium source in the irradiator (Figure 2-1) and increasing the time of irradiation as the dose rate was reduced, to deliver a similar total dose. The radiation chemical yield (*G* value) was calculated by plotting the concentration of pro-drug measured by HPLC, versus the absorbed dose. For all of the compounds tested, reduction of the nitro group induced the release of DEANO, presumably by electron transfer through the nitro radical anion or through higher reduction products (Eq. 5-5) (discussed in (Wardman 2001)).

$$\text{R-NO}_2 \xrightarrow{2e^-} \text{R-NO} \xrightarrow{2e^-} \text{R-NHOH} \xrightarrow{2e^-} \text{R-NH}_2. \qquad (5\text{-}5)$$

The *G* value for loss of the pro-drug gives an indication as to the mechanism involved, as between one and four electron equivalents are required to reduce the pro-drug to initiate drug release. The release of DEANO to which the nitroheterocycles were conjugated could not be detected by HPLC, despite the reported strong absorbance at 252 nm (Keefer *et al.* 1994), presumably because of its short lifetime and hydrophilic nature.

Using steady state radiolysis the *G* values for the loss of each of the pro-drugs under study following reaction with reducing radicals at pH 7.4 with varying dose rate was determined (Table 5-1). The 5-nitrofuran pro-drug was lost at close to 100% of the radical input yield (0.62 µM/Gy (Naylor *et al.* 1994)) at 0.5 Gy/min. However, on increasing the dose rate to > 2 Gy/min only ~70% of radical input could be accounted for by the loss of NF-DEANO, suggesting that at higher dose rates second order decay of NF-$NO_2^{\bullet -}$ through disproportionation or dimerization competes with the fragmentation (Eq. 5-3 and 5-4). At low dose rate NF-DEANO therefore appears to release DEANO through the radical anion (Scheme 5-1A). The reduction in *G* value at higher dose rates probably reflects the second-order decay of NF-$NO_2^{\bullet -}$ rather than a decrease in the rate of release of DEANO, as will be discussed later (§5.2.2).

Using steady state radiolysis the 4-nitrobenzylether pro-drug (NB-DEANO) is only lost with a *G* value of ~0.18 µM/Gy; ~30% of the radical input yield and is independent of dose rate (Table 5-1). This confirms that the radical anion decays largely by first order kinetics (Eq. 5-2), and suggests that release of DEANO may also occur through further reduction products, possibly the hydroxylamine (Scheme 5-1B).

	G (µmol / Gy)		
Dose rate Gy / min	**NB-DEANO**	**NF-DEANO**	**NI-DEANO**
0.5	0.16 ± 0.01	0.68 ± 0.02	0.52 ± 0.04
1.9	n.d	0.45 ± 0.02	n.d
13.5	0.22 ± 0.002	0.44 ± 0.02	0.44 ± 0.03
14.1	0.18 ± 0.003	0.41 ± 0.01	0.51 ± 0.01

Table 5-1 Effect of dose rate on the reduction of pro-drugs by reducing radicals (e_{aq}^- + $CO_2^{\bullet-}$) in N_2-saturated 0.1M sodium formate, 5 mM potassium phosphate buffer, pH 7.4.

In comparison the 2-mitro-5-methylimidazole pro-drug (NI-DEANO) is lost with a *G* value of ~0.5 µM/Gy; 80% of the radical yield, and the loss is independent of dose rate. Decay of nitro radicals of 2-nitroimidazoles is mainly by first order kinetics. Release of DEANO is proposed to occur mainly through the nitro radical anion but to a lesser extent through the hydroxylamine intermediate (Scheme 5-1C). Misonidazole is a well known 2-nitroimidazole developed as a hypoxic radiosensitizer over 30 years ago but withdrawn because of neurotoxicity. One-electron reduction of misonidazole gave a *G* value of 0.18 µM/Gy, a value in agreement with previous work suggesting that misonidazole is reduced by 4 electron equivalents (Whillans and Whitmore 1981). A *G* value of 0.19 µM/Gy was also achieved for the release of aspirin from a pro-drug with an ester linkage to 1-methyl-2-nitroimidazole and this was attributed to a four electron reduction occurring before aspirin is released (Everett *et al.* 1999). However, in the same studies, by comparison 1-methyl-2-nitroimidazole-5-methylbromide lost the bromide with a yield equivalent to the radical input, suggesting that release occurs through the one electron reduced nitro radical anion. The leaving group or linker region in bio-reductive pro-drugs also has a strong influence on the chemistry which occurs to catalyse cleavage of the active agent (Everett *et al.* 2002).

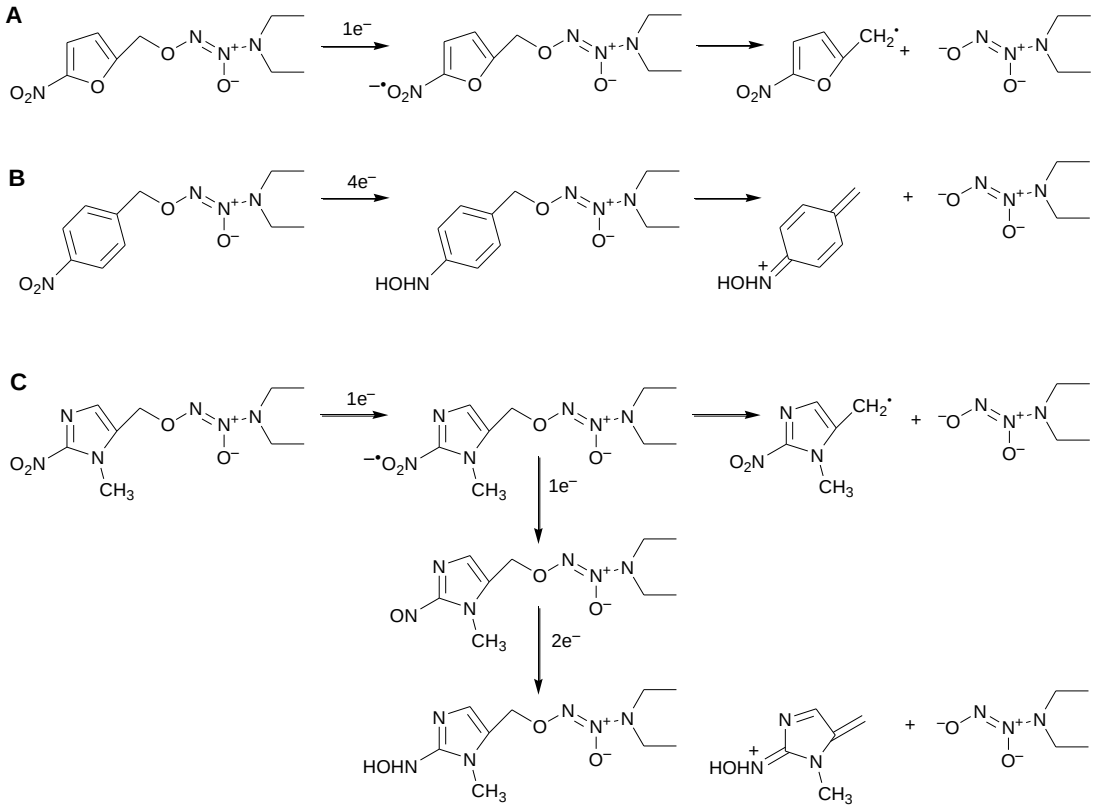

Scheme 5-1 Proposed mechanisms for the electron transfer associated with the release of conjugated DEANO following one-electron reduction of; (A) the 5-nitrofuran pro-drug; (B) the 4-nitrobenzyl alcohol pro-drug; (C) the 2-nitro-5-methylimidazole pro-drug.

5.2.2 Measurement of nitric oxide production following reduction by formate radicals

One-electron reduction of the nitroheterocycles in this study was expected to initiate release of DEANO to varying degrees (Scheme 5-1). At physiological pH DEANO could then decompose to form •NO (Scheme 5-2), detectable by chemiluminescence.

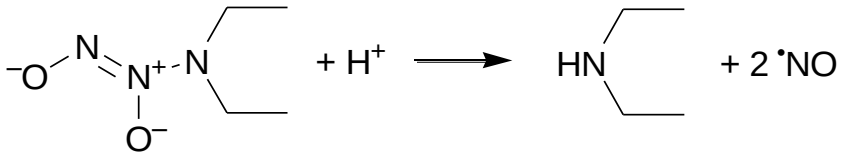

Scheme 5-2 Simple mechanism for the decomposition of diethylamine diazeniumdiolate (DEANO).

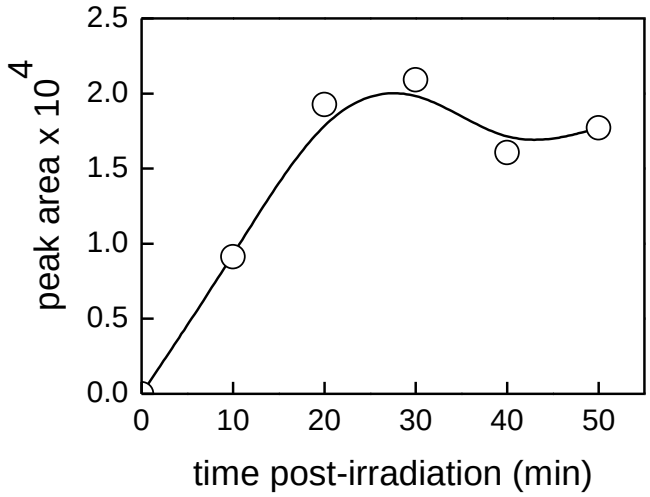

Figure 5-2 Representative data to show the effect of time on the yield of •NO at room temperature following reduction of NF-DEANO by $CO_2^{\bullet-}$ (56 Gy, 14.1 Gy/min) at pH 7.4 in N_2-saturated solutions.

DEANO has a $t_{½}$ of 16 min at 24 °C. Following γ-radiolysis (56 Gy) of 50 µM NF-DEANO at pH 7.4 and a dose rate of 14.1 Gy/min, the maximum formation of •NO was observed ~30 min following irradiation (Figure 5-2) and therefore all yields of •NO were measured at this time. Table 5-1 shows that the yield of radiation-induced loss of NF-DEANO is highest for a dose rate of 0.5 Gy/min. At a dose rate of only 2.2 Gy/min, NF-DEANO was lost linearly with dose with a *G* value of 0.47 ± 0.02 µM/Gy (Figure 5-3A). However, the subsequent formation of •NO was non-linear with dose (Figure 5-3B). As reduction of the pro-drug at 2.2 Gy/min takes ~27 min to reach 60 Gy, DEANO is released and can begin to breakdown to produce •NO during the irradiation period, based on the $t_{½}$ of 16 min. •NO may then be lost through other processes. For example it reacts with $CO_2^{\bullet-}$ with a second order rate constant of (k = 2.9 x 10^9 M^{-1} s^{-1}) (Czapski *et al.* 1994) producing a $NOCO_2^-$ adduct. It was therefore decided to do all further measurements of •NO production following radiolysis of the three pro-drugs at the highest dose rate possible (14.1 Gy/min) where it only takes ~4 min to reach 60 Gy relative to the 16 min half-life of DEANO.

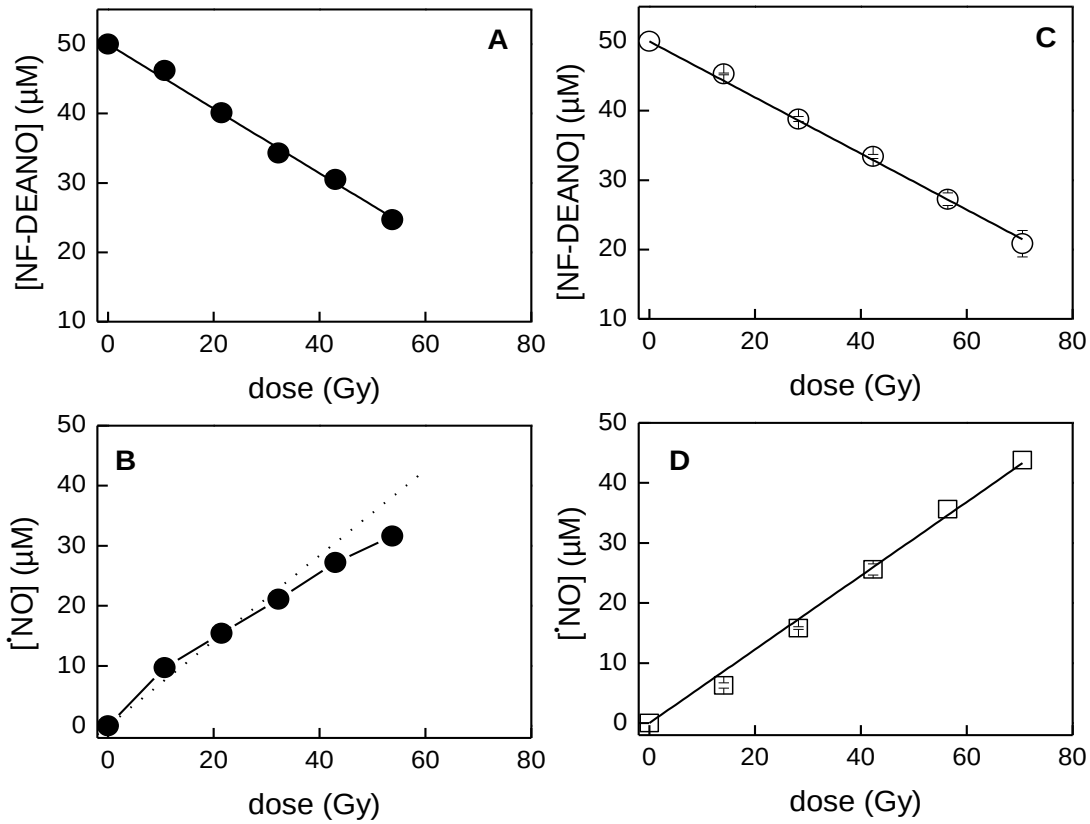

Figure 5-3 Dose dependent loss of NF-DEANO and formation of •NO measured 30 min following reduction by $CO_2^{\bullet-}$ at pH 7.4 at a dose rate of (A/B): 2.2 Gy / min and (C/D): 14.1 Gy / min.

At a dose rate of 14.1 Gy/min, NF-DEANO was lost linearly with dose following reduction by $CO_2^{\bullet-}$ + eaq^- in N_2-saturated solutions with a *G* value of 0.41 ± 0.01 μM/Gy (Figure 5-3C, Table 5-1). Under these conditions •NO is produced linearly with dose giving a *G* value of 0.61 ± 0.01 μM/Gy. A ratio of 1 : 1.5 of the loss of NF-DEANO to the amount of •NO released was determined. A previous report (Maragos *et al.* 1991) showed that one mole of DEANO releases 1.53 moles of •NO upon decomposition at physiological pH. Therefore in the radiolysis studies, for every mole of NF-DEANO reduced, 1 mole of DEANO is released. This adds further support that DEANO is mainly released directly from the nitro radical anion of the 5-nitrofuran through an electron transfer mechanism (Scheme 5-1A).

The yield of formation of •NO following one-electron reduction of NB-DEANO at 14.1 Gy/min has a *G* value of 0.15 ± 0.002 µM/Gy (Figure 5-4B, Table 5-2). Therefore, only ~1 mole of •NO is produced per mole of NB-DEANO reduced (Table 5-1), which suggests that when considering the stoichiometry of the number of reducing equivalents required to induce release, the hydroxylamine intermediate may be responsible for releasing DEANO.

	NB-DEANO	**NF-DEANO**	**NI-DEANO**
***G* •NO (µmol/Gy)**	0.15 ± 0.002	0.61 ± 0.01	0.47 ± 0.03

Table 5-2 Yields of nitric oxide measured 30 min following the reduction of the pro-drugs by reducing radicals in N_2-saturated 0.1M sodium formate, 5 mM potassium phosphate buffer pH 7.4 at a dose rate of 14.1 Gy / min.

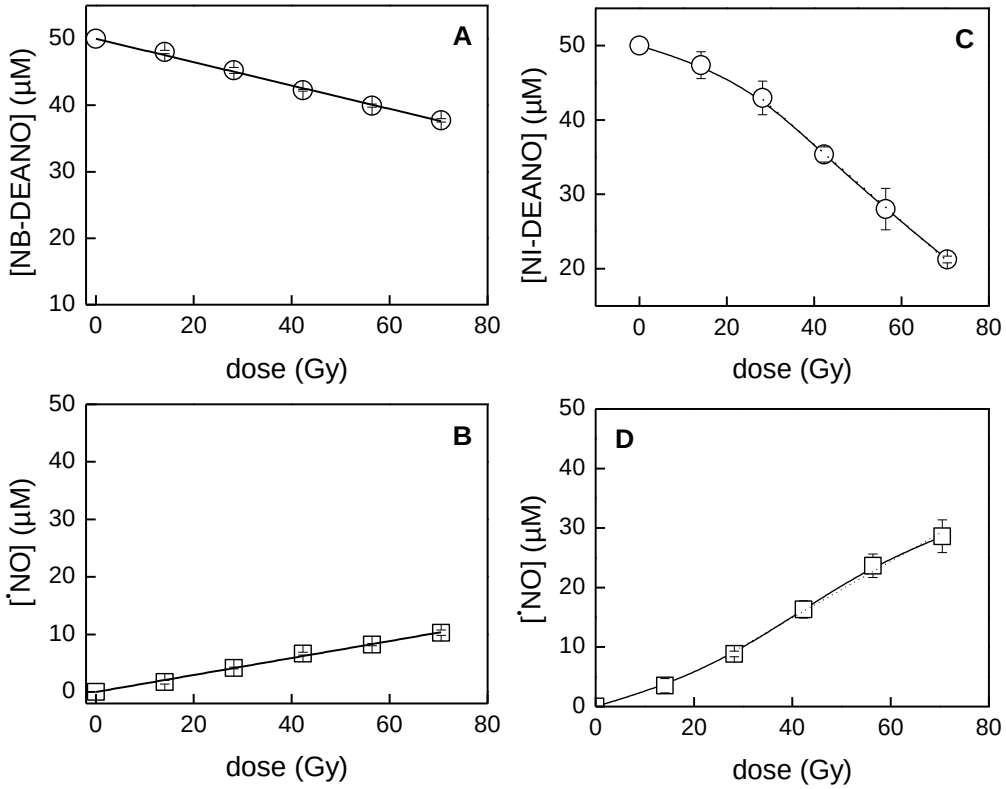

Figure 5-4 Dose dependent loss of (A) NB-DEANO and (B) subsequent formation of •NO; loss of (C) NI-DEANO and (D) subsequent formation of •NO measured 30 min after γ-radiolysis in N_2-saturated solutions at pH 7.4, following reduction by $CO_2^{\bullet-}$ radicals at 14.1 Gy / min.

The yield of formation of •NO following one-electron reduction of NI-DEANO at 14.1 Gy/min has a *G* value of 0.47 ± 0.001 μM/Gy (Figure 5-4D, Table 5-2). The dose dependent loss of NI-DEANO and formation of •NO showed a slight deviation from linearity at low doses (Figure 5-4C and D). As this was not seen with the other nitroheterocycles, an impurity may be present which reacts with the reducing radicals more efficiently than NI-DEANO until it is depleted. Once again only ~1 mole of •NO is produced per mole of NI-DEANO reduced. Unlike NB-DEANO, NI-DEANO is lost at ~85% of the radical input and therefore the majority of DEANO appears to be released from the nitro radical anion as seen with NF-DEANO and a smaller fraction from the reduced products shown in Scheme 5-1C.

5.2.3 Measurement of products following reduction of pro-drugs with $CO_2^{\bullet-}$

The loss of the pro-drugs and to some extent the formation of nitroheterocycle related products following reaction with reducing radicals could be followed by HPLC. Four products were observed following readuction of NF-DEANO (Figure 5-5A). All of the products have optical absorption spectra extending beyond 300 nm (Figure 5-5B). Monitoring at 314 nm, the yields of the products increased with dose but the relative yield of each product varied with the dose rate used. At a dose rate of 0.5 Gy/min, products **1** and **2** predominated, product **3** plateaued after ~5 Gy but product **4** was not observed (Figure 5-5C). At 13 Gy/min, all four products were observed with **3** being formed in the highest yield below ~50 Gy and then plateauing at higher doses (Figure 5-5D) when ~40% of NF-DEANO had been lost. Product **4** also reached a plateau at 50 Gy, but **1** and **2** were formed in similar yields to each other independent of dose rate and the yields increased with dose with an initial lag phase (Figure 5-5C and D).

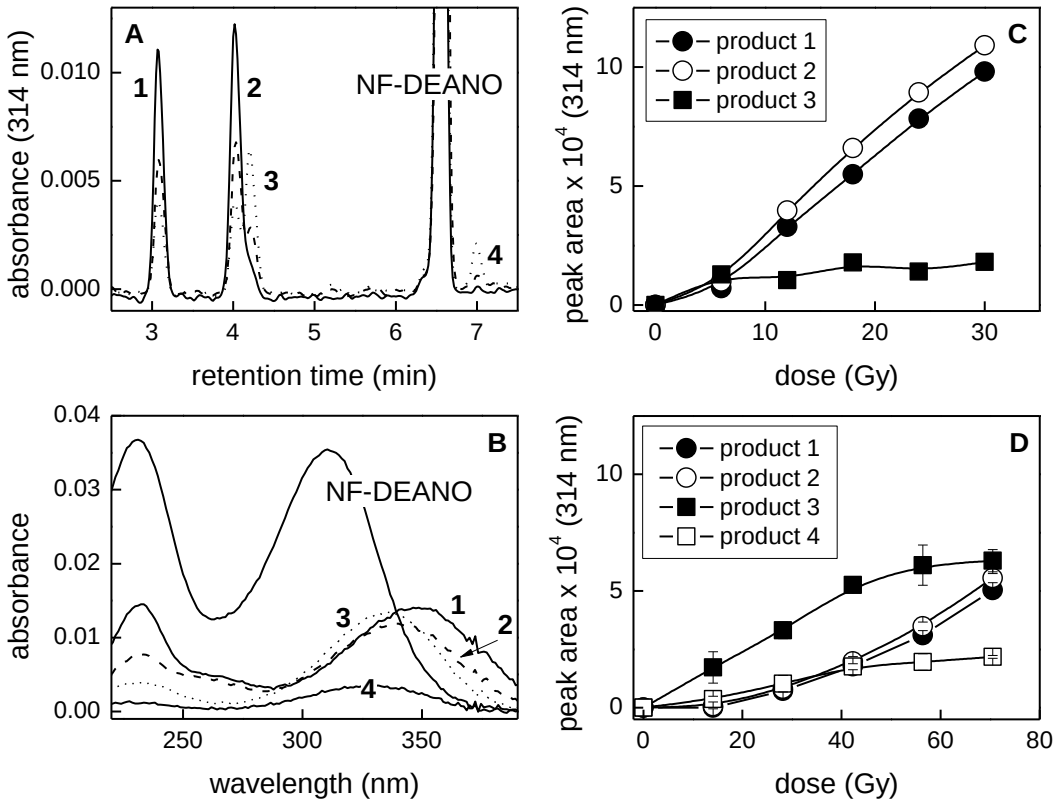

Figure 5-5 (A) Chromatograms showing the formation of products 1- 4 after ~30 Gy at dose rates of 0.5 (—), 1.9 (---) and 13.5 Gy/min (…); (B) absorption spectra of NF-DEANO and products; peak areas for products 1-4 following reaction of NF-DEANO with reducing radicals (e_{aq}^- + $CO_2^{\bullet-}$) in N_2 at pH 7.4 at (C) 0.5 Gy/min and (D) at 13.5 Gy/min.

The nitro radical anion of NF-DEANO, directly via radical fragmentation or following further reduction, may release DEANO leaving a 5-nitrofuran methyl radical (Scheme 5-1A). This type of radical could potentially dimerize by radical-radical combination as is seen with 2-nitroimidazole pro-drugs (Everett *et al.* 1999), or form other coupled products. Dimerization through the carbon-centred radicals would mean that nitro groups would remain on the molecule and could still be reduced by $CO_2^{\bullet-}$. Product **4** was only observed at a high dose rate and it is conceivable that **3** and/or **4** may be dimers which are reduced further, possibly to form **1** and **2**. Alternatively **3** and/or **4** may be formed as a result of a disproportionation reaction occurring, with the resulting products being further reduced to **1** and **2**. Products **1**-**4** are likely to be related to the nitrofuran moiety. 5-Nitrofurfuryl alcohol

does not co-elute with any of these products and was observed only as a very minor product with a retention time of 2.4 min. Products **1** and **2** have *m/z* of 155 (M-H). The ionisation of **3** was unsuccessful. Product **4** could only be ionised in ES^+ mode, and has *m/z* of 275 (M+H). However, this mass may represent a sodium ion adduct (as is seen with the parent pro-drug), although a fragment of *m/z* 252 (M+H) was not observed. No evidence of formation of a dimer was seen by mass spectral analysis.

The reaction of NB-DEANO by reducing radicals also showed the formation of a few products, with the major product (**5**) eluting with a retention time of 3.1 min by HPLC (Figure 5-6A), and a UV-visible spectrum with λ_{max} 275 nm (Figure 5-6B). A mass could not be measured for this product and the identity at the present time remains unknown.

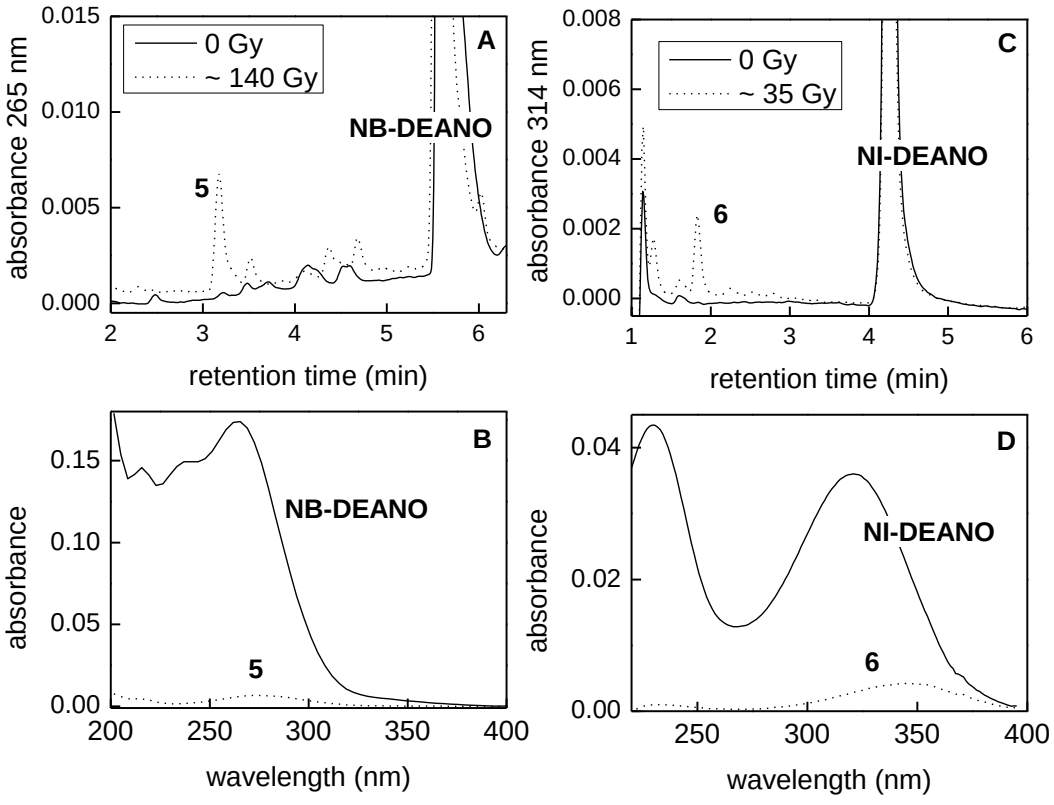

Figure 5-6 (A) Chromatograms showing the formation of product 5 from the reaction of NB-DEANO and $CO_2^{\bullet-}$ + eaq^- after ~140 Gy at a dose rate of 13.5 Gy/min; (B) absorption spectra of NB-DEANO and product 5; (C) Chromatograms showing the formation of product 6 from the reaction of NI-DEANO and $CO_2^{\bullet-}$ + eaq^- after ~35 Gy at a dose rate of 14.1 Gy/min.

Finally, the reduction of NI-DEANO produced products which could not be detected optimally by HPLC. However, an early eluting product was observed (Figure 5-6C, product **6**), with λ_{max} ~350 nm (Figure 5-6D) and *m/z* 142 (M+H). Product **6** was formed in a sigmoidal fashion with dose. As yet the identity of the product remains unknown but the low retention of the product on the column reflects the formation of a more hydrophilic compound.

5.3 Reduction of NF-DEANO by sodium dithionite

Sodium dithionite ($S_2O_4^{2-}$) is a powerful reductant which can reduce nitroaromatic compounds through consecutive one-electron steps following disassociation (Eq. 5-(6-7)).

$$S_2O_4^{2-} \rightleftharpoons SO_2^{\bullet-} + SO_2^{\bullet-} \qquad (5\text{-}6)$$

$$SO_2^{\bullet-} + R\text{-}NO_2 \rightarrow R\text{-}NO_2^{\bullet-} + SO_2. \qquad (5\text{-}7)$$

Addition of a bolus of dithionite can be equivalent to adding a high dose rate of reducing radicals, but rates are determined by the rate of disassociation compared to the rate of $SO_2^{\bullet-}$ with the reactant.

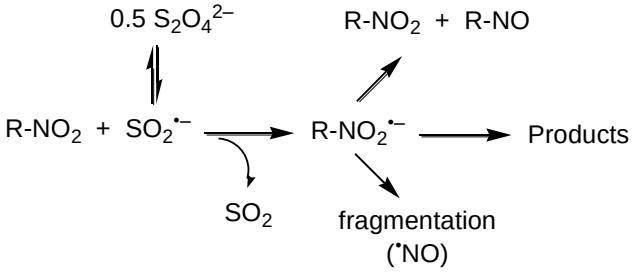

Scheme 5-3 Mechanisms proposed for the reduction of nitroaromatics by sodium dithionite.

Rate of reduction of viologens by dithionite has been shown to be proportional to the reduction potential (the more negative the reduction potential the slower the rate of reduction) (Tsukahara and Wilkins 1985) and it is assumed that the rate of reduction reflects the reduction potential of nitroheterocycles too. Nitrobenzenes for example are reduced by dithionite to form nitro radical anions (Kolker and Waters 1964) but the products of reaction

of dithionite with the pro-drugs will be dependent upon the competition between all the possible radical decomposition mechanisms (Scheme 5-3).

Reduction of NB-DEANO by dithionite was studied to see if any of the products formed are the same as those observed following radiolytic one-electron reduction of the pro-drug, where radicals are produced at ~0.3-8 μM/min, depending upon the dose rate (0.5–13 Gy/min). Only the reactions of NF-DEANO were studied because supplies of NB- and NI-DEANO were limited. It was proposed earlier from the stoichiometry of the products that DEANO is released from the NF-DEANO nitro radical anion. Dithionite may not induce the same chemistry. In N_2-saturated solution at pH 7.4, NF-DEANO was lost at a ratio of 0.61 ± 0.01 μM/μM dithionite. Two products were observed, one of which eluted with the same retention time as **3** (Figure 5-7) and has the same UV-visible spectrum. As product **3** is probably associated with the 5-nitrofuryl moiety, fragmentation must occur following reduction by dithionite, but not through the same reaction mechanisms as is predicted for one-electron reductants, and this may not result in the loss of DEANO per se. Attempts were made to measure the formation of $^{\bullet}NO$ in the solutions to understand whether dithionite-reduced products of the 5-nitrofuran pro-drug could expel the attached NONOate. Despite a very low concentration of $^{\bullet}NO$ being detected upon the addition of two equivalents of dithionite to NF-DEANO, the addition of further equivalents reduced the concentration of $^{\bullet}NO$ further. It has been reported that dithionite reacts with $^{\bullet}NO$ (k = 1.4 x 10^3 M^{-1} s^{-1} at pH 7, (Moore and Gibson 1976)) forming a SO_2-NO adduct, so even if DEANO is released following the reduction of NF-DEANO, any subsequent formation of $^{\bullet}NO$ which may occur could be removed by secondary reactions. In addition $SO_2^{\bullet-}$ may react with NF-DEANO through consecutive one-electron steps and reduce through to the various products shown in Eq. 5-5. The other product observed (**7)** has a λ_{max} of 300 nm and a molecular weight of 111 Da. At present the identity of this product and product **3** remains unknown.

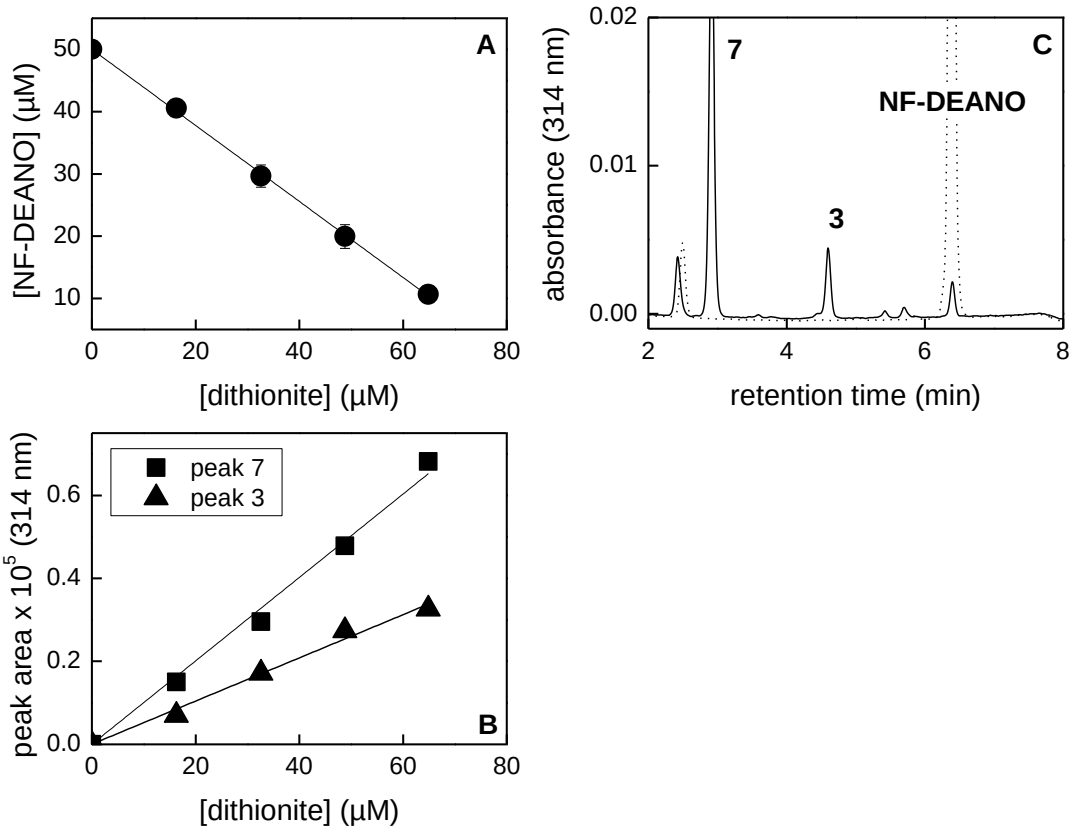

Figure 5-7 (A) Loss of NF-DEANO and (B) representative formation of products following the reduction of NF-DEANO by sodium dithionite in N_2 saturated solution at pH 7.4; (C) chromatogram of 50 μM NF-DEANO (…) with the addition of 100 μM dithionite (—).

5.4 Reduction of pro-drugs by P450 reductase supersomes

NADPH-cytochrome P450 reductase is able to reduce many bioreductive pro-drugs which have reduction potentials similar to or higher than those of the reductase domains (Wilson and Hay 2011) (FAD/FADH = ~ –330 mV; (FMN/FMNH) = ~ –160 mV (Munro *et al.* 2001)) (Scheme 5-4). NF-DEANO was readily reduced by P450 reductase supersomes in N_2 saturated solution to form products **1-3,** as observed by reaction with reducing radicals (Figure 5-8A). Unlike in the radiolysis studies, enzymatic reduction of NF-DEANO produced all three products at similar yields. At 314 nm, where the chromatograms are recorded, the three products have similar absorption intensities (Figure 5-5B) and therefore peak area should be indicative of relative yields of all of the products. NF-DEANO is lost at ~2

µM/min at 37 °C with cytochrome P450 supersomes (95 µg/ml protein (1300 nmole/min x mg protein cytochrome c reductase and 3600 pmol/mg protein cytochrome b_5)) (Figure 5-7C). In comparison the other pro-drugs were not so easily reduced by P450 reductase supersomes (Figure 5-7D). At 37 °C and 172 µg/ml of P450 reductase/cytochrome b5 protein (710 nmole/(min x mg protein cytochrome c reductase and 710 pmol/mg protein cytochrome b_5), NI-DEANO is metabolised at a rate of 0.54 µM ± 0.01 µM/min and NB-DEANO at a rate of 0.06 ± 0.01 µM/min. The slow rate of reduction of NI-DEANO and NB-DEANO by P450 reductase reflects that these compounds are not such good substrates for the enzyme.

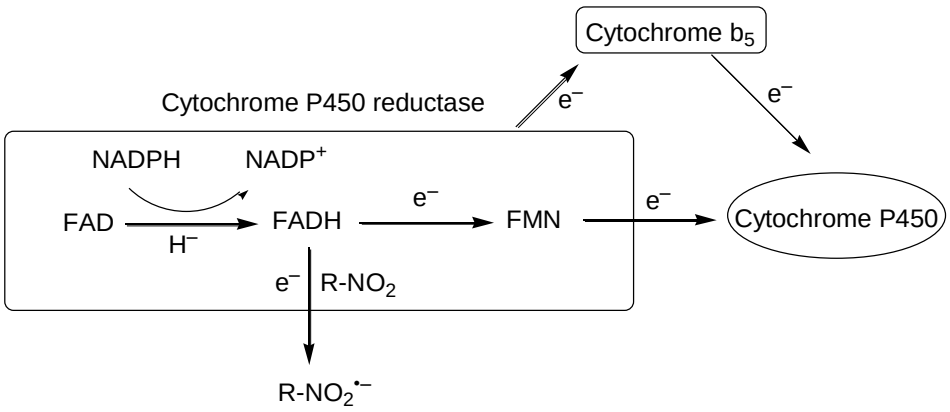

Scheme 5-4 Schematic showing the electron transfer chain of P450 reductase and possible mechanism for reduction of nitroaromatic pro-drugs in anoxia.

Measurement of the formation of •NO following the reduction of NF-DEANO with supersomes was difficult. DEANO has a $t_{½}$ of 2-3 min at 37 °C and 16 min at 25 °C and the DEANO released from NF-DEANO appeared to decompose within the •NO analyser giving broad peaks which took many minutes to return to baseline. However, the broad peaks did seem to increase in size with time of incubation with supersomes, reflecting an increase in the concentration of •NO. •NO is known to form a complex with the Fe-III centre of the cytochrome enzyme (Wink 1993) but this action if it occurs in these studies does not appear to inhibit the activity of the cytochrome P450 (Figure 5-8C).

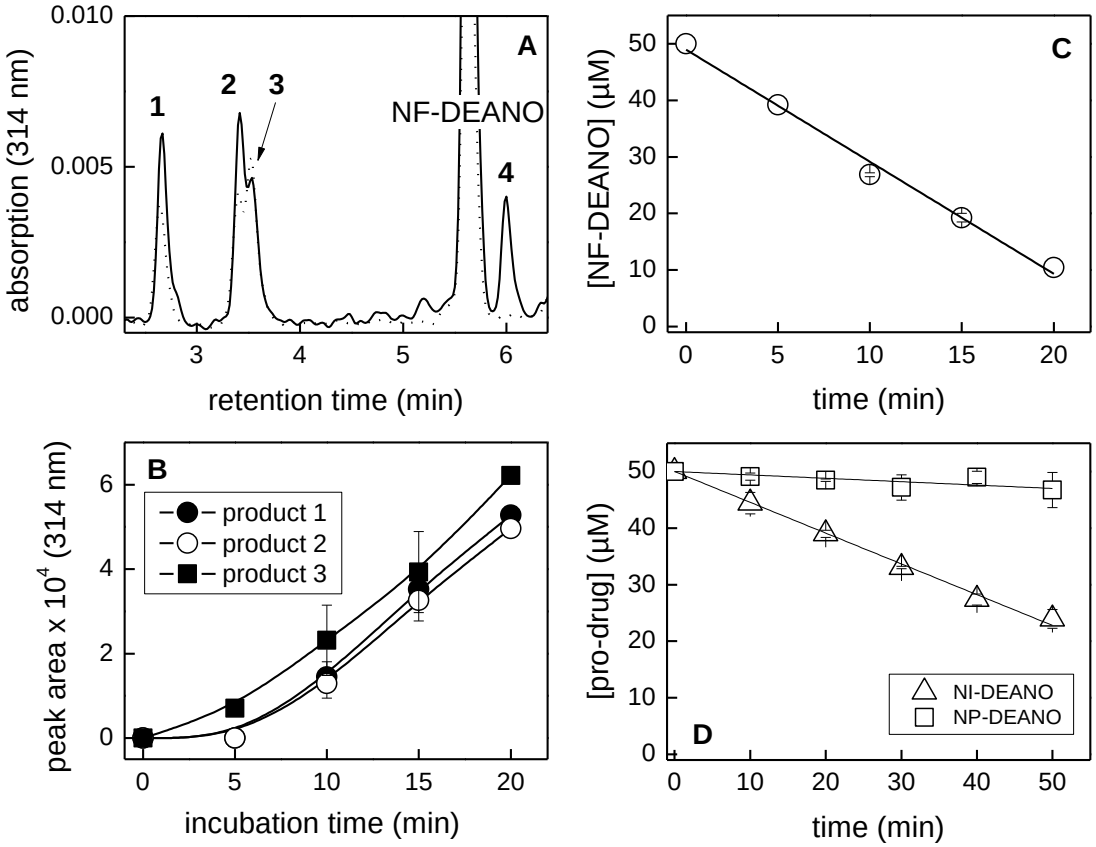

Figure 5-8 (A) Chromatograms showing the products resulting from the reduction of NF-DEANO with reducing radicals (54 Gy, 14.1 Gy/min) (—) and cytochrome P450 reductase supersomes (…); (B) Yield of products 1,2 and 3 during reduction with supersomes; (C) loss of NF-DEANO following reduction by cytochrome P450 reductase supersomes in anoxia at 37 °C; (D) loss of NI-DEANO and NP-DEANO following reduction by cytochrome P450 reductase supersomes in anoxia at 37 °C.

5.5 Reduction of pro-drugs by HepG2 Cells

NF-DEANO was readily reduced by HepG2 cell suspensions (~3 x10^7 cells/ml) in N_2-saturated solution. The presence of only ~0.25% (~3 μM) O_2 slowed the rate of reduction and metabolism and 1% O_2 (~13 μM) significantly reduced the loss of pro-drug (Figure 5-9A). Nitric oxide was not measured in these studies, therefore it can not be guaranteed that it is generated by bioreduction; however, metabolites are identical to those generated following reduction by supersomes containing cytochrome c reductase (Figure 5-9B) and formate radical reduction at a low dose rate (for which $^{\bullet}$NO production has been measured §5.2.2).

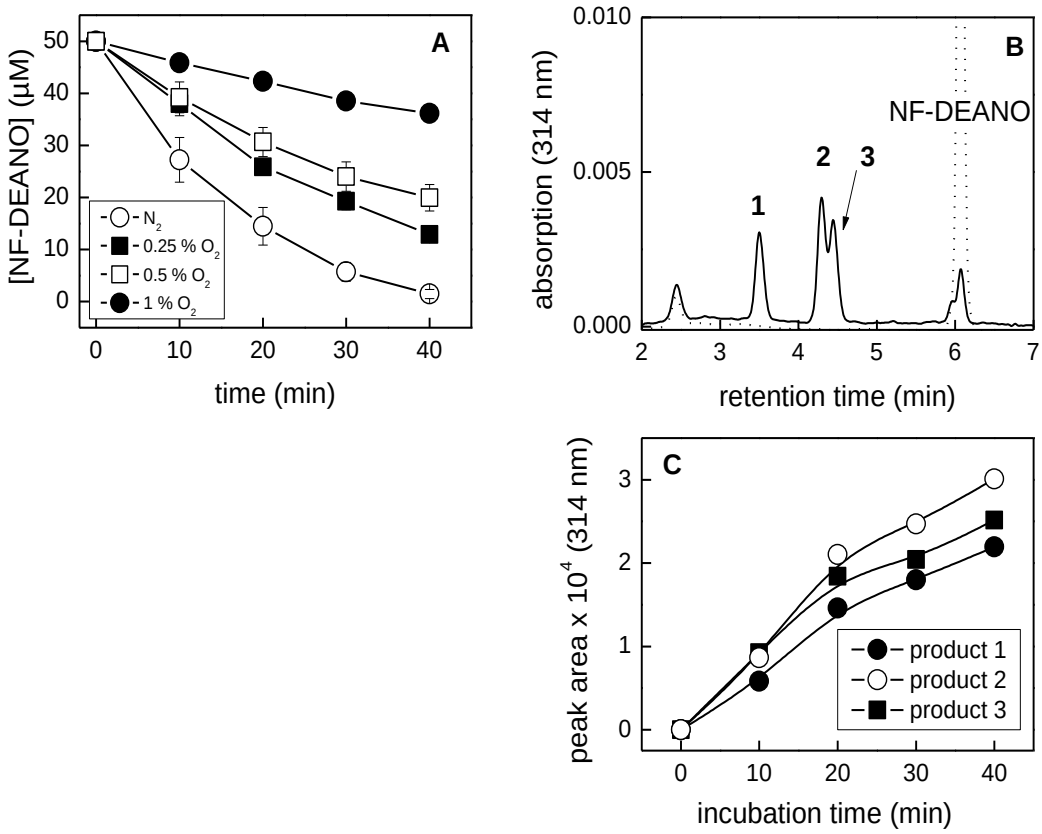

Figure 5-9 Effect of O_2 concentration on; (A) the metabolism of NF-DEANO by HepG2 cells (3.5 x 10^7/ml) at 37 °C in PBS; (B) chromatogram showing the formation of products 1-3 before and after 40 min incubation in anoxia at 37 °C; (C) representative yields of products 1-3 in these conditions.

NB-DEANO was not reduced readily by HepG2 cells even in N_2-saturated solutions (Figure 5-10A). NI-DEANO was reduced by HepG2 cells in anoxia more readily than NB-DEANO but at rates much lower than for NF-DEANO (Figure 5-10A). In 0.2% O_2, the turnover of NI-DEANO was virtually abolished (Figure 5-10B) reflecting rapid reaction of 2-nitroimidazole radical anions with oxygen (Wardman and Clarke 1976). It is possible that the uptake of NB- and NI-DEANO into HepG2 cells is less efficient than for NF-DEANO, which would be reflected in the lower rate of turnover of these pro-drugs. In addition these pro-drugs may not be such good substrates for the cellular reductases. This is shown to some extent by the low turnover of NI-DEANO in the presence of cytochrome c reductase supersomes where any possible variation in uptake (e.g. in whole cells) is not an issue (Figure 5-8D).

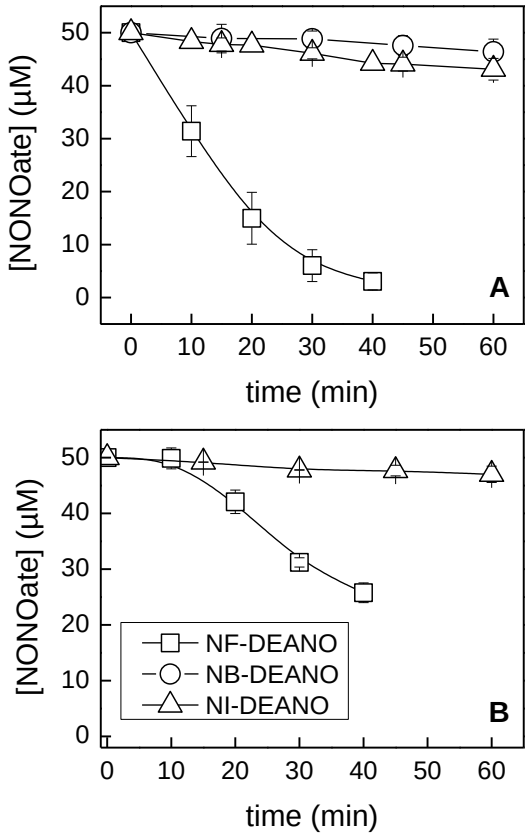

Figure 5-10 Metabolism of 50 µM NONOate pro-drugs by ~9 x 10^6 HepG2 cells/ml in PBS at 37 °C in; (A) N_2 saturated solution and (B) 0.2% O_2, 5% CO_2, 94.8% N_2 saturated solution; Results represent the mean and s.e.m of at least 2 independent experiments.

5.6 Radiosensitisation of V79-4 cells by NF-DEANO following reduction by supersomes

V79-4 cells were incubated with cytochrome c reductase supersomes in the presence of NF-DEANO in anoxia for 30 min at 37 °C which induced a loss of NF-DEANO of 6.3 ± 0.9 µM. These cells were then more radiosensitive than all control cells. A survival enhancement ratio (SER) of 2.2 at SF 0.4 was observed over cells irradiated in the presence of DMSO alone (Figure 5-11). Cells irradiated in the presence of un-metabolised NF-DEANO had an SER of 1.6 at SF 0.4 compared to cells incubated in N_2 alone (Figure 5-11) and cells incubated with supersomes alone showed no change in survival compared to control cells. As the studies were carried out in sealed glass syringes, the concentration of $^{\bullet}$NO likely to be present in the cell suspension following hydrolysis of the bioreductively-released DEANO is ~10 µM, although this was not confirmed.

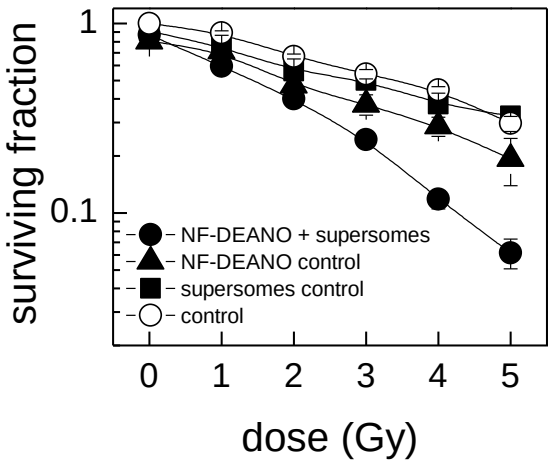

Figure 5-11 Radiosensitization of V79-4 cells by 20 μM NF-DEANO following reduction with P450 reductases for 30 min at 37 °C. Results represent the means and s.e.m of 3 independent experiments.

Nitroheterocycles are radiosensitizers of hypoxic cells themselves and are thought to interact directly with DNA radicals inducing DNA strand breaks and modified bases (Wardman 2007). The added radiosensitization, presumably by released •NO, amplifies the damage from the unmetabolised drug.

It is of course possible that the other products from the reduction of the 5-nitrofuran pro-drug are also radiosensitizers and it is these which increase the SER rather than •NO. To test this hypothesis NF-DEANO, in the presence of suspensions of V79-4 cells, was reduced with supersomes in sealed glass syringes for 30 min at 37 °C and then the cell suspensions were bubbled slowly with N_2 for 10 min before irradiating as above. Turnover of NF-DEANO was less than had been observed for the previous studies, with only 4.8 ± 3.2 μM loss of pro-drug over 30 min incubation in PBS in anoxia at 37 °C. However, cells which had been bubbled to remove any gaseous •NO were less radiosensitive than those which still had •NO present (Figure 5-12A). This suggests that it is •NO formed from the decomposition of bioreductively released DEANO which is acting as the radiosensitizer and not other potential furan products.

In addition, the cell samples were plated for DNA repair studies. Cell suspensions which still retained dissolved •NO showed more γH2AX foci (Figure 5-12B) and more cells expressed >3 foci (Figure 5-12C) than those cells which had been bubbled post supersomal-

incubation but pre γ-irradiation. This difference is particularly evident between 3-5 h after plating following 2 Gy. Although the repair of γH2AX foci is not as delayed as was seen with V79-4 cells saturated with 1% •NO (~18 µM) (Figure 4-7B) the data indicates that •NO is involved in the radiosensitization observed following the reduction of NF-DEANO.

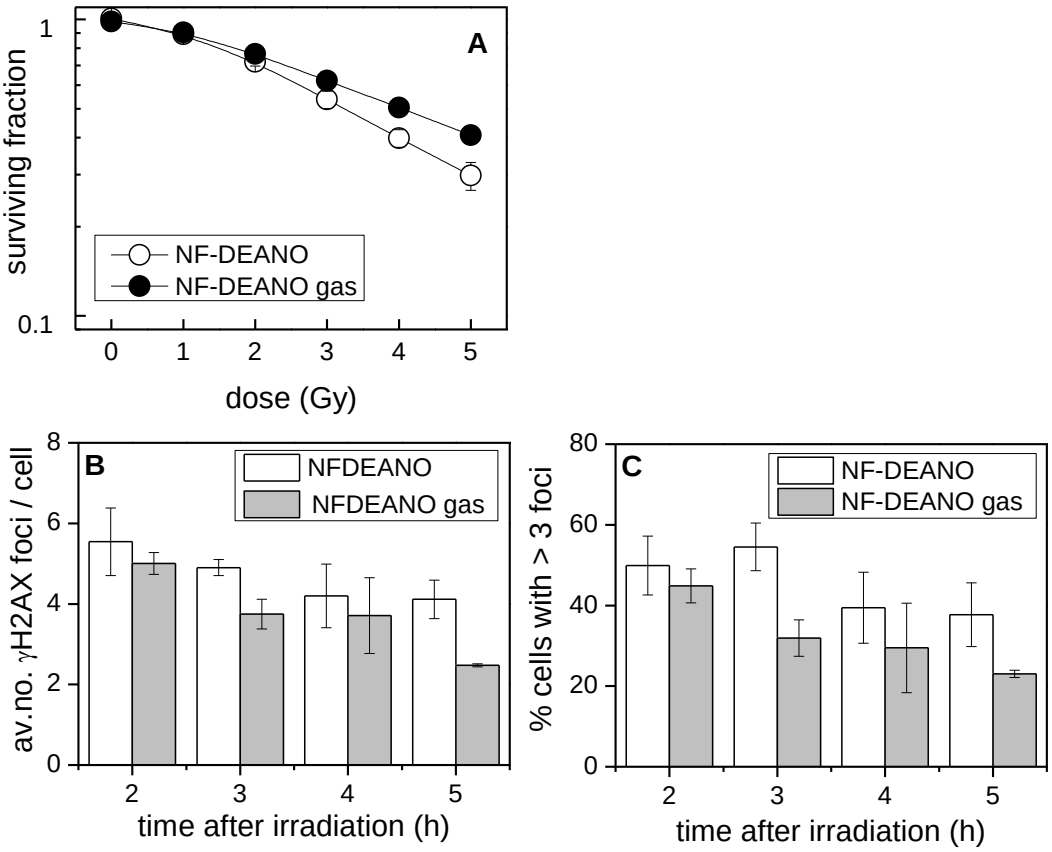

Figure 5-12 Effect of removal of released •NO by bubbling with N_2 following the reduction of NF-DEANO by cytochrome 450 supersomes in the presence of V79-4 cells on (A) surviving fraction of cells with dose; and formation and repair of γH2AX foci following γ-radiolysis (2 Gy); (A) average number of foci/cell; (B) percentage of cells showing >3 foci. Results represent the mean and s.e.m of 3 independent experiments.

5.7 Radiosensitization of HepG2 cells by NF-DEANO

Hepatoma G2 cells are not amenable to clonogenic survival assays, so a proliferation assay was used to study the effect of NF-DEANO metabolism on the radiosensitization of these cells. NF-DEANO increased the radiosensitivity of anoxic HepG2 cells and this effect

was enhanced further when it was reduced by endogenous reductases for 30 min at 37 °C in PBS (Figure 5-13). HepG2 cells (~10^7/ml) metabolised 22.9 ±1.7 µM NF-DEANO within this time. If •NO is produced at a ratio of 1:1.5 mole NF-DEANO: •NO as previously reported (Maragos *et al.* 1991) then ~34 µM •NO would be expected in the aqueous phase. In these experiments •NO produced in solution (1.5 ml) will equilibrate with the available headspace (8.5 ml) in the vial to some extent dependent upon the amount of agitation of the samples. As cells are present, the solutions were only swirled gently post-incubation at 37 °C before irradiation and therefore it is unlikely that full equilibration would have occurred between the gas and liquid phases. If complete equilibration did occur then the concentration of •NO remaining in the aqueous phase where the cells are, would be significantly lower than ~34 µM. However, •NO has a 6-8 times higher solubility in lipid than water, which may increase the concentration of dissolved •NO available to the cells during irradiations more than perhaps might be predicted for a simple aqueous solution. The most reliable method would be to measure the •NO produced in a sealed system with no headspace after incubation with the pro-drug. As so many HepG2 cells are required to get a reasonably efficient turnover of the pro-drug, a glass bubbling system similar to that used in V79-4 cell studies would have to be developed which could be used on volumes <2 ml. Preliminary studies were carried out degassing cells in inverted 2 ml glass syringes equipped with a PEEK tube through which N_2 was slowly bubbled. Although reasonable success with handing the cells was achieved, it was difficult to remove the headspace arising after sealing the syringes with luer type glass caps. Sampling of the cells during the irradiation period was also difficult, to prevent O_2 from entering the syringes. With time it is highly likely that a suitable vessel could be developed to carry out these studies but for this project, where proof of principle was the main aim, the actual concentration of •NO produced can for the time being be ignored.

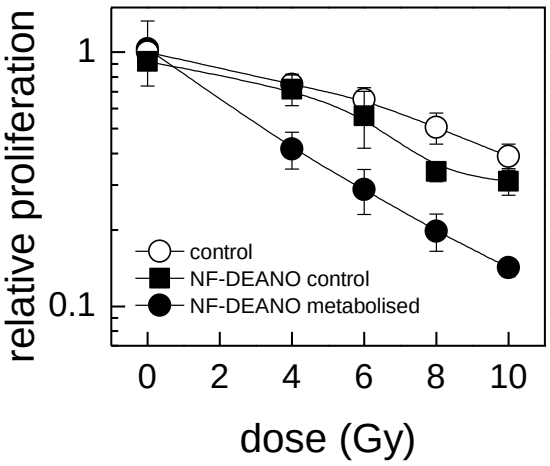

Figure 5-13 Radiosensitization of HepG2 cells by 40 μM NF-DEANO following reduction by HepG2 cells 30 min at 37 °C or unmetabolised pro-drug. Results represent the mean and s.e.m of at least 4 independent experiments.

5.8 General discussion

•NO has potential as a therapeutic agent in cancer treatment; however, administration to a tumour is difficult and •NO concentrations are tightly controlled in tissue. NONOate drugs which release •NO at physiological pH (Maragos *et al.* 1991; Keefer *et al.* 1996) have been investigated for the treatment of many disorders including heart disease. They have been conjugated with molecules showing specificity to tumours containing enhanced glutathione transferase activity, where the pro-drugs release the NONOate upon glutathionylation as has been investigated for multiple myeloma treatment (Kizlitepe *et al.* 2007). NONOates have also been targeted to tumour cells through peptide linkages specific to glioma cells (Safdar and Taite 2012). Linkage of NONOates to molecules which only allow the release of NO• in areas of very low oxygen could allow the targeting of •NO to hypoxic tumours. Auto-oxidation of •NO would be low in these conditions and diffusion to adjacent cells would be possible, allowing •NO to act as radiosensitizer of hypoxic radioresistant cells. The vasodilatory action of released •NO could also aid radiotherapy as an increase in blood flow would lead to increased oxygenation and radiosensitization (Oronsky *et al.* 2011; Oronsky *et al.* 2012).

The •NO releasing pro-drugs discussed in this chapter show a proof of principle. They are all stable at physiological pH and break down, releasing DEANO, upon one-electron

reduction. This effect was also observed in low oxygen conditions relevant to a hypoxic tumour. •NO is then released from the decomposition of DEANO at physiological pH. However, other products may be produced which could potentially give toxic side effects, for example alkylating agents and diethyl nitrosamine, and other NONOate drugs should be investigated.

The nitro heterocycles used for synthesizing these pro-drugs have a large effect upon the reducibility of the nitro groups and release of the active DEANO drug. The nitro radicals formed following one-electron reduction have different properties dependent upon the heterocycle. 5-Nitrofurans are very electron affinic compounds. Electron affinity is directly correlated with rate of reduction and metabolism of a drug (Wardman and Clarke 1976; Olive 1979). However, despite good results *in vitro*, early studies with nitrofurans showed little success as radiosensitizers *in vivo* and they showed high toxicities (Durand and Olive 1981). In fact early studies did not show that the most highly electron-affinic compounds were the best hypoxic radiosensitizers which may be due to their rapid metabolism. Nitro compounds with the most positive reduction potentials, including 5-nitrofurans, showed the highest toxicities in air (Adams *et al.* 1976) and hypoxia (Adams *et al.* 1980). *In vivo* relatively high concentrations of drugs (~0.1 mM) were necessary to induce significant radiosensitization in hypoxic cells and therefore the lipophilicity of the radiosensitizer was shown to be important, to allow sufficient uptake into the cells after administration for radiosensitization to occur (Brown and Workman 1980). However, lipophilicity was not shown to be important for effectiveness *in vitro,* where reduction potential was the most important factor (Adams *et al.* 1979). Despite showing the highest activity in the studies presented in this project 5-nitrofuran pro-drugs may not be the best choice for a bioreductive pro-drug. No common bioreductive pro-drugs which have been studied in the past contain nitrofuran moieties (Wilson and Hay 2011).

2-Nitroimidazoles have been well studied in tumours as their redox properties allow them to act as markers of hypoxia. In addition, pro-drugs have been developed which upon one-electron reduction release an active drug and are showing success in the clinic (Weiss *et al.* 2011). The reaction of nitro radical anions of 2-nitroimidazoles with O_2 is slower than for other effector molecules (for example quinones), which allows sufficient time for active drug release in hypoxia. 2-Nitroimidazoles are also well tolerated in humans (Coleman *et al.* 1990; Bleehen *et al.* 1991; Dische 1991). 2-Nitroimidazole pro-drugs may release the active drug through a non-radical process, where four-electron reduction of the nitro group to a hydroxylamine then allows elimination of the active dug (Everett *et al.* 1999). The remaining effector molecule is then likely to fragment and may form glyoxal and guanidines and alkylating species which may give potential side-effects through binding to DNA and other biomolecules. The 1-methyl-2-nitroimidazole pro-drug used in this project shows evidence that release of the active drug occurs through the nitro radical anion, as well as through further reduced products. Nitro radicals may also be responsible for toxic side effects because of their reactivity with DNA (discussed in (Tocher 1997)). Interestingly it has also been reported that sanazole, a 3-nitrotriazole releases nitric oxide upon reduction (although the techniques used measured $^{\bullet}NO$ production indirectly as nitrite and might therefore actually reflect nitrite release) (Kondakova *et al.* 2004), which may add to the radiosensitizing properties of this drug.

Chemical radiosensitizers must be present at the instant of radiotherapy. Nitroaromatic radiosensitizers show selective toxicity to hypoxic cells by reacting with DNA radicals produced during IR to form radical adducts which may lead to DNA strand breaks (Wardman 2007). In addition, metabolic products including nitroso and hydroxylamine derivatives may induce toxicity because of thiol or DNA binding. Activation of a pro-drug to release the active drug is dependent upon the expression and activity of cellular reductases, the oxygen concentration and the tissue penetration. NADPH dependent flavoproteins like

cytochrome P450 reductase and iNOS are one-electron reductants and can reduce some nitro compounds to nitro radical anions. These reactions are oxygen sensitive which allows some specificity to hypoxia but also can influence the formation of superoxide by futile redox cycling (Scheme 1-1). Inducible nitric oxide synthase is a one-electron reductase and is upregulated in hypoxia although its activity does require O_2. However, it may be a potential target for activation of pro-drugs. Two-electron reductases, which remove the potential for futile redox cycling, are also capable of reducing nitro compounds and reduction of indolequinone pro-drugs by this method have recently been shown to release conjugated diazeniumdiolates (Sharma *et al.* 2013). However, pro-drugs which fragment through the nitro radical anion would potentially be insensitive to activation through these types of enzymes (see (Wilson and Hay 2011) for a recent review).

Pro-drugs which are only activated in severe hypoxia (< 1 μM O_2) remove the risk of activation in moderately hypoxic cells. However, it is these moderately hypoxic cells which are the most important to eradicate during radiotherapy. Development of pro-drugs which release $^{\bullet}NO$ in severe hypoxia/anoxia offer the potential for diffusion to adjacent, more oxygenated cells. $^{\bullet}NO$ is more lipophilic than O_2 and can diffuse ~1.4 times further than O_2 (Singh and Gupta 2011) and could therefore be a very efficient radiosensitizer specific to severe and moderate hypoxia.

6 Reactivity of tyrosine radicals with nitric oxide

6.1 Introduction

Tyrosine is a critical component of many enzymes and membrane proteins and the oxidation of tyrosine (tyr) residues to phenoxyl radicals (tyr$^{\bullet}$) is essential for some enzyme functions. Tyrosine is readily oxidised by reactive oxygen and nitrogen species forming 3-3′-dityrosine (dityr), 3-nitrotyrosine ($3NO_2$tyr) and 3-hydroxytyrosine (3OHtyr) and their presence can be indicators of oxidative and/or nitrosative stress in cells. One-electron oxidation of tyr forms tyr$^{\bullet}$ in the first instance. Antioxidants can protect against the formation of stable products by reducing tyr$^{\bullet}$ back to tyr (Hunter *et al.* 1989; Folkes *et al.* 2011). In addition, tyr$^{\bullet}$ reacts slowly with O_2 (Hunter *et al.* 1989), but at near diffusion-controlled rates with $^{\bullet}$NO (Eiserich *et al.* 1995). Ribonucleotide reductase (RR), which is involved in the conversion of ribonucleotides to deoxyribonucleotides for DNA synthesis and repair (§1.7.1), has an essential tyr unit in its active site. $^{\bullet}$NO inhibits the activity of RR in a reversible reaction (Kwon *et al.* 1991; Lepoivre *et al.* 1992; Roy *et al.* 1995) but the mechanism for its action is unclear. The products from the reaction of tyr$^{\bullet}$ with $^{\bullet}$NO are unknown but it has been speculated that an intermediate tyrosine nitroso product is formed.

RR is a very attractive target for cancer therapy, particularly as it is inactivated in hypoxic conditions. Therefore, the aim of this project was to increase our understanding of tyrosine radical chemistry, focusing on the effect which O_2 and $^{\bullet}$NO have on product formation. Further knowledge on the mechanisms by which enzymes such as RR are inhibited by $^{\bullet}$NO and the $^{\bullet}$NO-releasing drug, hydroxyurea, may be beneficial to the development of future anti-cancer agents.

6.2 Oxidation of tyrosine by hydroxyl radicals

Hydroxyl radicals are an extremely reactive breakdown product of peroxynitrite (§1.6.1) and are enhanced in oxidative stress. They are strong one-electron oxidants, and they react with tyr through addition/elimination reactions forming in the majority $^{\bullet}$OH-adduct intermediates (Scheme 6-1, reaction 1) (k = 1.3 x 10^{10} M^{-1} s^{-1} at pH 7, (Solar *et al.* 1984)). It has been reported that ~50% $^{\bullet}$OH add to the position *ortho* (C-3) to the phenol and ~35% at the *meta* position (C-4) with ~5% of $^{\bullet}$OH directly leading to the formation of tyr$^{\bullet}$ and the remaining 10% reacting at other sites (Solar *et al.* 1984). Oxygen reacts rapidly with the C-3($^{\bullet}$OH) adduct forming 3OHtyr (otherwise known as L-DOPA) (k = 1.7 x 10^{9} M^{-1} s^{-1} (Cudina and Josimovic 1987)) and releasing $O_2^{\bullet-}$ (Scheme 6-1, reaction 2). 3OHtyr is also formed in cells through non-radical mechanisms by the reaction of tyrosine hydroxylase with tyr and is the precursor to the neurotransmitter catecholamines (dopamine, noradrenaline and adrenaline) and is used as a treatment for Parkinson's disease. In the absence of, or with low concentrations of O_2, the *ortho* position tyr-($^{\bullet}$OH) adduct dehydrates forming tyr$^{\bullet}$ (k = 1.8 x 10^{4} M^{-1} s^{-1}, H_2O (Solar *et al.* 1984)) (Scheme 6-1, reaction 3) in a reaction which is catalysed by phosphate (HPO_4^{2-}) (Land and Ebert 1967). Disproportionation and dimerisation are a minor pathway ($2k$ = 3 x 10^{8} M^{-1} s^{-1} (Solar *et al.* 1984)). In comparison, the *meta* position tyr-($^{\bullet}$OH) adduct is thought to decay through second order reactions only and does not dehydrate to form tyr$^{\bullet}$ ($2k$ = 2 x 10^{9} M^{-1} s^{-1}, (Solar *et al.* 1984)).

The majority of interest in tyrosine radical chemistry is with tyr$^{\bullet}$ which is produced directly by one-electron oxidants (Scheme 6-1, reaction 4) including $^{\bullet}NO_2$, $Br_2^{\bullet-}$ and $CO_3^{\bullet-}$ as well as through the dehydration of the C-3($^{\bullet}$OH) adduct. The ability of $^{\bullet}$NO to react with tyr$^{\bullet}$ is well known and this reaction is thought to be responsible for the inhibition of certain enzymes. It is unknown whether $^{\bullet}$NO can react with $^{\bullet}$OH-adducts of tyr, but the reaction is of interest as C-3($^{\bullet}$OH) is an intermediate for the formation of tyr$^{\bullet}$ and 3OHtyr. Oxidation of tyr by $^{\bullet}$OH in N_2O-saturated solution formed fluorescent dityr (Figure 6-1). In the presence of

20% O_2 (~260 µM), the yield of dityr was virtually abolished and 3OHtyr was observed (Figure 6-1). In N_2O-saturated solution at pH 7.4, dityr was formed with a yield of ~0.1 µM/µM •OH radical input (assuming ~0.6 µM •OH produced/Gy) (Figure 6-2) irrespective of the presence of 10 or 1 mM phosphate buffer. With both buffer concentrations, tyr was depleted at ~0.5 µM/µM •OH radical input. Two tyr molecules combine to form one dityr molecule, therefore about half of tyr lost forms dityr following reaction with •OH. As ~50% of •OH add at position C-3 (Solar *et al.* 1984) the vast majority of these adducts may form dityr, probably following dehydration to tyr• (Scheme 6-1, reaction 3). With the addition of 20% O_2, the formation of dityr was not significant but 3OHtyr was formed linearly with dose. The yield of 3OHtyr was ~40% higher in 1 mM phosphate compared to in 10 mM phosphate (0.23 ± 0.01 and 0.12 ± 0.01 µM/µM •OH radical input respectively) (Figure 6-2E and B). Lowering the concentration of O_2 to 10% (~130 µM) reduced the yield of 3OHtyr ~1.6-fold in 1 mM phosphate buffer (0.15 ± 0.01 µM/µM •OH radical input) and ~4-fold in 10 mM phosphate buffer (0.03 ± 0.01 µM/µM •OH radical input) but the yield of dityr remained extremely low. Loss of tyr was not significantly affected by O_2 concentration in 10 mM phosphate buffer (Figure 6-2A); however, in 1 mM phosphate, where dehydration of the radical adduct would be slower, the presence of 20% O_2 slightly increased the dose dependent loss of tyr (Figure 6-2D). Other mechanisms may exist, including the possibility that disproportionation may yield 3OHtyr and tyr (Getoff 1992), but as there is no evidence for the formation of 3OHtyr in anaerobic conditions, this pathway is expected to be very minor. On average only ~50% tyr is lost compared to the radical input, which suggests that disproportionation reactions may occur, as has been seen for similar reactions with salicylate (Maskos *et al.* 1993). Alternatively, dimerisation or disproportionation reactions involving the •OH-adducts at C-4 may also occur, to account for the yield of dityr being lower than the relative loss of tyr. Other products have as yet not been identified.

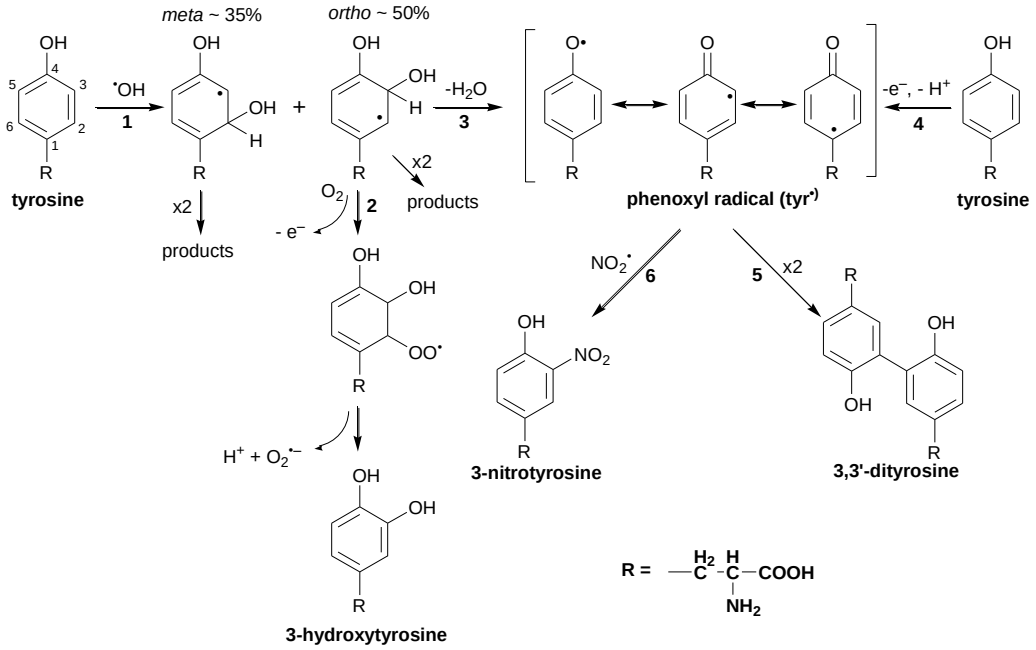

Scheme 6-1 Proposed mechanisms for the reaction of tyrosine with oxidising radicals and product formation.

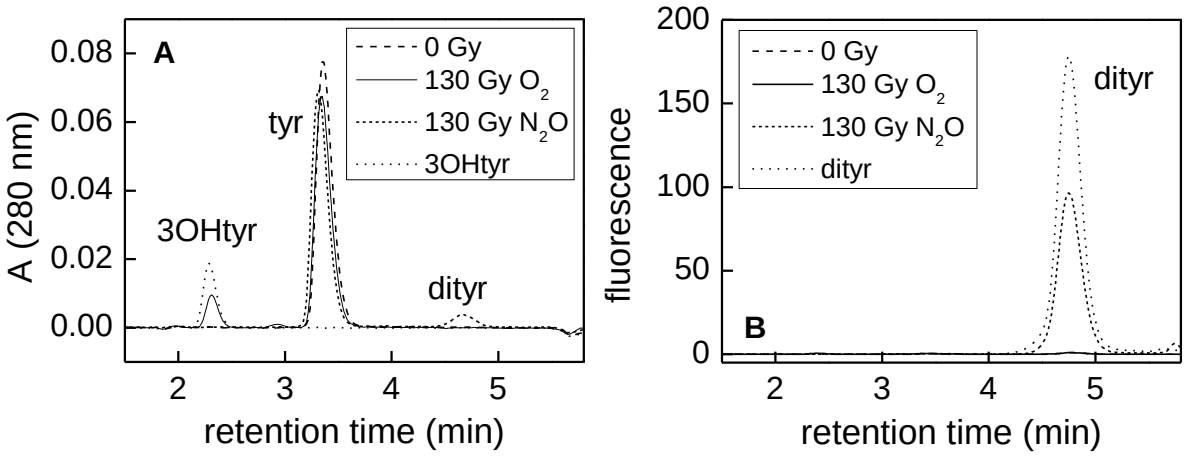

Figure 6-1 Chromatograms showing the formation of products from the reaction of tyrosine (0.5 mM) in 1 mM phosphate buffer (pH 7.4) with •OH in N_2O or N_2O/20% O_2 saturated solution; (A) monitoring at 260 nm showing 42 µM 3-hydroxytyrosine standard and (B) monitoring with fluorescence at Ex 294, Em 401 nm showing 18 µM dityrosine standard.

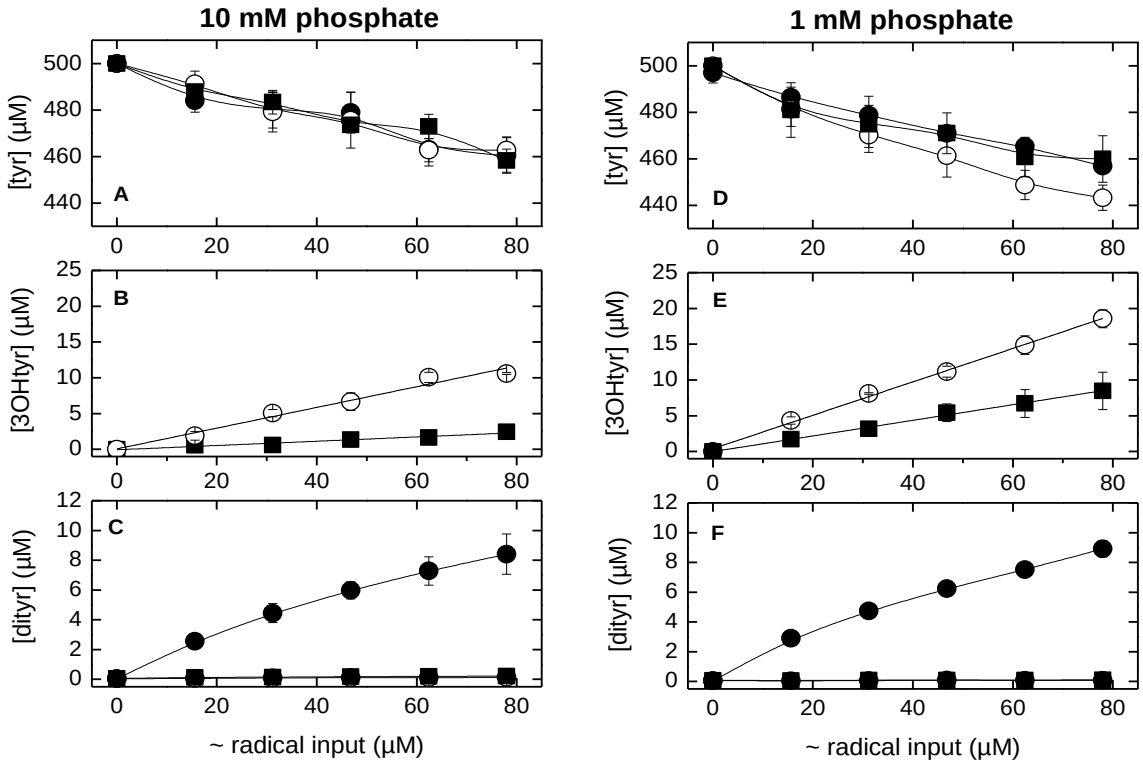

Figure 6-2 (A/D) Loss of tyrosine; (B/E) formation of 3-hydroxytyrosine and (C/F) formation of dityrosine following oxidation of tyrosine in 10 mM or 1mM phosphate, pH 7.4 with •OH in N_2O-saturated solution in the absence (●) or presence of ~260 µM O_2 (○) or ~130 µM O_2 (■). Results represent the means and SD of at least 2 independent experiments.

When tyr (0.5 mM) was irradiated in N_2O-saturated solution in the presence of a constant supply of •NO (~1.8 µM), the dose-dependent loss of tyr was unchanged compared to in the absence of •NO (Figure 6-3A, Figure 6-2) In comparison, the yield of dityr was reduced by ~100-fold (Figure 6-2B, Figure 6-3B) and although the yield was three-fold higher in 10 mM phosphate buffer compared to 1mM phosphate at pH 7.4, it was still sub-micromolar when •NO was present (Figure 6-3B); $3NO_2$tyr was not observed (Figure 6-2D). HPLC analysis showed the presence of two NO-related products, which had longer retention times than dityr (Figure 6-3D, products **1** and **2**). These products may account for the loss of tyr observed. The UV-visible spectra of the products are similar to that of tyr (Figure 6-3E).

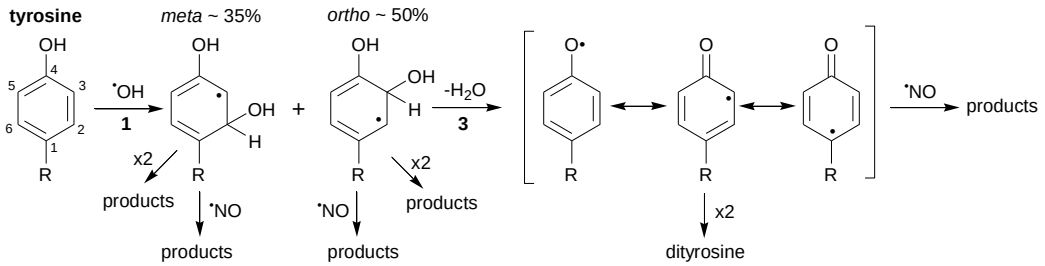

Scheme 6-2 Proposed reactions of •NO with tyrosine hydroxyl radical adducts.

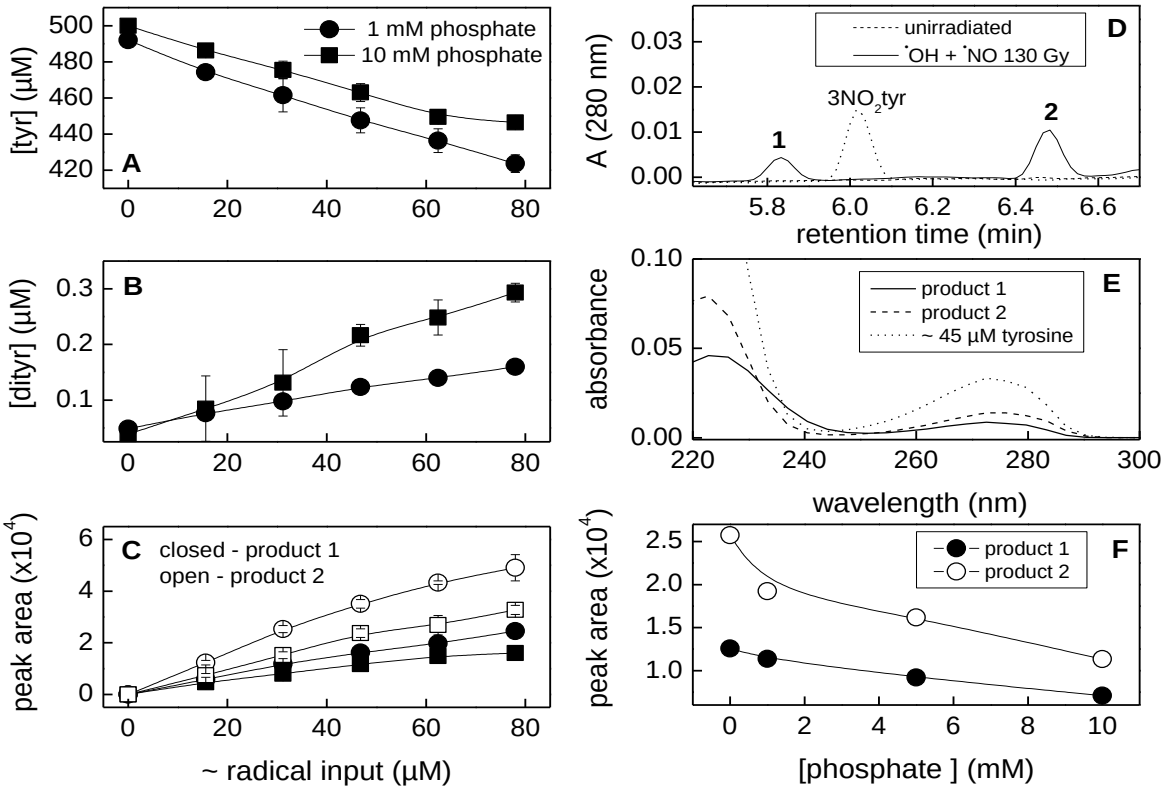

Figure 6-3 (A) Loss of tyrosine; (B) formation of dityrosine and (C) formation of products 1 and 2 following oxidation of tyrosine (0.5 mM) in 1 mM (●) or 10 mM (■) phosphate, pH 7.4 with •OH in the presence of ~1.8 μM •NO; (D) Chromatograms showing the formation of 1 and 2 at 280 nm - the retention of authentic 3-nitrotyrosine is shown to indicate that it is not formed during the reaction; (E) UV-visible spectra of products 1 and 2; (F) Effect of phosphate concentration on the yield of products 1 and 2 (280 nm) arising from the oxidation of tyrosine (1 mM) by •OH in the presence of ~1.8 μM •NO (~39 μM radical input). Results represent the means and SD of at least 2 independent experiments, apart from (F) where n=1.

The yields of these products (monitoring at 280 nm) were dependent upon phosphate concentration, with an approximate halving in peak area in 10 mM phosphate at pH 7.4

compared to buffer free solutions (Figure 6-3F). This suggests that the reaction of •NO with *ortho* tyr-(•OH) adducts may be in competition with phosphate catalysed dehydration which produces tyr•. The low concentration of dityr observed could then also be as a result of •NO reacting with tyr•, which is an extremely fast reaction (Eiserich *et al.* 1995) (Scheme 6-2). LCMS analysis of products **1** and **2** showed that both products are ionised with the major ion at *m/z* 181 (M-H), implying a molecular weight of 182, 1 Da greater than tyr. Increasing the cone voltage applied to the samples during ionisation increased fragmentation of the major ion.

Compound	***m/z***	**Fragments (*m/z*)**		
	(M-H)	**ES^- 20V**	**ES^- 30V**	**ES^- 40V**
Tyrosine	180	180	180	119, 163, 180
Product 1	181	119, 181	119, 151, 181	119
Product 2	181	181	135, 163, 181	119, 135, 163, 181

Table 6-1 Mass and fragmentation patterns of tyrosine and products 1 and 2 using LCMS analysis in ES^- mode, with cone voltages of 20-40V.

Products **1** and **2** show different sensitivities to the cone voltage applied and variations in the fragmentation patterns (Table 6-1). The 'nitrogen rule' for mass spectroscopy of organic compounds can predict that an even mass is representative of zero or an even number of N atoms and an odd mass can represent an odd number of N atoms. As tyr has a molecular weight of 181 Da and one N atom, the even mass measured for products **1** and **2** suggests that an extra N atom has been added, or indeed a N atom removed. It is therefore possible that the chemistry which is observed between the reaction of guanine C-8(•OH) or adenine C-8(•OH) adducts and •NO to form 8-azaguanine (§3.2.2) and 8-azaadenine respectively (§3.3.3) may also occur with tyr-(•OH) adducts, as a mass increase of one is observed between product **1**

and **2** and tyr. To investigate this hypothesis further, 4-hydroxybenzoic acid was utilised as a phenolic substitute for tyr, where •OH forms ~65% adducts on C-3 (Anderson 1987). However, no evidence was seen for the formation of 6-hydroxypyridine-3-carboxylic acid when 4-hydroxybenzoic acid was oxidized by •OH in the presence of ~1.8 μM •NO, suggesting that the aromatic C-3 is not replaced by a N in this molecule.

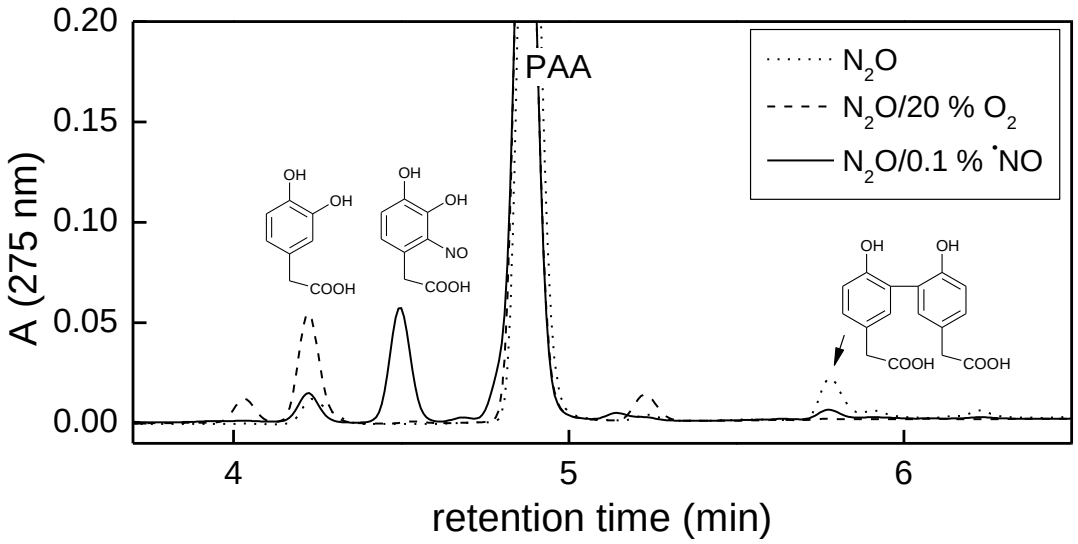

Figure 6-4 Chromatograms showing the possible products from the reaction of 4-hydroxyphenylacetic acid (PAA) (0.5 mM) with •OH (195 Gy) in 1 mM phosphate buffer, pH 7.4 in the presence of 20% O_2 (~260 μM) or 0.1% •NO (~1.8 μM). Chromatography conditions used a Hydro RP column with an eluent of 10 mM formic acid and a gradient of 0-80% methanol in 6 min.

The use of 4-hydroxyphenylacetic acid (PAA) as a more closely related substitute for tyr, showed significant differences in product formation compared to tyr. The formation of hydroxylated PAA was more efficient than for equivalent reactions with tyr and was observed even in the absence of O_2 (Figure 6-4). The presence of 20% O_2 increased the yield of mono-hydroxylated (*m/z* 167 (M-H)) products and also decreased the abundance of dimers (*m/z* 301 (M-H)) which are observed in N_2O-saturated solutions. In the presence of ~1.8 μM •NO the major hydroxylated product was still observed, but dimerisation was less efficient and a •NO-dependent product was also formed. This product has a low intensity ion of *m/z* 197 (M-H) and a fragment at *m/z* 154 and is likely to be an –OH and –NO adduct (with fragmentation

releasing $-COO^-$ (*m/z* 44) as shown in Figure 6-4. There is no evidence that tyr-(•OH) adducts react with •NO to form similar products and the chemistry which occurs with PAA and •OH is far less sensitive to •NO and O_2 than the equivalent reactions with tyr.

Fragmentation patterns shown in Table 6-1 for products **1** and **2** and tyr show that particularly for **2**, the major fragments observed are similar to those of tyr. This similarity might suggest that modifications have occurred to the aliphatic chain of tyr rather than the phenolic ring. It has been reported that <10% •OH react by H-atom abstraction with the alanine side-chain of tyr (Solar *et al.* 1984). To investigate if a reaction may have occurred with the alanine unit of tyr, the pH of the HPLC eluent was altered. The amino acid group of tyr is zwitterionic with an isoelectric point of 5.66. Preliminary HPLC analysis of **1** and **2** used a linear gradient comprising methanol and 10 mM formic acid (pH ~2.8), where both the COOH (p*K*a 2.2) and NH_3^+ (p*K*a 9.21) groups will be largely protonated and exhibit an overall positive charge. Exchanging the aqueous component of the eluent to 10 mM ammonium formate (pH ~ 6.9) will ensure that tyr will largely exist as a zwitterion with a net charge of zero. Rather surprisingly, the retention time of tyr was hardly changed by increasing the pH of the eluent. In comparison, the retention times of **1** and **2** were much reduced and they eluted close to tyr (Figure 6-5). The retention times of PAA and products were also significantly reduced when chromatographed using the higher pH eluent, showing that deprotonation to $-COO^-$ reduces the interaction of PAA with the hydrophobic C-18 packing in the column.

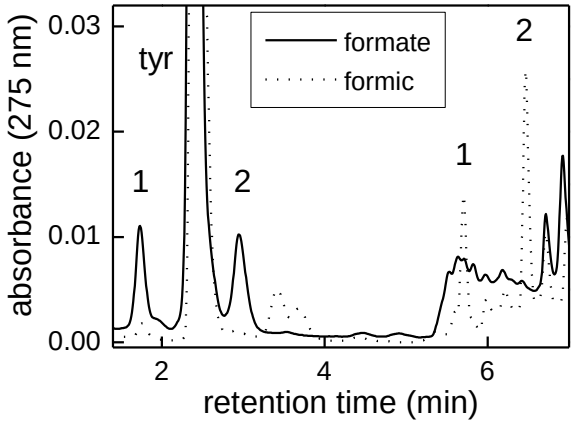

Figure 6-5 Chromatograms showing the elution of products 1 and 2 using 10 mM formic acid (…) or 10 mM ammonium formate (—) eluent with gradients of 0-80% methanol in 6 min and a flow rate of 0.8 ml/min.

There is evidence that a minor number of •OH-adducts form on the C-1 of tyr in peptides following Fenton reactions and that reactions of superoxide with tyr• also form adducts at C-1. These superoxide adducts can undergo intramolecular Michael addition to form bicyclic indolic *p*-hydroperoxide derivatives (Möller *et al.* 2012). It is possible that similar reactions may occur through the formation of •NO-adducts on the C-1 position. However, UV-visible spectra of **1** and **2** are very similar to that of tyr, which would not be expected if ring formation and loss of aromaticity had occurred. The identification of **1** and **2** requires more extensive analytical techniques and the formation of 2- or 3-azatyrosine cannot be ruled out, but the fact that •NO alters the product profile following the reaction of •OH with tyr is important. Inflammation can result in enhanced oxidative and nitrosative stress, situations which could potentially lead to simultaneous generation of •OH and •NO and therefore modification of tyrosine residues other than those currently known about may also be occurring.

6.3 Oxidation of tyrosine by one-electron oxidants (•NO_2, $Br_2^{\bullet-}$or N_3•)

The reaction of tyr by one-electron oxidants proceeds through an initial phenoxyl radical (tyr•) where the yield of tyr• is unaffected by the concentration of O_2 (Hunter *et al.* 1989). Tyr• reacts with •NO_2 to form $3NO_2$tyr (k~3 x 10^9 M^{-1} s^{-1} (gly-tyr) (Prütz *et al.* 1985)) (Scheme 6-1, reaction 6). In addition, tyr• dimerizes to form dityr (Scheme 6-1, reaction 5), and this is the major route taken for other one-electron oxidants.

Reaction of tyr with •NO_2 at pH 7.4 in N_2O-saturated 10 mM phosphate buffer formed $3NO_2$tyr and dityr at yields of ~40% of the loss of tyr (Table 6-2, Figure 6-6). Dityr formation also only accounted for ~40% of the loss of tyr following oxidation by N_3• and $Br_2^{\bullet-}$. These results suggest that disproportionation of tyr•, dimerization to form products other than dityr or other as yet unidentified products may occur.

	tyr loss			dityr			$3NO_2$tyr			nitrite
	N_2O	O_2	$^{\bullet}NO$	N_2O	O_2	$^{\bullet}NO$	N_2O	O_2	$^{\bullet}NO$	$^{\bullet}NO$
$^{\bullet}NO_2$	0.67	0.54	0.13	0.09	0.07	<0.002	0.11	0.1	0	nd
$N_3^{\bullet}$	0.60	0.47	0.12	0.12	0.09	<0.015	0	0	0	nd
$Br_2^{\bullet-}$	0.67	0.59	0.30	0.13	0.11	<0.002	0	0	0	0.89

Table 6-2 Approximate loss of tyrosine and yields of products (in µM/µM radical input, assuming ~0.6 µM radical/Gy) following oxidation by one-electron oxidants in N_2O-saturated 10 mM phosphate buffer, pH 7.4, with the addition of 20% (~260 µM) O_2 or 0.1% (~1.8 µM) $^{\bullet}NO$.

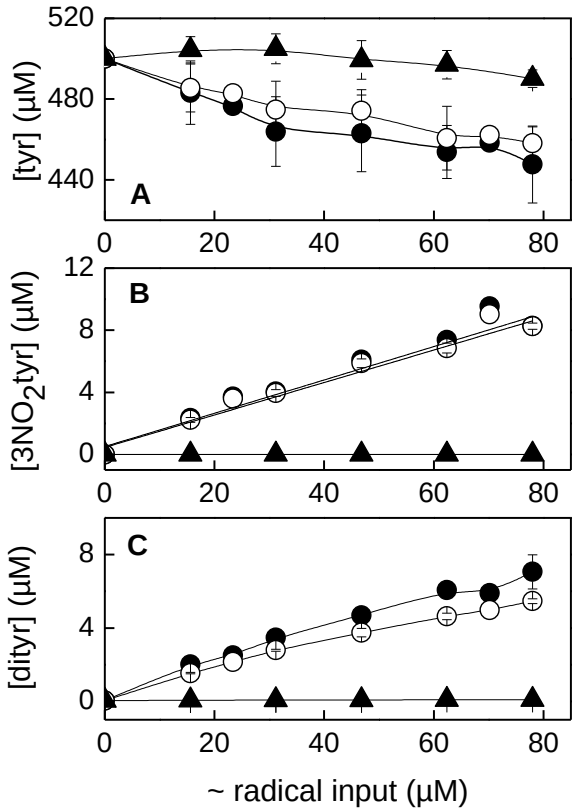

Figure 6-6 (A) Loss of tyrosine; (B) formation of 3-nitrotyrosine; (C) formation of dityrosine following oxidation of tyrosine (0.5 mM) by $^{\bullet}NO_2$ in 10 mM phosphate, pH 7.4 in the absence (●) or presence of either ~260 µM O_2 (○), or ~1.8 µM $^{\bullet}NO$ (▲). Results represent the means and SD of at least 2 independent experiments.

The presence of O_2 (260 µM) during γ-radiolysis had no effect upon the yield of $3NO_2$tyr following oxidation of tyr by $^{\bullet}NO_2$ (Table 6-2, Figure 6-6B). In comparison, the yields of dityr were reduced by ~20% following oxidation by all of the one-electron oxidants

in the presence of O_2, with similar reductions in the loss of tyr (Table 6-2, Figure 6-6 and 6-7). Oxygen reacts slowly with tyr$^{\bullet}$ ($k < 10^3$ M^{-1} s^{-1}) (Hunter *et al.* 1989; Jin *et al.* 1993) but the products which might arise from this reaction are unknown. The presence of $^{\bullet}NO$ (~1.8 µM) in N_2O-saturated solution during γ-radiolysis significantly reduced the formation of all products arising from the oxidants studied (Table 6-2, Figure 6-6 and 6-7). No alternative products were observed by HPLC, but the radiation-induced loss of tyr was much lower in the presence of $^{\bullet}NO$ for all oxidants (Table 6-2, Figure 6-6A, Figure 6-7 A and C). Measuring a small loss of tyr from a 0.5 mM initial concentration is prone to inaccuracies, but certainly there is evidence that some regeneration of tyr is occurring, suggesting that $^{\bullet}NO$ may be able to react with tyr$^{\bullet}$ to regenerate tyr with concomitant formation of nitrite. $^{\bullet}NO$ did not react with tyr directly in these anaerobic conditions.

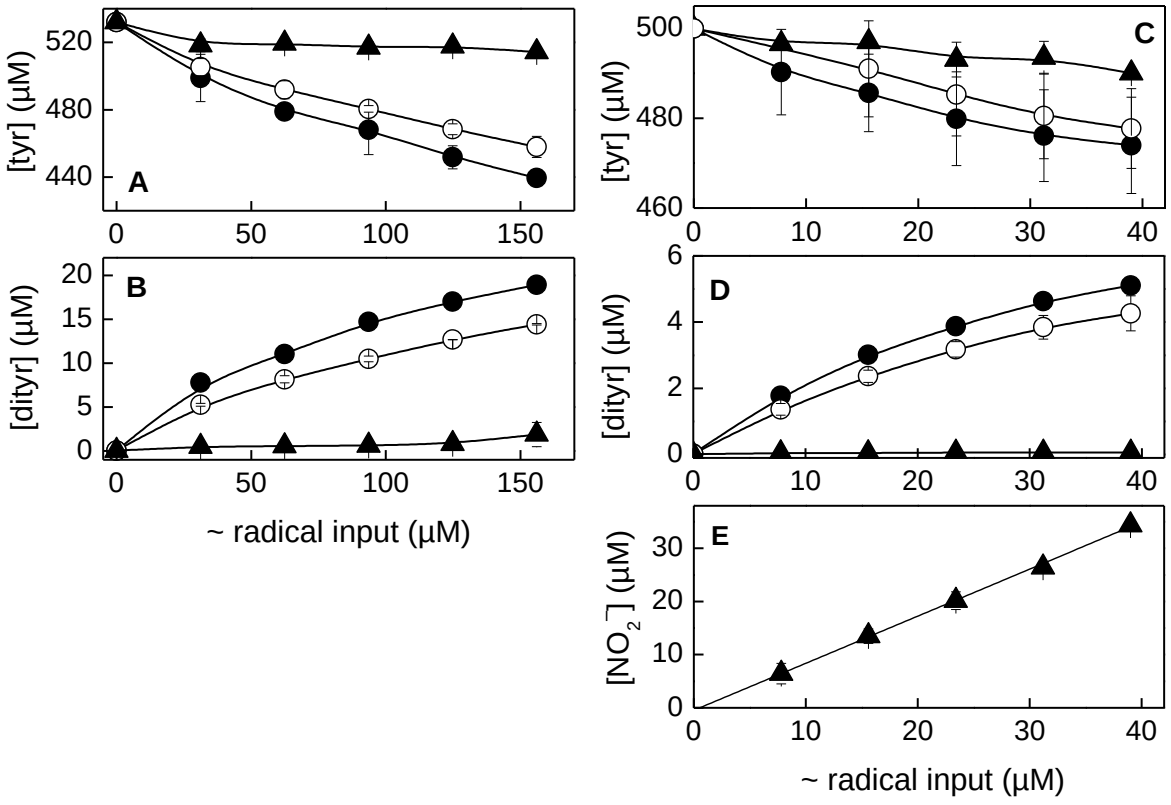

Figure 6-7 (A) Loss of tyrosine and (B) formation of dityrosine following oxidation of tyrosine (0.5 mM) with $N_3^{\bullet}$; (C) loss of tyrosine and (D) formation of dityrosine and (E) formation of nitrite following oxidation of tyrosine (0.5 mM) with $Br_2^{\bullet-}$ in the presence of ~1.8 µM $^{\bullet}NO$; all studies were carried out in 10 mM phosphate buffer, pH 7.4, in the absence (●) or presence of either ~260 µM O_2 (○) or ~1.8 µM $^{\bullet}NO$ (▲). Results represent the means and SD of at least 3 independent experiments.

6.4 Discussion of the reaction between •NO and tyrosine phenoxyl radical (tyr•)

It has been reported that •NO can react with tyrosine radicals in, for example, ribonucleotide reductase (Kwon *et al.* 1991; Lepoivre *et al.* 1992), prostaglandin H synthase-2 (Gunther *et al.* 1997; Sanakis *et al.* 1997) and photosystem II (Szalai and Brudvig 1996). The rate constant for the reaction of •NO with tyr• is extremely rapid (k~10^9 M^{-1} s^{-1} (Eiserich *et al.* 1995; Goldstein *et al.* 2000). Although the reaction has been well studied it is not fully understood, but it is generally accepted that some sort of reversibility of the reaction occurs (Janzen *et al.* 1993; Eiserich *et al.* 1995; Roy *et al.* 1995). 3-Nitrosotyrosine (3NOtyr) has been proposed to be formed from the reaction, in equilibrium with tyr• and •NO (Eq. 6-1). 3NOtyr may be enzymatically oxidized to an iminoxyl radical, identified through electron spin resonance spectroscopy (Sturgeon *et al.* 2001). Tyrosine iminoxyl radicals may be further oxidized to $3NO_2$tyr, as suggested in studies with prostaglandin H synthase-2 (Gunther *et al.* 1997). No direct evidence has been reported for the formation of 3NOtyr or O-nitrosotyrosine and neither of these products or $3NO_2$tyr was observed in these current studies either. It has been discussed that reversibility of the reaction between tyr• and •NO through a 3NOtyr intermediate (Eq. 6-1) may be misinterpreted as re-formation of tyr (Eq. 6-2) (Goldstein *et al.* 2000)

$$\text{tyr}^{\bullet} + {}^{\bullet}\text{NO} \leftrightharpoons \text{tyrONO} \qquad (6\text{-}1)$$

$$\text{tyrONO} + H_2O \rightarrow \text{tyr} + NO_2^- + H^+. \qquad (6\text{-}2)$$

When tyr is oxidized by $^{\bullet}NO_2$, $N_3^{\bullet}$ or $Br_2^{\bullet-}$ in the presence of •NO, the loss of tyr is significantly reduced (Figure 6-6 and 6-7), which supports the proposal that tyr is re-formed following reaction of tyr• with •NO, possibly through Eq. 6-2. Other alternative mechanisms may exist which could explain the fact that tyr is regenerated without the apparent formation of intermediates. •NO may directly reduce tyr• in an equilibrium reaction forming tyr and nitrosonium ion (NO^+) (Eq. 6-3).

$$tyr^{\bullet} + {}^{\bullet}NO + H^{+} \leftrightharpoons tyr + NO^{+} \quad (6\text{-}3)$$

$$NO^{+} + H_2O \leftrightharpoons H^{+} + HNO_2 \quad (6\text{-}4)$$

$$HNO_2 \leftrightharpoons H^{+} + NO_2^{-}. \quad (6\text{-}5)$$

NO^+ has a lifetime of 5-200 ns in water and would rapidly hydrolyse to nitrite in solution (Eq. 6-(4-5)) (k = 4.6 x 10^6 – 1.5 x 10^8 s^{-1} (Goldstein and Czapski 1996; Hughes 1999)). The reaction of tyr (0.5 mM) with $Br_2^{\bullet-}$ and ~1.8 µM $^{\bullet}NO$ in 10 mM phosphate at pH 7.4 produces nitrite at a yield of 0.88 ± 0.02 µM/µM $Br_2^{\bullet-}$ (Figure 6-7E). No significant formation of nitrite was seen in the absence of radiation. Although formation of nitrite through Eq. 6-2 can not be excluded, formation of nitrite in these solutions also supports reaction by Eq. 6-3.

The reduction potential of NO^+ has been estimated as $E°(NO^+/{}^{\bullet}NO)$ = 1.21 V (Stanbury 1989). NO^+ is therefore more electron-affinic than $tyr^{\bullet}$ at pH 7 by about 0.3 V ($E^0_7(tyr^{\bullet}, H^+/tyr)$ = 0.904 V (Folkes *et al.* 2011)). Thermodynamically, the ability of $^{\bullet}NO$ to reduce $tyr^{\bullet}$ is therefore unlikely, but there are examples of thermodynamically unfavorable reactions being 'driven' by a product being removed from the equilibrium. For example it has been proposed that $^{\bullet}NO$ can reduce Cu(II) complexes to Cu(I) with the formation of NO^+ which is rapidly removed by direct reaction with the solvent (Lim and Lippard 2006).

While a reaction between $tyr^{\bullet}$ and $^{\bullet}NO$ has been postulated to involve the formation of an adduct (Eiserich *et al.* 1995; Roy *et al.* 1995; Gunther *et al.* 1997)), no evidence has been presented for the isolation of such a product and exponential decay of $tyr^{\bullet}$ with a rate constant first-order in $^{\bullet}NO$ could also be compatible with an equilibrium involving NO^+ and tyr as products (Eq. 6-3). There is little doubt that $^{\bullet}NO$ reacts with $tyr^{\bullet}$, although the nature of the reaction and the products which form are still unclear. Scheme 6-4 shows all of the pathways which might occur. NO^+ is a powerful oxidant and may also nitrosylate tyr to form 3NOtyr, which following further oxidations may give $3NO_2$tyr. Formation of NO^+ through Eq. 6-3 may explain why $3NO_2$tyr has been observed in some studies (Gunther *et al.* 1997). Further work is necessary to fully ascertain whether $^{\bullet}NO$ is able to reduce $tyr^{\bullet}$ rather than forming an

as yet unidentified nitroso adduct. It remains to understand why •NO reacts so rapidly with tyr• whilst the same reaction by O_2 is slow. O_2 is not a reducing agent and cannot react in a similar way as the putative reaction of •NO with tyr• thereby 'repairing' tyr. Adduct formation with tyr• should theoretically be possible with both molecules, but reaction with O_2 would remove the aromaticity of the phenolic ring which may be unfavourable. Stable products have not been reliably identified from either •NO or O_2 reacting with tyr•.

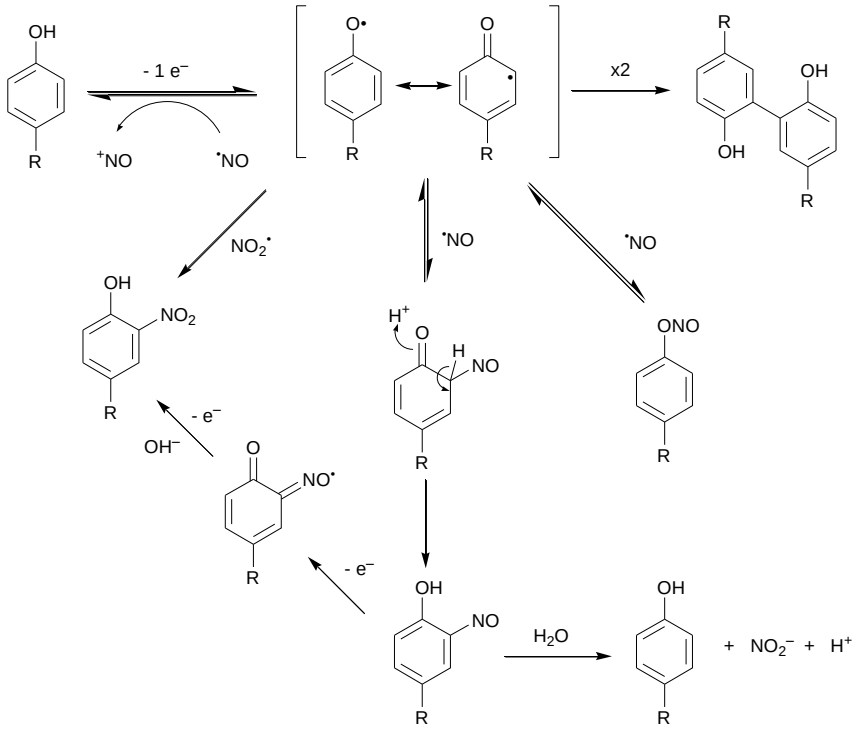

Scheme 6-3 Proposed mechanisms for the reaction and possible repair of tyrosine phenoxyl radical with nitric oxide.

6.5 Discussion into the release of nitric oxide from hydroxyurea

Studying the reaction between •NO and tyr• may help to explain the biological effect of a well used drug. Hydroxyurea (HU) is used as a treatment for sickle cell anaemia, various cancers and as a radiosensitizer for cervical cancer treatment (Navarra and Preziosi 1999; Candelaria *et al.* 2006). One of the mechanisms believed to be involved in its action is through the inhibition of RR, which has the effect of stalling DNA replication forks through

the depletion of 2′-deoxynucleoside triphosphates (dNTPs). Hydroxyurea administration to patients with sickle cell disease has been shown to generate •NO (Gladwin *et al.* 2002) and this metabolism may be one of the pathways by which HU elicits its effect. As •NO can inhibit the activity of RR (Kwon *et al.* 1991; Lepoivre *et al.* 1992), which is an important target for anti-cancer therapies, it seems pertinent to study the mechanisms by which •NO is released from HU in tissue, to understand the role which HU has in inhibiting DNA synthesis and how it might act as a radiosensitizer.

HU is oxidised by horseradish peroxidase (HRP) (Huang *et al.* 2002) and catalase in the presence of H_2O_2 (Huang *et al.* 2004) with rapid release of bursts of •NO and the formation of NH_3 and CO_2. HRP is an enzyme which oxidizes substrates through two consecutive one-electron steps, proceeding from a native ferric state, to compound I (HRP I), compound II (HRP II) and back to native form, with H_2O_2 essential for conversion of native ferric enzyme to HRP I (Eq. 6-6). It can be used as a model for biologically relevant peroxidases like myeloperoxidase and other one-electron oxidants. Using double-mix stopped-flow spectroscopy, the second order rate constants for the reaction of HRP I and II with HU at 37 °C are 2.91 ± 0.08 and 0.31 ± 0.01 x 10^4 M^{-1} s^{-1} respectively (results not shown). The rate of reaction of HU with HRP I is approximately 10-fold higher than with HRP II and the rate of both reactions is double at 37 °C compared to at 25 °C at pH 7 (1.65 ± 0.03 and 0.16 ± 0.01 x 10^4 M^{-1} s^{-1} for HRP I and HRP II respectively). The lifetime of observed HRP II is proportional to the concentration of H_2O_2, as was observed previously (Huang *et al.* 2002) and native HRP is regenerated from the reaction, presumably when H_2O_2 has been depleted and can no longer recycle the enzyme. The mechanisms for the reactions are uncertain but equally unclear are the mechanisms involved in the generation of •NO from these reactions. The studies of Huang *et al.* showed that the addition of small volumes of H_2O_2 to a solution of argon-saturated HU (1mM) and HRP (0.2 μM) produces a rapid burst of short-lived •NO which with repeated additions of H_2O_2 continues to be generated. The

lifetime of •NO is short in these studies but the reason for this is unclear. •NO reacts with the haem centre of ferric HRP and ferrous HRP to form stable nitroso adducts (Yonetani *et al.* 1972) but it is thought that these reactions do not irreversibly inhibit the enzyme, and addition of H_2O_2 may release bound •NO and reactivate the enzyme (Huang *et al.* 2002). In the studies by Huang *et al.* the apparent concentration of •NO produced after each addition of H_2O_2 was similar and did not increase significantly after each addition of H_2O_2. If •NO reacts with HRP to form a complex from which it is released upon further additions of H_2O_2, as well as further •NO being released from HU from oxidation by HRP I, it would be expected that the concentration of •NO would increase after each subsequent aliquot of H_2O_2 was added. •NO reacts efficiently with HRP I and II with apparent second order rate constants of 7.0×10^5 and 7.4×10^5 M^{-1} s^{-1} (20 °C) respectively (Glover *et al.* 1999), an unusually fast reaction with HRP II. The authors suggest that this fast rate may indicate direct oxidation of •NO to NO_2^- from the ferrous HRP II (Eq. 6-8).

$$\text{HRP} + H_2O_2 \rightarrow \text{HRP I} + H_2O \qquad (6\text{-}6)$$

$$\text{HRP I} + {}^{\bullet}NO \rightarrow \text{HRP II} + NO^+ \qquad (6\text{-}7)$$

$$\text{HRP II} + {}^{\bullet}NO \rightarrow \text{HRP} + NO_2^-. \qquad (6\text{-}8)$$

The apparent fast reactions of •NO with HRP I and II, ~70-700 fold faster than equivalent reactions with HU, could account for the rapid loss of •NO from solutions and the apparent high yields of nitrite/nitrate from these reactions (Huang *et al.* 2002) as any NO^+ formed would rapidly form NO_2^- in water (Eq. 6-4). Stopped-flow studies suggest that HRP is not inactivated during the reaction of HU with HRP in the presence of 100-fold excess H_2O_2 and no complex formation is observed, supporting the proposals by Glover *et al*. The apparent short lifetime of •NO could also then be accounted for by the reaction of •NO with radical intermediates from the oxidation of HU, as was discussed previously (Huang *et al.* 2002) and shown in Scheme 6-4.

There is no doubt that HU reacts with HRP and releases •NO. HRP is a one electron oxidant, and HU requires 3 electron equivalents to release •NO (Burkitt and Raafat 2006), if it is derived from nitroxyl (HNO) (Scheme 6-5). However, it is also possible that •NO is released directly from the nitroxide radical intermediate (Huang *et al.* 2002). This was investigated by using •OH to try to induce a one-electron oxidation of HU to the nitroxide radical intermediate. HU (1 mM) reacted with •OH with a loss of HU, measured using LCMS with single-ion monitoring at *m/z* 77 (M+H) of 0.24 ± 0.05 µM/Gy with a dose rate of 13.9 Gy/min. Using the Griess assay, nitrite was formed with a *G* value of only 0.028 ± 0.004 µM/Gy. With a *G* value of ~0.6 µM/Gy for the production of •OH in N_2O-saturated solution, the loss of HU is ~50 % of the radical input (results not shown).

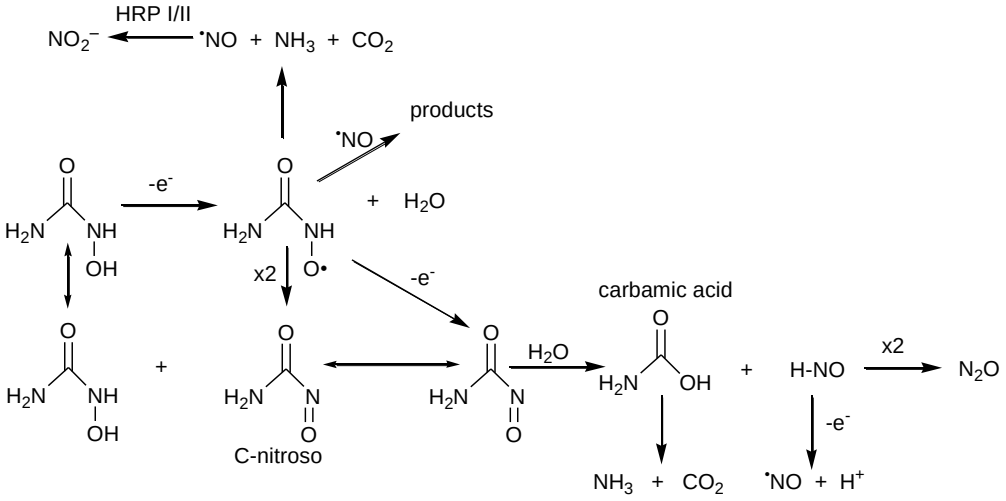

Scheme 6-4 Proposed mechanisms for the oxidation of hydroxyurea with HRP I and II or one-electron oxidants and the potential for the production and reactions of nitric oxide (adapted from (Huang *et al* 2002)).

This suggests that the nitroxide radical intermediate of HU may indeed disproportionate, as was proposed previously (Huang *et al.* 2002), with some of the nitroxide intermediates breaking down to form •NO, or that a two-electron step is required to oxidize HU to carbamic acid and HNO (Scheme 6-4).

Hypochlorous acid (HOCl) is a strong oxidant produced from the myeloperoxidase-catalysed oxidation of chloride ions by H_2O_2 and it could also be involved in the metabolism of HU. In the presence of metal ions (Candeias *et al.* 1994) and superoxide (Long and Bielski 1980; Candeias *et al.* 1993) HOCl can produce $^{\bullet}$OH. In addition, reaction with amines forms chloramines through electrophilic reactions which do not involve free-radical mechanisms (Folkes *et al.* 1995). HOCl reacts with HU to produce HNO (Cline *et al.* 2013) but no rate constants were presented and HNO requires a further one-electron oxidation step to release $^{\bullet}$NO (Scheme 6-5). Preliminary studies showed that the reaction of HOCl with an excess of HU produced a short burst of $^{\bullet}$NO. Nitrite reacts with HOCl to form nitryl chloride (Cl-NO_2), an agent capable of chlorinating and nitrating tyrosine (Eiserich *et al.* 1996) and this reaction may help to explain the apparent short lifetime of $^{\bullet}$NO in these reactions. Notably, complex mechanisms exist for the oxidation of HU and subsequent formation of $^{\bullet}$NO but the mechanisms warrant further studies to help towards the potential development of new drugs based upon the actions of $^{\bullet}$NO.

6.6 General Discussion

Nitric oxide is a free radical molecule produced *in vivo*, particularly following inflammation. Tyr is a common component of many membrane glycoproteins and the presence of dityr and 3NO_2tyr in cells is enhanced in regions of inflammation and in some pathologies (Radi 2004).

Hydroxyl radicals are highly reactive molecules produced during oxidative stress (and radiotherapy) which react with tyrosine to form in the majority $^{\bullet}$OH adducts. Major products from these reactions are 3OHtyr and dityr. In this project it is shown that $^{\bullet}$NO reacts with the radical intermediates to form two products, as yet unidentified, which may also be involved in some of the modifications which occur to tyr in regions of oxidative and nitrosative stress in tissue and could be responsible for some of the deleterious effects of inflammation.

Confirmation of the structure of these products is necessary. Identification of the products within cells would increase our understanding of tyr chemistry.

Tyr is also an essential amino acid in the activity of ribonucleotide reductase. RR is inactivated by $^{\bullet}NO$ which may reflect reactions with $tyr^{\bullet}$. The data described in this chapter may help to explain the reaction of $^{\bullet}NO$ with $tyr^{\bullet}$ further. By using steady state γ-radiolysis and oxidising radicals to oxidize tyr in the presence of hundreds of micromolar O_2 or low micromolar concentrations of $^{\bullet}NO$, evidence is shown for the ability of $^{\bullet}NO$ to react with $tyr^{\bullet}$ radicals, regenerating tyr and forming nitrite. This reaction may occur through the formation of the nitrosium ion (NO^+) (Eq. 6-3), or via a nitroso intermediate which may decay to tyr and nitrite (Eq. 6-2). In the reactions studied in this project, no evidence is seen for the formation of a nitrosotyrosine intermediate, suggesting that if the reaction proceeds through Eq. 6-2 (Goldstein *et al.* 2000), the proposed nitroso intermediate is extremely unstable and undetectable. Although reduction of $tyr^{\bullet}$ by $^{\bullet}NO$ is thermodynamically unfavourable, it cannot at this stage be ruled out. Production of NO^+ could potentially induce further damage as it is a potent nitrosylating agent and reaction with $tyr^{\bullet}$ in membranes may be particularly relevant in the hydrophobic environment where its lifetime will be considerably longer than in water.

Ribonucleotide reductase is an important target for cancer therapy and HU is an inhibitor of RR, although high concentrations of the drug are required to inhibit RR (ID_{50} ~5 10^{-4} M (Elford *et al.* 1979)). Cytotoxicity is an unfortunate side-effect (discussed in (Burkitt and Raafat 2006)) and understanding the role which HU has in the inhibition of RR could help to develop novel, less toxic drugs. Part of the action of HU may be through its poorly understood ability to release $^{\bullet}NO$. HU can be oxidised by for example, peroxidases, $^{\bullet}OH$ and HOCl, but complex mechanism exist and $^{\bullet}NO$ release may proceed through the formation of HNO. Formation of the nitroxide radical intermediate of HU following reaction with H_2O_2 has complex kinetics showing a lag-phase and lifetime dependent upon the experimental conditions, but visible by ESR up to 75 min after initiation (Lassmann and B.Liebermann

1989). These radicals if long-lived *in vivo*, could potentially react with tyr$^{\bullet}$ by electron transfer, or could decay to produce $^{\bullet}$NO directly. A steady production of $^{\bullet}$NO following the administration of HU in tissue where diffusion from the site of generation will occur may explain the role of $^{\bullet}$NO in some of the actions of HU.

Apart from reactions which might occur between $^{\bullet}$NO and tyrosyl radicals, reaction with the cysteinyl radicals generated in the catalytic cycle of RR (Scheme 1-7, steps 3 and 6) (Fontecave 1998) could also inhibit the enzyme (Roy *et al.* 1995). Unlike the proposed reversibility of the reaction between tyr$^{\bullet}$ and $^{\bullet}$NO, reaction between $^{\bullet}$NO and cysteinyl radicals, which would be equally fast (Madej *et al.* 2008), would form S-nitrosothiols which may inhibit RR for longer periods. Although S-nitrosothiols of free amino acids have been suggested to be relatively unstable, those created in proteins have been proposed to be longer lived (Roy *et al.* 1995).

Inhibition of RR by $^{\bullet}$NO through reactions with the metabolic tyrosine and cytosine radicals present in the active site, in conjunction with $^{\bullet}$NO-associated radiation-induced DNA damage, may explain the kinetics of DSB formation and repair observed in Chapter 4. A reduction in the available dNTPs through inhibition of RR would delay repair of DSB. These reactions may therefore offer additional benefits to the use of $^{\bullet}$NO as a hypoxic cell radiosensitizer.

7 Final discussion and future studies

Radiotherapy is an effective technique for treating cancer and is used for approximately 50% of cases, dependent upon type and location of a tumour. Radiation doses required to bring about tumour cure are a balance between limiting surrounding normal tissue damage and minimising radiation-induced mutagenesis. DNA damage, especially DSB, are thought to be the most lethal of radiation-induced DNA damage. The energy and intensity of the radiotherapy beam and the tumour microenvironment determines the specificity and level of repairability of any DNA damage arising within cells, in excess of that which occurs constantly through the action of endogenous oxidative stress. The research described in this thesis adds to our understanding of how the microenvironment of a cell can determine the types and severity of DNA damage which occurs following radiotherapy, with focus on the role of the endogenous molecule nitric oxide, in modifying the radiation response.

Ionizing radiation creates a plethora of types of DNA lesions including base modifications, abasic sites, SSB and DSB. The presence of •NO during the radiation exposure, affects the types of DNA damage observed. In particular, specific base modifications are generated from γ-irradiation of model nucleotides in anoxia in the presence of •NO. Base modifications which have been positively identified include xanthine and 8-azaguanine from guanine and hypoxanthine and 8-azaadenine from adenine. Other modifications also occur, in addition to those which occur to the pyrimidines, but further work is necessary to fully characterise these products. 8AzadGMP has been identified in γ-irradiated plasmid DNA in the presence of •NO, giving evidence that these types of changes may also occur in genomic DNA.

In studying the radical chemistry involved in the reaction of •NO with DNA radicals it was possible to address a topic in current debate. There has been much discussion as to the sites of reactivity of •OH with guanine molecules, particularly whether •OH can abstract a H-

atom from the primary amine on C-2 of guanine (discussed in Dizdaroglu and Jaruga 2012). The majority of studies following free radical reactions with DNA bases involve pulse radiolysis. This technique allows extremely fast (sub microsecond) changes in absorbance to be monitored and spectra of arising radicals to be recorded. Assigning these spectra and absorbancies to a particular species generally has a degree of ambiguity in the absence of any additional information and distinguishing between different species can be difficult, as optical absorption spectra can be a mixed composite of several radicals. The results described in this thesis show that 'fixing' a radical through its reaction with •NO has allowed a new hypothesis to be proposed as to the mechanisms involved in the •OH-induced changes which occur to guanine. These results help to explain the contrasting data obtained in previous studies and have led to an alternative interpretation of the previous pulse radiolysis data.

The reaction of •NO with DNA radicals generated by IR may also explain the DNA damaging effects which are seen in irradiated cells. Nitric oxide protects in part double-stranded plasmid DNA from SSB formation. However, incubation of these plasmids with a glycosylase increases the yields of SSB and DSB and demonstrates that base lesions are created, which are recognised, at least in non-cellular systems, by a bacterial endonuclease, and removed to create a strand break, and in the case of clustered damage some additional DSB. In mammalian cells, the yields of SSB are not significantly affected by •NO in anoxia, however DSB are enhanced, but only several hours after radiation exposure. The base lesions formed in the presence of •NO may be difficult to repair by conventional base excision repair as they may not be recognised by DNA repair enzymes, although this prediction requires testing. In addition, these lesions may occur within clustered damage, which account for ~30% of damage from low LET radiation including γ-rays. The presence of lesions in these clusters could induce DSB through a cluster encountering a replication fork, causing stalling or fork collapse. Indeed, cells undergoing replication are particularly sensitive to •NO during IR, and DSB repair is delayed several hours after most prompt DSB would have been

repaired. The results discussed in this thesis add evidence to the formation of •NO-associated damage within clusters being particularly difficult to repair. The data also supports a role for •NO in its ability to inhibit ribonucleotide reductase. Depletion of cellular deoxyribonucleotides would also lead to a delay in the repair of DNA damage until such a time as the pool is replenished, thereby allowing •NO to radiosensitize through an additional function other than modifying DNA damage.

The enhancement which oxygen has on cell death during IR is decreased with the increasing LET of the radiation (in (Hall 2000)). Approximately 2-3 times higher dose is required to kill anoxic cells compared to air-saturated cells by low LET X-rays at 250 keV but for high LET 2.5 MeV α-particles, the oxygen enhancement ratio is unity. Therefore hypoxia is not such an efficient radioprotector with high LET radiation. High LET radiation such as ion therapy creates complex clusters of damage compared to those induced by low LET radiation and damage is generally due to direct rather than indirect effects (Goodhead 1994). Repairability of these lesions is less efficient than those formed in more simple clusters (Eccles *et al.* 2011). It may be that •NO would also not be an efficient radiosensitizer with high LET compared to low LET radiation. This could potentially be studied using α-particles to irradiate cells, if a system could be developed to ensure anoxia and •NO exposure.

Although •NO is an endogenous molecule, which is elevated in tissue inflammation, delivery of the molecule to a hypoxic tumour may allow these regions to be sensitized to radiation and invoke better tumour cure. This thesis describes the development of novel pro-drugs of •NO which have the required properties to ensure the release of •NO only in low oxygen conditions through bioreductive activation for release of •NO. Administration of •NO through the use of NONOates which release large concentrations of •NO in short periods of time have been shown to induce tumour blood flow shutdown through the 'steal effect' (described in Sonveaux *et al.* 2009). This effect may only be relevant at high concentrations

of •NO which will may not be relevant to hypoxia selective •NO pro-drugs. This is a phenomenon which would have to be considered if work progressed into *in vivo* studies.

7.1 Future Work

Future work will concentrate on the biochemical responses of cells when exposed to extreme or moderate hypoxia. In particular, the rate of depletion and regeneration of cellular thiols following exposure to anoxia could be investigated to ascertain if data obtained *in vitro* may be as a result of changes in the cells antioxidant levels, which may not be replicated *in vivo*. In the same way, the kinetics of disappearance and reappearance of cellular deoxyribonucleotide pools following exposure to reduced O_2 tensions could be investigated further, and the effect which exposure to •NO may have on these levels and their rate of recovery. The nucleotide pool is essential to provide the building blocks required in many DNA repair pathways.

Evidence for the formation of •NO-associated lesions in DNA occurring in cells following ionizing radiation could be gained by the development of antibodies against 8azadGMP for example, which could be used for immunofluorescent techniques, as is already used for 8oxodGMP detection. Whether 8-azaguanine, in particular, is a substrate for mammalian glycosylases involved in DNA repair is as yet unknown, but development of model oligonucleotides containing 8azadGMP would allow this process to be studied in more detail. Further studies can be carried out on plasmid DNA and whole cells to investigate the nature of the formation of clustered damage by •NO during ionizing radiation using pulse field gel electrophoresis and digestion with glycosylases as described in previous studies (Sutherland *et al.* 2000; Gulston *et al.* 2002).

Future work on identifying the chemical modifications which occur to the other nucleotides following reaction with •OH in the presence of •NO which were briefly discussed in Chapter 3 is required.

Finally, if pulse radiolysis becomes available, in parallel with steady state radiolysis techniques, further studies could be carried out to investigate the hypothesis of the formation of the guanine aminyl radical following reaction of guanine with •OH as discussed in Chapter 3. In addition, differences in product formation following reaction of •OH in the presence of •NO with bases compared to nucleosides/nucleotides could be investigated further, which will increase our understanding of the chemistry associated with radiation-induced DNA damage.

References

Adams, G. E., E. D. Clarke, I. R. Flockhart, R. S. Jacobs, D. S. Sehmi, I. J. Stratford, P. Wardman, M. E. Watts, J. Parrick, R. G. Wallace and C. E. Smithen (1979). Structure-activity relationships in the development of hypoxic cell radiosensitizers: I. Sensitization efficiency. *Int J Radiat Biol* **35**: 133-150.

Adams, G. E., E. D. Clarke, R. S. Jacobs, I. J. Stratford, R. G. Wallace, P. Wardman and M. E. Watts (1976). Mammalian cell toxicity of nitro compounds: dependence upon reduction potential. *Biochem Biophys Res Comms* **72**: 824-829.

Adams, G. E., I. J. Stratford, R. G. Wallace, P. Wardman and M. E. Watts (1980). The toxicity of nitro compounds towards hypoxic mammalian cells in vitro: dependence upon reduction potential. *J Natl Cancer Inst* **64**: 555-560.

Adhikary, A., A. Kumar, D. Becker and M. D. Sevilla (2006). The guanine cation radical: investigation of deprotonation states by ESR and DFT. *J Phys Chem B* **110**: 24171-24180.

Alfassi, Z. B. (1987). Selective oxidation of tyrosine – oxidation by NO_2 and ClO_2 at basic pH. *Radiat. Phys. Chem.* **29**: 405-406.

Anderson, R. (1987). Radical spectra and product distribution following electrophilic attack by the $OH^{\bullet}$ radical on 4-hydroxybenzoic acid and subsequent oxidation. *J. Chem. Soc., Faraday Trans. 1* **83**: 3177-3188.

Aziz, K., S. Nowsheen, G. Pantelias, G. Iliakis, G. Gorgoulis and A. G. Georgakilas (2011). Targeting DNA damage and repair: Embracing the pharmacological era for successful cancer therapy. *Pharmac. Ther.* **133**: 334-350.

Balasubramanian, B., W. K. Pogozelski and T. D. Tullius (1998). DNA strand breaking by the hydroxyl radical is governed by the accessible surface areas of the hydrogen atoms of the DNA backbone. *Proc Nat. Acad Sci USA* **95**: 9738-9743.

Bamatraf, M. M. M., P. O'Neill and B. S. M. Rao (1998). Redox dependence of the rate of interaction of hydroxyl radical adducts of DNA nucleobases with oxidants: consequences for DNA strand breakage. *J Am Chem Soc* **120**: 11852-11857.

Banath, J. P., D. Klokov, S. H. MacPhail, A. Banuelos and P. L. Olive (2010). Residual γ-H2AX foci as an indication of lethal DNA lesions. *BioMed Central Cancer* **10**(4): 1471-2407.

Bartberger, M. D., W. Lui, E. Ford, K. M. Miranda, C. Switzer, J. M. Fukuto, P. J. Framer, D. A. Wink and K. N. Houk (2002). The reduction potential of nitric oxide (NO) and its impotance to NO biochemistry. *Proc Natl Acad Sci* **99**: 10958-10963.

Bartesaghi, S., V. Valez, M. Trujillo, G. Peluffo, N. Romero, H. Zhang, B. Kalyanaraman and R. Radi (2006). Mechanistic studies of peroxynitrite-mediated tyrosine nitration in membranes using the hydrophobic probe *N*-*t*-BOC-L-tyrosine *tert*-butyl ester. *Biochemistry* **45**: 6813-6825.

Bartesaghi, S., J. Wenzel, M. Trujillo, M. Lopez, J. Joseph, B. Kalyanaraman and R. Radi (2010). Lipid peroxyl radicals mediate tyrosine dimerization and nitration in membranes. *Chem Res Toxicol*.

Beckman, J. S., T. W. Beckman, J. Chen, P. A. Marshall and B. A. Freeman (1990). Apparent hydroxyl radical production by peroxynitrite: implications for endothelial injury from nitric oxide and superoxide. *Proc Natl Acad Sci USA* **87**: 1620-1624.

Begg, A. C., F. A. Stewart and C. Vens (2011). Strategies to improve radiotherapy with targeted drugs. *Nat. Rev. Cancer* **11**: 239-253.

Bergeron, F., F Auvré, J. P. Radicella and J-L. Ravanat (2010). HO• radicals induce an unexpected high proportion of tandem base lesions refractory to repair by DNA glycosylases. *Proc Natl Acad Sci USA* **107**: 5528-5533.

Berry, R. J., E. J. Hall and J. Cavanagh (1970). Radiosensitivity and the oxygen effect for mammalian cells cultured *in vitro* in stationary phase. *Br J Radiol* **43**: 81-90.

Bhide, S. A. and C. M. Nutting (2010). Recent advances in radiotherapy. *BMC Med.* **8:25**: 1-5.

Bleehen, N. M., T. S. Maughan, P. Workman, H. F. Newman, S. Stenning and R. Ward (1991). The combination of multiple doses of etanidazole and pimonidazole in 48 patients: a toxicity and pharmacokinetic study. *Radiother Oncol* **20 suppl. 1**: 137-142.

Bonini, M. G., R. Radi, G. Ferrer-Sueta, A. M. Da C Ferreira and O. Augusto (1999). Direct EPR detection of the carbonate radical anion produced from peroxynitrite and carbon dioxide. *J Biol Chem* **274**: 10802-10806.

Borde, V. and J. Cobb (2009). Double functions for the MRE11 complex during DNA double-strand break repair and replication. *Int J Biochem Cell Biol* **41**: 1249-1253.

Breen, A. P. and J. A. Murphy (1995). Reactions of oxyl radicals with DNA. *Free Radi. Biol Med.* **18**(6): 1033-1077.

Bristow, R. G. and R. P. Hill (2008). Hypoxia and metabolism. Hypoxia, DNA damage and genetic instability. *Nat. Rev. Cancer* **8**: 180-192.

Brown, J. M. (1981). Radiosensitizers: rationale and potential. *Cancer Treatment Reports* **65**: 95-102.

Brown, J. M. and P. Workman (1980). Partition coefficient as a guide to the development of radiosensitizers which are less toxic than misonidazole. *Radiat Res* **82**: 171-190.

Bryan, N. S. and M. B. Grisham (2007). Methods to detect nitric oxide and its metabolites in biological samples. *Free Radic. Biol. Med.* **43**: 645-657.

Bump, A. D., N. Y. Yu and J. M. Brown (1982). Radiosensitization of hypoxic tumor cells by depletion of intracellular glutathione. *Science* **217**: 544-545.

Burkitt, M. J. and A. Raafat (2006). Nitric oxide generation from hydroxyurea: significance and implications for leukemogenesis in the management of myeloproliferative disorders. *Blood* **107**: 2219-2222.

Burney, S., J. L. Caulfield, J. C. Niles, J. S. Wishnok and S. R. Tannenbaum (1999). The chemistry of DNA damage from nitric oxide and peroxynitrite. *Mutation Res.* **424**: 37-49.

Burris III, H. A., H. S. Rugo, S. J. Vukelja, C. L. Vogel, R. A. Borson, S. Limentani, E. Tan-Chiu, I. E. Krop, R. A. Michaelson, S. Girish, L. Amler, M. Zheng, Y.-W. Chu, B. Klencke and J. A. O'Shaughnessy (2011). Phase II study of the antibody drug conjugate trastuzumab-DM1 for the treatment of human epidermal growth factor receptor 2 (HER2) –positive breast cancer after prior HER2-directed therapy. *J. Clin. Oncol.* **29**: 398-405.

Buxton, G. V., C. L. Greenstock, W. P. Helman and A. B. Ross (1988). Critical review of rate constants for reactions of hydrated electrons, hydrogen atoms and hydroxyl radicals ($^{\cdot}OH/^{\cdot}O^{-}$) in aqueous solution. *J Phys Chem Ref Data* **17**: 513-886.

Candeias, L. P., K. B. Patel, M. R. L. Stratford and P. Wardman (1993). Free hydroxyl radicals are formed on reaction between the neutrophil-derived species superoxide anion and hypochlorous acid. *FEBS Letts* **333**: 151-153.

Candeias, L. P. and S. Steenken (1989). Structure and acid-base properties of one-electron-oxidized deoxyguanosine, guanosine and 1-methylguanosine. *J Am Chem Soc* **111**: 1094-1099.

Candeias, L. P. and S. Steenken (2000). Reaction of HO• with guanine derivatives in aqueous solution: formation of two different redox-active OH-adduct radicals and their unimolecular transformation reactions. Properties of G(-H)•. *Chem Eur J* **6**: 475-484.

Candeias, L. P., M. R. L. Stratford and P. Wardman (1994). Formation of hydroxyl radicals on reaction of hypochlorous acid with ferrocyanide, a model iron(II) complex. *Free Radic Res* **20**: 241-249.

Candelaria, M., A. Garcia-Arias, L. Cetina and A. Dueñas-Gonzalez (2006). Radiosensitizers in cervical cancer. Cisplatin and beyond. *Radiat. Oncol.* **1**: 1-17.

Caulfield, J. L., J. S. Wishnok and S. R. Tannenbaum (1998). Nitric oxide-induced deamination of cytosine and guanine in deoxynucleosides and oligonucleosides. *J Biol Chem* **273**: 12689-12695.

Chapman, J. D., J. A. Raleigh, J. Borsa, R. G. Webb and R. Whitehouse (1972). Radiosensitization of mammalian cells by p-nitroacetophenone. II. Effectiveness of analogues. *Int J Radiat Biol* **21**: 475-482.

Chapman, J. D., A. P. Reuvers, J. Borsa, A. Petkau and D. R. McCalla (1972). Nitrofurans as radiosensitizers of hypoxic mammalian cells. *Cancer Res* **32**: 2616-2624.

Chatgilialoglu, C., M. D'Angelantonio, M. Guerra, P. Kaloudis and Q. G. Mulazzani (2009). A reevaluation of the ambident reactivity of the guanine moiety towards hydroxyl radicals. *Angew. Chem.* **48**: 2214-2217.

Chatgilialoglu, C., M. D'Angelantonio, G. Kciuk and K. Bobrowski (2011). New insights into the reaction paths of hydroxyl radicals with 2'deoxyguanosine. *Chem Res Toxicol* **24**: 2200-2206.

Chatterjee, A. (2013). Reduced glutathione: a radioprotector or a modulator of DNA-repair activity. *Nutrients* **5**: 525-542.

Chen, S. N. and M. Z. Hoffman (1973). Rate constants for the reaction of the carbonate radical with compounds of biochemical interest in neutral aqueous solution. *Radiat Res* **56**: 40-47.

Chien, Y.-H., D.-T. Bau and K.-Y. Jan (2004). Nitric oxide inhibits DNA-adduct excision in nucleotide excision repair. *Free Radic Bio. Med* **36**: 1011.

Choi, I.-K., R. Strauss, M. Richter, C.-O. Yun and A. Lieber (2013). Strategies to increase drug penetration in solid tumours. *Frontiers Oncol.* **3**(Article 193): 1-18.

Chowdhury, R., L. C. Godoy, A. Thiantanawat, L. J. Trudel, W M Deen and G. N. Wogan (2012). Nitric oxide produced endogenously is responsible for hypoxia-induced HIF-1α stabilization in colon carcinoma cells. *Chem Res Toxicol* **25**: 2194-2202.

Cline, M. R., T. A. Chavez and J. P. Toscano (2013). Oxidation of N-hydroxy-L-arginine by hypochlorous acid to form nitroxyl (HNO). *J. Inorg. Biochem.* **118**: 148-154.

Coleman, C. N., T. H. Wasserman, R. C. Urtasun, J. Halsey, L. Noll, S. Hancock and T. L. Phillips (1990). Final report of the phase I trial of the hypoxic cell radiosensitizer SR 2508 (etanidazole) Radiation Therapy Oncology Group 83-03. *Int J Radiat Oncol Biol Phys* **18**: 389-393.

Colsky, J., L. E. Meiselas, S. J. Rosen and I. Schulman (1955). Response of patients with leukemia to 8-azaguanine. *Blood* **10**: 482-492.

Contreras, J. G. and S. T. Madariaga (2003). Structure and the energy of base pairing in non-natural bases of nucleic acids: the azaguanine-cytosine and azaadenine-thymine base pairs. *Bioorg Chem* **31**: 367-377.

Cook, T., Z. Wang, S. Alber, K. Liu, S. C. Watkins, Y. Vodovotz, T. R. Billiar and D. Blumberg (2004). Nitric oxide and ionizing radiation synergistically promote apoptosis and growth inhibition of cancer by activating p53. *Cancer Res* **64**: 8015-8021.

Coulter, J. A., H. O. McCarthy, J. Worthington, T. Robson, S. Scott and D. G. Hirst (2008). The radiation-inducible pE9 promoter driving inducible nitric oxide synthase radiosensitizes hypoxic tumour cells to radiation. *Gene Ther.* **15**: 495-503.

Cudina, I. and L. J. Josimovic (1987). The effect of oxygen on the radiolysis of tyrosine in aqueous solutions. *Radiat Res* **109**: 206-215.

Czapski, G., J. Holcman and B. H. J. Bielski (1994). Reactivity of nitric oxide with simple short-lived radicals in aqueous solutions. *J Am Chem Soc* **116**: 11465-11469.

Davies, K. M., D. A. Wink, J. E. Saavedra and L. K. Keefer (2001). Chemistry of the diazeniumdiolates. 2. Kinetics and mechanism of dissociation to nitric oxide in aqueous solution. *J Am Chem Soc* **123**: 5473-5481.

Denny, W. A., W. R. Wilson and M. P. Hay (1996). Recent developments in the design of bioreductive drugs. *Br J Cancer* **74 (Suppl. XXVII)**: S32-S38.

Dikomey, E. and J. Franzke (1986). DNA repair kinetics after exposure to X-irradiation and to internal β-rays in CHO cells. *Radiat. Env. Biophys.* **25**: 189-194.

Dische, S. (1991). A review of hypoxic cell radiosensitization. *Int J Radiat Oncol Biol Phys* **20**: 147-152.

Dizdaroglu, M. and P. Jaruga (2012). Mechanisms of free radical-induced damage to DNA. *Free Radic. Res.* **46**: 382-419.

Dizdaroglu, M. and M. G. Simic (1984). Radiation-induced crosslinking of cytosine. *Radiat Chem* **100**(1): 41-46.

Dizdaroglu, M. and C. V. Sonntag (1975). Strand breaks and sugar release by gamma-radiation of DNA in aqueous solution. *J Am Chem Soc* **97**: 2277-2278.

Dobrowsky, W., N. G. Huigol, R. S. Jayatilake, N. I. Kizilbash, S. Okkan, V. T. Kagiya and H. Tatsuzaki (2007). AK-2123 (Sanazol) as a radiation sensitizer in the treatment of stage III cervical cancer: Results of an IAEA multicentre randomised trial. *Radiother Oncol* **82**: 24-29.

Dourado, M., A. B. Sarmento, S. V. Pereira, V. Alves, T. Silva, A. M. Pinto and M. S. Rosa (2007). CD26/DPPIV expression and 8-azaguanine response in T-acute lymphoblastic leukaemia cell lines in culture. *Pathophysiology* **14**: 3-10.

Duda, D. G., D. Fukumura and R. K. Jain (2004). Role of eNOS in neovascularization:NO for endothelial progenitor cells. *Trends in Molecular Medicine* **14**: 143-145.

Dunford, H. B. (1999). Heme Peroxidases. New York, Wiley-VCH.

Durand, R. E. and P. L. Olive (1981). Evaluation of nitroheterocyclic radiosensitizers using spheroids. *Adv Radiat Biol* **9**: 75-107.

Eccles, L. J., P. O'Neill and M. E. Lomax (2011). Delayed repair of radiation induced clustered DNA damage: friend or foe? *Mutation Res.* **711**: 134-141.

Eiserich, J. P., J. Butler, A. Van der Vliet, C. E. Cross and B. Halliwell (1995). Nitric oxide rapidly scavenges tyrosine and tryptophan radicals. *Biochem J* **310**: 745-749.

Eiserich, J. P., C. E. Cross, A. D. Jones, B. Halliwell and A. van der Vliet (1996). Formation of nitrating and chlorinating species by reaction of nitrite with hypochlorous acid. *J Biol Chem* **271**: 19199-19208.

Ekmekcioglu, S., J. A. Ellerhorst, V. G. Prieto, M. M. Johnson, L. D. Broemeling and E. A. Grimm (2006). Tumor iNOS predicts poor survival for stage III melanoma patients. *Int J Cancer* **119**: 861-866.

Elford, H. L., G. L. Wampler and B. v. t. Riet (1979). New ribonucleotide reductase inhibitors with antineoplastic activity. *Cancer Res* **39**: 844-851.

Everett, S. A., M. A. Naylor, K. B. Patel, M. R. L. Stratford and P. Wardman (1999). Bioreductively-activated prodrugs for targeting hypoxic tissues: elimination of aspirin from 2-nitroimidazole derivatives. *Bioorg Med Chem Letts* **9**: 1267-1272.

Everett, S. A., E. Swann, M. A. Naylor, M. R. L. Stratford, K. B. Patel, N. Tian, R. G. Newman, B. Vojnovic, C. J. Moody and P. Wardman (2002). Modifying rates of reductive elimination of leaving groups from indolequinone prodrugs: a key factor in controlling hypoxia-selective drug release. *Biochem Pharmacol* **63**: 1629-1639.

Faraggi, M., F. Broitman, J. B. Trent and M. H. Klapper (1996). One-electron oxidation reactions of some purine and pyrimidine bases in aqueous solutions. Electrochemical and pulse radiolysis studies. *J Phys Chem* **100**: 14751-14761.

FitzGerald, J. E., M. Grenon and N. F. Lowndes (2009). 53BP1: function and mechansims of focal recruitment. *Biochem. Soc. Trans.* **37**: 897-904.

Folkes, L. K., S. Bartesaghi, M. Trujillo, R. Radi and P. Wardman (2012). Kinetics of oxidation of tyrosine by a model alkoxyl radical. *Free Radic. Res.* **46**: 1150-1156.

Folkes, L. K., L. P. Candeias and P. Wardman (1995). Kinetics and mechanisms of hypochlorous acid. *Arch Biochem Biophys* **323**: 120-126.

Folkes, L. K., M. Trujillo, S. Bartesaghi, R. Radi and P. Wardman (2011). Kinetics of reduction of tyrosine phenoxyl radicals by glutathione. *Arch Biochem Biophys* **506**: 242-249.

Folkes, L. K. and P. Wardman (2004). Kinetics of the reaction between nitric oxide and glutathione: implications for thiol depletion in cells. *Free Radic Biol Med* **37**: 549-556.

Folkes, L.K. and P. O'Neill (2013a). Modification of DNA damage mechanisms by nitric oxide during ionizing radiation. *Free Radic Biol Chem* **58**:14-25.

Folkes, L.K. and P. O'Neill (2013b). DNA damage induced by nitric oxide during ionizing radiation is enhanced at replication. *Nitric Oxide* **34**: 47-55.

Fontecave, M. (1998). Ribonucleotide reductases and radical reactions. *CMLS Cellular and Molecular Sciences* **54**: 684-695.

Frérart, F., P. Sonveaux, G. Rath, A. Smoos, A. Meqor, N. Charlier, B. F. Jordan, J. Saliez, A. Noël, C. Dessy, B. Gallez and O. Feron (2008). The acidic tumor microenvironment promotes the reconversion of nitrite into nitric oxide: towards a new and safe radiosensitizing strategy *Clin Cancer Res* **14**: 2768-2774.

Fuciarelli, A. F., B. J. Wegher, W. F. Blakely and M. Dizdaroglu (1990). Yields of radiation-induced base products in DNA: effects of DNA confirmation and gassing conditions. *Int J Radiat Biol* **58**: 397-415.

Fukumura, D., S. Kashiwagi and R. K. Jain (2006). The role of nitric oxide in tumour progression. *Nat Rev Cancer* **6**: 521-534.

Fulford, J., H. Nikjoo, D. T. Goodhead and P. O'Neill (2001). Yields of SSB and DSB induced in DNA by Al_k ultrasoft X-rays and α-particles: comparison of experimental and simulated yields. *Int J Radiat Biol* **77**: 1053-1066.

Gajewski, E., G. Rao, Z. Nackerdien and M. Dizdaroglu (1990). Modification of DNA bases in mammalian chromatin by radiation-generated free radicals. *Biochemistry* **29**: 7876-7882.

Gerasimov, O. V. and S. V. Lymar (1999). The yield of hydroxyl radical from the decomposition of peroxynitrous acid. *Inorg Chem* **38**: 4317-4321.

Getoff, N. (1992). Pulse radiolysis of amino acids-state of the art. *Amino acids* **2**: 195-214.

Gladwin, M. T., J. H. Shelhamer, F. P. Ognibene, M. E. Pease-Fye, J. S. Nichols, B. Link, D. B. Patel, M. A. Jankowski, L. K. Pannell, A. N. Schechter and G. P. Rodgers (2002). Nitric oxide donor properties of hydroxyurea in patients with sickle cell disease. *Br. J. Haematol.* **116**: 436-444.

Glover, R. E., V. Koshkin, H. B. Dunford and R. P. Mason (1999). The reaction rates of NO with horseradish peroxidase compounds I and II. *Nitric Oxide* **3**: 439-444.

Glynn, S. A., B. J. Boersma, T. H. Dorsey, M. Yi, H. G. Yfantis, L. A. Ridnour, D. N. Martin, C. H. Switzer, R. S. Hudson, D. A. Wink, D. H. Lee, R. M. Stephens and S. Ambs (2010). Increased NOS2 predicts poor survival in estrogen receptor-negative breast cancer patients *J Clin Invest* **120**: 3843-3854.

Goldstein, S. and G. Czapski (1996). Formation of peroxynitrite from the oxidation of hydrogen peroxide by nitrosonium ion (NO+): a pulse radiolysis study. *Inorg. Chem.* **35**: 7735-7740.

Goldstein, S., G. Czapski, J. Lind and G. Merényi (2000). Tyrosine nitration by simultaneous generation of $^{\bullet}NO$ and $O_2^{\bullet-}$ under physiological conditions. *J Biol Chem* **275**: 3031-3036.

Goldstein, S., G. Czapski, J. Lind and G. Merényi (2001). Carbonate radical ion is the only observable intermediate in the reaction of peroxynitrite with CO_2. *Chem Res Toxicol* **14**: 1273-1276.

Goodarzi, A. A., A. T. Noon, D. Deckbar, Y. Ziv, Y. Shiloh, M. Löbrich and P. A. Jeggo (2008). ATM signaling facilitates repair of DNA double-strand breaks associated with heterochromatin. *Mol. Cell* **31**: 167-177.

Goodhead, D. T. (1994). Initial events in the cellular effects of ionizing radiations: clustered damage in DNA. *Int J Radiat Biol* **65**: 7-17.

Graeber, T. G., C Osmanian, T. Jacks, D. E. Housman, C. J. Koch, S. W. Lowe and A. J. Giaccia (1996). Hypoxia-mediated selection of cells with diminished apoptopic potential in solid tumours. *Nature* **379**: 88-91.

Gray, L. H., A. D. Conger, M. Ebert, S. Hornsey and O. C. A. Scott (1953). The concentration of oxygen dissolved in tissues at the time of irradiation as a factor in radiotherapy. *Br J Radiol* **26**: 638-648.

Gray, L. H., F. O. Green and C. A. Hawes (1958). Effect of nitric oxide on the radiosensitivity of tumour cells. *Nature (London)* **182**: 952-953.

Groth, P., M. L. Orta, I. Elvers, M. M. Majumber, A. Lagerqvist and T. Helleday (2012). Homologous recombination repairs secondary replication induced DNA double-strand breaks after ionizing radiation. *Nucleic Acids Res* **40**: 6585-6594.

Gulston, M., J. Fulford, T. Jenner, C. d. Lara and P. O'Neill (2002). Clustered DNA damage induced by γ-radiation in human fibroblasts (HF19), hamster (V79-4) cells and plasmid DNA is revealed as Fpg and Nth sensitive sites. *Nucleic Acids Res* **30**: 3464-3472.

Gulston, M. J., C. deLara, T. Jenner, E. Davis, P. O'Neill (2004). Processing of clustered DNA damage generates additional double-strand breaks in mammalian cells post-irradiation. *Nucleic Acids. Res* **32**:1602-1609.

Gunther, M. R., L. C. Hsi, J. F. Curtis, J. K. Gierse, L. J. Marnett, T. E. Eling and R. P. Mason (1997). Nitric oxide trapping of the tyrosyl radical of prostaglandin H synthase-2 leads to tyrosine iminoxyl radical and nitrotyrosine formation. *J Biol Chem* **272**: 17086-17090.

Hall, C. N. and J. Garthwaite (2009). What is the real physiological NO concentration *in vivo*? *Nitric Oxide* **21**: 92-103.

Hall, E. J. (2000). Radiobiology for the Radiologist. Philadelphia, Lippincott Williams & Wilkins.

Hanot, M., A. Boivin, C. Malésys, M. Beuve, A. Colliaux, M. Foray, T. Douki, D. Ardail and C. Rodriguez-Lafrasse (2012). Glutathione depletion and carbon ion radiation potentiate clustered DNA lesions, cell death and prevent chromosomal changes in cancer cells progeny. *PLoS ONE* **7**(11): e44367.

Harding, S. M. and R. G. Bristow (2012). Discordance between phosphorylation and recruitment of 53BP1 in response to DNA double-strand breaks. *Cell Cycle* **11**: 1432-1444.

Harper, J. V., J. A. Anderson and P. O'Neill (2010). Radiation induced DNA DSBs: contribution from stalled replication forks? *DNA Repair* **9**: 907-913.

Harris, A. L. (2002). Hypoxia – a key regulatory factor in tumour growth. *Nat Rev Cancer* **2**: 38-47.

Harrison, L. and K. Blackwell (2004). Hypoxia and anemia: factors in decreased sensitivity to radiation therapy and chemotherapy? *The Oncologist* **9(suppl 5)**: 31-40.

Harrison, L. B., M. Chadha, R. J. Hill, K. Hu and D. Shasha (2002). Impact of tumor hypoxia and anemia on radiation therapy outcomes. *The Oncologist* **7**: 492-508.

Hayon, E. and M. Simic (1973). Addition of hydroxyl radicals to pyrimidine bases and electron transfer reactions of intermediates to quinones. *J Am Chem Soc* **95**: 1029-1035.

He, B., H. Qing and Y. W. Kow (2000). Deoxyxanthosine in DNA is repaired by *Escherichia coli* endonuclease V. *Mutation Res.* **459**: 109-114.
Heldin, C.-H., K. Rubin, K. Pietras and A. Ostman (2004). High interstitial pressure - an obstacle in cancer therapy. *Nat. Rev. Cancer* **4**: 806-813.
Helleday, T. (2003). Pathways for mitotic homogous recombination in mammalian cells. *Mutation Res.* **532**: 103-115.
Hems, G. (1958). Effect of ionizing radiation on aqueous solutions of guanylic acid and guanosine. *Nature* **181**: 1721-1722.
Hicks, M. and J. M. Gebicki (1986). Rate constants for reaction of hydroxyl radicals with Tris, Tricine and Hepes buffers. *FEBS Letts* **199**: 92-94.
Hodges, G. R. and K. U. Ingold (1999). Cage-escape of geminate radicals pairs can produce peroxynitrate from peroxynitrite under a wide variety of experimental conditions. *J Am Chem Soc* **121**: 10695-10701.
Hodgkins, P. S., M. P. Fairman and P. O'Neill (1996). Rejoining of gamma-radiation-induced single-strand breaks in plasmid DNA by human cell extracts: dependence on the concentration of the hydroxy radical scavenger,Tris. *Radiat Res* **145**: 24-30.
Howard-Flanders, P. (1957). Effect of nitric oxide on the radiosensitivity of bacteria. *Nature (London)* **180**: 1191-1192.
Huang, J., D. B. Kim-Shapiro and S. B. King (2004). Catalase-mediated nitric oxide formation from hydroxyurea. *J. Med. Chem.* **47**: 3495-3501.
Huang, J., E. M. Sommers, D. B. Kim-Shapiro and S. B. King (2002). Horseradish peroxidase catalyzed nitric oxide formation from hydroxyurea. *J Am Chem Soc* **124** (3473-3480).
Hughes, M. N. (1999). Relationships between nitric oxide, nitroxyl ion, nitrosonium cation and peroxynitrite. *Biochim Biophys Acta* **1411**: 263-272.
Hummel, S. G., A. J. Fischer, S. M. Martin, F. Q. Schafer and G. R. Buettner (2005). Nitric oxide as a cellular antioxidant: a little goes a long way. *Free Radic Biol Med* **40**: 501-506.
Hunter, E. P. L., M. F. Desrosiers and M. G. Simic (1989). The effect of oxygen, antioxidants and superoxide radical on tyrosine phenoxyl radical dimerization. *Free Radic Biol. Med.* **6**: 581-585.
Idriss Ali, K. M. (1979). Formation of dimers in the gamma radiolysis of aqueous solutions of pyrimidines and N_2O. *J Radiat Res* **20**: 84-94.
Idriss Ali, K. M. and G. Scholes (1979). Radiolysis products analysis of aqueous thymine and N_2O solutions. *J. Radiat. Res* **20**: 146-156.
Ignarro, L. J., Ed. (2000). Nitric Oxide. Biology and Pathobiology. San Diego, Academic Press.
Ishibashi, T., M. Himeno, N. Imaizumi, K. Maejima, S. Nakano, K. Uchida, J. Yoshida and M. Nishio (2000). NOx contamination in laboratory ware and effect of countermeasures. *Nitric oxide* **4**(5): 516-525.
Jain, R. K. (1994). Barriers to drug delivery in solid tumors. *Scientific American* **271**: 58-65.
Janssens, M. Y., V. N. Verovski, D. L. V. d. Berge, C. Monsaert and G. A. Storme (1999). Radiosensitization of hypoxic tumour cells by S-nitroso-N-acetylpenicillamine implicates a bioreductive mechanism of nitric oxide generation. *Br J Cancer* **79**: 1085-1089.
Janzen, E. G., A. L. Wilcox and V. Manoharan (1993). Reactions of nitric oxide with phenolic antioxidants and phenoxyl radicals. *J Org Chem* **58**: 3597-3599.
Jarry, A., L. Charrier, C. Bou-Hanna, M.-C. Devilder, V. Crussaire, M. G. Denis, G. Vallette and C. L. Laboisse (2004). Position in cell cycle controls the sensitivity of colon cancer cells to nitric oxide-dependent programmed cell death. *Cancer Res* **64**: 4227-4234.
Jeggo, P. A., V. Geuting and M. Löbrich (2011). The role of homologous recombination in radiation-induced double-strand break repair. *Radiother Oncol* **101**: 7-12.

Jenner, T. J., C. M. deLara, P. O'Neill and D. L. Stevens (1993). Induction and rejoining of DNA double-strand breaks in V79-4 mammalian cells following gamma- and alpha-irradiation. *Intl J Radiat Biol* **64**: 265-273.

Jiang, H., M. D. Ridder, V. N. Verovski, P. Sonveaux, B. F. Jordan, K. Law, C. Monsaert, D. L. V. d. Berge, D. Verellen, O. Feron, B. Gallez and G. A. Storme (2010). Activated macrophages as a novel determinant of tumor cell radioresponse: the role of nitric oxide-mediated inhibition of cellular respiration and oxygen sparing. *Int J Oncol Biol Phys* **76**: 1520-1527.

Jin, F., J. Leitich and C. von Sonntag (1993). The superoxide radical reacts with tyrosine-derived phenoxyl radicals by addition rather than by electron transfer. *Journal of the Chemical Society, Perkin Transactions 2* **1583-1588**.

Joffe, A., S. Mock, B. H. Yun, A. Kolbanovskiy, N. E. Geacintov and V. Shafirovich (2003). Oxidative generation of guanine radicals by carbonate radicals and their reactions with nitrogen dioxide to form site specific 5-guanidino-4-nitroimidazole lesions in oligodeoxynucleotides. *Chem Res Toxicol* **16**: 966-973.

Jones, G. D. D. and P. O'Neill (1990). The kinetics of radiation-induced strand breakage in polynucleotides in the presence of oxygen: a time-resolved light-scattering study. *Int J Radiat Biol* **6**: 1123-1139.

Jones, G. D. D. and P. O'Neill (1991). Kinetics of radiation-induced strand break formation in single-stranded pyrimidine polynucleotides in the presence and absence of oxygen: a time-resolved light-scattering study. *Int J Radiat Biol* **59**: 1127-1145.

Jones, G. D. D. and M. Weinfeld (1996). Dual action of tirapazamine in the induction of DNA strand breaks. *Cancer Res* **56**: 1584-1590.

Jones, R. M. and E. Petermann (2012). Replication fork dynamics and the DNA damage response *Biochem J* **443**: 13-26.

Jordan, B. F., N. Beghein, M. Aubry, V. Grégoire and B. Gallez (2003). Potentiation of radiation-induced regrowth delay by isosorbide dinitrate in FSAII murine tumors. *Int J Cancer* **103**: 138-141.

Jordan, B. F., V. Grégoire, R. J. Demeure, P. Sonveaux, O. feron, J. O'Hara, V. P. Vanhulle, N. Delzenne and B. Gallez (2002). Insulin increases the sensitivity of tumors to irradiation: involvement of an increase in tumor oxygenation mediated by a nitric oxide-dependent decrease of the tumor cells oxygen consumption. *Cancer Res* **62**: 3555-3561.

Jordan, B. F. and P. Sonveaux (2012). Targeting tumor perfusion and oxygenation to improve the outcome of anticancer therapy. *Frontiers Pharmacol.* **3**(94): 1-15.

Jordan, B. F., P. Sonveaux, O. Feron, V. Grégoire, N. Beghein, C. Dessy and B. Gallez (2004). Nitric oxide as a radiosensitizer: evidence for an intrinsic role in addition to its effect on oxygen delivery and consumption. *Int J Cancer* **109**: 768-773.

Kaanders, J. H., I. W. K, H. A. Marres, A. S. Ljunkvist, L. A. Pop, F. J. v. d. Hoogen, P. C. d. Wilde, J. Bussink, J. A. Raleigh and A. J. v. d. Kogel (2002). Pimonidazole binding and tumour vascularity predict for treatment outcome in head and neck cancer. *Cancer Res* **62**: 7066-7074.

Kaanders, J. H., L. A. Pop, H. A. Marres, I. Bruaset, F. J. v. d. Hoogen, M. A. Merkx and A. J. v. d. Kogel (2002). ARCON: experience in 215 patients with advanced head-and-neck cancer. *Int. J. Radiat Oncol Biol Phys* **52**: 759-778.

Kaiya, T., K. Nakamura, M. Tanaka, N. Miyata and K. Kohda (2004). Product analyses of ozone mediated nitration of benzimidazole derivatives with nitrogen dioxide: formation of 1-nitrobenzimidazoles and conversion to benzotriazoles. *Chem. Pharm. Bull.* **52**: 570-576.

Kasai, H. and S. Nishimura (1984). Hydroxylation of deoxyguanosine at the C-8 position by ascorbic acid and other reducing agents. *Nucleic Acids Res* **12**: 2137-2145.

Keefer, L. K., D. Christodoulos, T. M. Dunams, J. A. Hrabie, C. M. Maragos, J. E. Saavedra and D. A. Wink (1994). Chemistry of the "NONOates": Unusual *N*-nitroso compounds formed by reacting nitric oxide with nucleophiles. Nitrosamines and Related *N*-nitroso Compounds. Chemistry and Biochemistry. R. N. Loeppky and C. J. Michejda. Washington, American Chemical Society**:** 136-146.

Keefer, L. K., R. Nims, K. Davies and D. Wink (1996). "NONOates" (1-substituted diazen-1-ium-1,2-diolates) as nitric oxide donors: convenient nitric oxide dosage forms. Methods Enzymol. P. L, Academic press. **268:** 281-293.

Keefer, L. K. and D. A. Wink (1996). DNA Damage and Nitric Oxide. Biological Reactive Intermediates. V. Basic Mechanistic Research in Toxicology and Human Risk Assessment (Advances in Experimental Medicine and Biology, vol. 387). R. Snyder, J. J. Kocsis, I. G. Sipeset al. New York, Plenum Press**:** 177-185.

Kent, C. R. H., J. J. Eady, G. M. Ross and G. G. Steel (1995). The comet moment as a measure of DNA damage in the comet assay. *Int. J. Radiat. Biol*. **67**:655-660.

Kidder, G. W., V. C. Dewey, R. E. Parks and G. L. Woodside (1951). Further evidence on the mode of action of 8-azaguanine (Guanazolo) in tumour inhibition. *Cancer Res* **11**: 204-211.

Kim, J. J. and I. F. Tannock (2005). Repopulation of cancer cells during therapy: an important cause of treatment failure. *Nat. Rev. Cancer* **5**: 516-525.

King, S. B. (2004). Nitric oxide production from hydroxyurea. *Free Radic. Biol. Med.* **37**: 737-744.

Kizlitepe, T., T. Hideshima, K. Ishitsuka, E. M. Ocio, N. Raje, L. Catley, C.-Q. Li, L. J. Trudel, H. Yasui, S. Vallet, J. L. Kutok, D. Chauhan, C. S. Mitsiades, J. E. Saavedra, G. N. Wogan, L. K. Keefer, P. J. Shami and K. C. Anderson (2007). JS-K, a GST-activated nitric oxide generator, induces DNA double-strand breaks, activates DNA damage response pathways, and induces apoptosis in vitro and in vivo in human multiple myeloma cells. *Blood* **110**: 709-718.

Kjellen, E., M. C. Joiner, J. M. Collier, H. Johns and A. Rojas (1991). A therapeutic benefit from combining normobaric carbogen or oxygen with nicotinamide in fractionated X-ray treatments. *Radiother Oncol* **22**: 81-91.

Koch, C. J. and R. B. Painter (1975). The effect of extreme hypoxia on the repair of DNA single-strand breaks in mammalian cells. *Radiat Res* **64**: 256-269.

Kolker, P. L. and W. A. Waters (1964). The radical-anions of para-substituted aromatic nitro-compounds. *J Chem Soc*: 1136-1141.

Kondakova, I. V., V. V. Tcheredova, G. V. Zagrebelnaya, N. V. Cherdyntseva, T. V. Kagiya and E. L. Choinzonov (2004). Production of nitric oxide by hypoxic radiosensitizer sanazole. *Exp. Oncol.* **26**: 331-333.

Koppenol, W. H. (1998). The basic chemistry of nitrogen monoxide and peroxynitrite. *Free Radic Biol Med* **25**: 385-391.

Kumareswaran, R., O. Ludkovski, A. Meng, J. Sykes, M. Pintilie and R. G. Bristow (2012). Chronic hypoxia compromises repair of DNA double strand breaks to drive genetic instability. *J. Cell Sci* **125**: 1-11.

Kwon, N. S., D. J. Stuehr and C. F. Nathan (1991). Inhibition of tumor cell ribonucleotide reductase by macrophage-derived nitric oxide. *J Exp Med* **174**: 761-767.

Lambert, J. M. (2013). Drug-conjugated antibodies for the treatment of cancer. *Br. J. Clin. Pharmacol.***76**:248-262.

Land, E. J. and M. Ebert (1967). Pulse radiolysis studies of aqueous phenol. *Trans Faraday Soc* **63**: 1181-1190.

Lassmann, G. and B.Liebermann (1989). ESR studies of structure and kinetics or radicals from hydroxyurea. *Free Radic. Biol. Med.* **6**: 241-244.

Lavin, M. F. (2004). The MRE11 complex and ATM: a two-way fuctional interaction in recognising and signaling DNA double strand breaks. *DNA Repair (Amst)* **3**: 1515-1520.

Leatherbarrow, E. L., J. V. Harper, F. A. Cucinotta and P. O'Neill (2006). Induction and quantification of γH2AX foci following low and high LET-irradiation. *Int J Radiat Biol* **82**: 111-118.

Lee, H., H.-J. Kwak, I.-T. Cho, S. H. Park and C.-H. Lee (2009). S1219 residue of 53BP1 is phosphorylated by ATM kinase upon DNA damage and required for proper execution of DNA damage response. *Biochem Biophys Res Commun* **378**: 32-36.

Lehnig, M. (1999). Radical mechansims of the decomposition of peroxynitrite and the peroxynitrite-CO_2 adduct and of reactions with L-tyrosine and related compounds as studied by (15)N chemically induced dynamic nuclear polarization. *Arch Biochem Biophys* **368**: 303-318.

Lepoivre, M., J.-M. Flamand and Y. Henry (1992). Early loss of the tyrosyl radical in ribonucleotide reductase of adenocarcinoma cells producing nitric oxide. *J Biol Chem* **267**: 22994-23000.

Li, F., P. Sonveaux, Z. N. Rabbani, S. Lui, B. Yan, Q. Huang, Z. Vujaskovic, M. W. Dewhirst and C. Y. Li (2007). Regulation of HIF-1α stability through S-nitrosolation. *Mollecular Cell* **26**: 63-74.

Lim, M. H. and S. J. Lippard (2006). Fluorescent nitric oxide detection by copper complexes bearing anthracenyl and dansyl fluorophore ligands. *J Inorg Chem* **45**: 8980-8989.

Lobrich, M., A. Shibata, A. Beucher, A. Fisher, M. Ensminger, A. A. Goodarzi, O. Barton and P. A. Jeggo (2010). Gamma H2AX foci analysis for monitoring DNA double-strand break repair: strengths, limitations and optimization. *Cell Cycle* **9**: 662-669.

Long, C. A. and B. H. J. Bielski (1980). Rate of reaction of superoxide radical with chloride-containing species. *J Phys Chem* **84**: 555-557.

Lucas, L. T., D. Gatehouse, G. D. D. Jones and D. E. G. Shuker (2001). Characterization of DNA damage at purine residues in oligonucleotides and calf thymus DNA induced by the mutagen 1-nitroso-3-acetonitrile. *Chem Res Toxicol* **14**: 158-164.

Lymar, S. V. and J. K. Hurst (1998). CO_2-catalyzed one-electron oxidations by peroxynitrite: properties of the reactive intermediate. *Inorg Chem* **37**: 294-301.

Madej, E., L. K. Folkes, P. Wardman, G. Czapski and S. Goldstein (2008). Thiyl radicals react with nitric oxide to form S-nitrosothiols with rate constants near the diffusion-controlled limit. *Free Radic Biol Med* **44**: 2013-2018.

Makings, L. R. and R. Y. Tsien (1994). Caged nitric oxide. *J Biol Chem* **269**: 6282-6285.

Maloney, D. G., A. J. Grillo-Lo´pez, C. A. White, D. Bodkin, R. J. Schilder, J. A. Neidhart, N. Janakiraman, K. A. Foon, T.-M. Liles, B. K. Dallaire, K. Wey, I. Royston, T. Davis and R. Levy (1997). IDEC-C2B8 (Rituximab) anti-CD20 monoclonal antibody therapy in patients with relapsed low-grade Non-Hodgkin's Lymphoma. *Blood* **90**: 2188-2195.

Maragos, C. M., D. Morley, D. A. Wink, T. M. Dunams, J. E. Saavedra, A. Hoffman, A. A. Bove, L. Isaac, J. A. Hrabie and L. K. Keefer (1991). Complexes of NO with nucleophiles as agents for the controlled biological release of nitric oxide. Vasorelaxant effects. *J. Med. Chem.* **34**: 3242.

Marková, E., N. Schulz and I. Y. Belyaev (2007). Kinetics and dose-response of residual 53BP1/γ -H2AX foci: co-localization, relationship with DSB repair and clonogenic survival. *Int J Radiat Biol* **83**: 319-329.

Maskos, Z., J. D. Rush and W. H. Koppenol (1993). The hydroxylation of the salicylate anion by a Fenton reaction and gamma-radiolysis: a consideration of the respective mechanisms *Free Radic. Biol. Med.* **8**: 153-162.

Mason, R. P. and J. L. Holtzman (1975). The role of catalytic superoxide formation in the O_2 inhibition of nitroreductase. *Biochem Biophys Res Comm* **67**: 1267-1274.

Metzen, E., J. Zhou, W. Jelkmann, J. Fandrey and B. Brune (2003). Nitric Oxide Impairs Normoxic Degradation of HIF-1 alpha by Inhibition of Prolyl Hydroxylases. *Mol. Biol. Cell* **14**.

Miaskiewicz, K. and R. Osman (1994). Theoretical study on the deoxyribose radicals formed by hydrogen abstraction. *J Am Chem Soc* **116**: 232-238.

Michaels, H. B. and J. W. Hunt (1973). Reactions of the hydroxyl radical with polynucleotides. *Radiat Res* **56**: 57-70.

Mitchell, J. B., J. A. Cook, M. C. Krishna, W. DeGraff, J. Gamson, F. Fisher, D. Christodoulou and D. A. Wink (1996). Radiation sensitisation by nitric oxide releasing agents. *Br J Cancer* **74 (Suppl. XXVII)**: S181-S184.

Mitchell, J. B., D. A. Wink, W. DeGraff, J. Gamson, L. K. Keefer and M. C. Krishna (1993). Hypoxic mammalian cell radiosensitization by nitric oxide. *Cancer Res* **53**: 5845-5848.

Mladenov, E. and G. Iliakis (2011). Induction and repair of DNA double strand breaks: the increasing spectrum of non-homologous end joining pathways. *Mutation Res.* **711**: 61-72.

Möller, M. N., D. M. Hatch, H.-Y. H. Kim and N. A. Porter (2012). Superoxide reaction with tyrosyl radicals generates para-hydroperoxyl and para-hydroxy derivatives of tyrosine. *J Am Chem Soc* **134**: 16773-16780.

Moore, E. G. and Q. H. Gibson (1976). Cooperativity in the dissociation of nitric oxide from heamoglobin. *J Biol Chem* **271**: 2788-2794.

Munro, A. W., M. A. Noble, L. Robledo, S. N. Daff and S. K. Chapman (2001). Determination of the redox properties of human NADPH-cytochrome P450 reductase. *Biochemistry* **40**: 1956-1963.

Mvula, E., M. N. Schuchmann and C. V. Sonntag (2001). Reactions of phenol-OH-adduct radicals. Phenoxyl radical formation by water elimination vs. oxidation by dioxygen. *J Chem Soc, Perkin Trans 2*: 264-268.

Naumov, h. and C. von Sonntag (2008). Guanine-derived radicals: dielectric constant-dependent stability and UV/Vis spectral properties: A DFT study. *Radiat Res* **169**: 364-372.

Navarra, P. and P. Preziosi (1999). Hydroxyurea: new insights into an old drug. *Crit. Rev. Oncol. Hematol.* **29**: 249-255.

Naylor, M. A., B. M. Sutton, J. Nolan, P. O'Neill, E. M. Fielden, G. E. Adams and I. J. Stratford (1994). Radiolytic and photochemical reduction of the hypoxic cytotoxin 1,2-dihydro-8-(4-methylpiperazinyl)-4-phenylimidazo[1,2-α] pyrido [3,2-*e*] pyrazine 5-oxide (RB90740) and a potential mechanism for hypoxia-selective toxicity. *Int J Radiat Oncol BiolPhys* **29**: 333-337.

Nelson, D. P. and L. A. Kiesow (1972). Enthalpy of decomposition of hydrogen peroxide by catalase at 25 °C (with molar extinction coefficients of H_20_2 solutions in the UV). *Anal. Biochem.* **49**: 474-478.

Ng, Q.-S., V. Goh, J. Milner, M. R. Stratford, L. K. Folkes, G. M. Tozer, M. L. Saunders and P. J. Hoskin (2007). Effect of nitric-oxide synthesis on tumour blood volume and vascular activity: a phase I study. *The Lancet* **8**: 111-118.

Nguyen, T., D. Brunson, C. L. Crespi, B. W. Penman, J. S. Wishnok and S. R. Tannenbaum (1992). DNA damage and mutation in human cells exposed to nitric oxide *in vitro*. *Proc Nat. Acad Sc. USA* **89**: 3030-3034.

Nikjoo, H., S. Uehara, W. E. Wilson, M. Hoshi and D. T. Goodhead (1998). Track structure in radiation biology: theory and applications. *Int J Radiat Biol* **73**: 355-364.

Ning, S., M. Bednaarski, B. Oronsky, J. Scicinski, G. Saul and S. J. Knox (2012). Dinitroazetidines are a novel class of anticancer agents and hypoxia-activated radiation sensitizers developed from highly energetic materials. *Cancer Res* **72**: 2600-2608.

Nordsmark, M., S. M. Bentzen, V. Rudat, D. Brizel, E. Lartigau, P. Stadler, A. Becker, M. Adam, M. Molls, J. Dunst, D. J. Terris and J. Overgaard (2005). Prognostic value of tumor oxygenation in 397 head and neck tumors after primary radiation therapy. An international multi-center study. *Radiother Oncol* **77**(1): 18-24.

Nouspikel, T. (2009). Nucleotide excision repair: variations on versatility. *Cell Mol. Life Sci.* **66**: 994-1009.

O'Neill, P., P. W. Chapman and D. G. Papworth (1985). Repair of hydroxyl radical damage of dA by antioxidants. *Life Sci. Rep.* **3**: 62-69.

O'Neill, P. (1983). Pulse radiolytic study of the interaction of thiols and ascorbate with OH adducts of dGMP and dG: implications for DNA repair processes. *Radiat Res* **96**: 198-210.

O'Neill, P. and P. W. Chapman (1985). Potential repair of free radical adducts of dGMP and dG by a series of reductants. A pulse radiolytic study. *Int J Radiat Biol* **47**: 71-80.

Olive, P. L. (1979). Correlation between metabolic reduction rates and electron affinity of nitroheterocycles. *Cancer Res* **39**: 4512-4515.

Oronsky, B. T., S. J. Knox and J. Scicinski (2011). Six degrees of separation: the oxygen effect in the development of radiosensitizers. *Trans Onc* **4**: 189-198.

Oronsky, B. T., S. J. Knox and J. J. Scicinski (2012). Is nitric oxide (NO) the last word in radiosensitization? A review. *Trans Onc* **5**: 66-71.

Overgaard, J., J. G. Eriksen, M. Nordsmark, J. Alsner, M. R. Horsman and D. H. a. N. C. S. Group (2005). Plasma osteopontin, hypoxia, and response to the hypoxia sensitiser nimorazole in radiotherapy of head and neck cancer: results from the DAHANCA 5 randomised double-blind placebo-controlled trial. *Lancet Oncol* **6**: 757-764.

Pagano, M., R. Pepperkok, F. Verde, W. Ansorge and G. Draetta (1992). Cyclin A is required at two points in the human cell cycle. *EMBO Journal* **11**: 961-971.

Palmer, R. M. J., A. G. Ferrige and S. Moncada (1987). Nitric oxide release accounts for the biological activity of endothelium-derived relaxing factor. *Nature (London)* **327**: 524-526.

Patterson, D. M., M. Zweifel, M. R. Middleton, P. M. Price, L. K. Folkes, M. R. L. Stratford, P. Ross, S. Halford, J. Peters, J. Balkissoon, D. J. Chaplin, A. R. Padhani and G. J. S. Rustin (2012). Phase 1 clinical and pharmacokinetic evaluation of the vascular-disrupting agent OXi4503 in patients with advanced solid tumours. *Clin Cancer Res* **18**: 1415-1425.

Peddi, P., D. C. Francisco, A. M. Cecil, J. M. Hair, M. I. Panayiotidis and A. G. Georgakilas (2008). Processing of clustered DNA damage in human breast cancer cells MCF-7 with partial DNA-PKcs deficiency. *Cancer Lett.* **269**: 174-183.

Phadatare, S. D., K. K. K. Sharma, B. S. M. Rao, S. Naumov and G. K. Sharma (2011). Spectral characterization of guanine C4-OH adduct: A radiation and quantum chemical study. *J Phys Chem B* **115**: 13650–13658.

Pires, I. M., Z. Bencokova, M. Milani, L. K. Folkes, J.-L. Lang, M. R. L. Stratford, A. L. Harris and E. M. Hammond (2010). Effects of acute versus chronic hypoxia on DNA damage responses and genomic instability. *Cancer Res* **70**: 925-935.

Portess, D. I., G. Bauer, M. A. Hill and P. O'Neill (2007). Low-dose irradiation of nontransformed cells stimulates the selective removal of precancerous cells via intercellular induction of apoptosis. *Cancer Res* **67**: 1246-1253.

Pouget, J.-P., S. Frelon, L.-L. Ravanat, I. Testard, F. Odin and J. Cadet (2002). Formation of modified DNA bases in cells exposed either to gamma radiation or to high-LET particles. *Radiat Res* **157**: 589-595.

Prütz, W. A., H. Monig, J. Butler and E. Land (1985). Reactions of nitrogen dioxide in aqueous model systems:oxidation of tyrosine units in peptides and proteins. *Arch Biochem Biophys* **243**(1): 125-134.

Radi, R. (2004). Nitric oxide, oxidants, and protein tyrosine nitration. *Proc Natl Acad Sci USA* **101**: 4003-4008.

Rafi, A. A. and C. M. Wheeler (1973). On the radiation-induced hyperchromicity of DNA. *Int J Radiat Biol* **24**(3): 321-323.

Raleigh, J. A. and C. J. Koch (1990). Importance of thiols in the reductive binding of 2-nitroimidazoles to macromolecules. *Bioche Pharmacol* **40**: 2457-2464.

Rauth, A. M., T. Melo and V. Misra (1998). Bioreductive therapies: an overview of drugs and their mechanisms of action. *Int J Radiat Oncol Biol Phys* **42**: 755-762.

Reynolds, P., J. A. Anderson, J. V. Harper, M. A. Hill, S. W. Botchway, A. W. Parker and P. O'Neill (2012). The dynamics of Ku70/80 and DNA-PKcs at DSBs induced by ionizing radiation is dependent on the complexicity of damage. *Nucleic Acids Res* **40**: 10821-10831.

Richardson, A. R., K. C. Soliven, M. E. Castor, P. D. Barnes, S. J. Libby and F. C. Fang (2009). The base excision repair system of *Salmonella enterica* serovar Typhimurium counteracts DNA damage by host nitric oxide *PLoS Pathogens* **5**(5): e1000451.

Rischin, D., R. J. Hicks, R. Fisher, D. Binns, J. Corry, S. Porceddu and L. J. Peters (2006). Prognostic significance of [18F]-misonidazole positron emission tomography-detected tumor hypoxia in patients with advanced head and neck cancer randomly assigned to chemoradiation with or without tirapazamine: a substudy of Trans-Tasman Radiation Oncology Group Study 98.02. *J Clin Oncol* **24**(13): 2098-2104.

Rischin, D., L. J. Peters, B. O'Sullivan, J. Giralt, R. Fisher, K. Yuen, A. Trotti, J. Bernier, J. Bourhis, J. Ringash, M. Henke and L. Kenny (2010). Tirapazamine, cisplatin and radiation versus cisplatin and radiation for advanced squamous cell carcinoma of the head and neck (TROG 02.02, HeadSTART): a phase III trial of the Trans-Tasman Radiation Oncology Group. *J. Clin. Oncol.* **28**: 2989-2995.

Robertson, A. B., A. Klungland, T. Rognes and I. Leiros (2009). Base excision repair: the long and short of it. *Cell Mol. Life Sci.* **66**: 981-993.

Rogakou, E. P., D. R. Pilch, A. H. Orr, V. S. Ivanova and W. M. Bonner (1998). DNA double-stranded breaks induce histone H2AX phosphorylation on serine 139. *J Biol Chem* **273**: 5858-5865.

Roots, R. and S. Okada (1975). Estimation of life times and diffusion distances of radicals involved in X-ray-induced DNA strand breaks or killing of mammalian cells. *Radiat Res* **64**: 306-320.

Rothkamm, K. and M. Löbrich (2003). Evidence for a lack of DNA double-strand break repair in human cells exposed to very low x-ray doses. *Proc Natl Acad Sci USA* **100**: 5057-5062.

Roy, B., M. Lepoivre, Y. Henry and M. Fontecave (1995). Inhibition of ribonucleotide reductase by nitric oxide derived from thionitrites: reversible modifications of both subunits. *Biochemistry* **34**: 5411-5418.

Ruane, P. H., K. M. Bushan, C. M. Pavlos, R. A. D'Sa and J. P. Toscano (2002). Controlled photochemical release of nitric oxide from *o*-benzyl-substituted diazeniumdiolates. *J Am Chem Soc* **124**: 9806-9811.

Rustin, J. S., S. M. Galbraith, H. Anderson, M. Stratford, L. Folkes, LSena, L. Gumbrell and P. Price (2003). Phase 1 clinical trial of weekly combretastatin A4 Phosphate (CA4P): clinical and pharmacokinetic results. *J. Clin. Oncol.***21**:2815-1822.

Safdar, S. and L. J. Taite (2012). Targeted diazeniumdiolates: localized nitric oxide release from glioma-specific peptides and proteins. *Int. J. Pharm.* **422**: 264-270.

Saleh-Gohari, N., H. E. Bryant, N. Schultz, K. M. Parker, T. N. Cassel and T. Helleday (2005). Spontaneous homologous recombination is induced by collapsed replication forks that are caused by endogenous DNA single-strand breaks. *Mol Cell Biol* **25**: 7158-7169.

Sambrook, J. and D. W. Russell (2001). Molecular cloning, a laboratory Manual. New York, Cold Spring Harbor Laboratory Press.

Sanakis, Y., C. Goussias, R. P. Mason and V. Petrouleas (1997). NO interacts with the tyrosine radical $Y_D^{\bullet}$ of photosystem II to form an iminoxyl radical. *Biochemistry* **36**: 1141-1417.

Saparbaev, M. and J. Laval (1994). Excision of hypoxanthine from DNA containing dIMP residues by the Escherichia coli, yeast, rat, and human alkylpurine DNA glycosylases. *Proc Natl Acad Sci USA* **91**: 5873-5877.

Saunders, M., S. Dische, A. Barrett, A. Harvey, G. Griffiths and M Parmar (1999). Continuous, hyperfractionated, accelerated radiotherapy (CHART) versus conventional radiotherapy in non-small cell lung cancer: mature data from the randomised multicentre trial. *Radiother. Oncol*. **52**:137-148.

Schmid, T. E., G. Dollinger, W. Beisker, V. Hable, C. GreubelL, S. Auer, A. Mittag, A. Tarnok, A. A. Friedl, M. Molls and B. Roper (2010). Differences in the kinetics of gamma-H2AX fluorescence decay after exposure to low and high LET radiation. *Int J Radiat Biol* **86**(682-691).

Scholes, G., R. L. Willson and M. Edbert (1969). Pulse radiolysis of aqueous solutions of deoxyribonucleotides and of DNA: reaction with hydroxy-radicals. *Chem. Commun.*: 17-18.

Schouten, K. A. and B. Weiss (1999). Endonuclease V protects *Escherichia coli* against specific mutations caused by nitrous acid. *Mutation Res.* **435**: 245-254.

Schultz, L. B., N. H. Chehab, A. Malikzay and T. D. Halazonetis (2000). p53 Binding protein 1 (53BP1) is an early participant in the cellular response to DNA double-strand breaks. *J. Cell Biol.* **151**: 1381-1390.

Seddon, W. A., J. W. Fletcher and F. C. Sopchyshyn (1973). Pulse radiolysis of nitric oxide in aqueous solution. *Can. J. Chem.* **51**: 1123-1130.

Seela, F. and S. Lampe (1994). Synthesis, base pairing and structural transitions of oligodeoxyribonucleotides containing 8-aza-2'-deoxyguanosine. *Helv Chim Acta* **77**: 1003-1017.

Seela, F., I. Munster, U. Lochner and H. Rosemeyer (1998). 8-Azaadenosine and its 2'-deoxyribonucleoside: synthesis and oligonucleotide base-pair stability. *Helvetica Chimica Acta* **81**: 1139-1155.

Sessa, W. C. (2007). Nitric oxide synthase inhibition and cancer. *Lancet* **8**: 88-89.

Shami, P., J. Saavedra, L. Wang, C. Bonifant, B. Diwan, S. Singh, Y. Gu, S. Fox, G. Buzard, M. Citro, D. Waterhouse, K. Davies, X. Ji and L. Keefer (2003). JS-K a glutathione/glutathione S-transferase-activated nitric oxide donor of the diazenimdiolate class with potent antineoplastic activity. *Mol Cancer Ther* **2**: 409-417.

Shan, S. Q., G. L. Rosner, R. D. Braun, J. Hahn, C. Pearce and M. W. Dewhirst (1997). Effects of diethylamine/nitric oxide on blood perfusion and oxygenation in the R3230Ac mammary carcinoma. *Br J Cancer* **76**: 429-437.

Shao, C., M. Aoki and Y. Furusawa (2003). Bystander effect of cell growth stimulation in neoplastic HSGc cells induced by heavy-ion irradiation. *Radiat. Env. Biophys.* **42**: 183-187.

Sharma, K., A. Iyer, K. Sengupta and H. Chakrapani (2013). INDQ/NO, a bioreductively activated nitric oxide prodrug. *Org. Lett.* **15**: 2636-2639.

Singh, S., R. L. Cowen, E. C. Chinje and I. J. Stratford (2009). The impact of intracellular generation of nitric oxide on the radiation response of human tumour cells. *Radiat Res* **171**: 572-580.

Singh, S. and A. K. Gupta (2011). Nitric oxide: role in tumour biology and iNOS/NO-based anticancer therapies. *Cancer Chemother. Pharmacol.* **67**: 1211-1224.

Siim, B. G., G. J. Altwell and W. R. Wilson (1994). Oxygen dependendence of the cytotoxicity and metabolic activation of 4-alkylamino-5-nitroquinoline bioreductive drugs. *Br J Cancer* **70**: 596-603.

Solar, S., W. Solar and N. Getoff (1984). Reactivity of OH with tyrosine in aqueous solution studied by pulse radiolysis. *J. Phys. Chem.* **88**: 2091-2095.

Sonveaux, P., B. F. Jordan, B. Gallez and O. Feron (2009). Nitric oxide delivery to cancer: why and how? *Eur J Cancer* **45**: 1352-1369.

Spinks, J.W.T and R. J. Woods (1976). An introduction to radiation chemistry, second edition, New York, Wiley Interscience: 91-98.

Stanbury, D. M. (1989). Reduction potentials involving inorganic free radicals in aqueous solution. *Adv Inorg Chem* **33**: 69-138.

Steel, G. G., T. J. McMillan and J. H. Peacock (1989). The 5Rs of radiobiology. *Int J Radiat Biol* **56**: 1045-1048.

Steenken, S. (1989). Purine bases, nucleosides, and nucleotides: aqueous solution redox chemistry and transformation reactions of their radical cations and e^- and OH adducts. *Chem. Rev.* **89**: 503-520.

Stewart, G. D., J. Nandi, E. Katz, K. J. Bowman, J. G. Christie, D. J. G. Brown, D. B. Mclaren, A. C. P. Riddick, J. A. Ross, G. D. D. Jones and F. K. Habib (2011). DNA srand breaks and hypoxia response inhibition mediate the radisensitisation effect of nitric oxide donors on prostrate cancer under varying oxygen concentrations. *Biochem Pharmacol* **81**: 203-210.

Stiff, T., M. O'Driscoll, N. Rief, K. Iwabuchi, M. Löbrich and P. A. Jeggo (2004). ATM and DNA-PK function redundantly to phosphorylate H2AX after exposure to ionizing radiation. *Cancer Res* **64**: 2390-2396.

Stratford, I. J. and P. Workman (1998). Bioreductive drugs into the next millenium. *Anti-Cancer Drug Design* **13**: 519-528.

Stubbe, J. and W. A. van der Donk (1995). Ribonucleotide reductases: radical enzymes with suicidal tendencies. *Chem. Biol.* **2**: 793-801.

Stuehr, D. J., J. Santolini, Z.-Q. Wang, C.-C. Wei and S. Adak (2004). Update on mechanism and catalytic regulation in the NO synthases. *J Biol Chem* **279**: 36167-36170.

Sturgeon, B. E., R. E. Glover, Y.-R. Chen, L. T. Burka and R. P. Mason (2001). Tyrosine iminoxyl radical formation from tyrosyl radical/nitric oxide and nitrosotyrosine. *The J Biol Chem* **276**: 45516-45521.

Su, X., A. Takahashi, N. Kondo, Y. Nakagawa, T. Iwasaki, G. Guo and T. Ohnisho (2011). Nitric oxide radical-induced radioadaptation and radiosensitization are G_2/M phase-dependent. *J. Radiat. Res* **52**: 609-615.

Sutherland, B. M., P. V. Bennett, O. Sidorkina and J. Laval (2000). Clustered DNA damages induced in isolated DNA and in human cells by low doses of ionizing radiation. *Proc. Natl. Acad. Sci. USA* **97**: 103-108.

Suzuki, T., H. Ide, M. Yamada, N. Endo, K. Kanaori, K. Tajima, T. Morii and K. Makino (2000). Formation of 2'deoxyoxanosine from 2'-deoxyguanosine and nitrous acid: mechanisms and intermediates. *Nucleic Acids Res* **28**: 544-551.

Suzuki, T., K. Iwakura, Y. Takashima, N. Kasajima and M. Inukai (2009). Formation of diazoate intermediate upon nitrous acid and nitric oxide treatment of 2'-deoxyadenosine. *Bioorg. Med. Chem. Lett.* **19**: 788-791.

Suzuki, T., Y. Matsumura, H. Ide, K. Kanaori, K. Tajima and K. Makino (1997). Deglycosylation susceptibility and base-pairing stability of 2'-deoxyoxanosine in oligodeoxynucleotide. *Biochemistry* **36**: 8013-8019.

Suzuki, T., R. Yamaoka, M. Nishi, H. Ide and K. Makino (1996). Isolation and characterization of a novel product, 2'-deoxoxanosine, from 2'-deoxyguanosine, oligodeoxynucleotide, and calf thymus DNA treated by nitrous acid and nitric oxide. *J Am Chem Soc* **118**: 2515-2516.

Szalai, V. A. and G. W. Brudvig (1996). Reversible binding of nitric oxide to tyrosyl radicals in photosystem II. Nitric oxide quenches formation of the S3 EPR signal species in acetate-inhibited photosystem II. *Biochemistry* **35**: 15080-15087.

Tannenbaum, S. R., S. Tamir, T. de Rojas-Walker and J. S. Wishnok (1994). DNA damage and cytotoxicity caused by nitric oxide. Nitrosamines and Related *N*-nitroso Compounds. Chemistry and Biochemistry. R. N. Loeppky and C. J. Michejda. Washington, American Chemical Society**:** 120-135.

Terato, H., A. Masaoka, K. Asagoshi, A. Honsho, Y. Ohyama, T. Suzuki, M. Yamada, K. Makino, K. Yamamoto and H. Ide (2002). Novel repair activities of AlkA (3-methyladenine DNA glycosylase II) and endonuclease VIII for xanthine and oxanine, guanine lesions induced by nitric oxide and nitrous acid. *Nucleic Acids Res* **30**: 4975.

Thomas, D. D., X. Liu, S. P. Kantrow and J. R. Lancaster, Jr. (2001). The biological lifetime of nitric oxide: implications for the perivascular dynamics of NO and O_2. *Proc Natl Acad Sci USA* **98**: 355-360.

Thomlinson, R. H. and L. H. Gray (1955). The histological structure of some human lung cancers and the possible implications for radiotherapy. *Br J Cancer* **9**: 539-549.

Tocher, J. H. (1997). Reductive activation of nitroheterocyclic compounds. *Gen. Pharmac.* **28**: 485-487.

Tsukahara, K. and R. G. Wilkins (1985). Kinetics of reduction of eight viologens by dithionite ion. *J Am Chem Soc* **107**: 2632-2635.

Valavanidis, A., T Vlachogianni and C. Fiotakis (2009). 8-hydroxy-2'-deoxyguanosine (8-OHdG): A critical biomarker of oxidative stress and carcinogenesis. *Journal of Environmental Science and Health Part C* **27**: 120-139.

Varia, M. A., D. P. Calkins-Adams, L. H. Rinker, A. S. Kennedy, D. B. Novotny, W. C. Fowler and J. A. Raleigh (1998). Pimonidazole: A novel hypoxia marker for complementary study of tumor hypoxia and cell proliferation in cervical carcinoma. *Gynecol. Oncol.* **71**: 270-277.

Vieira, A. J. S. C. and S. Steenken (1987). Pattern of OH radical reaction with 6- and 9-substituted purines. Effect of substituents on the rates and activation parameters of the unimolecular transformation reactions of two isomeric OH adducts. *J Phys Chem* **91**: 4138-4144.

Vieira, A. J. S. C. and S. Steenken (1990). Pattern of OH radical reaction with adenine and its nucleosides and nucleotides. Characterization of two types of isomeric OH adduct and their unimolecular transformation reactions. *J Am Chem Soc* **112**: 6986-6994.

von Sonntag, C. (1987). The Chemical Basis of Radiation Biology. London, Taylor & Francis.

von Sonntag, C. (2006). Free-radical-induced DNA damage and its repair. Hiedelberg, Springer.

Vongchampa, V., M. Dong, L. Gingipalli and P. Dedon (2003). Stability of 2'-deoxyxanthosine in DNA. *Nucleic Acids Res* **31**: 1045-1051.

Wang, L., G. G. Shi, J. C. Yao, W. Gong, D. Wei, T.-T. Wu, J. A. Ajani, S. Huang and K. Xie (2005). Expression of endothelial nitric oxide synthase correlates with the angiogenic phenotype of and predicts poor prognosis in human gastric cancer. *Gastric Cancer* **8**: 18-28.

Ward, J. F. (1988). DNA damage produced by ionizing radiation in mammalian cells: identities, mechanisms of formation, and reparability. *Prog Nucleic Acid Res Mol Biol* **35**: 95-125.

Ward, J. F. (1994). The complexity of DNA damage: relevance to biological consequences. *Int J Radiat Biol* **66**: 427-432.

Wardman, P. (1985). Lifetimes of the radical-anions of medically-important nitroaryl compounds in aqueous solution. *Life Chem Rep* **3**: 22-28.

Wardman, P. (1989). Reduction potentials of one-electron couples involving free radicals in aqueous solution. *J Phys Chem Ref Data* **18**: 1637-1755.

Wardman, P. (2001). Electron transfer and oxidative stress as key factors in the design of drugs selectively active in hypoxia. *Current Med Chem* **8**: 739-761.

Wardman, P. (2007). Chemical radiosensitizers for use in radiotherapy. *Clin. Oncol. (R. Coll. Radiol.)* **19**: 397-417.

Wardman, P. and E. D. Clarke (1976). Oxygen inhibition of nitroreductase: electron transfer from nitro radical-anions to oxygen. *Biochem Biophys Res Comms* **69**: 942-949.

Wardman, P. and E. D. Clarke (1985). Electron transfer and radical-addition in the radiosensitization and chemotherapy of hypoxic cells. New Chemo and Radiosensitizing Drugs. A. Breccia and J. F. Fowler. Bologna, lo Scarabeo**:** 21-38.

Wardman, P., K. Rothkamm, L. K. Folkes, M. Woodcock and P. J. Johnston (2007). Radiosensitization by nitric oxide at low radiation doses. *Radiat Res* **167**: 475-484.

Weiner, L. M., M. V. Dhodapkar and S. Ferrone (2009). Monoclonal antibodies for cancer immunotherapy. *The Lancet* **373**: 1033-1040.

Weiss, G. J., J. R. Infante, E. G. Chiorean, M. J. Borad, J. C. Bendell, J. R. Molina, R. Tibes, R. K. Ramanathan, K. Lewandowski, S. F. Jones, M. E. Lacouture, V. K. Langmuir, H. Lee, S. Kroll and H. A. Burris (2011). Phase I study of the safety, tolerability, and pharmacokinetics of TH-302, a hypoxia-activated prodrug, in patients with advanced solid malignancies. *Cancer Therapy: Clinical* **17**: 2997-3004.

Whillans, D. W. and G. F. Whitmore (1981). The radiation reduction of misonidazole. *Radiat Res* **86**: 311-324.

Willson, R. L. (1970). The reaction of oxygen with radiation-induced free radicals in DNA and related compounds. *Int J Radiat Biol* **17**: 349-358.

Willson, R. L. (1974). Electron-transfer reactions studied by pulse radiolysis. *Biochem Soc Trans* **2**: 1082-1084.

Wilson, W. R. and M. P. Hay (2011). Targeting hypoxia in cancer therapy. *Nature Reviews* **11**: 393-410.

Wink, D. A. (1993). Inhibition of cytochromes P450 by nitric oxide and a nitric oxide-releasing agent. *Arch Biochem Biophys* **300**: f115-123.

Wink, D. A., J. F. Darbyshire, R. W. Nims, J. E. Saavedra and P. C. Ford (1993). Reactions of the bioregulatory agent nitric oxide in oxygenated aqueous media: determination of the kinetics for oxidation and nitrosation by intermediates generated in the NO/O_2 reaction. *Chem Res Toxicol* **6**: 23-27.

Wink, D. A., K. S. Kasprzak, C. M. Maragos, R. K. Elespuru, M. Misra, T. M. Dunams, T. A. Cebula, W. H. Koch, A. W. Andrews, J. S. Allen and L. K. Keefer (1991). DNA deaminating ability and genotoxicity of nitric oxide and its progenitors. *Science* **254**: 1001-1003.

Wise, D. L. and G. Houghton (1968). Diffusion coefficients of neon, krypton, xenon, carbon monoxide and nitric oxide in water at 10-60 °C. *Chem Eng Sci* **23**: 1211-1216.

Wiseman, H. and B. Halliwell (1996). Damage to DNA by reactive oxygen and nitrogen species: role in inflammatory disease and progression to cancer. *Biochem J* **313**: 17-29.

Worthington, J., H. O. McCarthy, E. Barrett, C. Adams, T. Robson and D. G. Hirst (2004). Use of the radiation-inducible WAF1 promoter to drive iNOS gene therapy as a novel anti-cancer treatment. *J. Gene Med.* **6**: 673-680.

Wu, L. L., C.-C. Chiou, P.-Y. Chang and J. T. Wu (2004). Urinary 8-OHdG: a marker of oxidative stress to DNA and a risk factor for cancer, atherosclerosis and diabetics. *Clin Chim Acta* **339**: 1-9.

Wuenschell, G. E., T. R. O'Connor and J. Termini (2003). Stability, miscoding potential, and repair of 2'-deoxyxanthosine in DNA:Implications for nitric oxide-induced mutagenesis. *Biochemistry* **42**: 3608-3616.

Yamazaki, H., S. Nakamura, T. Nishimura, N. Kodani, T. Tsubokura, T. Kimoto, H. Sihomi, N. Aibe, K. Yoshida, M. Koizumi and T. Kagiya (2013). Hypofractionated stereotactic radiotherapy with the hypoxic sensitizer AK-2123 (sanazole) for reirradiation of brain metastases: a preliminary feasibility report. *Anticancer Res.* **33**: 1773-1776.

Yaromina, A., M. Krause and M. Baumann (2012). Individualization of cancer treatment from radiotherapy perspective. *Mol. Oncol.* **6**: 211-221.

Yaromina, A., T. Kroeber, A. Meinzer, S. Boeke, H. Thames, M. Baumann and D. Zips (2011). Exploratory study of the prognostic value of microenvironmental parameters during fractionated irradiation in human squamous cell carcinoma xenografts. *Int. J. Radiat. Oncol. Biol. Phys.* **80**: 1205-1213.

Yermilov, V., J. Rubio and H. Ohshima (1995). Formation of 8-nitroguanine in DNA treated with peroxynitrite *in vitro* and its rapid removal from DNA by depurination. *FEBS Letts* **376**: 207-210.

Yonetani, T., H. Yamamoto, J. E. Erman, J. J. S. Leigh and G. H. Reed (1972). Electromagnetic properties of hemoproteins. *J Biol Chem* **247**: 2447-2455.

Yousafzai, F. K and R. R. Eady (2002). Dithionite reduction kinetics of the dissimilatory copper-containing nitrite reductase of *Alcalegenesxylosoxiadans*. *J BiolChem* **277**: 34067-64073.

Zacharia, I. G. and W. M. Deen (2005). Diffusibility and solubility of nitric oxide in water and saline. *Annals of Biomedical Engineering* **33**: 214-222.

Zhang, H., J. Joseph, J. Feix, N. Hogg and B. Kalyanaraman (2001). Nitration and oxidation of a hydrophobic tyrosine probe by peroxynitirite in membranes: comparison with nitration and oxidation of tyrosine by peroxynitrite in aqueous soution. *Biochemistry* **40**: 7675-7686.

Zhang, W., S. Tan, E. Paintsil, G. E. Dutschman, E. A. Gullen, E. Chu and Y.-C. Cheng (2011). Analaysis of deoxyribonucleotide pools in human cancer cells lines using a liquid chromatography coupled with tandem mass spectrometry technique. *Biochem Pharmacol* **84**: 411-417.

Zhong, H., A. M. D. Marzo, E. Laughner, M. Lim, D. A. Hilton, D. Zagzag, P. Buechler, W. B. Isaacs, G. L. Semenza and J. W. Simons (1999). Overexpression of hypoxia-inducible factor 1a in common human cancers and their metastases. *Cancer Res* **59**: 5830-5835.

Publications

Folkes, L.K and P O'Neill. (2013). Modification of DNA damage mechanisms by nitric oxide during ionizing radiation. *Free Radic Biol Med* **58**, 14-25.

Folkes, L.K and P O'Neill. (2013). DNA damage induced by nitric oxide during ionizing radiation is enhanced at replication. *Nitric oxide* **34**, 47-55.

Lomax, M.E., L.K. Folkes and P O'Neill. (2013). Biological consequences of radiation-induced DNA damage: relevance to radiotherapy. *Clin Oncol* **25**, 578-585.